

University of Alberta

**The Schaft Creek Porphyry Cu-Au-Mo-Ag Deposit,
Northwestern British Columbia**

by

James Edward Scott



A thesis submitted to the Faculty of Graduate Studies and Research
in partial fulfillment of the requirements for the degree of

Master of Science

Department of Earth and Atmospheric Sciences

**Edmonton, Alberta
Spring 2008**



Library and
Archives Canada

Published Heritage
Branch

395 Wellington Street
Ottawa ON K1A 0N4
Canada

Bibliothèque et
Archives Canada

Direction du
Patrimoine de l'édition

395, rue Wellington
Ottawa ON K1A 0N4
Canada

Your file *Votre référence*

ISBN: 978-0-494-45883-9

Our file *Notre référence*

ISBN: 978-0-494-45883-9

NOTICE:

The author has granted a non-exclusive license allowing Library and Archives Canada to reproduce, publish, archive, preserve, conserve, communicate to the public by telecommunication or on the Internet, loan, distribute and sell theses worldwide, for commercial or non-commercial purposes, in microform, paper, electronic and/or any other formats.

The author retains copyright ownership and moral rights in this thesis. Neither the thesis nor substantial extracts from it may be printed or otherwise reproduced without the author's permission.

AVIS:

L'auteur a accordé une licence non exclusive permettant à la Bibliothèque et Archives Canada de reproduire, publier, archiver, sauvegarder, conserver, transmettre au public par télécommunication ou par l'Internet, prêter, distribuer et vendre des thèses partout dans le monde, à des fins commerciales ou autres, sur support microforme, papier, électronique et/ou autres formats.

L'auteur conserve la propriété du droit d'auteur et des droits moraux qui protègent cette thèse. Ni la thèse ni des extraits substantiels de celle-ci ne doivent être imprimés ou autrement reproduits sans son autorisation.

In compliance with the Canadian Privacy Act some supporting forms may have been removed from this thesis.

Conformément à la loi canadienne sur la protection de la vie privée, quelques formulaires secondaires ont été enlevés de cette thèse.

While these forms may be included in the document page count, their removal does not represent any loss of content from the thesis.

Bien que ces formulaires aient inclus dans la pagination, il n'y aura aucun contenu manquant.

■ ■ ■
Canada

ABSTRACT

Schaft Creek is a calc-alkaline porphyry Cu-Mo-Au deposit located in northwestern British Columbia. Hosted by Late Triassic basaltic to andesitic volcanic rocks of the Stuhini Group, the deposit formed as a result of crystallization of the underlying Hickman/Yehiniko batholith complex which released granodioritic porphyritic dykes and fluids into the overlying volcanic sequence. The age of the Hickman/Yehiniko batholith complex is approximately constrained by a composite U-Pb zircon date of 222.1 ± 9.6 Ma, which is in broad agreement with a well-constrained age for mineralization of 222.0 ± 0.8 Ma (Re-Os molybdenite). The deposit shares characteristics of both the classic and diorite porphyry models, with silica-poor sericite-chlorite alteration in mafic country rocks instead of more normal phyllic alteration. Mineralization occurs in hydrothermal veins and breccias and consists of bornite, chalcopyrite, molybdenite, and pyrite with potassic and sericite-chlorite alteration. Significant structural modification of the deposit occurred during and after its formation.

ACKNOWLEDGMENTS

This project was generously funded by a research grant to Jeremy Richards (University of Alberta) from CopperFox Metals Inc. Additional funding was provided by the University of Alberta through the Bruce Nesbitt Memorial Graduate Award, and the Department of Earth and Atmospheric Sciences through a Graduate Teaching Assistantship for one semester.

I would like to thank Jeremy Richards for accepting me to work on this project, and for his invaluable guidance and support over the past few years. I would also like to thank Guillermo Salazar for his assistance in getting the project off the ground in its early stages, for providing generous field support, and for sharing his first-hand knowledge of the deposit from the Hecla exploration days.

I would also like to acknowledge the terrific work done by Rob Creaser, Larry Heaman, and Antonio Simonetti at the Radiogenic Isotope Facility (University of Alberta) in helping to unravel some of the mysteries of the geochronology of Schaft Creek. A huge thank-you goes out to Walter Hanych, Peter Fischer, and Sheena Ewanchuk for their companionship and assistance in the field, and for stimulating scientific debate and exchange of ideas regarding the nature of the deposit.

Thanks also go out to Don Resultay and Mark Labbe in the thin section lab for making flawless sections which form a large part of this thesis; and to Kim Ferguson for her assistance in processing my U-Pb samples for analyses. Big thanks also to Sarah Gleeson for her assistance as a committee member during the first two years of the project and for helpful feedback and encouragement during the early stages of work. Stimulating geological discussions regarding porphyry system geology and northern Cordilleran tectonics with Taras Nahnybida and Walter Loogman contributed in a large part to some of the early ideas which ultimately ended up in the thesis.

Of course, I must also acknowledge those from my research group without whom I may never have finished this project in the first place; Mike Moroskat, Suzy Byron, Bronwen Wallace, Ali Imer, Tracye Davies, and Mike Lawson. I'd also like to thank Luke Harris, Bronwen Wallace, Mike Moroskat, and Melissa Bowerman for putting me up in their respective places when I was without a home. In particular, Mike and Melissa put up with a loud and sometimes obnoxious James in a quite small apartment for over three months. I'd also like to thank Luke Harris for helping me keep my sanity during the most challenging parts of the thesis through biking, good food, good drinks, and good times. Thanks also to Breanna Uzelman for helping me to make it through the some of most stressful final parts of the thesis, when at times I would forget where I was going or what I was doing.

Of course, no set of acknowledgements would be complete without thanking all my colleagues in this closely-knit and supportive department – you all know who you are.

Lastly, I'd like to thank my family for their boundless encouragement and support, and for always trying to understand what I'm working on despite how technical the work can sometimes be – it has been most appreciated.

TABLE OF CONTENTS

1 – INTRODUCTION.....	1
2 – REGIONAL GEOLOGICAL AND TECTONIC SETTING.....	3
3 – ANALYTICAL METHODS.....	10
4 – LOCAL GEOLOGY, PETROLOGY, GEOCHEMISTRY, AND GEOCHRONOLOGY.....	12
4.1 – Petrography.....	12
4.1.1 – <i>Volcanic rocks</i>	15
4.1.2 – <i>Mafic intrusive rocks</i>	18
4.1.3 – <i>Intermediate to felsic intrusive rocks</i>	18
4.1.4 – <i>Intrusive breccias</i>	21
4.1.5 – <i>Late mafic dykes</i>	22
4.2 – Mineral Chemistry.....	22
4.3 – Whole-Rock Geochemistry.....	26
4.3.1 – <i>Major element geochemistry</i>	26
4.3.2 – <i>Trace element geochemistry</i>	28
4.4 – Geochronology.....	34
4.4.1 – <i>Previous data</i>	34
4.4.2 – <i>Current data</i>	35
5 – GEOLOGY OF THE SCHAFT CREEK PORPHYRY SYSTEM.....	41
5.1 – Alteration.....	41
5.1.1 – <i>Potassic alteration</i>	41
5.1.2 – <i>Sericite-Chlorite alteration</i>	44
5.1.3 – <i>Propylitic alteration</i>	47
5.1.4 – <i>Hematization</i>	47
5.1.5 – <i>Carbonate alteration</i>	47
5.1.6 – <i>Silicification</i>	52
5.2 – Veining and Mineralization.....	52
5.2.1 – <i>Vein types</i>	52
5.2.2 – <i>Syn- and post-mineralization deformation</i>	59
5.2.3 – <i>Nature of mineralization</i>	62
5.2.4 – <i>Nature of ore distribution</i>	66
6 – DISCUSSION.....	72

6.1 – Tectonic Setting.....	72
6.2 – Nature of the Schaft Creek Porphyry System.....	74
6.3 – Schaft Creek compared with other porphyry systems in northern British Columbia...81	
6.4 – Deposit Exploration.....	82
7 - CONCLUSIONS.....	86
REFERENCES.....	88
APPENDICES.....	93
Appendix 1 – Geochemical Quality Control: Standards and Duplicates.....	93
<i>Appendix 1.1 – ICP-OES analyses.....</i>	<i>93</i>
<i>Appendix 1.2 – Instrumental neutron activation analyses.....</i>	<i>96</i>
<i>Appendix 1.3 – ICP-MS analyses.....</i>	<i>97</i>
<i>Appendix 1.4 – Total dissolution ICP-OES analyses.....</i>	<i>101</i>
Appendix 2 – Lithochemistry.....	102
<i>Appendix 3.1 – Major element geochemistry.....</i>	<i>102</i>
<i>Appendix 3.2 – Trace element geochemistry.....</i>	<i>104</i>
Appendix 3 – Mineral Chemistry.....	110
Appendix 4 – Sample Descriptions and Locations.....	122
Appendix 5 – Selected Petrographic Descriptions.....	140
Appendix 6 – 2006 Schaft Creek Outcrop Mapping Data.....	155

LIST OF TABLES

		Page
Table 2.1	Published geochronological results for Schaft Creek and environs	8
Table 4.1	Representative mineral chemistry for pyroxene and plagioclase grains from the Stuhini Group volcanic rocks at Schaft Creek	25
Table 4.2	Summary of Logan et al. (2000) U-Pb zircon results for Schaft Creek	33
Table 4.3	Schaft Creek U-Pb zircon results	36
Table 4.4	Schaft Creek in-situ LA-ICP-MS U-Pb zircon results; Sample 06CF287	36
Table 4.5	Schaft Creek Re-Os molybdenite results	39
Table 6.1	A comparison of northern Cordilleran porphyry deposits to classic porphyry deposit models	75

LIST OF FIGURES

		Page
Figure 1.1	Superterranes of the Canadian Cordillera	2
Figure 2.1	Key Cordilleran tectonic terranes with respect to porphyry Copper deposit formation	4
Figure 2.2	Simplified regional geology	5
Figure 4.1	Geological map of the Schaft Creek deposit	13
Figure 4.2	850 m elevation plan – Geology	14
Figure 4.3	Textures of basaltic to andesitic volcanic rocks	16
Figure 4.4	Textures of basaltic to andesitic pyroclastic volcanic rocks	17
Figure 4.5	Gabbro, diorite, granodiorite, and quartz-feldspar porphyry textures	19
Figure 4.6	Photomicrographs of felsic intrusive rocks	20
Figure 4.7	Compositional plot for intermediate to felsic non-porphyritic intrusive rocks by modal mineralogy	21
Figure 4.8	Textures of the intrusive breccia unit and the late mafic dykes	23
Figure 4.9	Clinopyroxene compositions for Schaft Creek volcanic rocks	24
Figure 4.10	Total alkali-silica plot for all geochemical samples collected at Schaft Creek	27
Figure 4.11	Alkali - iron oxide - magnesium oxide diagram	28
Figure 4.12	Harker diagrams for Schaft Creek lithochemical samples	29
Figure 4.13	Trace element plots for Schaft Creek lithochemical samples	30
Figure 4.14	Rare-earth element plots for Schaft Creek samples	31
Figure 4.15	U-Pb zircon TIMS data from the Schaft Creek deposit	34
Figure 4.16	U-Pb zircon LA-ICP-MS from sample 06CF287	38
Figure 4.17	Re-Os molybdenite samples from Schaft Creek	39
Figure 5.1	Alteration map of the Schaft Creek deposit	42
Figure 5.2	850 m elevation plan – alteration	43
Figure 5.3	Potassic and phyllic alteration facies textures	45

Figure 5.4	Phyllic and propylitic alteration facies textures	48
Figure 5.5	Hematization alteration textures	49
Figure 5.6	Two examples of multi-fluid veins from within the deposit	51
Figure 5.7	Paragenetic sequence of events forming the Schaft Creek deposit	52
Figure 5.8	Different types of veins commonly observed at Schaft Creek	53
Figure 5.9	Photomicrographs of two different types of mineralized veins	54
Figure 5.10	Mineralized stringers and mineralized quartz-tourmaline veins	56
Figure 5.11	West Breccia Zone mineralization	57
Figure 5.12	Molybdenite fracture coating and late Pb-Zn mineralization	58
Figure 5.13	Late veins common in the Schaft Creek deposit area	60
Figure 5.14	Structural features from within the Schaft Creek deposit area	61
Figure 5.15	Different mineralization textures represented in the deposit area	63
Figure 5.16	850 m elevation plan – copper grades	68
Figure 5.17	850 m elevation plan – molybdenum grades	69
Figure 5.18	850 m elevation plan – gold grades	70
Figure 5.19	850 m elevation plan – silver grades	71

LIST OF ABBREVIATIONS AND SYMBOLS

AFM	<i>alkali - iron oxide - magnesium oxide</i>
And	<i>andesite</i>
a.s.l	<i>above sea level</i>
Bn	<i>bornite</i>
Bt	<i>biotite</i>
Carb	<i>carbonate</i>
Chl	<i>chlorite</i>
Cpy	<i>chalcopyrite</i>
Cc	<i>chalcocite</i>
Epi	<i>epidote</i>
Fluor	<i>fluorite</i>
Gal	<i>galena</i>
Gran	<i>granodiorite</i>
Gyp	<i>gypsum</i>
Hm	<i>hematite</i>
ICP-MS	<i>inductively coupled plasma mass spectrometry</i>
ICP-OES	<i>inductively coupled plasma optical emission spectroscopy</i>
K-spar	<i>potassium feldspar</i>
kV	<i>kilovolts</i>
λ	<i>lambda - decay constant</i>
LA	<i>laser ablation</i>
Ma	<i>unit - age, maga-annum, million years</i>
MC	<i>multi-collector</i>
Min	<i>mineralization</i>
Mo	<i>molybdenite</i>
MSWD	<i>mean standard weighted deviation</i>
Mt	<i>unit - million tonnes</i>
Mt	<i>magnetite</i>
m.y.	<i>million years</i>
n	<i>number in sample</i>
nA	<i>nanoamperes</i>
NAD 83	<i>North American Datum, 1983 standard</i>
NTS	<i>National topographic system</i>
Plag	<i>plagioclase feldspar</i>
PPL	<i>plane-polarized light</i>
Py	<i>pyrite</i>
Qtz	<i>quartz</i>
QV	<i>quartz vein</i>
REE	<i>rare earth element</i>
Rho	<i>correlation coefficient</i>
RL	<i>reflected light</i>
Ser	<i>sericite</i>
Sphal	<i>sphalerite</i>
TIMS	<i>thermal ionization mass spectrometer</i>
Tour	<i>tourmaline</i>
UTM	<i>universal transverse mercator</i>
vol. %	<i>volume percent</i>
wt. %	<i>weight percent</i>
XPL	<i>cross-polarized light</i>
ZAF	<i>atomic number (Z), absorption (A), and fluorescence (F)</i>

1 - INTRODUCTION

The Schaft Creek porphyry Cu-Mo-Au deposit is a major unexploited mineral deposit in northwestern British Columbia. The deposit is located roughly 60 km south of the town of Telegraph Creek, and roughly 1100 km northwest of Vancouver, on NTS mapsheet 104G07W at 57°21'N and 131°00'W (Fig. 1.1). The deposit lies between the Schaft Creek and Mess Creek rivers, on the west-facing slopes above Schaft Creek at an average elevation of 1000 m. Current access is by fixed wing aeroplane or helicopter from the Bob Quinn or Barrage air strips on the Stewart-Cassiar highway.

The deposit was first discovered by the BIK Syndicate in 1957 during regional prospecting. A number of companies subsequently operated various exploration programs in the following years. During the late 1960s to early 1980s the property was intensely explored by Hecla Mining Company and then Teck Corporation, in two programs that produced a total of 60,000 m of diamond drill core which is preserved on-site. In 1982, decreasing metal prices made development of the deposit uneconomic, and no further work was conducted until the beginning of renewed exploration in 2005. Copper Fox Metals Inc., under option agreement with Teck Cominco Ltd., drilled an additional 12,000 m of core during the 2005 and 2006 field seasons.

The most recent resource estimate for the Schaft Creek deposit was completed in June 2007 by Associated Geosciences Ltd. Measured and indicated resources total 1,393 Mt grading 0.25 wt. % Cu, 0.019 wt. % Mo, 0.18 g/t Au, and 1.55 g/t Ag. Inferred resources account for an additional ~186 Mt of similar grade.

The purpose of this study is to take a new, modern look at the Schaft Creek deposit and define the nature of the system, including its petrology, mineral chemistry, litho-geochemistry, paragenesis, and age of formation. Through construction of a robust dataset for the deposit, the aim is to provide a solid base for comparison of this system to existing porphyry models, and other similar deposits in the northern Cordillera.

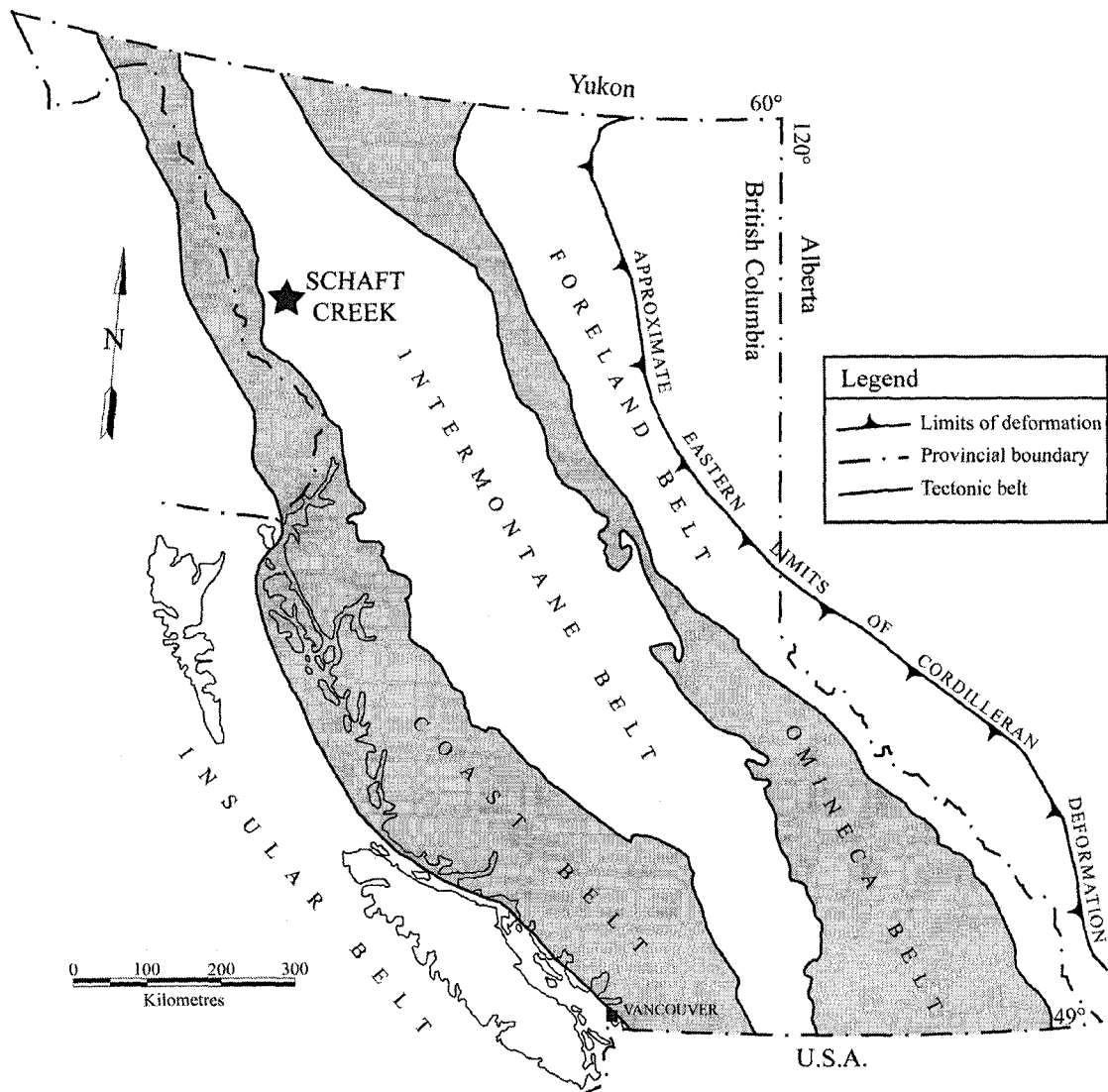


Figure 1.1 - Superterranes of the Canadian Cordillera. Figure modified after McMillan et al. (1992)

2 – REGIONAL GEOLOGICAL AND TECTONIC SETTING

The Schaft Creek porphyry Cu-Mo-Au deposit is one of a number of porphyry deposits of similar age and affinity distributed throughout the Canadian Cordillera (Fig. 2.1). The Cordillera is comprised of a number of disparate tectonic terranes which formed independently prior to amalgamation as four distinct superterranes (Monger, 1989). From the eastern Foreland belt of ancient North America and moving west these superterranes are the Omineca, Intermontane, Coast, and Insular belts. Paleomagnetic, paleontological, and stratigraphic studies by a number of authors (Monger et al., 1972; Monger, 1977; Monger and Price, 1981) indicate that the Intermontane belt that hosts the Schaft Creek deposit is allochthonous with respect to the ancestral margin of North America.

The Intermontane belt includes three terranes that are known to host significant porphyry copper mineralization. East to west, these are the Quesnel, Cache Creek, and Stikinia terranes (Fig. 2.1). Some workers have suggested that prior to amalgamation with ancestral North America, the eastern Cache Creek terrane and western Stikinia terranes amalgamated sometime prior to the Middle to Late Jurassic (Monger et al., 1978). These terranes and their host superterranes were then accreted to the ancestral margin of North America sometime shortly thereafter, but possibly as late as the Early Cretaceous, forming the modern Cordillera (Monger et al., 1982; McMillan, 1992a,b; McMillan et al., 1995).

The Stikinia terrane is the westernmost and most extensive terrane of the Intermontane belt. The terrane was formed in an island-arc setting that was located on the western margin of the North American plate, separated from the North American craton by a back-arc basin (Monger and Price, 2002). The Stikinia terrane is composed of Devonian to Jurassic island arc-related volcanic and sedimentary rocks with coeval plutons (McMillan et al., 1995).

The Stikinia terrane is the largest of the allochthonous terranes, and bears a unique pre-Jurassic geological history, paleontological assemblage, and paleomagnetic signature (Brown et al., 1996; Logan et al., 2000), all indicating an origin spatially separated from

the paleomargin of North America (Gabrielse and Yorath, 1991). The Stikinia terrane is made up of a number of assemblages: the most important with respect to the Schaft Creek deposit are the Devonian to Permian Stikine assemblage, and the Triassic Stuhini Group (Fig. 2.2; McMillan et al., 1995; Brown et al., 1996; Logan et al., 2000).

The Stikine assemblage comprises a submarine succession of tholeiitic basalt flows, breccias, and epiclastic rocks of island arc affinity interspersed with carbonate rocks (Logan et al., 2000). Logan et al. (2000) proposed that the periods of carbonate accumulation coincided with periods of volcanic quiescence in the area. On the eastern flank of the Mess

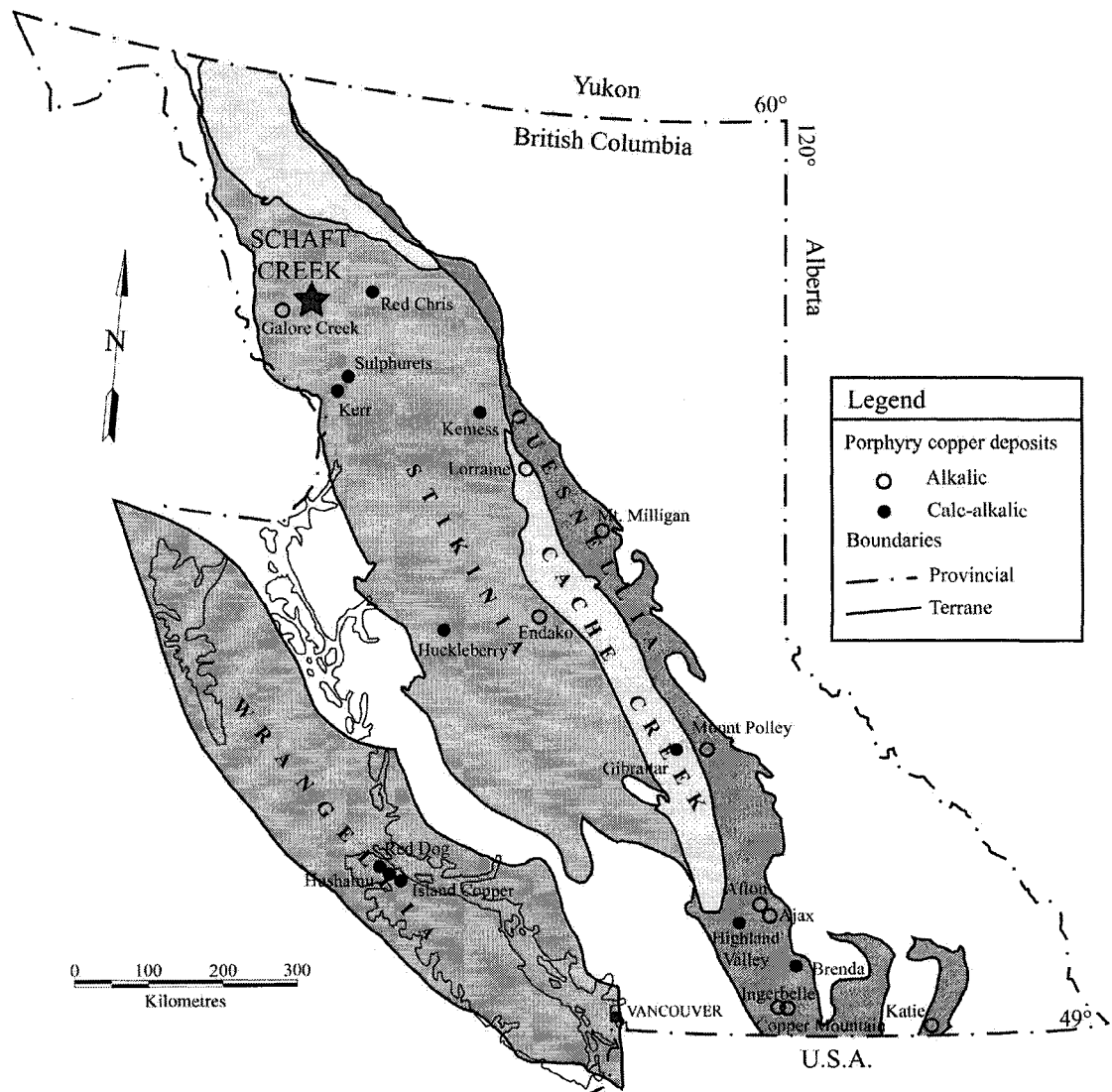


Figure 2.1 - Key Cordilleran tectonic terranes with respect to porphyry copper formation. Selected porphyry copper deposits are shown. Figure modified after McMillan et al. (1992).

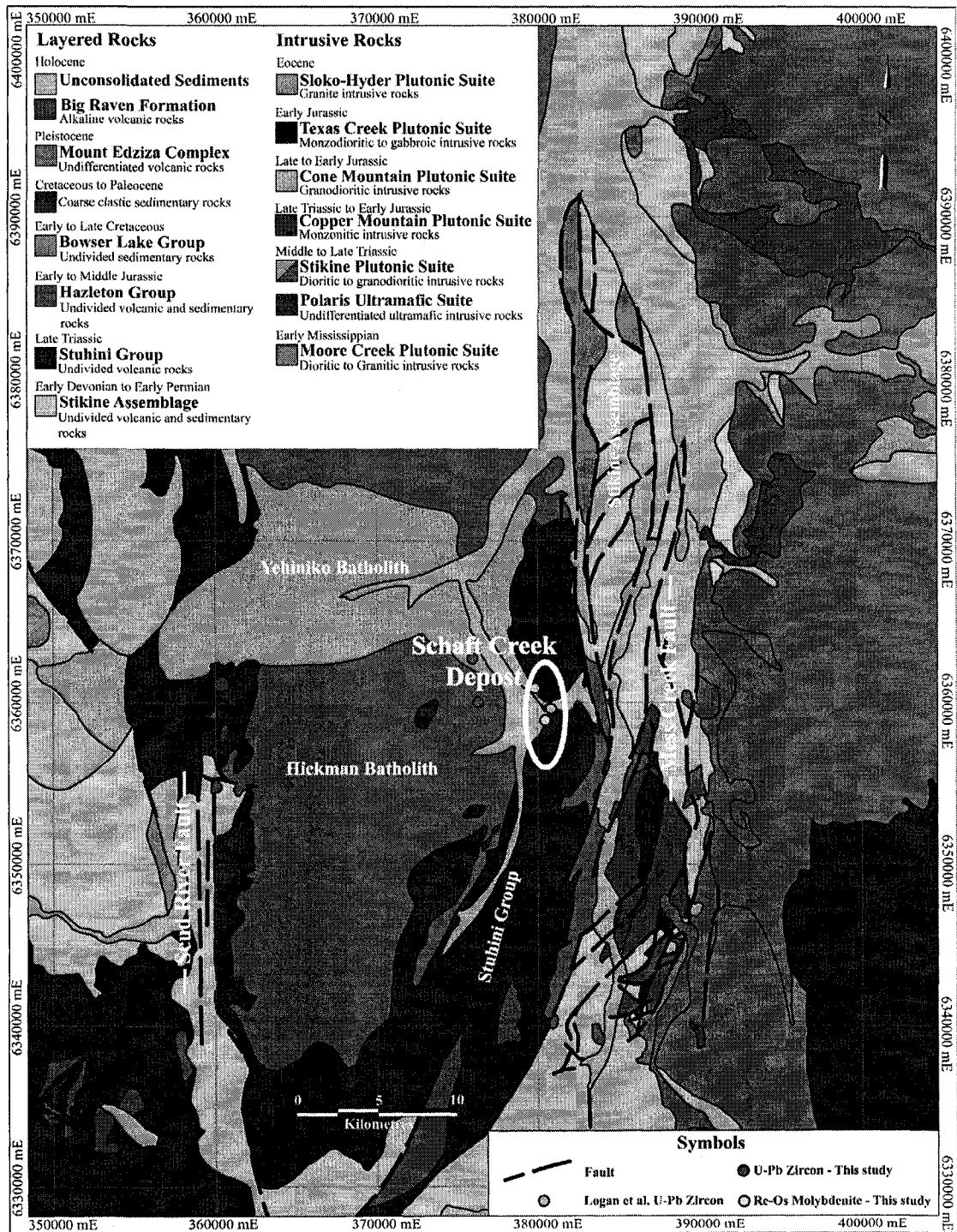


Figure 2.2 - Simplified regional geology of the area surrounding Schaft Creek. Mapping compiled from published British Columbia Geological Survey maps including Brown et al. (1996) and Logan et al. (2000). Maps by Brown et al. (1996) and Logan et al. (2000) attribute the Yehiniko batholith to the Jurassic Three Sisters Plutonic Suite based upon K-Ar and Rb-Sr dating by Holbek (1988). U-Pb data presented below indicate the Yehiniko batholith instead belongs to the Triassic Stikine Plutonic Suite. See discussion below.

Creek valley directly east of the Schaft Creek deposit, a sample of Late Carboniferous rhyolite from the Stikine Assemblage has been dated by U-Pb zircon geochronology at 311.7 ± 2 Ma (Logan et al., 2000). Above the Late Carboniferous rhyolite unit lies a thick succession of Early Permian carbonate rocks, which terminates in a major disconformity that separates it from the overlying Late Triassic Stuhini Group rocks (Souther, 1971; Logan et al., 2000). This disconformity is believed to be related to the Tahltanian Orogeny which similarly affected pre-Jurassic rocks of the Stikinia, Quesnellia, and Slide Mountain terranes (Souther, 1971; Gabrielse and Yorath, 1991). The earliest rocks to be deposited following this disconformity were a series of thinly bedded marine sediments which were followed by mafic picritic tuffs marking the beginning of Late Triassic Stuhini volcanism (Logan et al., 2000).

The Stuhini Group comprises a package of volcanic and sedimentary rocks that occurs throughout the Stikine terrane to the northwest of the Bowser Basin (Fig. 2.2; the Bowser Basin is to the southeast, roughly 20 km outside of the map area). The rocks of the Stuhini Group are believed to represent an emerging island arc environment with a proximal volcanic facies to the west, and distal re-worked volcanoclastic rocks to the east (Holbek, 1988; Logan et al., 2000). The Schaft Creek deposit is hosted in the Mess Lake facies of the Stuhini Group volcanic sequence. The Mess Lake facies forms a north-south-trending belt roughly 30 km long and generally less than 4 km wide. This facies of the Stuhini Group is comprised of a complex package of subaerial tuffs and mafic lava flows of basaltic to andesitic composition (Brown et al., 1996; Logan et al., 2000). The generalized stratigraphy of the Mess Lake facies, as described by Logan et al. (2000), consists of a basal sedimentary or mafic tuffaceous succession overlain by a medial volcanic succession of mafic flows and breccias with a central tuffaceous unit, and capped by a tuffaceous sedimentary succession. Orientations of the strata are typically steep and dip either to the northeast or southwest (Logan et al., 2000). It is not known whether the strata are folded because fold hinges are not observed, possibly due to the largely massive nature of the

strata and the general lack of distinct bedding (Brown et al., 1996; Logan et al., 2000).

The Mess Lake facies volcanic rocks are unconformably overlain by Early Jurassic conglomerates of the Hazelton Group both to the west of Mess Creek and at the eastern margin of the volcanic rocks (Brown et al., 1996; Logan et al., 2000). To the south, the Triassic volcanic rocks are in fault contact with Paleozoic rocks of various affinities from the Stikine assemblage (Logan et al., 2000). To the west, they are intruded by the Late Triassic Hickman batholith, and possibly a second intrusion, the Yehiniko batholith of supposed Middle Jurassic age (Brown et al., 1996; Logan et al., 2000; see discussion of U-Pb dating of these units below).

The Hickman batholith is a complexly-zoned, roughly north-south-trending intrusive body with dimensions of ~65 km by 17 km (Souther, 1972; Holbek, 1988; Brown et al., 1996; Logan et al., 2000). Part of the calc-alkaline Stikine intrusive suite, the Hickman batholith is believed to be coeval with the Stuhini Group volcanic rocks (Holbek, 1988; Logan et al., 2000). Holbek (1988) dated the intrusive body using K-Ar on biotite and hornblende, and Rb-Sr on biotite and whole-rock samples, and obtained dates ranging from roughly 233 to 209 Ma (published geochronological data are presented in Table 2.1, and new U-Pb data are presented and discussed below).

The Hickman batholith is made up of three distinct phases: the main phase, the southerly mafic phase, and the western diorite phase (Brown et al., 1996). To the east of the Schaft Creek deposit in the Mess Creek valley lies a dioritic body which Logan et al. (2000) suggested to be cogenetic with the western diorite phase described by Brown et al. (1995). It is believed that both diorite phases represent possible border phases to the main phase of the Hickman batholith, but this relationship is unclear (Logan et al., 2000). The southerly mafic phase bounds the batholith to the south, and is predominantly a medium-grained, equigranular hornblende gabbro to plagioclase-bearing hornblendite (Brown et al., 1996). At the southern contact, the main phase is locally gradational and carries mafic xenoliths, indicating that the mafic phase is earlier than the main phase (Brown et al.,

Table 2.1: Published geochronological results from the Schaft Creek deposit and area.

BCGS results, Logan et al. (2000)

Sample	Method	Date (Million years)
Quartz-feldspar porphyry dyke within deposit area, mineralized	U-Pb - Zircon	216.6 ± 2 Ma

Holbek (1988) Unpublished M.Sc thesis, UBC

Sample	Method	Date (Million years)
Yehiniko (81-HA19a)	Rb-Sr - Biotite	170 ± 16 Ma
Yehiniko (81-HA19a)	K-Ar - Biotite	172 ± 6 Ma
Yehiniko (81-HA19a)	Rb-Sr - Whole-rock	178 ± 11 Ma
Hickman (81-HA10a)	K-Ar - Biotite	209 ± 15 Ma
Hickman (81-HA10a)	Rb-Sr - Biotite	216 ± 4 Ma
Hickman (81-HA10a)	K-Ar - Hornblende	221 ± 8 Ma
Hickman (81-HA10a)	Rb-Sr - Whole-rock	233 ± 23 Ma

Panteleyev and Dudas, BC Gov. annual report (1972, p. 527)

Sample	Method	Date (Million years)
Mineralized biotite hornfels (DDH 52 @ 370')	K-Ar - Whole-rock	182 ± 5 Ma

1996). The main phase itself is a medium- to fine-grained hornblende biotite granodiorite to quartz monzonite, which grades into the diorite phase near the western margin where it intrudes the Stuhini Group rocks (Brown et al., 1996; Logan et al., 2000). Along this western margin, Brown et al. (1996) described numerous aplitic dykes that extend outwards from the pluton and cross-cut the rocks of the Stuhini Group, although they are too small to be shown in Figure 2.2 (Brown et al., 1996; Logan et al., 2000). The eastern contact of the batholith with the Mess Lake facies of the Stuhini Group rocks is poorly exposed and relationships are difficult to discern. However, the dykes that are commonly observed in the Schaft Creek area may be the eastern equivalents of the western aplitic dykes.

The Yehiniko batholith is described as predominantly medium-grained equigranular biotite hornblende granite with numerous aplitic and rhyolitic dykes cutting into and locally altering the surrounding volcanic rocks (Holbek, 1988; Brown et al., 1996; Logan et al., 2000). Contacts between the Yehiniko and Hickman batholiths are obscured by overburden, however, and field relationships have not been determined (Brown et al., 1996; Logan et al., 2000). Brown et al. (1996) and Logan et al. (2000) both assigned the Yehiniko Batholith to the Middle Jurassic Three Sisters plutonic suite. Dating by Holbek (1988) roughly

constrains the age of the intrusive body to between 170 and 178 Ma using K-Ar and Rb-Sr on biotite and Rb-Sr on whole-rocks (but see the discussion below).

Significant regional structural disturbance has occurred since emplacement of the intrusive bodies. The most significant structural feature affecting the deposit area is the Mess Creek fault zone. This fault zone is a roughly 7 km-wide, north-south-trending structural feature occurring to the immediate east of the Schaft Creek deposit, with splays crossing the Skeeter Lake and Schaft Creek valleys. The fault zone separates the Late Triassic Stuhini Group rocks to the west from Paleozoic basement rocks and the Pliocene Edziza volcanic complex to the east (Logan et al., 2000). There have been repeated complex motions along the Mess Creek fault which are not fully understood, but evidence suggests there was an early period of eastern uplift and erosion down to the Paleozoic basement, followed by eruption of the Pliocene volcanic rocks (Logan et al., 2000). In order to juxtapose the Triassic volcanic rocks with Paleozoic (Devonian) strata, a minimum vertical offset of 800 m is required (800 m being the estimated minimum thickness of the preserved Stuhini Group volcanic rocks; Logan et al., 2000). This significant vertical motion is believed to have been accommodated by compound movement along the major fault in the Mess Creek valley, and its splays in the Mess Lake and Schaft Creek valleys (Logan et al., 2000). The best estimate for timing of the eastern uplift along the fault system is early Tertiary to late Miocene (Logan et al., 2000), which post-dates intrusion of the Hickman batholith to the west.

3 – *SAMPLES AND ANALYTICAL METHODS*

Over 300 samples were collected from drillcore and outcrop during field seasons in 2005 and 2006. Samples were collected to provide a representative suite of all host rocks and intrusions, alteration facies, and mineralization styles within the deposit. Twenty-one samples were selected for geochemical analysis of the major lithologic units within the immediate deposit area.

Geological mapping was primarily completed during a two-week period in 2006. Surface exposure in the deposit area is limited, and the majority of outcrop occurs at the peripheries of the system. Much of the deposit itself is covered by 5 to 40 m of talus and glacial till. It was therefore necessary to combine drillhole data with outcrop data in order to produce a bedrock geological map. This was done by selecting the dominant alteration facies and lithology over the upper 50 m of the drillhole and projecting it to surface. Maps were also projected at 850 m a.s.l. by taking collar elevation coordinates, dip, and azimuth, and calculating the depth and location at which that drillhole would intersect the 850 m elevation plane. Elevation across the system varies from 825 m to 1200 m with gently sloping topography. The 850 m elevation plane provides the greatest number of drillhole pierce points without omitting any significant zones of drilling. At each pierce point, the alteration and lithology were plotted from the unique 3 m logging and sampling interval.

Twenty-one geochemical samples were submitted for analysis in two batches to Activation Laboratories in Ancaster, Ontario. Quality control standard and duplicate analytical results are presented in Appendix 1, and sample data are presented in Appendix 2.

Quantitative analyses of primary minerals in the volcanic rocks were completed using a JEOL JXA-8900 SuperProbe at the University of Alberta, Department of Earth and Atmospheric Sciences Electron Microprobe laboratory, using wavelength-dispersive analysis with an accelerating potential of 15.0 kV and beam current of 15 nA. Count times

for most analyzed elements were 20 s for the peak, and 10 s for background on either side of the peak. The count times for Mn were longer with a peak measurement of 30 s, and background measurements of 15 s per side.

To convert the raw X-ray data to elemental weight percent, a ZAF correction was applied. The ZAF correction accounts for effects due to the atomic number, which affect electron backscattering and stopping power, as well as the X-ray absorption and fluorescence. When calibrated to a standard, the ZAF correction enables the determination of the elemental weight percentages presented. Typical analytical error for the electron microprobe is 1-2 relative % for the major elements, and 3-10 relative % for elements with concentrations of less than 1 weight %.

The majority of U-Pb zircon work and isotopic analyses was completed at the University of Alberta's Radiogenic Isotope Facility using a Vacuum Generators VG354 thermal ionization mass spectrometer (TIMS). Samples were prepared for analyses through a multi-stage pulverizing, sieving, and separation process as described by Heaman et al. (2002). All age uncertainties and error ellipses are reported at two sigma.

In-situ U-Pb zircon isotopic analyses were completed at the University of Alberta's Radiogenic Isotope Facility using a Nu Instruments Plasma multi-collector inductively coupled plasma mass spectrometer (MC-ICP-MS) together with a New Wave Research UP213 laser ablation (LA) system. Analyses were completed using the methods described in Simonetti et al. (2006). All age uncertainties and error ellipses are reported at two sigma.

Two molybdenite samples were analyzed for Re-Os geochronology by isotope dilution mass spectrometry at the University of Alberta radiogenic isotope facility using methods described by Selby and Creaser (2001). Two sigma uncertainties for the Re-Os dates for molybdenite include uncertainties from the mass spectrometer measurements, standard and spike Re and Os isotopic compositions, and the calibration and gravimetric uncertainties of ^{185}Re and ^{187}Os .

4 – LOCAL GEOLOGY, PETROLOGY, GEOCHEMISTRY, AND GEOCHRONOLOGY

The Schaft Creek deposit occurs within a north–south-trending belt of Stuhini Group basaltic to andesitic volcanic rocks between the Mess Creek and Schaft Creek valleys (Fig. 2.2). Mineralization occurs on the eastern slopes above the Schaft Creek valley where granodioritic dykes from the Hickman and Yehiniko batholiths intrude and locally brecciate the basaltic to basaltic andesitic volcanic package (Fig. 4.1).

The deposit itself can be subdivided into three general zones based on common lithologic, alteration, and mineralization features (Fig. 4.1). The Paramount zone in the northwest of the map area features abundant equigranular and porphyritic granodiorite and intrusive breccia hosted by volcanic rocks of the Stuhini Group. To the southeast of the Paramount zone, intrusive rocks become less abundant and intrusive breccias are rare. This area of fewer intrusive rocks comprises the largest volume of mineralized rocks in the known deposit, and is referred to as the Main zone or historically as the Liard zone. To the west of the Main zone, and to the south of the Paramount zone, lies the West Breccia zone. The West Breccia zone hosts abundant hydrothermal breccias that cross-cut earlier intrusive breccias and volcanic host rocks. Details of alteration textures and mineralization styles that characterize these three zones are discussed below.

4.1 - Petrography

The main rock types in the immediate Schaft Creek deposit area are a thick sequence (> 800 m; Logan et al., 2000) of volcanic rocks of various affinities, which have been intruded by granodioritic dykes with corresponding intrusive breccia zones. Minor units include equigranular gabbros and diorites that may represent syngenetic feeders to the volcanic pile. A geological map and 850 m geological plan are presented in Figures 4.1

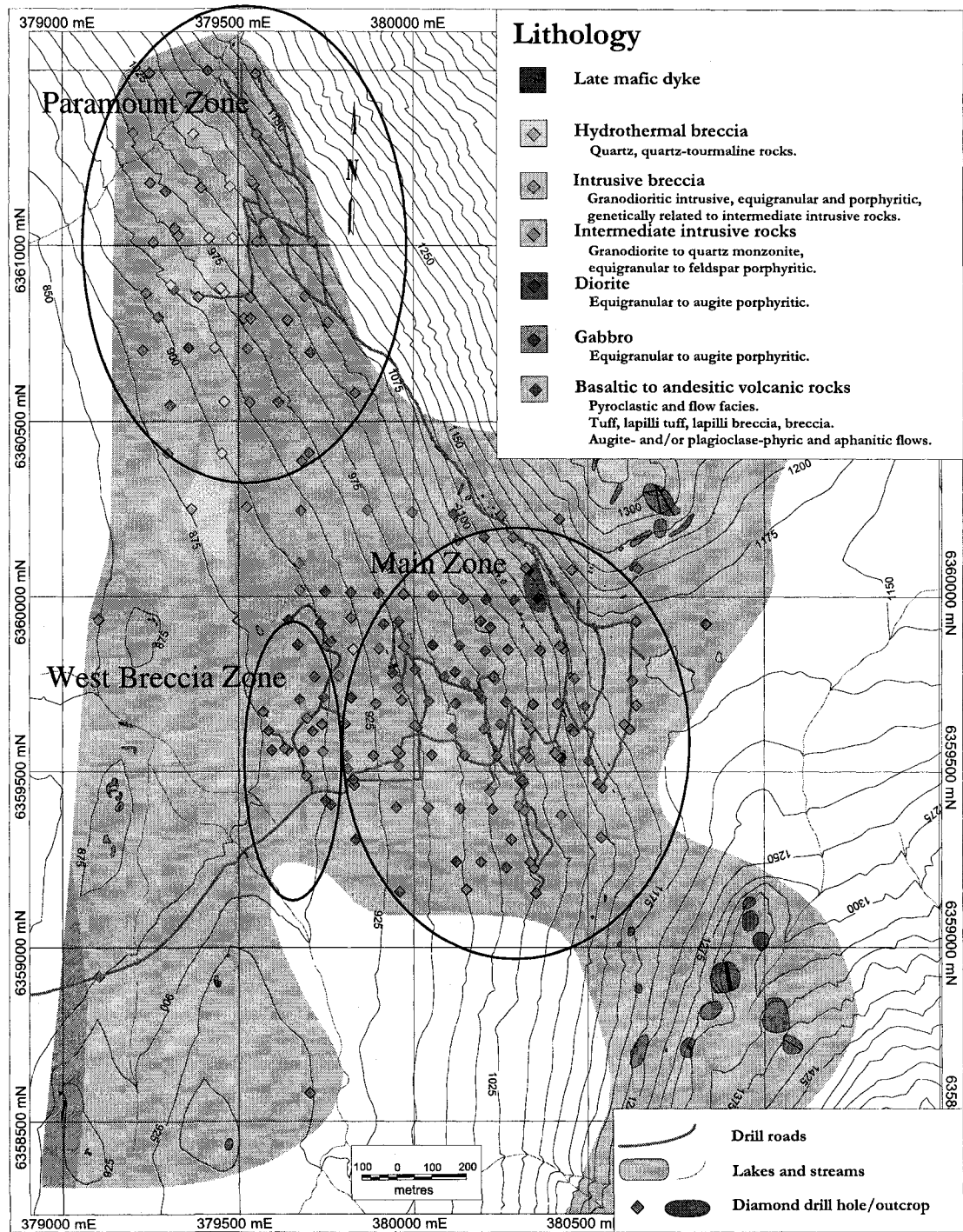


Figure 4.1 - Geology of the Shaft Creek deposit. Drillhole data (diamond shapes) are projected to surface. The dominant lithology for the upper 50 m of the drillcore is presented along with surface outcrop data. Coordinates are in UTM Zone 9V (NAD 83 datum). Deposit zone boundaries are approximate, based on the nature of geology, alteration, and mineralization.

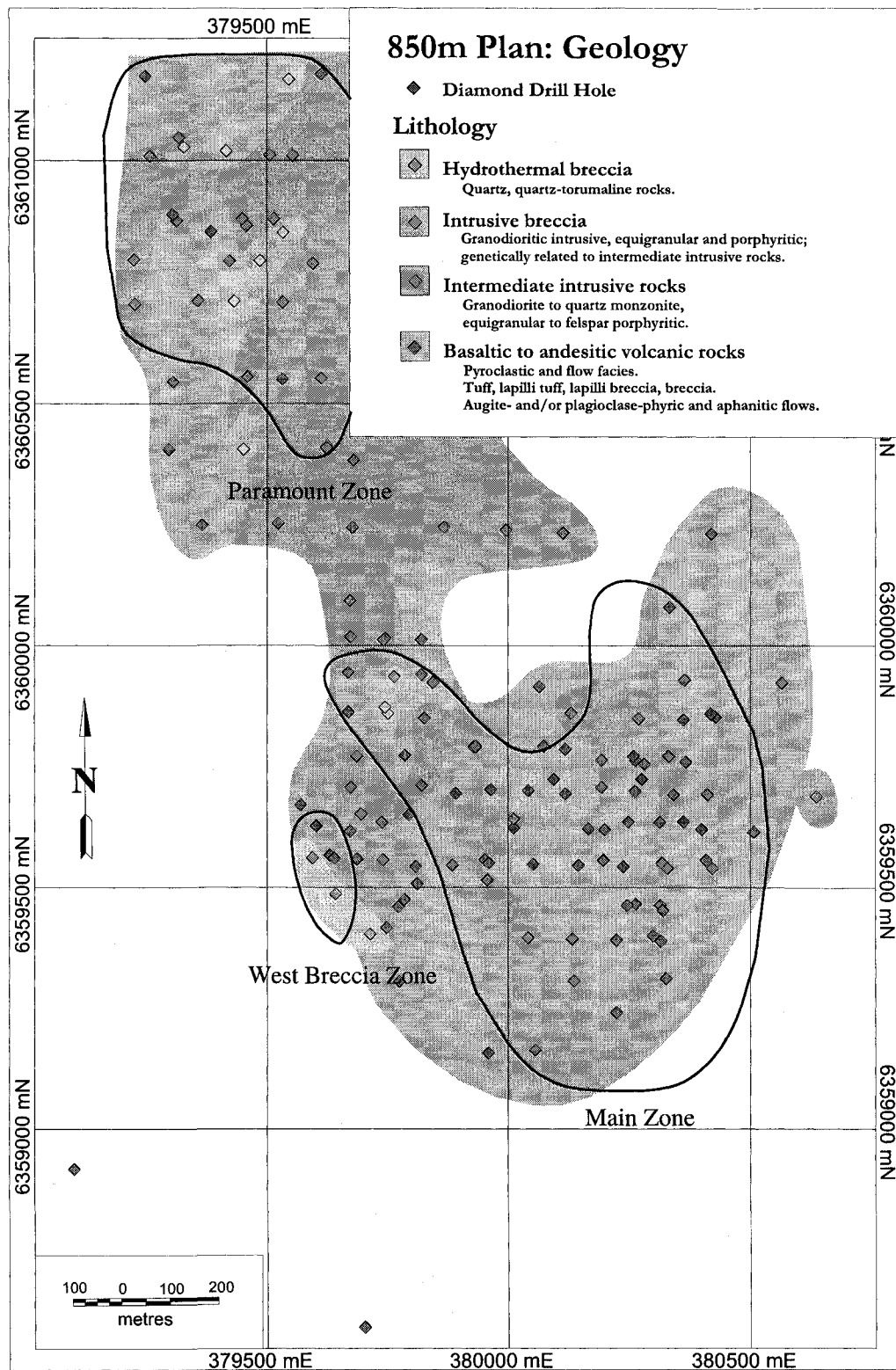


Figure 4.2 - 850 m elevation plan - Geology. Drillhole pierce points are calculated from surface elevation, drillhole azimuth, and dip. Geology is from the three metre sample interval that pierces the plane. Coordinates are in UTM Zone 9V (NAD 83 datum).

and 4.2. The descriptions of the primary textures described below reflect textures of the least-altered rocks.

4.1.1 - Volcanic rocks

The Schaft Creek deposit is hosted within a complex package of dominantly basaltic to andesitic volcanic rocks. The volcanic pile consists of numerous massive volcanic flows (Fig. 4.3a) and pyroclastic deposits which dip steeply to the north-northwest. The primary textures of the volcanic flows range from aphanitic to strongly plagioclase- and/or pyroxene-phyric, with up to 50 vol. % subhedral to euhedral phenocrysts of plagioclase and/or pyroxene (Fig. 4.3b). The groundmass is comprised of fine-grained acicular plagioclase with abundant secondary chlorite (Fig. 4.3c–f). Magnetite is also common as fine-grained disseminations in most facies of the volcanic rock and has locally been partly or wholly replaced by hematite. Variations between these facies are gradual and subtle with a lack of distinct marker horizons, making correlation of flow units across the deposit area difficult.

Basaltic to andesitic pyroclastic units exhibit a similar lack of unique marker horizons, but show a high degree of variability between tuff, crystal tuff, lapilli tuff, and breccia tuff facies (Fig. 4.4a–d). Clasts in the pyroclastic units are representative of other units in the volcanic pile, and no exotic clasts were observed. Clast sizes range from less than one centimetre to approximately two metres. One example of a fining-upwards succession at the top of a pyroclastic bed indicated that the steeply-dipping beds are not overturned (Fig. 4.4e). Bedding measurements ranged from 271°/78°N to 330°/52°NE, with an average orientation of 292°/67°NE (n = 5). No fold hinges were observed in the map area.

At the top of Mount LaCasse, ~200 m to the northeast of the mapped area in Figure 4.1, a number of outcrops of aphanitic rhyolitic volcanoclastic rocks were observed (Fig. 4.4g). Contacts between these and the more mafic volcanic rocks were not observed and

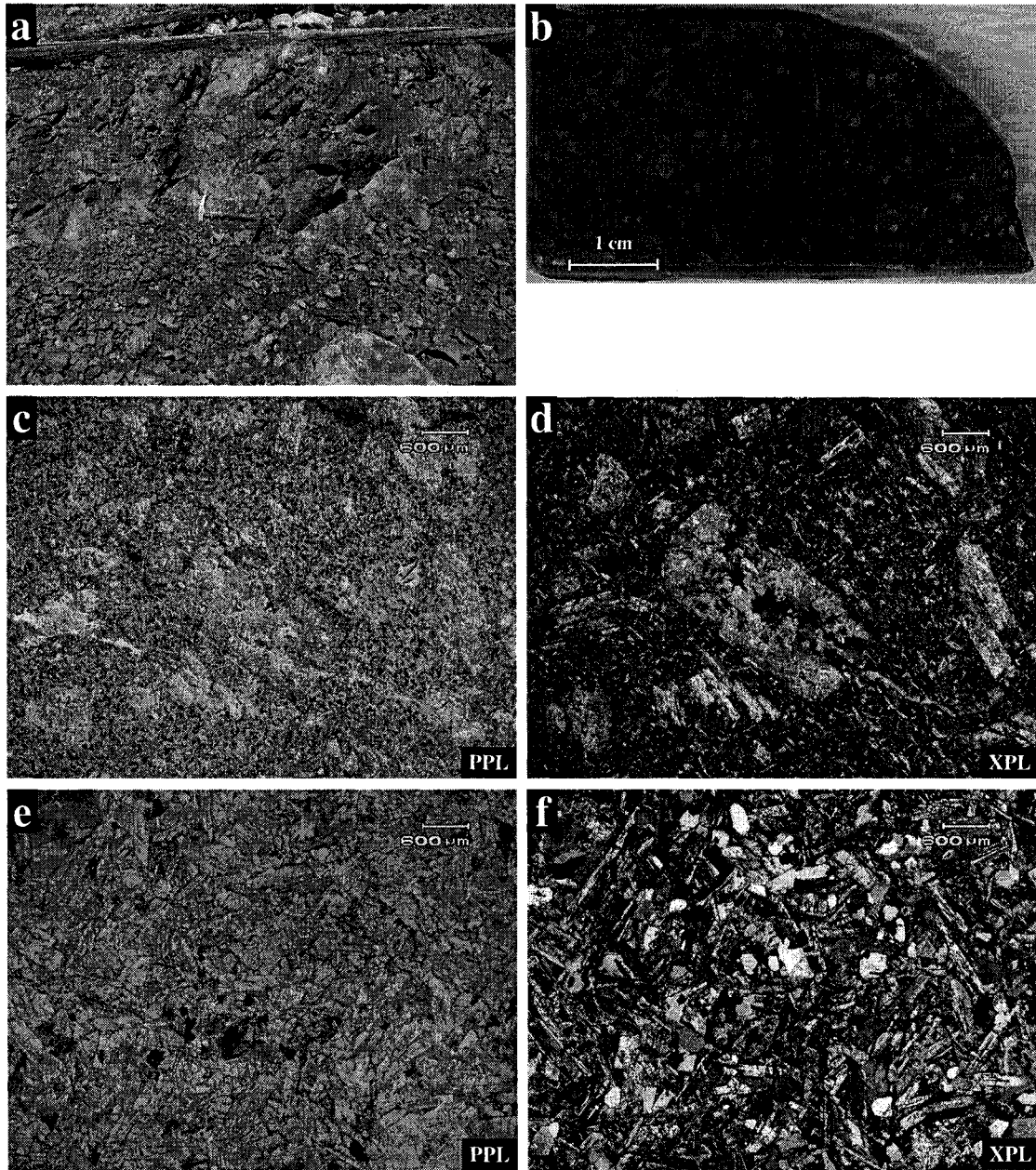


Figure 4.3 - (a) Outcrop of massive basaltic andesite flow. Purple colouration is the result of hematite alteration. Outcrop is typical of exposure and fracture density in the area. Coordinates (NAD83) 380262E, 635995N (b) Representative basaltic andesite with subhedral plagioclase and augite phenocrysts; sample 05-JES-136. (c & d) Photomicrograph of plagioclase-augite-phyric basalt. Fine-grained plagioclase comprises most of the groundmass; mafic constituents of the groundmass have been replaced by chlorite. Anhedral to subhedral fine to medium-grained plagioclase grains are moderately altered to carbonate, and the large euhedral augite grain in the centre of frame has been completely pseudomorphed by carbonate and chlorite. Sample 05-JES-136. (e & f) Photomicrograph of largely equigranular basalt. Fine-grained euhedral lath-shaped plagioclase with subhedral to anhedral augite. The sample has been weakly altered by chlorite and carbonate. Sample 05-JES-151.

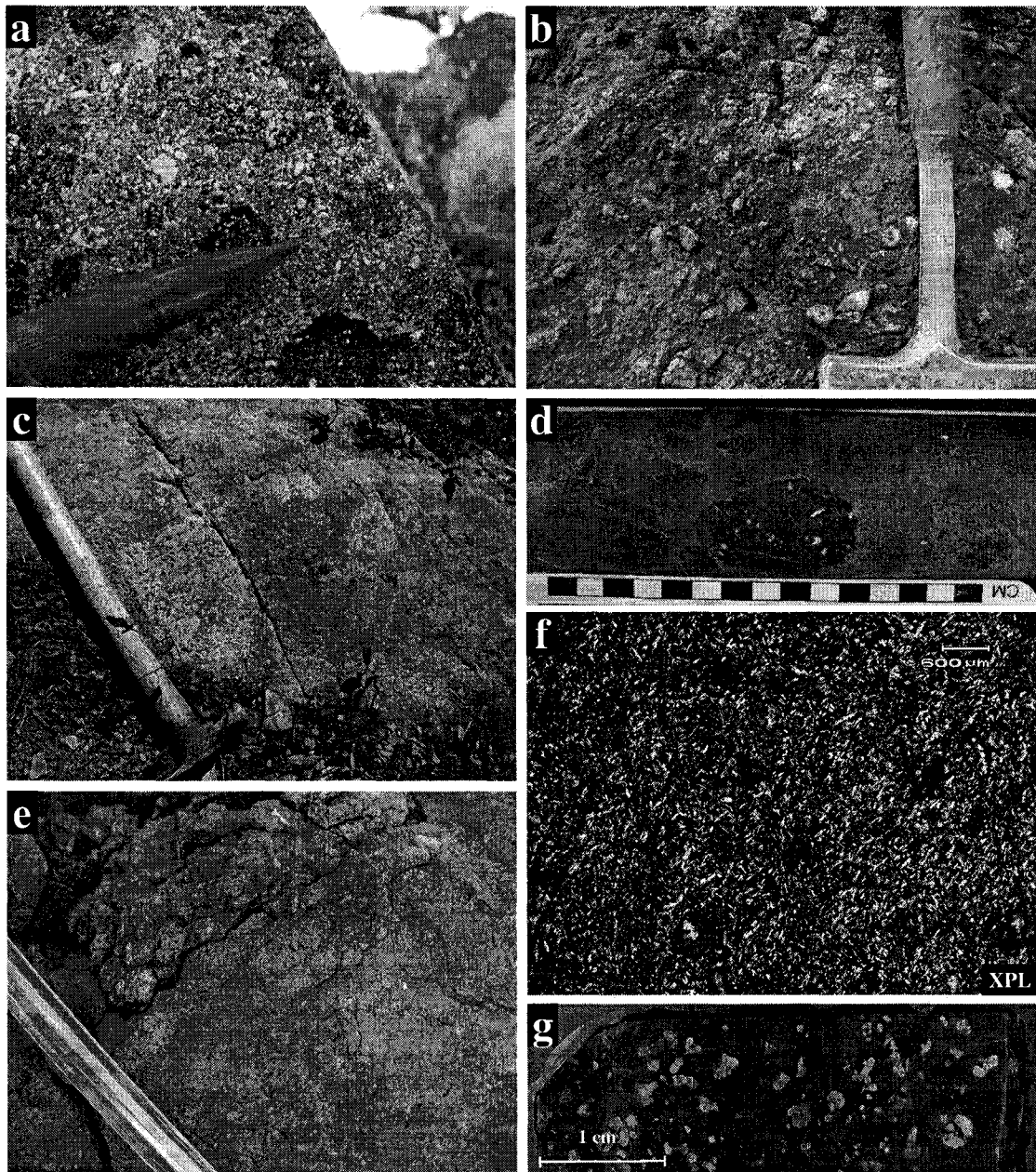


Figure 4.4 - (a) Representative crystal tuff with euhedral to subhedral fine to medium grained plagioclase crystals. Coordinates (NAD83) 380675E, 6360642N. (b) Representative weathered lapilli tuff from outcrop. Coordinates (NAD83) 380530E, 6359161N. (c) Volcanic breccia with large heterolithic andesitic to basaltic clasts that are angular to subangular. Coordinates (NAD83) 381087E, 6360584N. (d) Volcanic breccia with heterolithic, subrounded to subangular, andesitic to basaltic clasts. Sericite-chlorite alteration imparts a washed-out grey appearance to the drillcore. Drillhole 06CF273 at 235.15 m depth. (e) Best-exposed bedding in the deposit area. Photograph shows weak evidence of fining-upwards succession indicating right-way-up orientation. Coordinates (NAD83) 380521E, 6360132N. (f) Photomicrograph of a basaltic andesite tuff or an aphanitic flow. Fine-grained acicular plagioclase grains with rare augite phenocrysts (bottom left of frame), with weak chlorite and carbonate alteration (crossed polarized light; sample 05-JES-097). (g) Rhyolite sample from the peak of Mount LaCasse; sample 06-JES-061.

thus the relationship between these units remains unclear. However, these rocks are likely analogous to the roughly 150 m thick succession of tuffaceous siltstone-sandstone and well-bedded fine-grained tuffs that comprise the upper units of the Stuhini Group, and which are described by Logan et al. (2000) as conformably overlying the more mafic volcanic and volcanoclastic succession.

4.1.2 - Mafic intrusive rocks

The volcanic package is intruded by a number of equigranular to porphyritic plugs of gabbroic and dioritic composition. The rocks are comprised of a variable assemblage of clinopyroxene and plagioclase with accessory magnetite (Fig. 4.5a and b). These units are minor volumetrically with respect to the rest of the deposit area. It remains unclear if the diorite and gabbro are distinct intrusive phases or not, because no cross-cutting relationships were observed due to their spatial separation. The gabbroic intrusions occur in the southwest corner of the map area, whereas the dioritic units occur in the east-central portion of the map area where they intrude the volcanic rocks.

4.1.3 - Intermediate to felsic intrusive rocks

The volcanic rocks and mafic intrusions were subsequently intruded by a series of equigranular to porphyritic granodioritic to quartz monzodioritic dykes. These dykes have a roughly north-northwest strike and nearly vertical dip, and continue throughout the deposit over a strike length of greater than 1200 m. Figure 4.1 shows the discontinuous surface projection of some of the wider dykes. Dyke width is variable, and ranges from less than one metre to over ten metres. In addition, due to the lack of outcrop in much of the deposit area the continuity of the dykes cannot be mapped in Figure 4.1.

The contact of the dykes with the host volcanic rocks is typically sharp and irregular (Fig. 4.5c and d), but locally the volcanic rocks are brecciated by the dykes. The dykes are dominantly composed of plagioclase, quartz, potassium feldspar, amphibole, rare biotite,

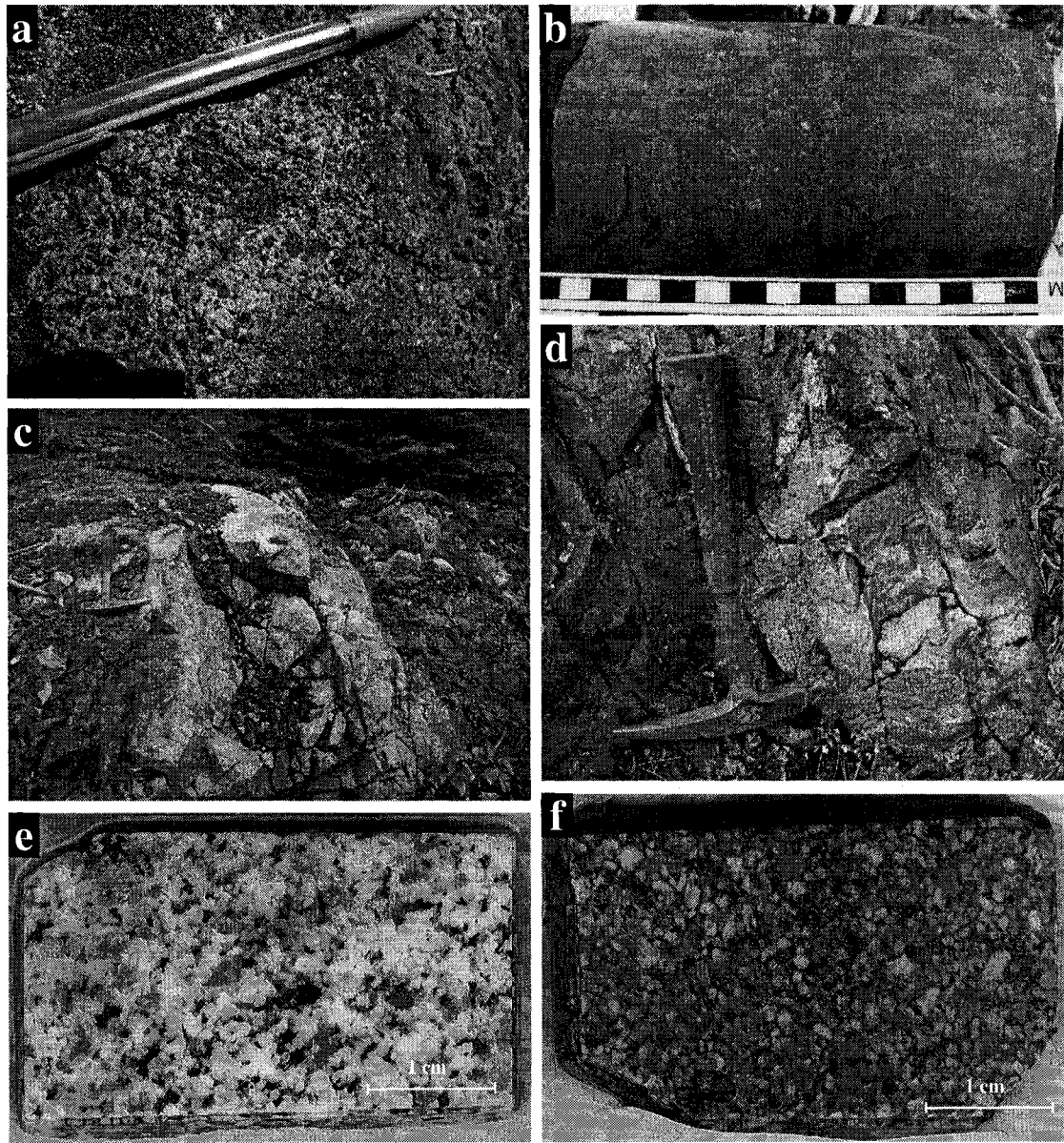


Figure 4.5 - (a) Outcropping weathered gabbro with weak sericite-chlorite alteration. Large subhedral pyroxene grains have been altered to chlorite but stand out clearly in the photograph; plagioclase grains are subhedral and medium grained and have been altered to sericite. Photo taken at coordinates 379052E, 6358436N. (b) Diorite sample from drillhole 06CF268 at 151.90 m depth (sample 06CF268-152). This is the least-altered diorite sample collected from the property, and has been subjected to weak sericite-chlorite alteration with weak overprinting carbonate alteration. (c) Granodiorite dyke in contact with volcanic rocks; dyke width is ~ 1 m. Photo taken at coordinates 379132E, 6359461N. (d) Tip of propagating dyke in sharp contact with augite-plagioclase-phyric basaltic andesite; same location as (c). (e) Granodiorite from the Hickman batholith showing weak potassic alteration characterized by secondary K-feldspar. Primary minerals are plagioclase, quartz, potassium feldspar, and amphibole in decreasing order of abundance. Sample 05-1008-6. (f) Sericite-chlorite alteration in feldspar porphyry dyke from within the deposit area (sample 05-JES-152). Modal mineralogy is the same as the Hickman granodiorite sample in (e).

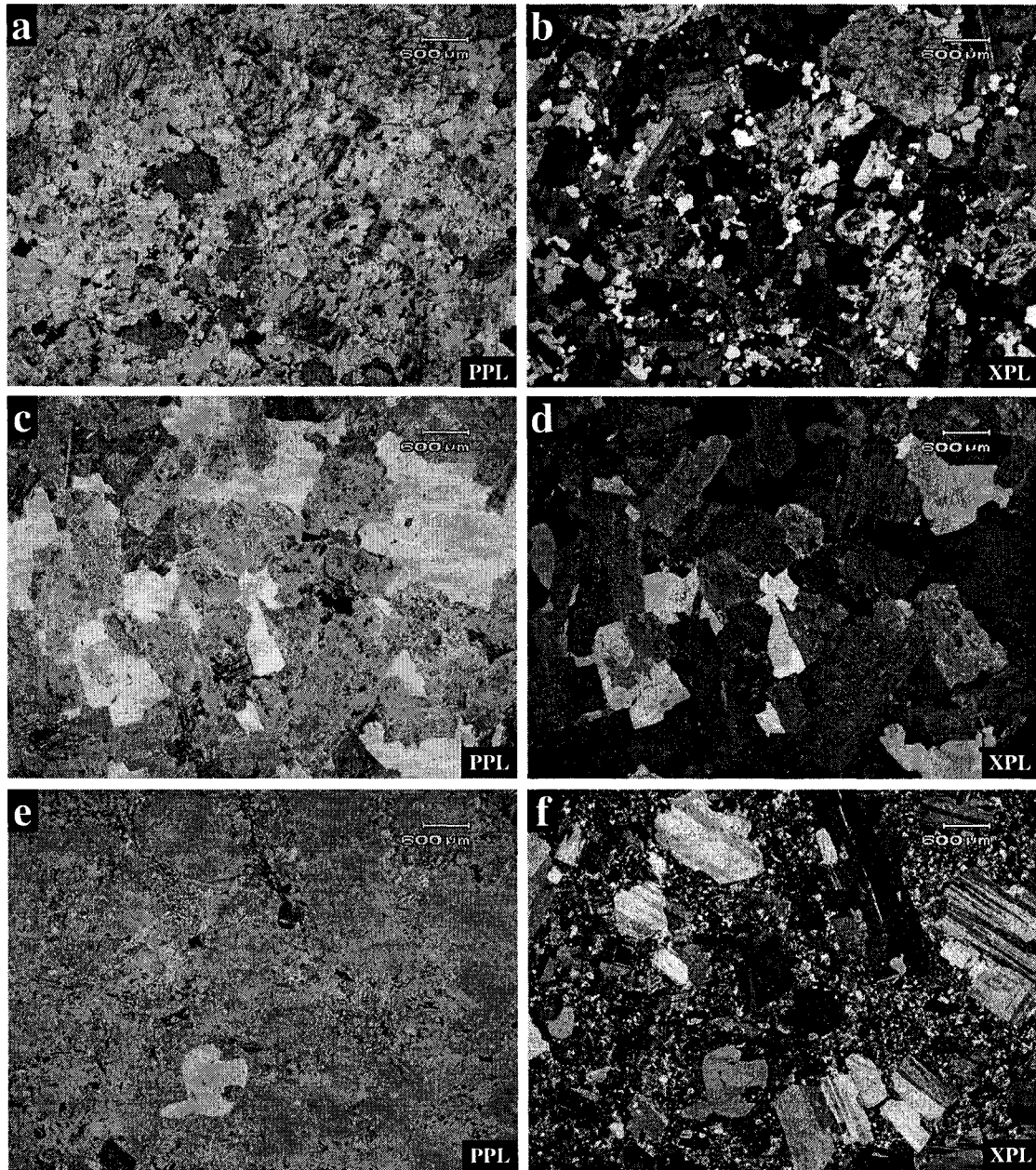


Figure 4.6 - (a & b) Photomicrographs of granodiorite from the Hickman batholith (sample 05-1008-1). Mineralogy is quartz, plagioclase, amphibole, potassium feldspar, and biotite in decreasing order of abundance. Feldspars are weakly to moderately altered by sericite, and amphibole has been weakly altered to chlorite. (c & d) Photomicrographs of coarse-grained granodiorite from the Hickman batholith (sample 05-1008-2). Mineralogy is plagioclase, quartz, potassium feldspar, and amphibole in decreasing order of abundance. Feldspars are pervasively sericitized and locally pseudomorphed, and mafic minerals are largely replaced by secondary chlorite. (e & f) Photomicrographs of feldspar-quartz porphyry from a mineralized dyke within the deposit (sample 05-JES-152). Plagioclase phenocrysts are coarse-grained, subhedral, and abundant, quartz phenocrysts are common, and potassium feldspar and mafic phenocrysts (biotite and hornblende) are rare. The groundmass is composed dominantly of fine-grained quartz with secondary chlorite. Alteration throughout is weak, mainly sericite and/or carbonate with weak to moderate chloritization of mafic phenocrysts.

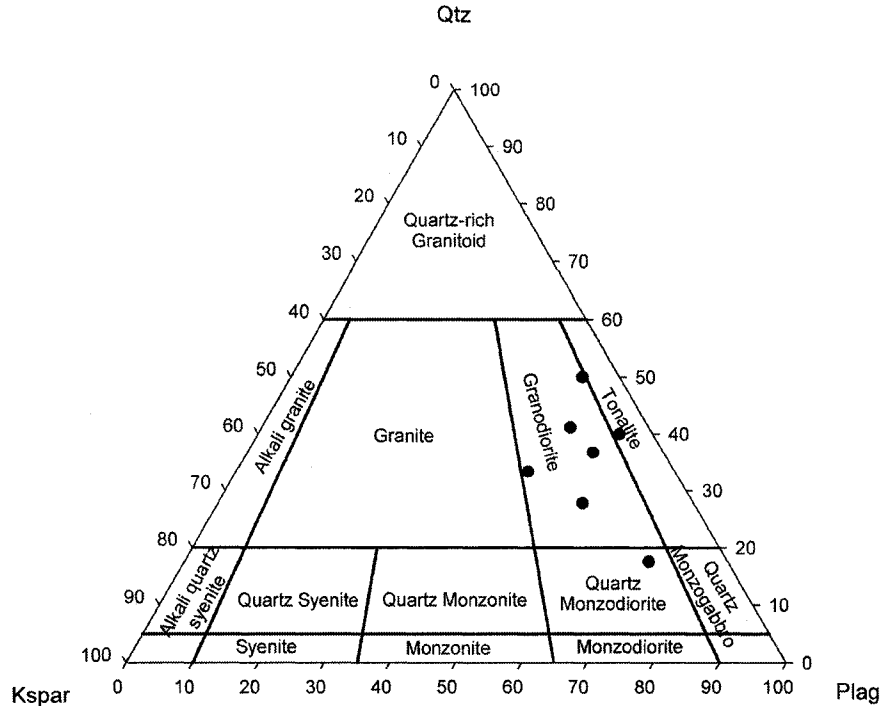


Figure 4.7 - Compositional plot for intermediate to felsic non-porphyritic intrusive rocks by modal mineralogy. Classification diagram after Streckeisen (1974, 1976).

and minor disseminated magnetite (Fig. 4.5e and f). These dykes are petrographically similar to the Hickman batholith, and the texture of the dykes becomes more porphyritic further from the batholith (Fig. 4.6a–f). Figure 4.7 shows a compositional plot of the non-porphyritic intermediate intrusive rocks by modal mineralogy.

4.1.4 - Intrusive breccias

Where the felsic intrusive rocks are in contact with the host volcanic rocks, the volcanic rocks are locally strongly brecciated. This is mainly observed in the Paramount and West Breccia zones, whereas in the Main zone of the deposit contacts with the intrusive units tend to be sharp, although commonly irregular as shown in Figures 4.5c and d. The timing of the intrusive brecciation event is complex. Clasts of granodiorite/feldspar porphyry and vein quartz show that brecciation followed at least one earlier period of intrusion and a period of barren quartz veining (Fig. 4.8a). Figure 4.8b shows porphyritic intrusive

material forming the matrix to brecciated volcanic host rock, but an earlier intrusive phase is lacking in this example.

Volcanic and intrusive clasts in the intrusive breccia are typically angular to subangular and range in size from <1cm to >10cm. Intrusive intervals in drill core can be quite thick in the northern part of the deposit (intersection of ~80 m thickness in drillhole 06CF287), where the unit is also more abundant in surface projection and at the 850 m a.s.l. plan level.

4.1.5 - Late mafic dykes

Late basaltic dykes are present throughout the deposit, and are observed to cross-cut all other lithologic units (Fig. 4.8c–e), as well as some vein types (Fig. 4.8f). The late mafic dykes are highly competent and mostly unaltered. Some of the dykes were observed to be vesicular at their margins, with secondary calcite filling these vesicles (Fig. 4.8e). Some late mafic dykes were observed to exhibit fine-grained irregular chilled margins as shown in Figures 4.8f and g.

Two different orientations of the mafic dykes were observed at roughly 075°/75° SE and at roughly 300°/90° NE. These two sets of dykes were not observed to cross-cut, and thus their relative timing could not be established.

4.2 - Mineral Chemistry

Five samples of basaltic and basaltic andesitic volcanic rocks were analyzed by electron microprobe for primary mineral chemistry of the pyroxenes and plagioclase. Unaltered phenocrysts were exceedingly rare in the sample suite. The pyroxene grains were typically weakly altered to chlorite in the basaltic andesite samples, and in the basalt sample the pyroxene grains were weakly to moderately uralitized. The plagioclase grains that were selected were the least altered, but in general they were weakly altered to fine-

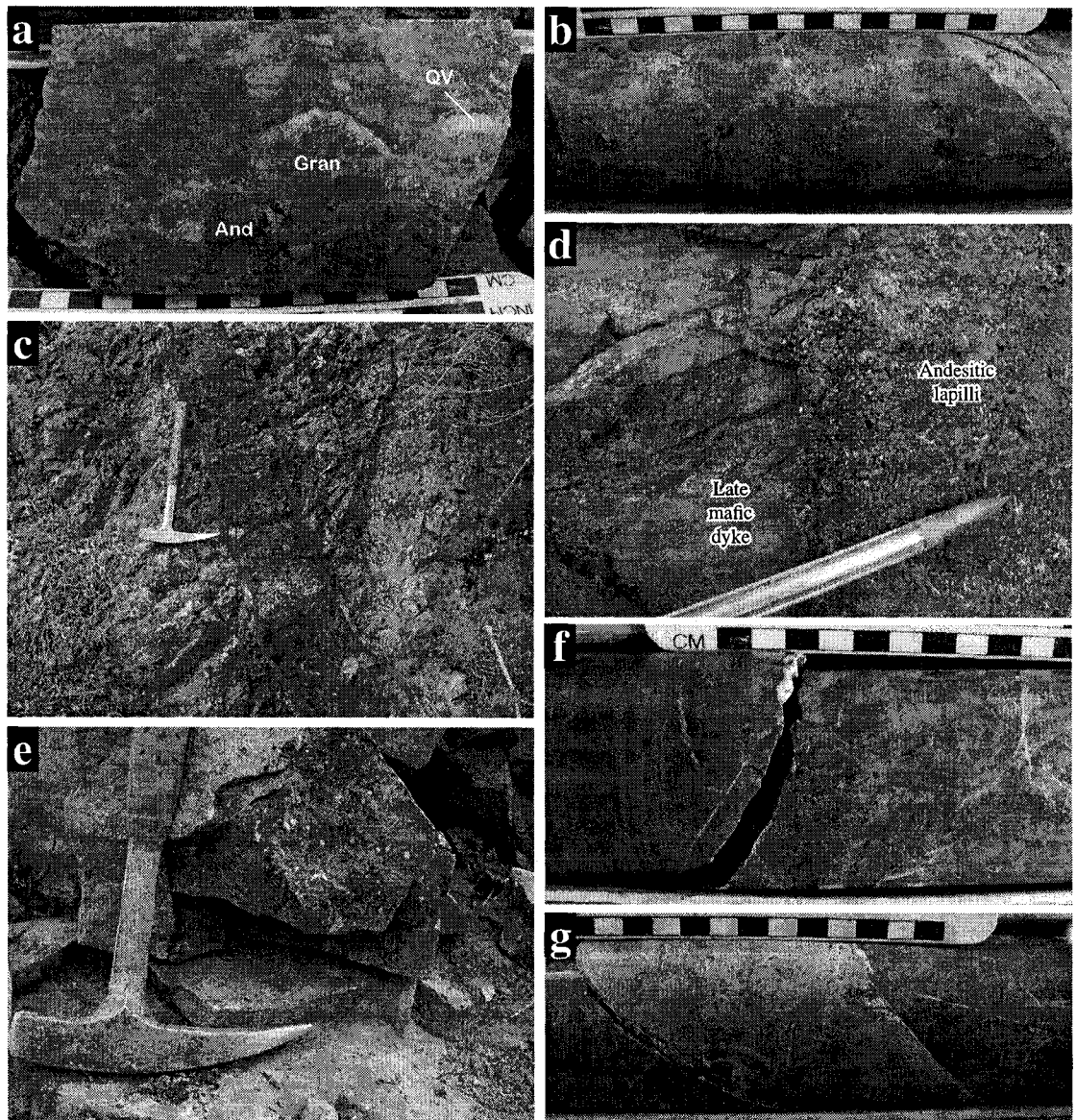


Figure 4.8 - (a) Intrusive breccia sample from the Paramount zone (sample 06CF287-14). The breccia contains clasts of the volcanic country rocks (And), granodiorite (Gran), and barren quartz veins (QV), indicating that some hydrothermal activity occurred prior to the brecciation. Disseminated chalcopyrite and molybdenite are present in the matrix. (b) Intrusive breccia from the Paramount zone (drillhole 06CF277 at 14.40 m depth), with clasts mainly of the host volcanic rocks. (c) Late mafic dyke (outlined in red) cross-cutting earlier volcanic rocks. Photo taken at coordinates 379420E, 6358927N. (d) Contact between late mafic dyke (left) and lapilli andesite (right), both of which have been subjected to hematite alteration (discussed in section 5). Photo taken at coordinates 380747E, 6358723N. (e) Larger (> 30 cm) late mafic dykes locally exhibit vesicles that increase in size (up to ~ 1 cm) towards the dyke margins, and are filled with secondary calcite. Photo taken at coordinates 380376E, 6360083N. (f) Example of the chilled contact of the late mafic dyke with the quartz-feldspar porphyry unit. Drillhole 06CF272 at 163.2 m depth. (g) Late mafic dyke, strongly chilled, following an earlier carbonate breccia vein. Remnants of the old vein are observed at the sides of the dyke. The centre of the dyke carries angular fragments of volcanic host rock and carbonate vein material. The dyke is in turn cross-cut by narrow (<1 mm) carbonate veinlets. Drillhole 06CF277 at 221.90 m.

Pyroxene Classification Diagram

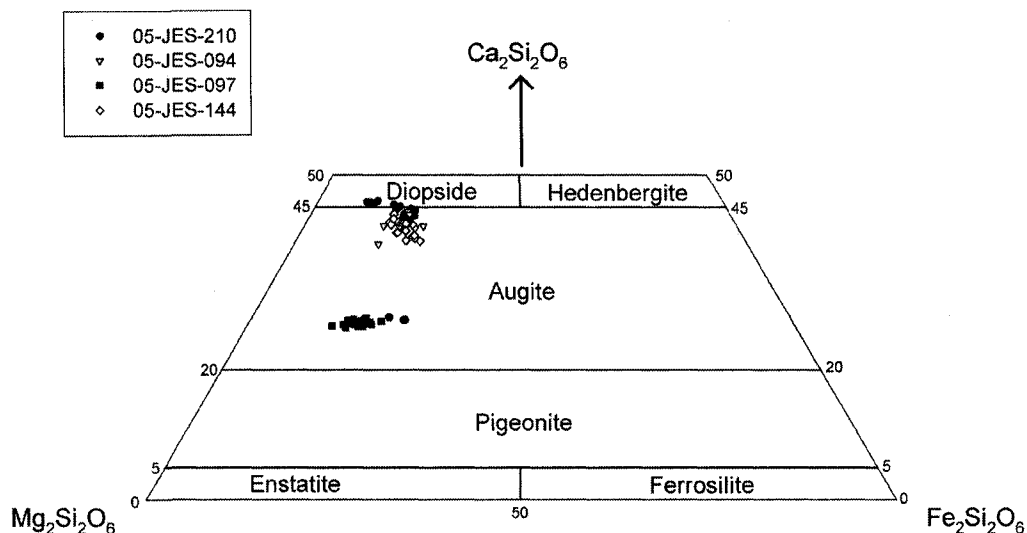


Figure 4.9 - Clinopyroxene compositions for Schaft Creek volcanic rocks. The results show two distinct compositional clusters, with sample 05-JES-210 having mineral grains that fall in both clusters.

grained carbonate. Representative results of the analyses are presented in Table 4.1, and full analyses are presented in Appendix 2.

Analyzed pyroxenes form two clusters on the pyroxene classification diagram of Deer et al. (1992; Fig. 4.9), with one cluster straddling the diopside/augite field boundary, and another cluster of less calcic augite that appears to have a fairly well-developed Mg-Fe trend with a low degree of Ca variability. One sample had pyroxene grains from both compositional clusters, indicating that there may be two generations of pyroxene crystallization. Plagioclase grains were all albitic, with typically less than 7% anorthite. Because mafic rocks are generally low in alkalis such as Na, the primary plagioclase grains associated with crystallization from the melt should be significantly more anorthitic (calcic) in composition. Thus, the observed albitic plagioclase compositions likely indicate that extensive albitization has occurred through hydrothermal alteration, as evidenced by the common presence of hydrothermal chlorite and sericite.

Table 4.1: Representative electron microprobe analyses of pyroxene and plagioclase grains from the Stuhini Group volcanic rocks at Schaft Creek.

Sample Mineral Lithology	05-JES-210A1		05-JES-210C7		05-JES-094A30		05-JES-097E47		05-JES-144B59		05-JES-136A3		05-JES-136G20	
	Diopside Andesite	Andesite	Augite Andesite	Andesite	Augite Andesite	Andesite	Augite Andesite	Andesite	Augite Andesite	Albite Andesite	Andesite	Albite Andesite	Andesite	
<i>Weight percent</i>														
SiO ₂	53.10	50.27	51.70	52.53	51.58	66.67	65.24	66.67	65.24	66.67	65.24	66.67	65.24	65.24
TiO ₂	0.21	0.55	0.40	0.50	0.50									
Al ₂ O ₃	1.73	4.05	2.92	3.99	3.13	20.64	21.37	20.64	21.37	20.64	21.37	20.64	21.37	21.37
FeO	4.85	8.02	9.29	8.78	8.00	0.04	0.01	0.04	0.01	0.04	0.01	0.04	0.01	0.01
MnO	0.12	0.18	0.31	0.55	0.21	0.00	0.02	0.00	0.02	0.00	0.02	0.00	0.02	0.02
MgO	16.74	14.64	14.96	18.17	16.06	0.01	0.02	0.01	0.02	0.01	0.02	0.01	0.02	0.02
CaO	22.72	21.53	20.16	11.90	19.98	0.89	1.89	0.89	1.89	0.89	1.89	0.89	1.89	10.58
Na ₂ O	0.21	0.40	0.38	0.65	0.38	11.09	10.58	11.09	10.58	11.09	10.58	11.09	10.58	10.58
Total	99.67	99.63	100.09	97.07	99.84	99.34	99.15	99.34	99.15	99.34	99.15	99.34	99.15	99.15
<i>Atomic Proportions</i>														
Si	1.95	1.88	1.92	1.96	1.91	2.94	2.89	2.94	2.89	2.94	2.89	2.94	2.89	2.89
Ti	0.01	0.02	0.01	0.01	0.01	0.00	0.00	0.01	0.00	0.00	0.00	0.00	0.00	0.00
Al	0.07	0.18	0.13	0.17	0.14	1.07	1.12	1.07	1.12	1.07	1.12	1.07	1.12	1.12
Al ^{IV}	0.05	0.12	0.08	0.04	0.09	0.06	0.11	0.06	0.11	0.06	0.11	0.06	0.11	0.11
Al ^{VI}	0.03	0.06	0.05	0.13	0.05	1.01	1.01	1.01	1.01	1.01	1.01	1.01	1.01	1.01
Cr	0.00	0.00	0.00	0.00	0.00	0.00	0.00	0.00	0.00	0.00	0.00	0.00	0.00	0.00
Total Fe	0.15	0.25	0.29	0.27	0.25	0.00	0.00	0.25	0.00	0.00	0.00	0.00	0.00	0.00
Mn	0.00	0.01	0.01	0.02	0.01	0.00	0.00	0.01	0.00	0.00	0.00	0.00	0.00	0.00
Mg	0.92	0.81	0.83	1.01	0.89	0.00	0.00	0.89	0.00	0.00	0.00	0.00	0.00	0.00
Ca	0.89	0.86	0.80	0.47	0.79	0.04	0.09	0.04	0.09	0.04	0.09	0.04	0.09	0.09
Na	0.01	0.03	0.03	0.05	0.03	0.95	0.91	0.95	0.91	0.95	0.91	0.95	0.91	0.91
Total cations	4	4	4	4	4	8	8	8	8	8	8	8	8	8
Oxygens	6	6	6	6	6	8	8	8	8	8	8	8	8	8

4.3 - Whole-Rock Geochemistry

Fourteen least-altered and four altered samples of volcanic and intrusive rocks representing each of the units observed in the Schaft Creek deposit area were collected and analyzed for their whole-rock geochemical compositions, along with three samples from the intrusive complex to the west of the deposit. The altered samples were not selected to characterize the geochemistry of strongly altered rocks in the deposit area, but rather were selected to form a complete sample set because unaltered samples of the given lithologies did not exist or were limited. The more altered samples include two mafic volcanic rocks, a sample of the diorite intrusive rock, and a weakly altered gabbroic intrusive rock. Alteration of these samples is characterized by weak chloritization and sericitization of the groundmass of the volcanic rocks, and plagioclase and pyroxene grains of all three rock types. Weak carbonate alteration affects nearly all collected samples, but the four altered samples have a moderate to strong carbonate overprint. Major and trace element geochemical data are presented in Appendices 3.1 and 3.2, respectively.

4.3.1 - Major element geochemistry

All analyzed samples are plotted on a total-alkali-silica diagram in Figure 4.10; both intrusive and extrusive rocks were plotted for comparative purposes, although only the volcanic rocks can be classified using this diagram. The least-altered mafic volcanic rocks plot within the basalt, basaltic andesite, and andesite fields, whereas the altered mafic volcanic samples are enriched in K and slightly depleted in Na. The gabbro sample plots close to the mafic volcanic rocks, but is slightly more alkali-rich, likely due at least in part to the weak alteration this sample has undergone. The diorite sample is enriched in alkalis due to its strong alteration, and would otherwise likely plot among the mafic volcanic rocks in the basaltic andesite field. The intermediate intrusive rocks cluster together near the dacite–trachyte field boundary, whereas the felsic volcanic sample from the top of Mount

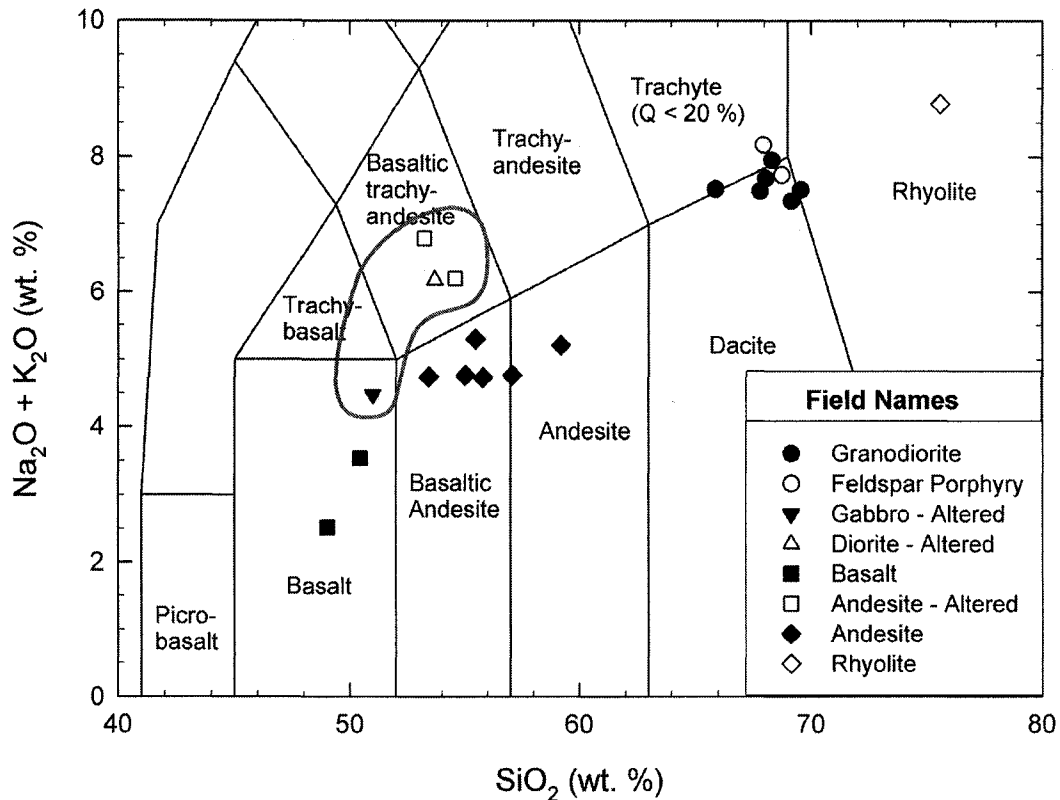


Figure 4.10 - Total alkali-silica plot for samples from Schaft Creek. Altered samples are enriched in K and are outlined in red.

LaCasse plots in the rhyolite field.

On the $\text{MgO}-\text{FeO}_{\text{Total}}-(\text{Na}_2\text{O} + \text{K}_2\text{O})$ diagram of Irvine and Baragar (1971) (Fig. 4.11), the samples are observed to loosely follow a typical calc-alkaline evolutionary trend. However, interpretation of any trend by the mafic volcanic rocks and intrusive rocks alone is difficult because of the small compositional range exhibited by the samples. The felsic intrusive rocks and rhyolite are plotted for illustrative purposes, and should not be considered to verify any trends.

Compositional trends versus silica are presented as Harker diagrams in Figure 4.12. Alumina and MnO appear to show no clear trend with SiO_2 , but Na_2O and K_2O show weak positive trends with increasing silica content. Other oxides ($\text{Fe}_2\text{O}_{3(\text{Total})}$, MgO , CaO , TiO_2 , and P_2O_5) show strong negative correlations. These trends can be explained by the early precipitation of olivine, diopside-augite, and plagioclase as phenocryst phases in the

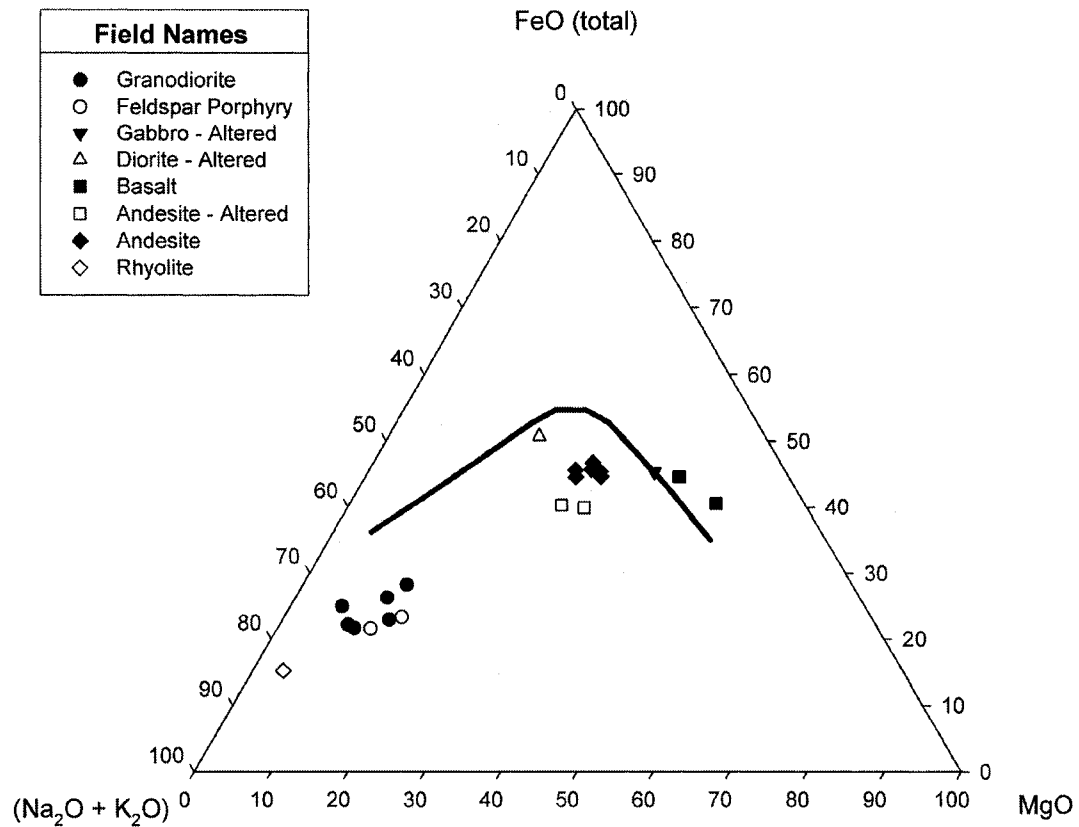


Figure 4.11 - Alkali - iron oxide - magnesium oxide (AFM) diagram after Irvine and Barager (1971). The black line separates the tholeiitic and calc-alkaline trends.

basaltic and andesitic volcanic rocks, and the retention of alkalis in the melt until potassium feldspar began to precipitate out in the intermediate intrusions. The rhyolite sample appears to differ from the patterns exhibited by the other samples in the suite, being depleted in Al_2O_3 and Na_2O , but enriched in Fe_2O_3 and weakly enriched in K_2O .

4.3.2 - Trace element geochemistry

Primitive mantle-normalized (Sun and McDonough, 1989) trace element plots are presented in Figure 4.13. All samples exhibit negative Ta, Nb, and Ti anomalies typical of arc magmas (Brenan et al., 1994; Foley et al., 2000). Rhyolites show strong depletion in P, Eu, and Ti, resulting from fractional crystallization of apatite, plagioclase, and mafic minerals and Fe-Ti oxides, respectively. Chondrite-normalized (Sun and McDonough,

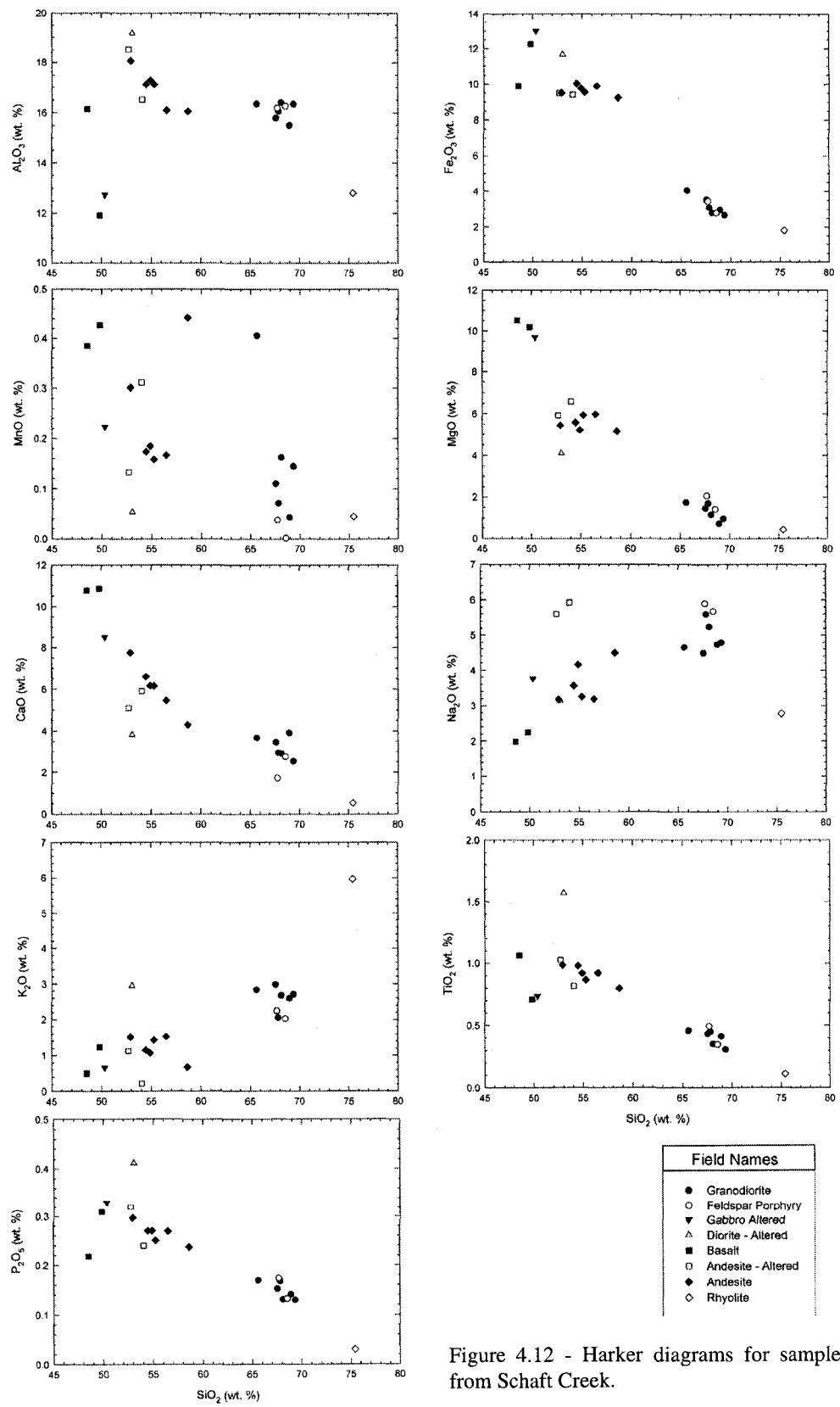


Figure 4.12 - Harker diagrams for samples from Schaft Creek.

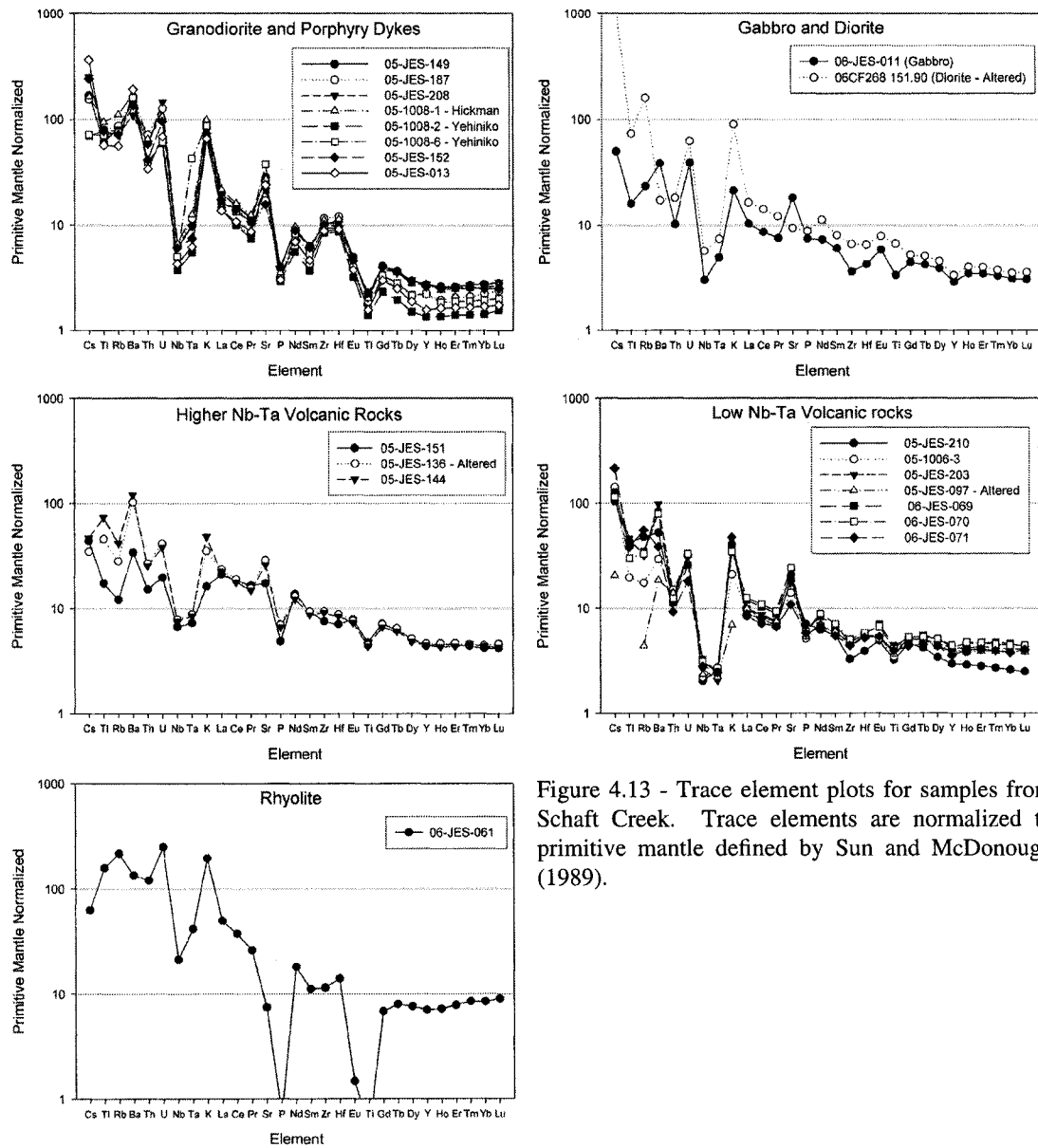


Figure 4.13 - Trace element plots for samples from Schaft Creek. Trace elements are normalized to primitive mantle defined by Sun and McDonough (1989).

1989) rare earth element plots are presented in Figure 4.14. The granodiorite samples show well-developed listric REE patterns indicative of hornblende fractionation (Frey et al., 1978; Hanson, 1980), whereas the more mafic rocks tend to have more flat-lying REE patterns. Both gabbro and diorite samples exhibit weak positive Eu anomalies, as do a number of the andesitic samples. This is likely the result of the magma being hydrous and oxidized, which are properties that would suppress plagioclase fractionation while promoting hornblende and clinopyroxene fractionation (Frey et al., 1978; Müntener et al.,

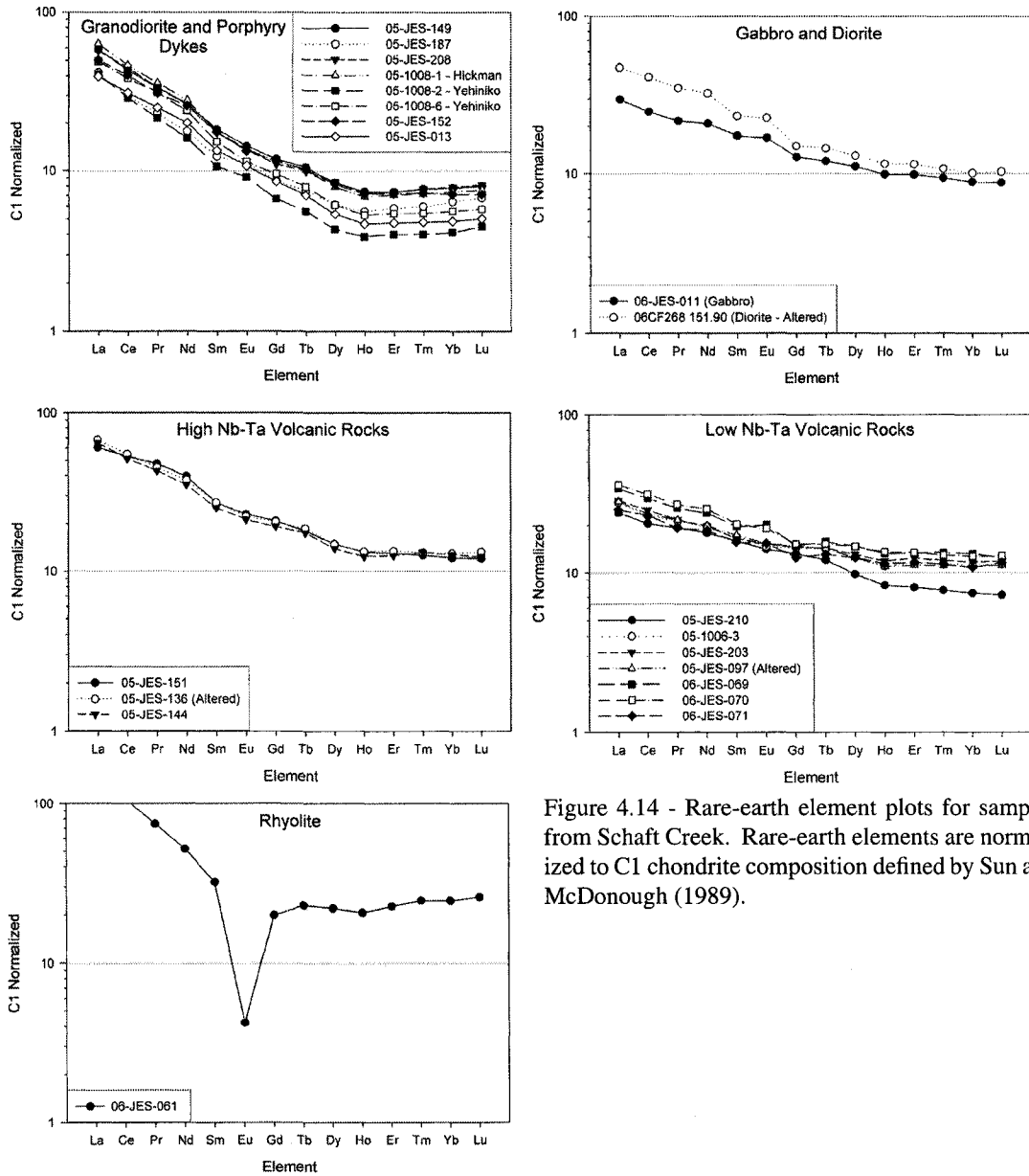


Figure 4.14 - Rare-earth element plots for samples from Shaft Creek. Rare-earth elements are normalized to C1 chondrite composition defined by Sun and McDonough (1989).

2001). In contrast to the rest of the samples, the rhyolite sample exhibits a strong negative Eu anomaly, consistent with strong plagioclase fractionation.

Mafic volcanic rocks can be separated into two distinct groups which are most easily recognized by a significant difference in Nb-Ta concentrations (Fig. 4.13). The difference is also apparent in the REE plots (Fig. 4.14), where the low Nb-Ta volcanic rocks exhibit more flat-lying curves relative to the high Nb-Ta volcanic rocks. The reasons for these differences remain unclear because no petrologic differences or differences in

spatial distribution were observed. Therefore, without the aid of geochemistry there is no way in which one could distinguish the two groups from each other in the field.

4.4 - Geochronology

The intrusive rocks from within the Schaft Creek deposit area and to the west of the Schaft Creek valley have been dated in a number of previous studies. The results from these studies are presented in Table 2.1, and new results from this work are discussed below.

4.4.1 – Previous results

The earliest dating was completed on mineralized biotite hornfels (the metamorphic equivalent of the andesitic unit) from drillhole 52 at 113 m depth by Panteleyev and Dudas (1972), and yielded a whole-rock K-Ar date of 182 ± 5 Ma. This date provided the first estimate of the timing of mineralization in the deposit.

A subsequent study by Holbek (1988) dated two samples from the intrusive bodies to the West of the deposit area using Rb-Sr and K-Ar dating of biotite, hornblende, and whole-rock samples. One sample was collected from within the Hickman batholith as mapped by Souther (1972), and the other from the Yehiniko batholith to the north. The Rb-Sr and K-Ar results from the Yehiniko sample indicated an approximate date of 173 ± 10 Ma (MSWD = 0.13; n = 3; 2 biotite, 1 whole-rock; inverse-variance weighted mean calculated using Isoplot by Ludwig, 2003). The geochronological data for the Hickman sample indicate a date slightly outside error of the Yehiniko sample with an approximate date of 216.9 ± 6.9 Ma (MSWD = 0.36; n = 4; 2 biotite, 1 hornblende, 1 whole-rock; inverse-variance weighted mean calculated using Isoplot by Ludwig, 2003). These results led Holbek (1988) to conclude that the Yehiniko and Hickman batholiths represented distinct intrusive episodes. However, it is important to consider a number

Table 4.2: Summary of U-Pb zircon results for Schaft Creek from Logan et al. (2000).

Fraction	$^{207}\text{Pb}/^{235}\text{U}$	$\pm 1\sigma \%$	$^{206}\text{Pb}/^{238}\text{U}$	$\pm 1\sigma \%$	Rho	$^{207}\text{Pb}/^{206}\text{Pb}$	$\pm 1\sigma \%$
a	0.2426	0.30	0.03474	0.14	0.500	0.05065	0.26
c	0.2394	0.75	0.03435	0.11	0.513	0.05056	0.70
d	0.2376	0.73	0.03402	0.14	0.441	0.05065	0.68
e	0.2433	0.16	0.03422	0.07	0.607	0.05155	0.13
g	0.2446	0.10	0.03488	0.08	0.869	0.05085	0.05
h	0.2426	0.18	0.03448	0.13	0.746	0.05103	0.12
i	0.2356	0.23	0.03386	0.11	0.840	0.05047	0.15
j	0.2131	0.27	0.03080	0.08	0.389	0.05019	0.25
k	0.2964	0.44	0.03699	0.17	0.621	0.05812	0.36

of factors in the interpretation of these data. First, the low closure temperature of biotite for argon diffusion ($\sim 300 \pm 50$ °C) makes the chronometer highly susceptible to resetting through metamorphism or hydrothermal processes (Hanes, 1991, and references therein). Hornblende has a higher closure temperature of $\sim 500 \pm 50$ °C (Hanes, 1991, and references therein), but in the Yehiniko sample hornblende was not analyzed. Second, the Rb-Sr system is highly susceptible to chronometer re-setting during alteration due to the mobile nature of both Rb and Sr (Hanes, 1991). These effects mean that neither the K-Ar nor Rb-Sr systems provide reliable age estimates in rocks that have experienced any degree of metamorphism or hydrothermal alteration.

A more recent study by Logan et al. (2000) dated a number of volcanic assemblages and intrusive rocks in the region by the more robust U-Pb zircon method. Important to this study are the data obtained for a sample of mineralized quartz-feldspar porphyry dyke from within the deposit area (collected from drillhole T-169 at 154–170 m depth). A summary of these data is presented in Table 4.2 and Figure 4.15a, with the exception of zircon fraction K which falls significantly to the right of the concordia curve outside of the plot area of Figure 4.15a, and likely exhibits significant inheritance from older zircon grains. Logan et al. (2000) selected fractions C, H, and I to calculate a $^{206}\text{Pb}/^{238}\text{U}$ age of 216.6 ± 2 Ma. Citing possible inheritance problems, concordant fractions D and A were not used in this calculation. Logan et al. (2000) preferred to use an average of the $^{206}\text{Pb}/^{238}\text{U}$ ages instead of the $^{207}\text{Pb}/^{206}\text{Pb}$ age because they considered the former to be a more reliable estimate of the

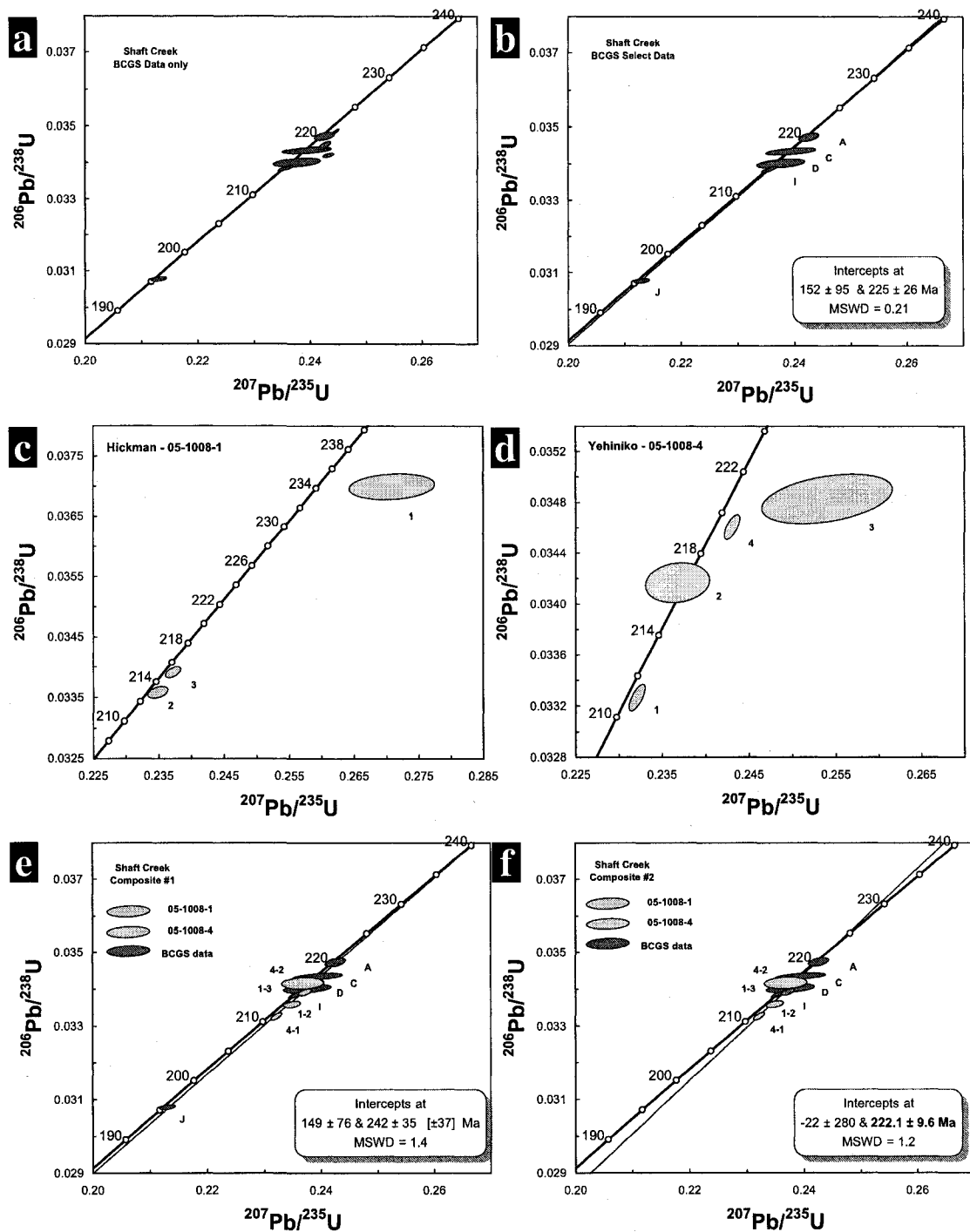


Figure 4.15 - U-Pb zircon TIMS data from the Shaft Creek deposit. All error ellipses are at two sigma. (a) Dataset from Logan et al. (2000). (b) Model 1 solution for selected fractions from Logan et al. (2000). (c) Hickman sample mineral fractions. (d) Yehiniko sample mineral fractions. (e) Composite model solution 1 from current data and selected fractions from Logan et al. (2000). (f) Composite model solution 2 from current data and selected fractions from Logan et al. (2000).

true age in the presence of likely lead-loss and inheritance.

These results are reinterpreted here by calculating the intercepts with concordia of a discordia line formed by zircon fractions with evidence of lead-loss, but excluding those with evidence of inheritance. By these criteria, all the concordant mineral fractions are included (fractions A, C, D, I, and J), and those that fall to the right of concordia are rejected (fractions E, G, H, and K). The best-fit line passing through the selected fractions has an upper intercept age of 225 ± 26 Ma and a lower intercept of 152 ± 95 Ma, with an MSWD of 0.21 (Fig. 4.15b).

4.4.2 – *Current data*

Geochronological analyses were completed in the current study in order to constrain which of the two previously distinguished intrusive bodies, the Hickman and Yehiniko batholiths, was responsible for the mineralization observed at Schaft Creek. Samples were collected from each of these major intrusive bodies, as mapped by Logan et al. (2000), for U-Pb zircon thermal ionization mass spectrometry (TIMS) analysis. Sample 05-1008-4 was collected from the northeast corner of the southern portion of the Hickman batholith, and sample 05-1008-1 was collected from the southeast corner of the Yehiniko batholith (Fig. 2.2). In addition, two molybdenite samples were collected from mineralized veins within the deposit for Re-Os dating. The intrusive host rock to one of these molybdenite-bearing vein samples was also dated by in-situ U-Pb zircon laser ablation inductively coupled plasma mass spectrometry (LA-ICP-MS) analysis.

4.4.2.1 — U-Pb TIMS data

Analyzed mineral fractions and results are presented in Table 4.3, and the data are illustrated in Figures 4.15c and 4.15d. Only one fraction from sample 05-1008-4 (representing the Yehiniko batholith) overlapped the concordia curve with a large 2σ error ellipse, and none of the mineral fractions from sample 05-1008-1 (representing the

Table 4.3: Schaft Creek U-Pb zircon results

Description	Weight (µg)	U (ppm)	Th (ppm)	Pb (ppm)	Th/U	TCPb (pg)	$^{206}\text{Pb}/^{204}\text{Pb}$	$^{206}\text{Pb}/^{238}\text{U}$	$^{207}\text{Pb}/^{235}\text{U}$	$^{207}\text{Pb}/^{206}\text{Pb}$	Model Ages (Ma)		% Disc	
											$^{206}\text{Pb}/^{238}\text{U}$	$^{207}\text{Pb}/^{235}\text{U}$		
051008-1														
1 col best largest frags 5NM (10)	21.9	120	41	6	0.345	32	208	0.03700±9	0.2708±27	0.05308±52	234.2±0.5	243.3±2.2	332.2±22.2	30.1
2 col equant euhed 6NM (5)	32.4	242	84	9	0.346	16	1049	0.03359±4	0.2349±6	0.05071±12	213.0±0.2	214.2±0.5	227.7±5.4	6.6
3 col 3:1 euhed prisms (11)	41.9	247	76	9	0.307	10	2117	0.03392±4	0.2372±5	0.05072±8	215.0±0.2	216.1±0.4	228.3±3.8	5.9
051008-4														
1 col best prisms MIH (27)	39.2	209	76	7	0.366	5	3284	0.03327±4	0.2322±4	0.05061±6	211.0±0.3	212.0±0.3	223.20±2.6	5.6
2 It tan larger 2:1 euhed prisms MIH (5)	11.8	204	78	9	0.383	42	271	0.03417±6	0.2368±15	0.05027±32	216.6±0.4	215.8±1.2	207.3±14.7	-4.5
3 best col euhed 3:1 prisms MIH (12)	17.9	195	66	8	0.341	21	388	0.03483±8	0.2540±31	0.05289±61	220.7±0.5	229.8±2.5	324.3±25.9	32.5
4 best col multi-fac prisms MIH (14)	49.9	232	78	8	0.337	11	2313	0.03461±4	0.2431±4	0.05095±6	219.3±0.2	220.9±0.3	238.4±2.6	8.1

Reported errors are 1 sigma. Abbreviations: col, colourless; It tan, light tan; euhed, euhedral; multi-fac, multi-faceted; frags, fragments; NM, non-magnetic at indicated angle of tilt on Frantz Isodynamic Separator. The number in parentheses corresponds to the number of individual grains.

Table 4.4: Schaft Creek in-situ LA-ICP-MS U-Pb zircon results. Sample 06CF287.

Grain	^{206}Pb (cps)	$^{206}\text{Pb}/^{204}\text{Pb}$	$^{207}\text{Pb}/^{206}\text{Pb}$	$^{207}\text{Pb}/^{206}\text{Pb}$	$\pm 2\sigma$	$^{207}\text{Pb}/^{235}\text{U}$	$\pm 2\sigma$	$^{206}\text{Pb}/^{238}\text{U}$	$\pm 2\sigma$	rho	Age (Ma)	$\pm 2\sigma$	$^{206}\text{Pb}/^{238}\text{U}$	
													Age (Ma)	$\pm 2\sigma$
5A	19453	9726	0.05136	0.00099	0.00099	0.2633	0.0102	0.0373	0.0013	0.87	257	±44	236	±8
4A	31635	1977	0.06613	0.00431	0.00431	0.3196	0.0237	0.0345	0.0013	0.47	810	±136	219	±8
4B	30726	infinite	0.05551	0.00086	0.00086	0.2576	0.0089	0.0339	0.0011	0.90	433	±34	215	±7
1A	39465	infinite	0.05254	0.00064	0.00064	0.2572	0.0108	0.0355	0.0015	0.96	309	±28	225	±9
2A	12236	infinite	0.05221	0.00072	0.00072	0.2672	0.0134	0.0377	0.0019	0.96	294	±32	239	±12
3A	12776	infinite	0.05020	0.00119	0.00119	0.2462	0.0113	0.0359	0.0014	0.86	204	±55	227	±9

Hickman batholith) were concordant. All fractions from both samples plot above 210 Ma, although six of the seven fractions lie off concordia.

Individually, the sample ages cannot be uniquely resolved due to a combination of inheritance and lead-loss problems, as noted previously in samples from these intrusions dated by Logan et al. (2000). However, if the data from the most concordant mineral fractions are combined, an approximate composite age for the two batholiths can be obtained. To this end, fractions 4 and 3 from sample 05-1008-4 (Yehiniko batholith) and fraction 1 from sample 05-1008-1 (Hickman batholith) were rejected because they lie significantly off the concordia curve. Combining the remaining fractions with those selected from Logan et al. (2000), a more consistent pattern emerges.

Two models were considered. The first model includes the selected fractions from the previously discussed Logan et al. (2000) data, as well as those from the two new samples. All fractions fall on or close to concordia along a lead-loss path with intercepts at 149 ± 76 Ma and 242 ± 35 Ma (MSWD = 1.4; Fig. 4.15e). However, by rejecting the outlying fraction J of Logan et al. (2000), which has experienced extensive Pb-loss, the error is decreased significantly, and the resulting discordia line has intercepts of -22 ± 280 Ma (i.e., a recent lead-loss event related to uplift and weathering), and 222.1 ± 9.6 Ma (MSWD = 1.2; Fig. 4.15f), which is interpreted to approximate the age of emplacement of the intrusions. It is important to note that this analysis finds no difference within error between the ages of the Yehiniko and Hickman batholiths, which may therefore be more closely related in age and origin than previously assumed.

4.4.2.2 — U-Pb LA-ICP-MS data

The U-Pb zircon LA-ICP-MS analysis of sample 06CF287 – 157.5 is preliminary, and to date only five zircons were tested (Table 4.4). These were analyzed in situ from a thin section of the sample. An approximate age was calculated from concordant analyses 5A and 3A, yielding a $^{207}\text{Pb}/^{206}\text{Pb}$ age of 231.6 ± 5.6 Ma (MSWD = 0.40; Fig. 4.16) which

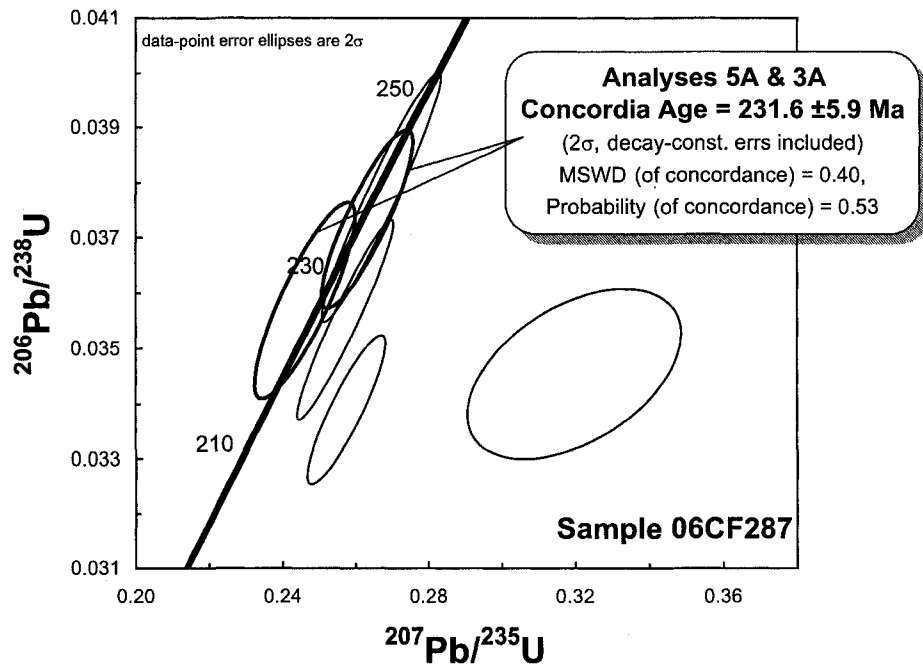


Figure 4.16 - U-Pb zircon LA-ICP-MS data from sample 06CF287.

overlaps within error the 222.1 ± 9.6 Ma age estimated for the Hickman and Yehiniko batholiths.

4.4.2.3 — Re-Os molybdenite data

Molybdenite samples were collected for Re-Os dating from quartz-rich chalcopyrite-molybdenite-bearing veins (Fig. 4.17a and b, Table 4.5). Sample 05-JES-078 was collected from drillhole H-084 at 299' depth, within the Main zone of the deposit. Sample 06CF287-157 was collected from drillhole 06CF287 at 157.5 m depth, within the Paramount zone.

Model ages are calculated from the simplified isotope equation: $t = \ln(^{187}\text{Os}/^{187}\text{Re} + 1)/\lambda$, where λ is the ^{187}Re decay constant ($1.666 \pm 0.005 \times 10^{-11} \text{ a}^{-1}$; Smoliar et al., 1996; Selby et al., 2007), which assumes that molybdenite crystallizes with only Re and no Os. The model ages calculated for the two samples are 221.2 ± 1.3 Ma and 222.4 ± 1.0 Ma, respectively. The close agreement of these two results provides strong evidence that these dates are valid estimates for the timing of mineralization, an average of which gives an age of 222.0 ± 0.8 Ma (MSWD = 2.1; inverse-variance weighted mean calculated using Isoplot

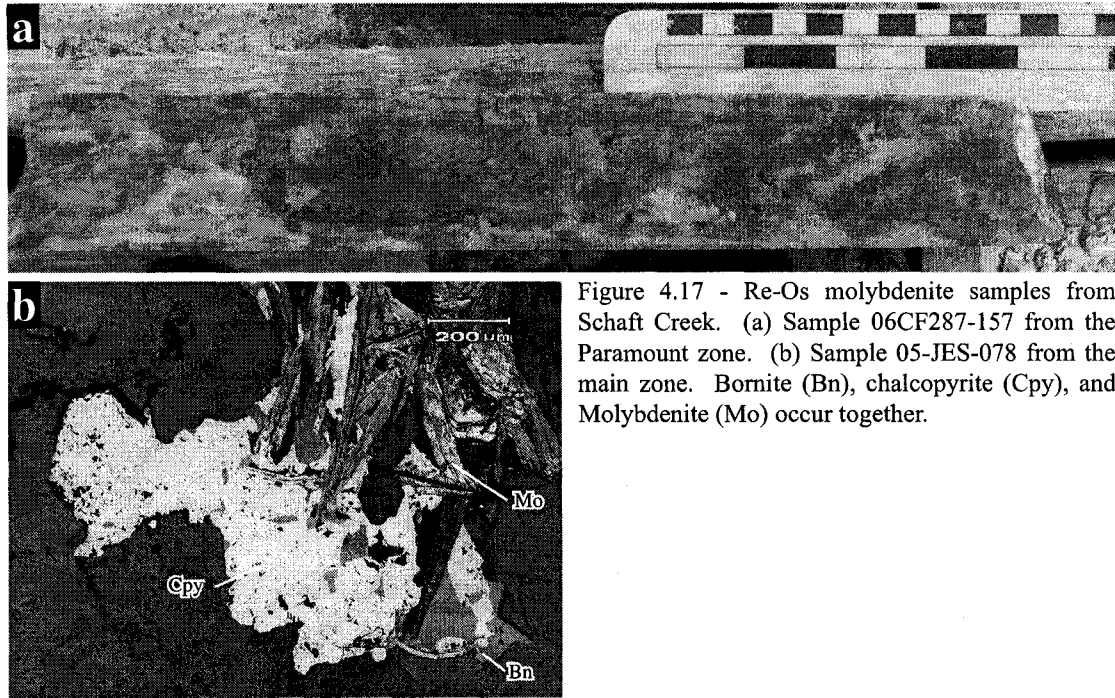


Figure 4.17 - Re-Os molybdenite samples from Schaft Creek. (a) Sample 06CF287-157 from the Paramount zone. (b) Sample 05-JES-078 from the main zone. Bornite (Bn), chalcopyrite (Cpy), and Molybdenite (Mo) occur together.

Table 4.5: Schaft Creek Re-Os molybdenite results.

Sample	Weight (g)	Re ppm	$\pm 2\sigma$	^{187}Re ppm	$\pm 2\sigma$	^{187}Os ppb	$\pm 2\sigma$	$^{187}\text{Os}/^{187}\text{Re}$ molar	$\pm 2\sigma$	TC Os (pg)	Model age (Ma)	$\pm 2\sigma$ absolute λ uncertainty included
05-JES-078	0.02532	745.0	3.8	468.3	2.4	1729	1	0.003692	0.000019	1.6	221.2	1.3
06CF287	0.05127	574.5	1.9	361.4	1.2	1341	1	0.003712	0.000007	4.8	222.4	1.0

Model Age is corrected for any common Os in excess of blank Os (i.e., >0.5 pg) using $^{187}/^{188}\text{Os}$ of 0.3
 TC Os pg is total common osmium in picograms

by Ludwig, 2003).

4.4.2.4 — Interpretation

Upon re-interpretation, the data from Logan et al. (2000) are shown to give an approximate $^{207}\text{Pb}/^{206}\text{Pb}$ age of crystallization of the granodioritic dykes of 225 ± 26 Ma, somewhat older than the $^{206}\text{Pb}/^{238}\text{U}$ age of 216.6 ± 2 Ma reported by Logan et al. (2000). When these data are combined with the TIMS U-Pb zircon data collected here, a composite $^{207}\text{Pb}/^{206}\text{Pb}$ age of 222.1 ± 9.6 Ma is obtained for intrusive rocks of the Hickman and Yehiniko batholiths. The LA-ICP-MS U-Pb zircon data from the mineralized sample yielded a date of 231.6 ± 5.6 Ma. The overlap of these ages (within error) indicates that the Yehiniko and Hickman batholiths and the mineralized dykes may have formed within broadly the same time interval (i.e., between approximately 235 and 220 Ma). The more

precise Re-Os molybdenite ages of 221.2 ± 1.3 Ma and 222.4 ± 1.0 Ma suggest that the two intrusions were emplaced prior to or close to 223 Ma. The mineralization was likely genetically related to this intrusive event, but these results do not enable distinction between the previously distinguished Yehiniko and Hickman batholiths as the causative pluton.

5 – GEOLOGY OF THE SCHAFT CREEK PORPHYRY SYSTEM

The Paramount, Main, and West Breccia zones that collectively make up the Schaft Creek porphyry system exhibit a multitude of alteration and mineralization styles which are distinct in each zone. Although each of these zones has unique features that define them, there is significant overlap of geology, alteration, and mineralization styles between these zones.

5.1 - Alteration

The deposit area has been subjected to significant hydrothermal alteration which has created a number of different alteration facies which are summarized below. A map of the alteration at surface is presented in Figure 5.1, and a plan map of alteration at 850 m a.s.l. is presented in Figure 5.2. From these maps, it is apparent that potassic alteration occurs in a roughly linear trend in the Paramount zone, and in an irregular pattern in the core of the Main zone. In the latter zone, it is of particular note that the potassic alteration is broadly encompassed by sericite-chlorite alteration (see below), which in turn gives way to propylitic alteration. This alteration pattern is similar to that described by Lowell and Guilbert (1970) for porphyry Cu deposits. The zoning is less pronounced in the Paramount zone where alteration has a roughly linear pattern without the typical concentric potassic-propylitic zoning. Late carbonate and hematite alteration overprint all earlier alteration phases, and are also described below.

5.1.1 - Potassic alteration

Potassic alteration at the Schaft Creek deposit is defined by the presence of secondary pink potassium feldspar, locally with rare secondary biotite. Alteration is variable in intensity, and where strong imparts a weak pink colouration to the host rocks (Fig. 5.3a),

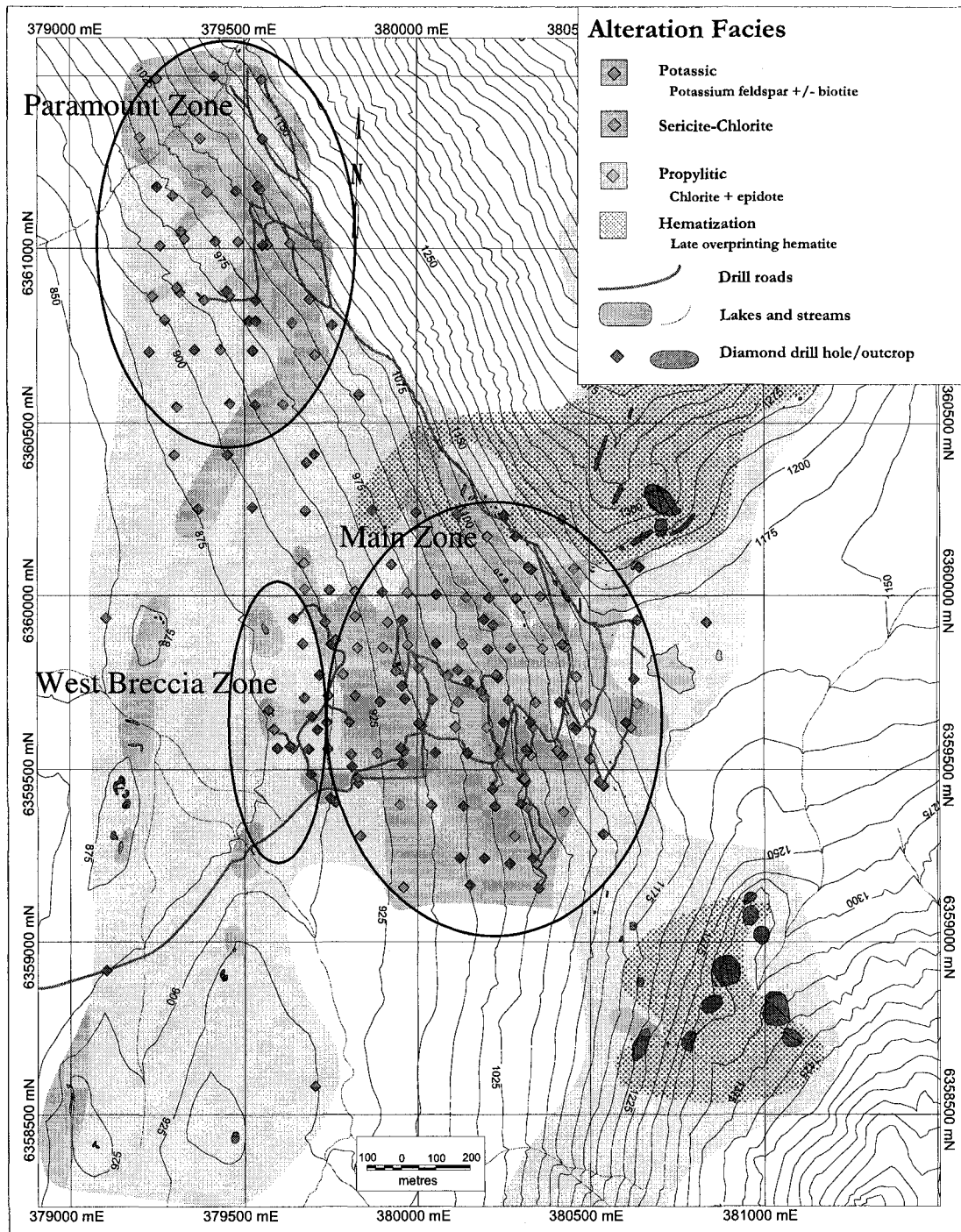


Figure 5.1 - Alteration of the Schaft Creek deposit. Drillhole data are projected to surface. The dominant alteration facies over the upper 50 m of the drillcore is presented along with surface outcrop data. Coordinates are in UTM Zone 9V (NAD 83 datum).

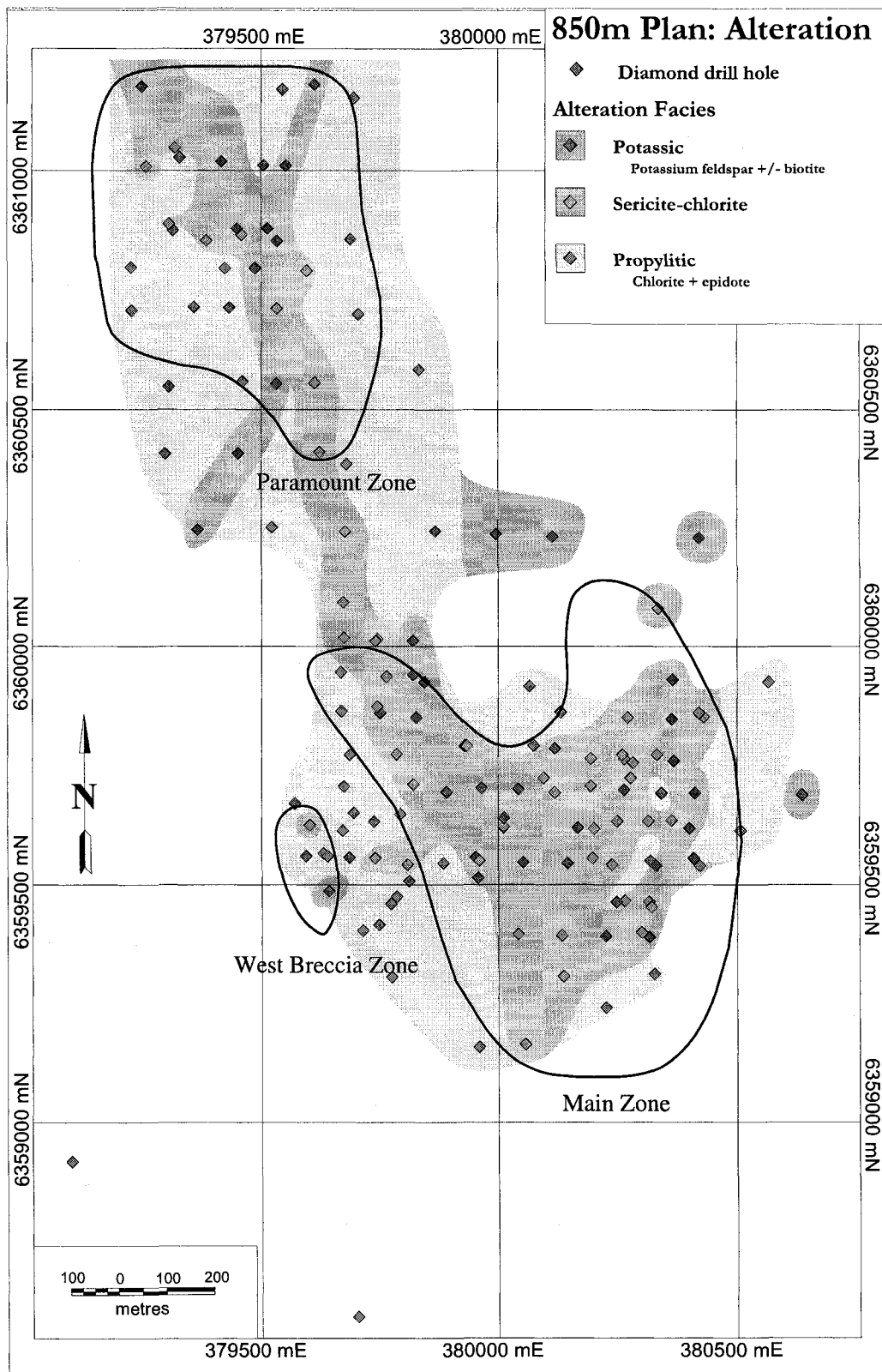


Figure 5.2 - 850 m elevation plan - Alteration. Drillhole pierce points are calculated from surface elevation, drillhole azimuth, and dip. Alteration is from the three metre sample interval that pierces the plane.

with complete replacement of groundmass and phenocrysts by K-feldspar. In a number of samples, well-formed secondary potassium feldspar rims are observed around earlier plagioclase grains (Fig. 5.3c and d).

Potassic alteration tends to be largely related to discrete veins, occurring as alteration halos surrounding veins of various affinities (Fig. 5.3b). In general, the width and intensity of the potassic alteration halo is directly proportional to the thickness of the central vein. Vein petrology associated with these potassic halos tends to be quartz-dominated, sometimes with associated mineralization that may also extend outside the vein into the surrounding altered wall rocks. The potassic zone is the most enriched in bornite relative to the rest of the deposit. Significant molybdenite and chalcopyrite are also present, but pyrite is rare to absent.

Potassic alteration is developed most strongly in the granodioritic dykes that cross cut the volcanic pile, especially where these dykes are widest and most numerous. Locally potassic alteration is pervasive, most notably in the core of the Main zone and in parts of the Paramount zone.

In the Main zone, potassic alteration displays an irregular multi-branching pattern when projected to surface. At depth, the potassic alteration is significantly more continuous (plan map, Fig. 5.2). Rocks of the Paramount zone to the north and continuing to the south on the west side of the deposit area are also potassically altered, roughly coincident with the granodioritic dykes.

5.1.2 – Sericite-chlorite alteration

A true phyllic zone as described by Lowell and Guilbert (1970) does not appear to exist at the Schaft Creek deposit. Lowell and Guilbert (1970) described the phyllic alteration as comprising a combination of sericite with quartz and pyrite. However, a transitional alteration zone with mineralization exists between the potassic and propylitic alteration zones at the Schaft Creek deposit. The alteration mineralogy of this zone is an

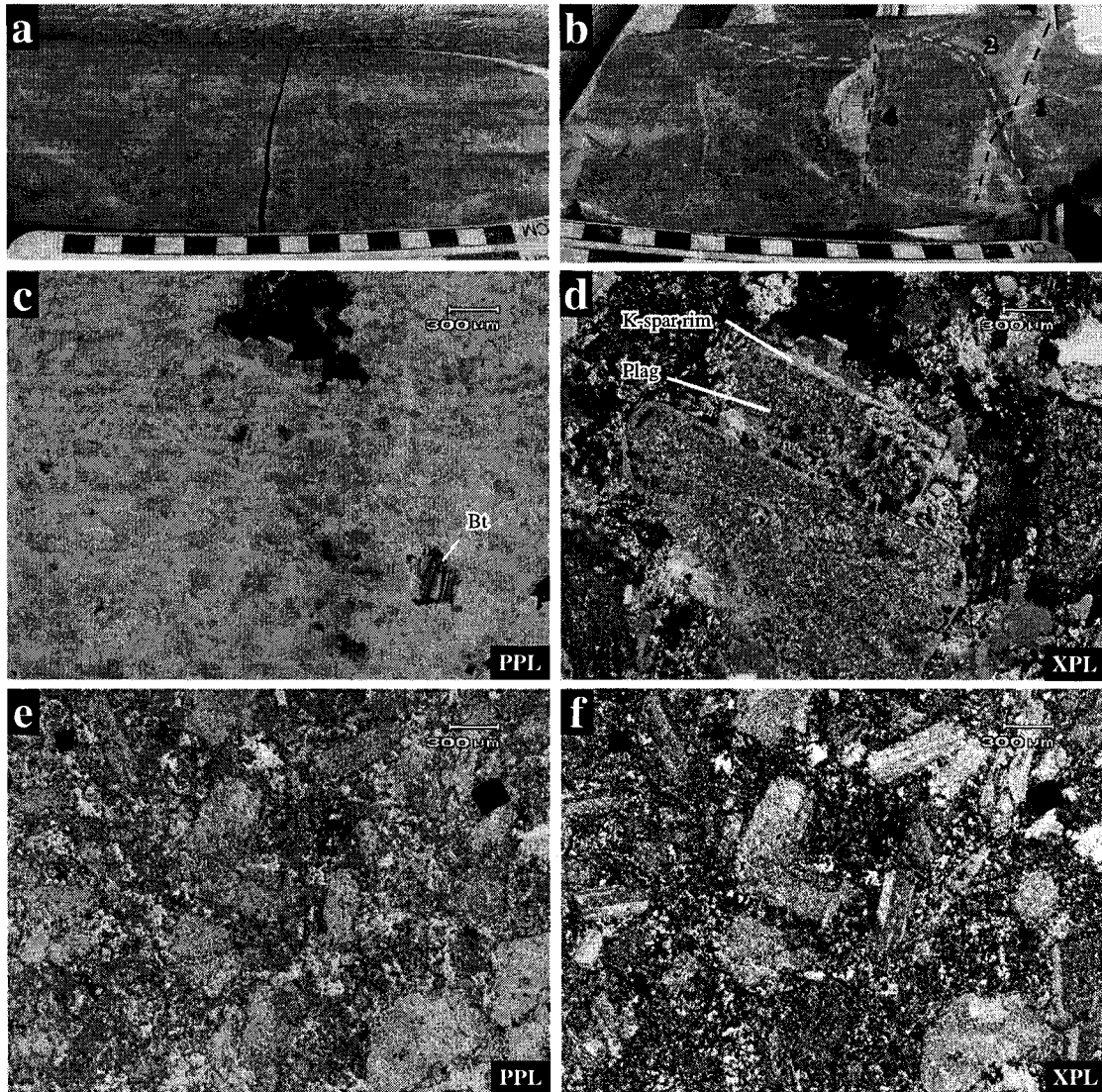


Figure 5.3 - (a) Pervasively potassically altered feldspar porphyry. Potassic alteration is weak to moderate and this interval hosts ~0.5 vol. % disseminated chalcopyrite grains. Drillhole 06CF277 at 167.5 m. (b) Plagioclase-pyroxene-phyric basaltic andesite. Sericite-chlorite alteration imparts dull green-grey colouration to the rock. Some of the cross-cutting quartz veins exhibit narrow potassic alteration halos. At least four distinct veining events are represented in this rock, and two deformational events. Events are numbered in the diagram. First vein set 1 cut the volcanic rock, then the molybdenite-mineralized vein cut this vein at an oblique angle (2). Vein 3 represents a plane of movement that offset vein 2 and subsequent in-fill veining. Vein 3 was then offset by movement along the plane of vein 4 which was also in-filled by quartz. Drillhole 06CF277 at 66.7 m. (c & d) Photomicrographs of potassic alteration of plagioclase-phyric basaltic andesite. Potassium feldspar (K-spar) rims the highly sericitized plagioclase (Plag) grains. Secondary biotite (Bt) has been largely replaced by secondary chlorite after the high-temperature potassic alteration phase. The replacement of biotite by chlorite in this sample, along with the replacement of plagioclase by sericite, indicate that the earlier potassic alteration was overprinted by later sericite-chlorite alteration. Sample 05-JES-091. (e & f) Sericite-chlorite-altered plagioclase-phyric andesite. Alteration in this sample is an assemblage of sericite, chlorite, quartz, and rare pyrite. Sample 05-JES-104. Abbreviations: Bt = biotite; Plag = plagioclase; K-spar = potassium feldspar.

assemblage of chlorite and sericite of variable intensity. Pyrite is locally observed, but is not present in the abundance typically associated with phyllic alteration zones. In contrast, chalcopyrite, bornite, and molybdenite are common. Quartz as an alteration mineral is also notably sparse. Typical alteration of the mafic volcanic rocks in this zone results in the sericitization of plagioclase phenocrysts and sometimes pyroxene phenocrysts. However, it is more common that the pyroxene phenocrysts are strongly altered to chlorite along with the groundmass. In more felsic rocks such as the granodiorites, sericitization of the feldspars and groundmass is dominant with significantly less chloritic alteration, reflecting the low proportion of mafic minerals in the intrusive rocks. Secondary quartz may locally be present in any sericite-chlorite-altered rocks, but is not typically abundant (Fig. 5.3e and f).

These alteration traits are roughly consistent with the diorite porphyry model proposed by Hollister (1975). In this model, no phyllic zone is present; instead, the relatively high iron and low silica content of the mafic host rocks results in the formation of abundant iron-rich silicate and oxide minerals such as chlorite and magnetite but little quartz, without significantly affecting the precipitation of iron-rich sulphides such as pyrite and chalcopyrite. This is consistent with the petrology of the chlorite-sericite alteration facies between the potassic and propylitic alteration zones observed at Schaft Creek.

Pervasive sericite-chlorite alteration as described above is common in large sections of the Main zone, and parts of the Paramount zone. The alteration imparts a grey-green or grey-tan washed-out appearance to the host volcanic rocks (Fig. 5.4a and b), and a tan to grey colouration to altered felsic intrusive rocks. Below surface (at 850m a.s.l.), sericite-chlorite alteration of the two zones converges into a single zone. In general, the sericite-chlorite alteration assemblage surrounds the higher-temperature potassic alteration, and separates it from the lower-temperature propylitic alteration (Figs. 5.1 and 5.2).

5.1.3 - Propylitic alteration

Propylitic alteration at the Schaft Creek deposit is similar to the sericite-chlorite zone described above, however this zone is differentiated from the former by the presence of epidote with minor pyrite. The propylitic alteration imparts a characteristic green colouration to the rocks, and coarse-grained epidote is distinctive of the assemblage locally (Fig. 5.4c–f). The propylitic alteration zone begins at the margins of the sericite-chlorite alteration zones and extends out beyond the current limits of mapping. Large portions of the West Breccia zone are also propylitically altered (Figs. 5.1 and 5.2).

5.1.4 - Hematization

Significant volumes of rock in the volcanic pile have been strongly hematized by oxidizing fluids related to quartz-carbonate-hematite veins (Fig. 5.5). These rocks have been locally referred to as the “Purple Volcanics” by previous workers (Linder, 1975; Fox et al., 1976; Seraphim et al., 1976; Spilsbury, 1995), and have been the subject of numerous debates (discussed below).

In these rocks, the hematization has replaced magnetite with hematite, either wholly or along rims and fractures of the magnetite grains. This alteration imparts a distinctive red to purple colouration to the affected volcanic rocks (Fig. 5.5). Significant areas of this late alteration occur to the north and south of the topographic saddle in the deposit area, and the alteration was also encountered at depth (drillhole 06CF284 at 216m depth; Fig. 5.5c). The hematization is observed to overprint earlier potassic, sericite-chlorite, and propylitic alteration, although it most commonly overprints propylitic alteration to the northeast and southeast of the Main zone.

5.1.5 - Carbonate alteration

Most of the rocks throughout the Schaft Creek deposit area have undergone a late overprint by carbonate alteration. In the volcanic rocks, pyroxene phenocrysts are

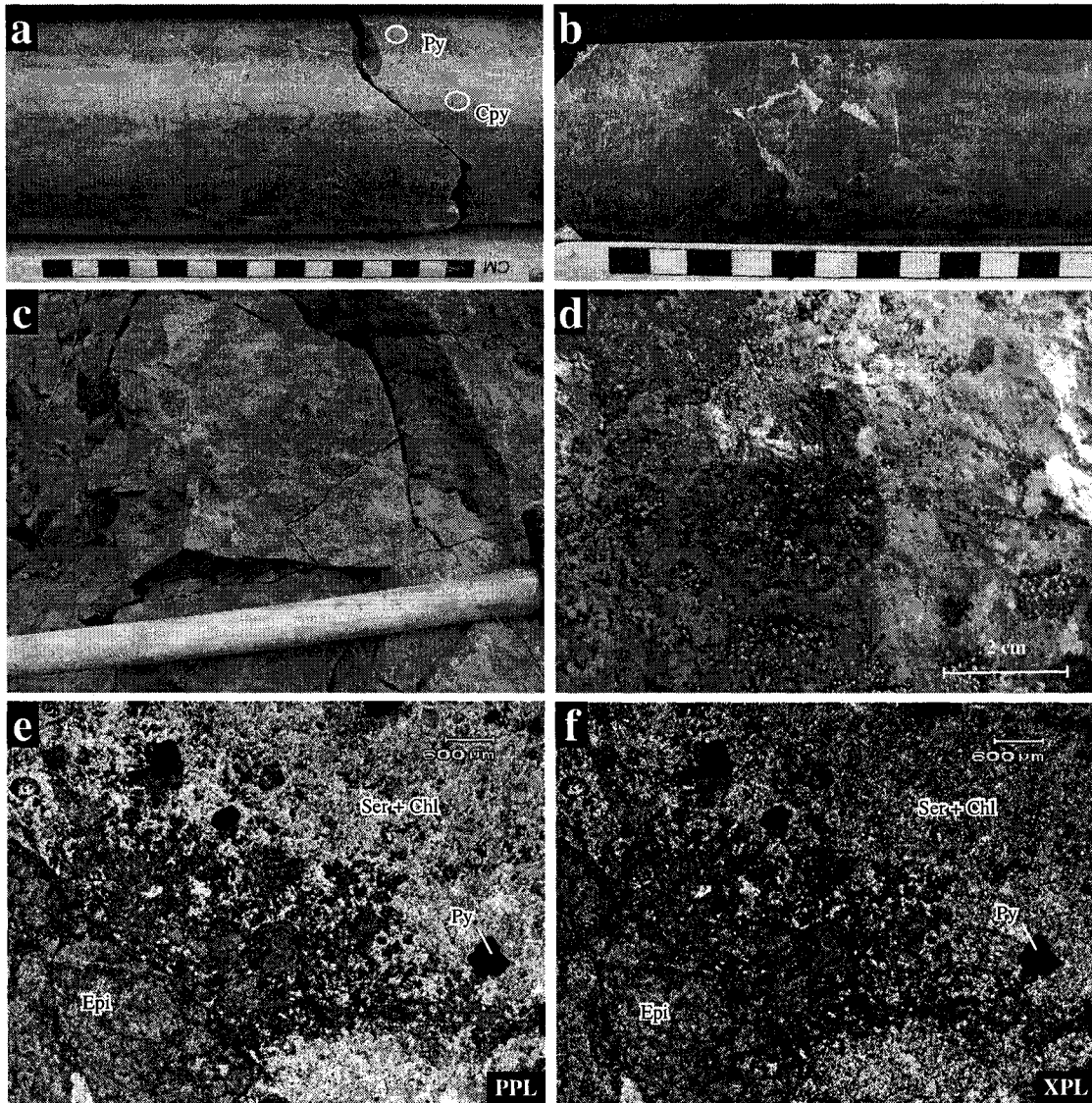


Figure 5.4 - (a) Sericite-chlorite alteration of plagioclase-pyroxene-pyritic andesite. The washed-out appearance and colouration are typical of sericite-chlorite alteration at the Schaft Creek deposit. Rare chalcopyrite (Cpy) occurs within thin quartz-chlorite veins (circled), and rare pyrite (Py) occurs as disseminations (circled). Drillhole 06CF264 at 133.0 m. (b) Pervasive sericite-chlorite alteration overprinting weak potassic alteration. The potassic alteration has left a subtle pink colouration which varies in intensity locally. The host rock was an andesitic breccia. It is unclear whether the chalcopyrite mineralization is associated with the earlier potassic alteration or the later sericite-chlorite alteration. Drillhole 06CF273 at 261.65 m. Ore grades for the 3 m interval that includes this sample are: 1.00 wt. % Cu, 0.030 wt. % Mo, 0.330 g/t Au, and 2.00 g/t Ag. (c) Propylitically altered andesitic breccia. Photo taken at coordinates 380111E, 6360384N. (d) Coarse-grained radiating mass of epidote grains forming a nodule within an epidote-altered volcanic clast in propylitically altered andesitic breccia. The presence of epidote marks the beginning of the propylitic alteration zone. Photo taken at coordinates 380434E, 6359986N. (e & f) Photomicrographs of propylitically altered andesitic volcanic breccia. Sample 05-JES-098. Abbreviations: Chl = chlorite; Cpy = chalcopyrite; Epi = epidote; Py = pyrite; Ser = sericite.

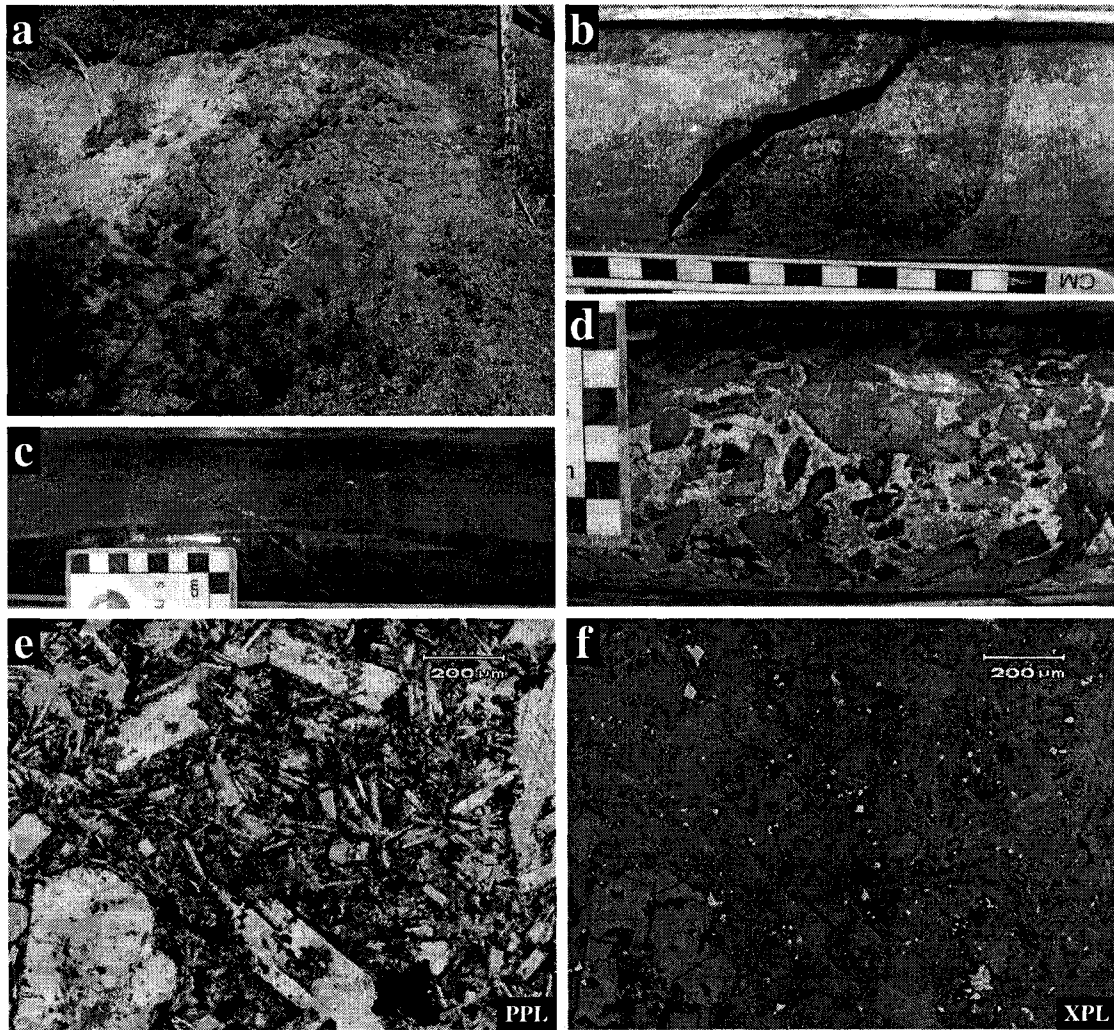


Figure 5.5 - (a) Aphanitic basaltic andesite, strongly altered by hematite. The colouration is typical of outcrops in the area that have undergone hematite alteration. Photo taken at coordinates 380300E, 6360159N. (b) A late vein of hematite + quartz + chlorite cross-cuts potassically altered quartz feldspar porphyry at depth. Drillhole 06CF277 at 150.5 m. (c) Hematized andesite at depth. The hematite imparts a weak purple colouration to the rock, overprinting the earlier potassic alteration. The earlier potassic alteration can be recognized by the weak washed-out pink-orange colour. Drillhole 06CF284 at 203.8 m. Ore grades from the 3 m sample interval that includes this depth were: 0.50 % Cu, <0.001 % Mo, 0.530 g/t Au, and 4.10 g/t Ag. Such grades indicate that the presence of hematite alteration is not mutually exclusive to the presence of mineralization. (d) Carbonate-hematite-gypsum vein brecciating potassically-altered host andesitic lapilli tuff. The presence of both hematite and gypsum indicate that at the time of this event the system was highly oxidizing. Chlorite commonly rims the andesite clasts. Drillhole 06CF256 at 302.70 m. (e & f) Photomicrographs of hematite alteration overprinting propylitically altered plagioclase-pyroxene-phyric basaltic andesite. Hematite is red to opaque in the plane-polarized photograph (e), and dull white-grey in the reflected light photograph (f). Sample 05-JES-204.

the most strongly affected by this alteration (Fig. 4.3d), and the groundmass of all rock types is carbonatized to some degree. Intrusive rocks are also affected, and some of the granodiorites have undergone significant carbonate replacement of feldspars.

The carbonate alteration may be related to a series of late wispy carbonate veins observed throughout the deposit and the surrounding area. The timing of this event relative to the hematization event is unclear, but they may be related because veins carrying both carbonate and hematite are commonly observed throughout the deposit, as discussed below.

5.1.6 - Silicification

Silicification occurs locally in the deposit area, but is rare. It typically occurs within highly fractured rocks and adjacent to fault zones where increased fluid flow has occurred. Typically the silicification is fine-grained and imparts a washed-out appearance to the rocks.

5.2 - Veining and Mineralization

Copper-molybdenum mineralization in the Schaft Creek deposit is closely linked to certain vein types. Mineralization occurs as disseminations only in restricted zones of pervasive potassic alteration, or within the alteration halos of mineralized veins. The greatest proportion of Cu-Mo mineralization is vein-hosted, thus making vein paragenesis important with respect to deposit formation.

5.2.1 - Vein types

Veining at the Schaft Creek deposit is complex and many generations of distinct veins cross cut one another at subtly to markedly different angles. Widths of the veins also vary dramatically from hairline to greater than 15 cm. Vein abundance is highly variable as

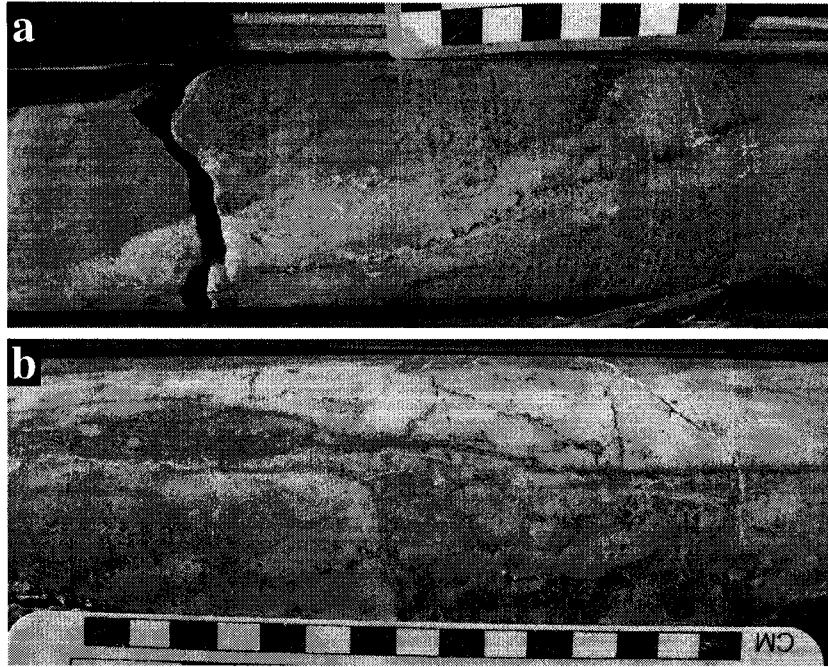


Figure 5.6 - (a) An example of a multi-stage vein in sericite-chlorite alteration of plagioclase-pyroxene-phyric basaltic andesite. The earlier wide quartz-dominated vein carries accessory carbonate, minor chlorite, and trace chalcopyrite. The core of this vein was later re-opened and carbonate was deposited with chlorite and molybdenite. Drillhole 06CF272 at 30.6 m. (b) A second example of multiple veining events overprinting along the same axes. Here a ~5 cm quartz-dominated vein hosting bornite and chalcopyrite cements brecciated potassically-altered plagioclase-pyroxene-phyric basaltic andesite. This vein is in turn brecciated and cemented by quartz + chlorite along its centre (outlined in red). Drillhole 06CF269 at 95.40 m.

well, ranging from 2 to 3 veins per metre to more than 100. Veins are frequently re-opened by later fluids of sometimes different compositions (Fig. 5.6). The vein sets can be loosely grouped into six major types, and their relative timing is illustrated in Figure 5.7.

5.2.1.1 - Pre-mineralization veins

The earliest sets of veins are barren quartz veins that either had asymmetrical vein walls at the time of formation, or have subsequently been deformed by tectonism. These veins typically exhibit wide but barren potassic halos, which are locally overprinted by later sericite-chlorite or propylitic alteration (Fig. 5.8a). In rare instances, these early barren quartz veins are re-used by narrow (<4 cm) feldspar porphyry dykes, indicating that some of these veins pre-dated at least one period of feldspar porphyry intrusion (Fig. 5.8b).

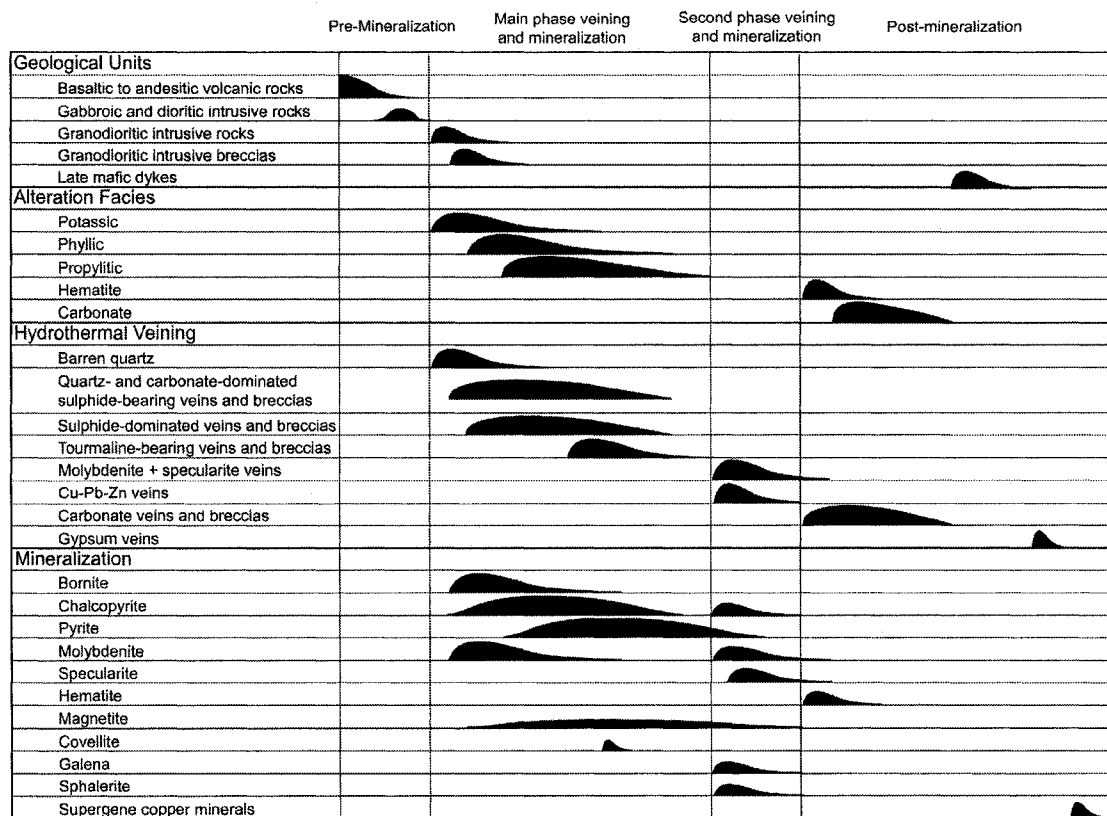


Figure 5.7 - Paragenetic sequence of events forming the Schaft Creek deposit.

5.2.1.2 - Quartz- and carbonate-dominated mineralized veins and breccias

Mineralized breccias and veins are generally quartz-dominated with significant carbonate and rare chlorite. Ore minerals in these veins include chalcopyrite, bornite, pyrite, and molybdenite, although pyrite and bornite do not coexist in the same vein. Rarely these veins may also contain magnetite and hematite, where hematite commonly replaces the magnetite as a result of oxidation. Widths of these veins vary significantly from hairline to greater than 10 cm. Ore minerals may occur along the vein margins, or along their centrelines (compare Figs. 5.8c and 5.8d). These veins occur at highly variable angles with respect to the core axes, and with strongly variable compositions and textures. Some of the high degree of variability in mineralized vein petrology is illustrated in Figures 5.8b through 5.8f. Two notable examples are shown in Figure 5.9, where one vein exhibits an assemblage of quartz-sericite-carbonate with molybdenite along the vein walls, and chalcopyrite at the core. The other vein is also quartz-dominated, but with less

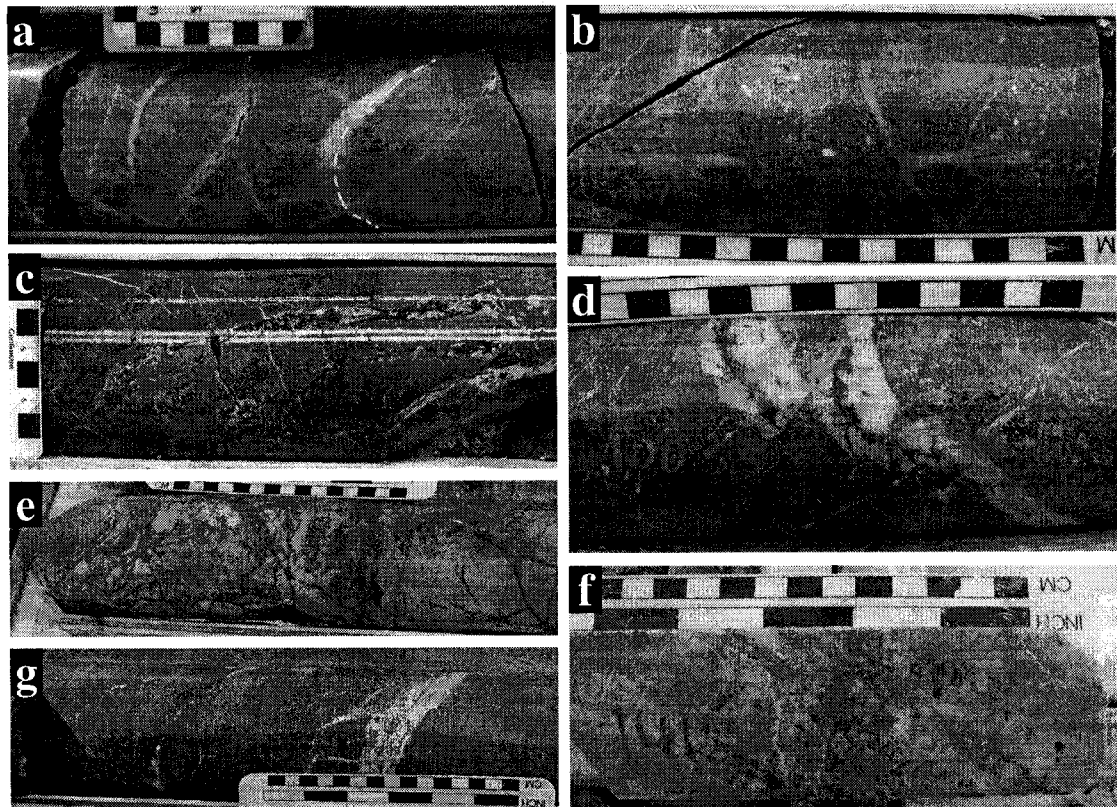


Figure 5.8 - (a) Pre-mineralization barren quartz veins (traced in red). Later quartz, quartz-chlorite, and carbonate-chlorite (traced in yellow) veins cross-cut the early asymmetrical barren veins. Potassic alteration is pervasive over this interval. Drillhole 06CF285 at 104.35 m. (b) Feldspar porphyry dykes following and cross-cutting early barren quartz vein. Remnants of the early vein can be seen at margins of the dyke on the left. Drillhole 06CF277 at 54.75 m. (c) Quartz-carbonate-chlorite vein with chalcopyrite mineralization and a strong potassic alteration halo. This vein locally brecciates the host volcanic rocks. Drillhole 06CF262 at 186.8 m. (d) Quartz vein with bornite mineralization predominantly in the vein centre. A weak potassic halo is present but is overprinted by chlorite, and the vein is offset by several small faults. Drillhole 06CF277 at 100.55 m. (e) Complex multi-stage quartz vein with molybdenite and bornite mineralization. The number of events is difficult to discern due to all phases being quartz-dominated. Drillhole 06CF257 at 210.6 m. (f) Quartz vein with chalcopyrite mineralization. The vein cuts quartz feldspar porphyry and does not appear to exhibit a well-developed alteration halo. Drillhole 06CF287 at 141.0 m. (g) Two different vein types cutting sericite-chlorite alteration in volcanic rocks. The vein to the left is carbonate-dominated with bornite and chalcopyrite mineralization over much of the vein width. The wide vein to the right is quartz-dominated with significant carbonate and trace chlorite, plus bornite and molybdenite. Neither vein exhibits a noticeable alteration halo. Drillhole 06CF257 at 168.3 m.

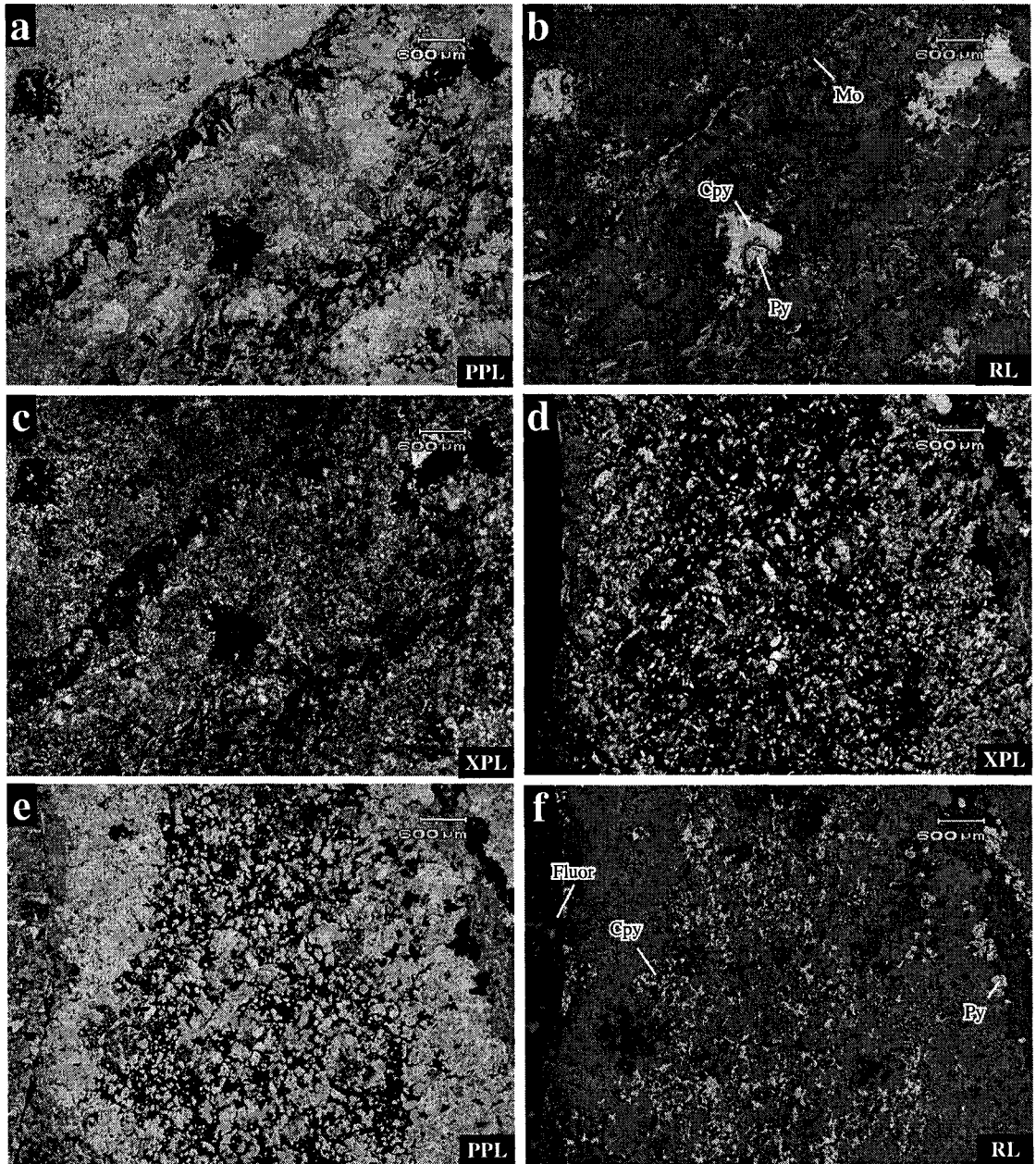


Figure 5.9 - (a - c) Mineralized quartz-sericite-carbonate vein. Molybdenite grains are found near the vein walls in this sample, with chalcopyrite at the vein centre, where it locally envelopes pyrite. Chalcopyrite disseminations are also present in the pervasively altered wall rock. Sample 05-JES-176. (d-f) Quartz-dominated vein with lesser carbonate and rare chlorite. Pyrite grains to the left of the frame occur in spatial association with the carbonate, whereas chalcopyrite occurs within the centre of the quartz-dominated region of the vein. To the left margin of the frame, a late fluorite vein follows and cross-cuts the quartz vein. Sample 05-JES-227. Abbreviations: Cpy = chalcopyrite, Fluor = fluorite, Mo = molybdenite, Py = pyrite.

carbonate and chlorite in the place of sericite. This vein is mineralized with an assemblage of chalcopyrite and pyrite.

5.2.1.3 – Sulphide-dominated mineralized veins

Sulphide-dominated veins that contain no appreciable gangue minerals are common within the potassic and sericite-chlorite alteration zones of both the Main zone and the Paramount zone, and are commonly composed of either chalcopyrite (Fig. 5.10a) or bornite, although sometimes both are present in a single vein. Pyrite stringers are found in the propylitic alteration zone but are not common. The width of these sulphide-only mineralized veins varies from hairline stringers up to veins of roughly 1 cm width, and in rare cases 2–3 cm; however, in zones with gangue-free veins the abundance of these veins is very high, sometimes with hundreds of veins at random orientations over a given metre interval, imparting a “crackle breccia” texture to the host rock (Fig. 5.10b).

5.2.1.4 - Tourmaline veins/breccias

Tourmaline is rare in the Main and Paramount zones of the deposit, but is abundant in the West Breccia zone, mainly occurring in hydrothermal breccia cements with quartz and chlorite. In the West Breccia zone, tourmaline is associated with significant amounts of chalcopyrite and pyrite (Figs. 5.10c, 5.11a–c). In the main zone, tourmaline locally occurs as disseminated radiating aggregates of acicular grains, and rarely within quartz-dominated veins (Fig. 5.10d).

5.2.1.5 - Molybdenite and specularite veins

Throughout the deposit, a combination of molybdenite and/or specularite is observed on fracture surfaces, often exhibiting slickensides. These minerals typically coat fractures and microfaults that cross-cut most other vein sets, indicating that these molybdenite/specularite veins possibly represent the most recent syndeformational mineralizing event



Figure 5.10 - (a) Chalcopyrite stringer with a sericite-chlorite alteration halo cross-cutting propylitic alteration in andesite. Drillhole 06CF258 at 222.8 m. (b) Bornite crackle breccia. Weak potassic vein-centric alteration has been overprinted by more pervasive sericite-chlorite alteration imparting a grey washed-out appearance to the volcanic rock. Drillhole 06CF254 at 81.1 m. (c) West Breccia zone mineralization. Hydrothermal breccia of sericite-chlorite altered volcanic rocks, cemented by tourmaline-quartz-carbonate with chalcopyrite and pyrite mineralization. Drillhole 05CF234 at 131.6 m. (d) Quartz-tourmaline vein with trace disseminated chalcopyrite. The vein locally brecciates the potassically altered volcanic host. The quartz portion of this vein does not contain any noticeable chalcopyrite mineralization. Drillhole 06CF277 at 156.1 m. Abbreviations: Bn = bornite, Cpy = chalcopyrite, Py = pyrite, Tour = tourmaline.

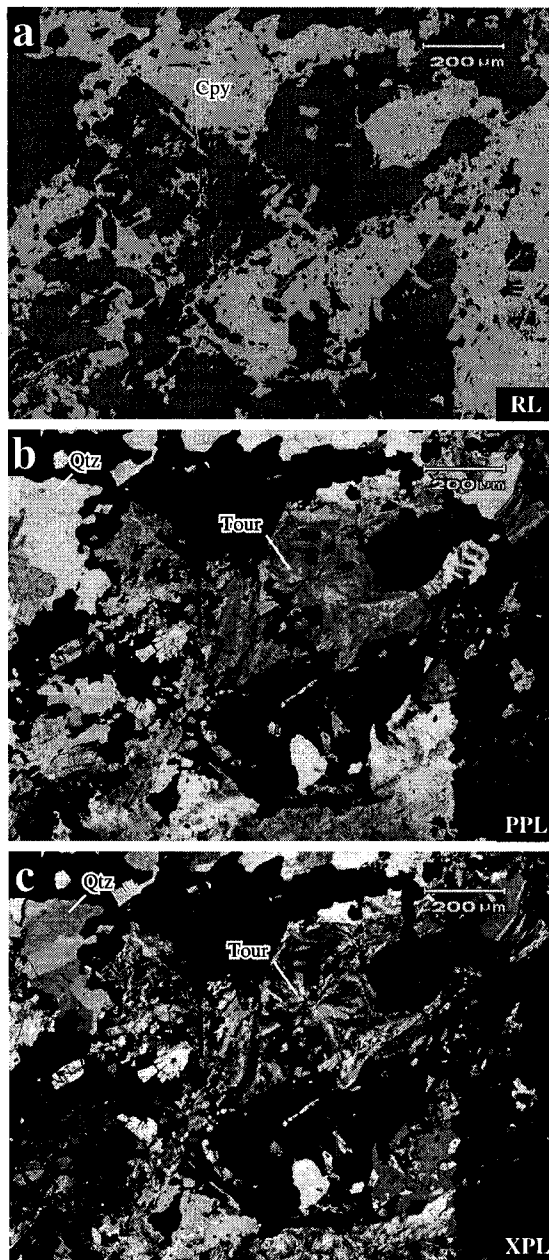


Figure 5.11 - West Breccia zone mineralization. Hydrothermal quartz + tourmaline occurring together with chalcopyrite mineralization. This mineral assemblage, often with pyrite, forms the matrix of the hydrothermal breccia system in the West Breccia zone. Sample 05-JES-227. Abbreviations: Cpy = chalcopyrite, Qtz = quartz, Tour = tourmaline.

(Fig. 5.12a). These veins can vary in thickness from hairline to centimetre-thick fracture coatings, typically at low angles to the core axes. Because most drill holes were drilled vertically or at less than 45° dip, this would indicate that these veins are likely close to vertical in their orientation.

5.2.1.6 – Late Cu-Pb-Zn veins

A small number of quartz-dominated veins with up to ~15 vol. % chalcopyrite + galena + sphalerite ± pyrite cross-cut mineralization within the West Breccia zone (Fig. 5.12b and c). Typically these veins are wide (up to ~25 cm), and have diffuse walls, flooding the surrounding rock with silica and carbonate (illustrated in Fig. 5.12b). The timing of this veining episode falls somewhere between the main mineralizing phase and the later barren carbonate veining phase (Fig. 5.12d–f).

5.2.1.7 - Post-mineralization veins

Hematite-bearing carbonate veins cross-cut earlier mineralizing veins and are abundant particularly at depth and in the eastern portion of the deposit. Locally these

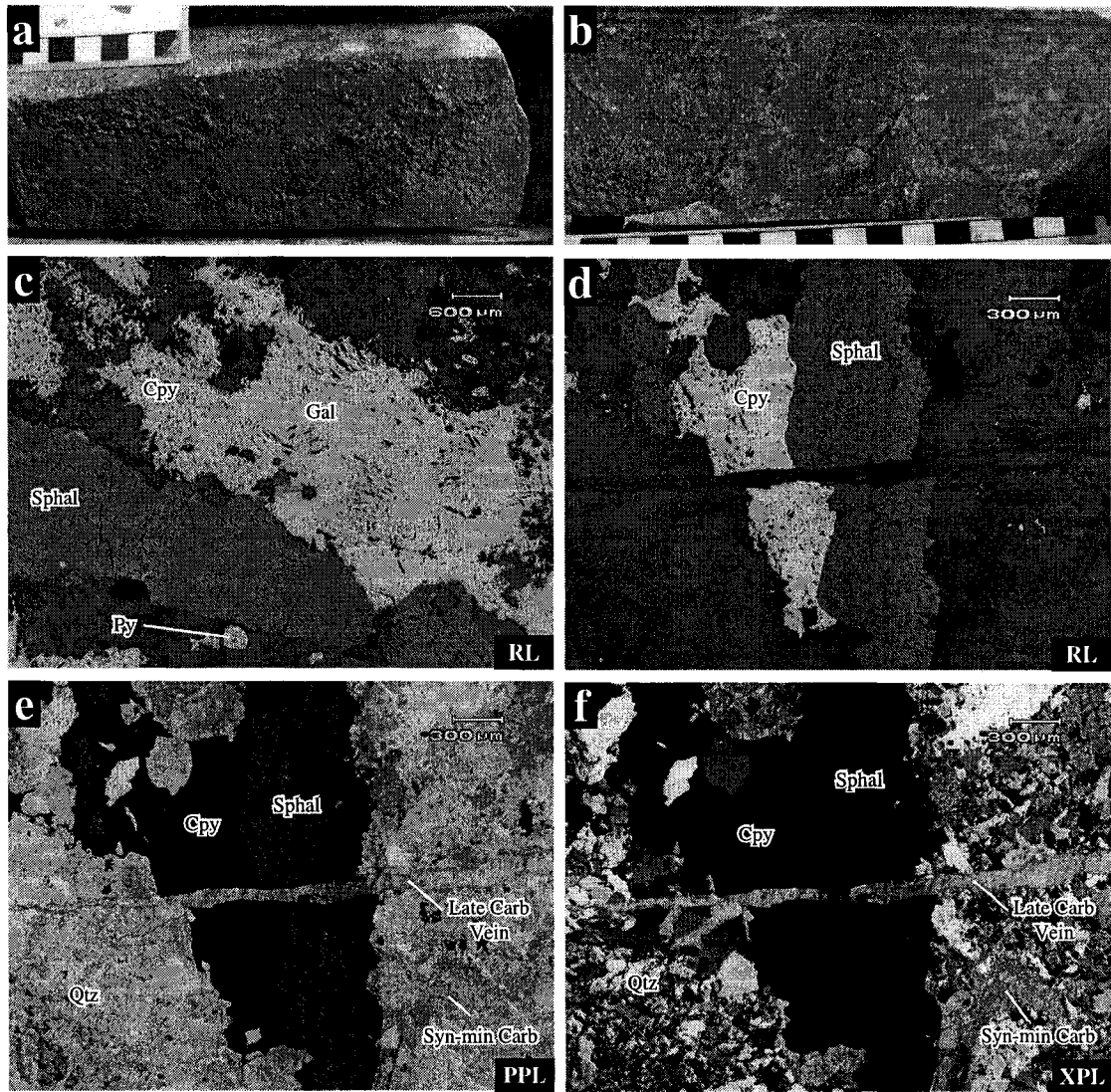


Figure 5.12 - (a) Molybdenite fracture surface coating. The fracture plane runs nearly parallel to the core axis, and the molybdenite coating is roughly 0.5 cm thick in this example. Drillhole 06CF256 at 180.9 m. (b) Quartz-carbonate-chalcopyrite-sphalerite-galena vein with intensely silicified halo making determination of the limits of the vein difficult. Total width of the vein zone in this example is roughly 25 cm. Drillhole 05CF234 at 48.3 m. (c) Typical mineralization assemblage within the Pb-Zn veins. In this example, the galena is surrounded by chalcopyrite, sphalerite with chalcopyrite blebs, and trace pyrite. The chalcopyrite blebs in the sphalerite and the replacement of galena by chalcopyrite indicate the chalcopyrite mineralization was later. Sample 05-JES-216. (d - f) Photomicrographs showing cross-cutting relationships which indicate the approximate timing of the Pb-Zn veins relative to other vein types. Here the chalcopyrite and sphalerite grains which occur together with carbonate and quartz are cross-cut by a later ~ 0.2 mm carbonate vein. Sample 05-JES-216. Abbreviations: Carb = carbonate, Cpy = chalcopyrite, Gal = galena, Qtz = quartz, Sphal = sphalerite, min = mineralization.

veins brecciate the host rock (as shown in Fig. 5.5b–d). These veins are common and likely explain the presence of the late hematite alteration observed in the deposit area.

Barren milky-white carbonate veins are common and cross-cut earlier quartz veins (Fig. 5.13a). However, the relative timing of the barren carbonate veins and the hematite-bearing veins remains unclear because cross-cutting relationships have not been observed. These barren veins are ubiquitous throughout the deposit area and take a number of forms including wispy asymmetrical veins of less than 1 cm thickness, breccias up to 10 cm wide (Fig. 5.13b), and locally abundant <5 mm-wide veins in random orientations forming a “crackle breccia” texture in the host rock (Fig. 5.13c).

The most recent veining episode in the deposit area was a period of gypsum veining that both cross-cuts and follows earlier barren carbonate veins. The gypsum is typically clear and colourless, but locally exhibits weak pink and/or purple colouration (Fig. 5.13d). A single fluorite vein of ~0.4 mm thickness was observed in thin section from a sample within the West Breccia zone. The vein followed an earlier barren carbonate vein, indicating that it is a later event. No sulphides were associated with the fluorite vein (Fig. 5.13e and f).

5.2.2 - Syn- and post-mineralization deformation

The local deformational history of the Schaft Creek deposit is complicated and spans a significant period of the history of the deposit. Much of the history of deformation is well preserved in veins, annealed faults, and shear zones. Small millimetre-scale faults commonly offset earlier veins along sharp planes, and these faults subsequently acted as conduits to later hydrothermal fluids, commonly repeatedly. In some instances more than four deformational events are preserved in this manner over a single metre of core (as shown in Figure. 5.3d). Some of the offset veins contain sulphides, and thus provide strong evidence that mineralization was syndeformational.

Larger faults are commonly preserved in the deposit area as partly annealed zones

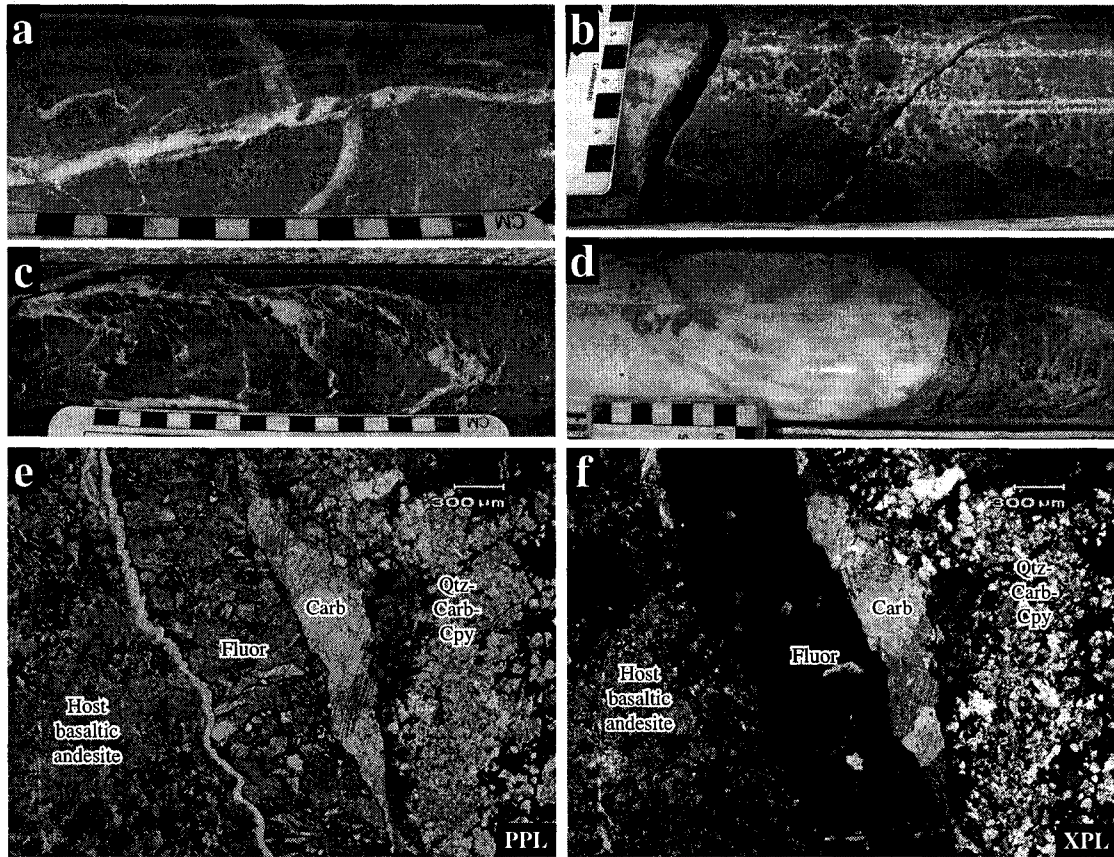


Figure 5.13 - (a) Late vuggy carbonate-chlorite vein cross-cutting and offsetting earlier quartz-carbonate-chlorite veins. Drillhole 06CF273 at 75.8 m. (b) Late barren carbonate-chlorite-cemented vein breccia in volcanic host rocks. Drillhole 06CF260 at 111.0 m. (c) Randomly-oriented, locally vuggy carbonate veins cross-cutting potassic alteration in andesitic lapilli. Drillhole 06CF273 at 275.2 m. (d) Late gypsum vein (Gyp), ~ 30 cm wide. Drillhole 05CF256 at 300.2 m. (e & f) Three vein generations are shown in this figure. The original host rock is at the left of the frame, and is intensely altered by carbonate and quartz. The first vein generation is the quartz-carbonate-chalcopyrite vein on the right of the frame. This vein was then followed by the carbonate vein in the centre of the frame. The carbonate was in turn followed by the late fluorite vein. To the immediate left of the fluorite vein is a fracture in the thin section, not an additional vein type. Sample 05-JES-227. Abbreviations: Carb = carbonate, Cpy = chalcopyrite, Fluor = fluorite, Gyp = gypsum; Qtz = quartz.

of fault gouge/rock flour, which may exhibit evidence for displacement in the form of mineral alignment and rotated grains (Fig. 5.14a). These zones locally host mineralization that was present prior to faulting and which is preserved as crushed sulphide clasts within the fault gouge. These fault zones were then partly healed by later hydrothermal fluids moving through the fault zone. These fault zones vary in width from <10 cm to ~2 m, are typically light grey to charcoal in colour, and host some preserved clasts of up to ~2 cm.

The most recent periods of deformation are more poorly preserved in unannealed

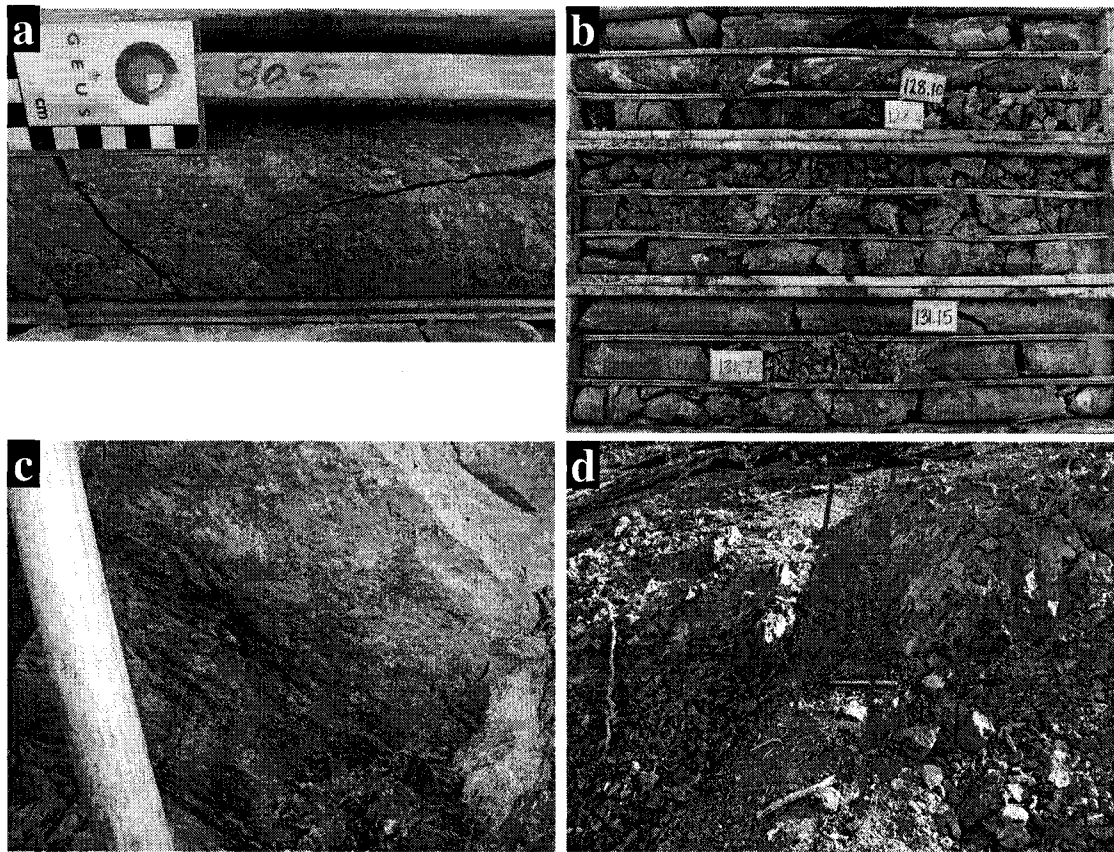


Figure 5.14 - (a) Partly annealed fault gouge and rock flour. The large grain in the centre of the frame has undergone some rotation/alignment possibly indicating a sinistral sense of shear along the fault. Drillhole 06CF284 at 80.5 m. (b) Fault zone preserved in core. These zones of rubble are common and are observed in all zones of the deposit. Some of the fracture surfaces exhibit slickensides, but due to the highly fractured nature of the core, it is not possible to determine the nature of movement along these late faults. Drillhole 06CF278 at 133.0 m. (c) Slickensides of hematite and epidote at surface. No sense of movement could be determined from this location because the block was not in-situ. Photograph taken at coordinates 380747E, 6358723. (d) Typical surface exposure of a narrow fault, recessively weathered. Wide faults are difficult to observe at surface because no outcrop is preserved. Photo taken at coordinates 380493E, 6360096.

fault zones throughout the deposit. These recent fault zones are abundant and are reflected in zones of rubbly fault gouge and zones of high fracture density (Fig. 5.14b). These fault zones were logged as distinct lithologies during the 2006 and 2007 field seasons, and accounted for varying percentages of the total logged core during that period. Fault zones in the Paramount, Main, and West Breccia zones accounted for 9%, 4%, and 2% of the logged core for each of those zones, respectively (Ewanchuk et al., 2007). Overall, this is a relative percentage of 5% of the total logged core for the deposit in the 2006 and 2007 field seasons. Regardless of the common presence of slickensides on fracture surfaces

(Fig. 5.14c), the sense of movement along these recent faults is difficult to determine due to their rubbly nature in core. The surface exposures of these faults are typically zones of fine-grained rubble, or are not preserved in outcrop at all due to their low resistance to weathering (Fig. 5.14d). Even small compound movement along such a significant number of faults could result in significant total offset across the deposit. Because the direction of movement on these faults is not well understood, reconstruction of the system prior to the recent faulting event is difficult. The same conclusion was reached by both Linder (1975, p. 55) and Fox et al. (1976, p. 221), the former describing the deposit as "... a shatter zone", and the latter describing the area as a "...fault mosaic that makes correlation of lithology, structure, and assay data from drill hole to drill hole difficult, if not highly interpretive."

5.2.3 - Nature of mineralization

Chalcopyrite, bornite, and molybdenite are the three primary ore minerals occurring in the Schaft Creek deposit, and occur in varying abundances in each of the three mineralized zones. All three ore minerals are observed in single veins, and are sometimes observed to be intergrown (e.g., Fig. 4.17b). Sphalerite and galena are also observed locally, but are generally rare in the deposit area. Galena is only observed in association with sphalerite in late cross-cutting quartz-carbonate veins, but sphalerite also commonly occurs in trace amounts with chalcopyrite. Both sphalerite and galena are most common within and adjacent to the West Breccia zone.

Non-ore sulphides and oxides are common in the deposit area, including significant amounts of pyrite, magnetite, and hematite both as disseminations and in veins. Rarely, magnetite is observed to occur together with ore minerals within single veins, although the magnetite may be commonly partly or wholly replaced by hematite (Fig. 5.15a). In thin section, chalcopyrite is commonly observed replacing pyrite along fractures (Fig 5.15b). In other instances, chalcopyrite is sometimes observed to be partly replaced by bornite, which in turn may be locally replaced by hematite (Fig. 5.15c). Some bornite grains are

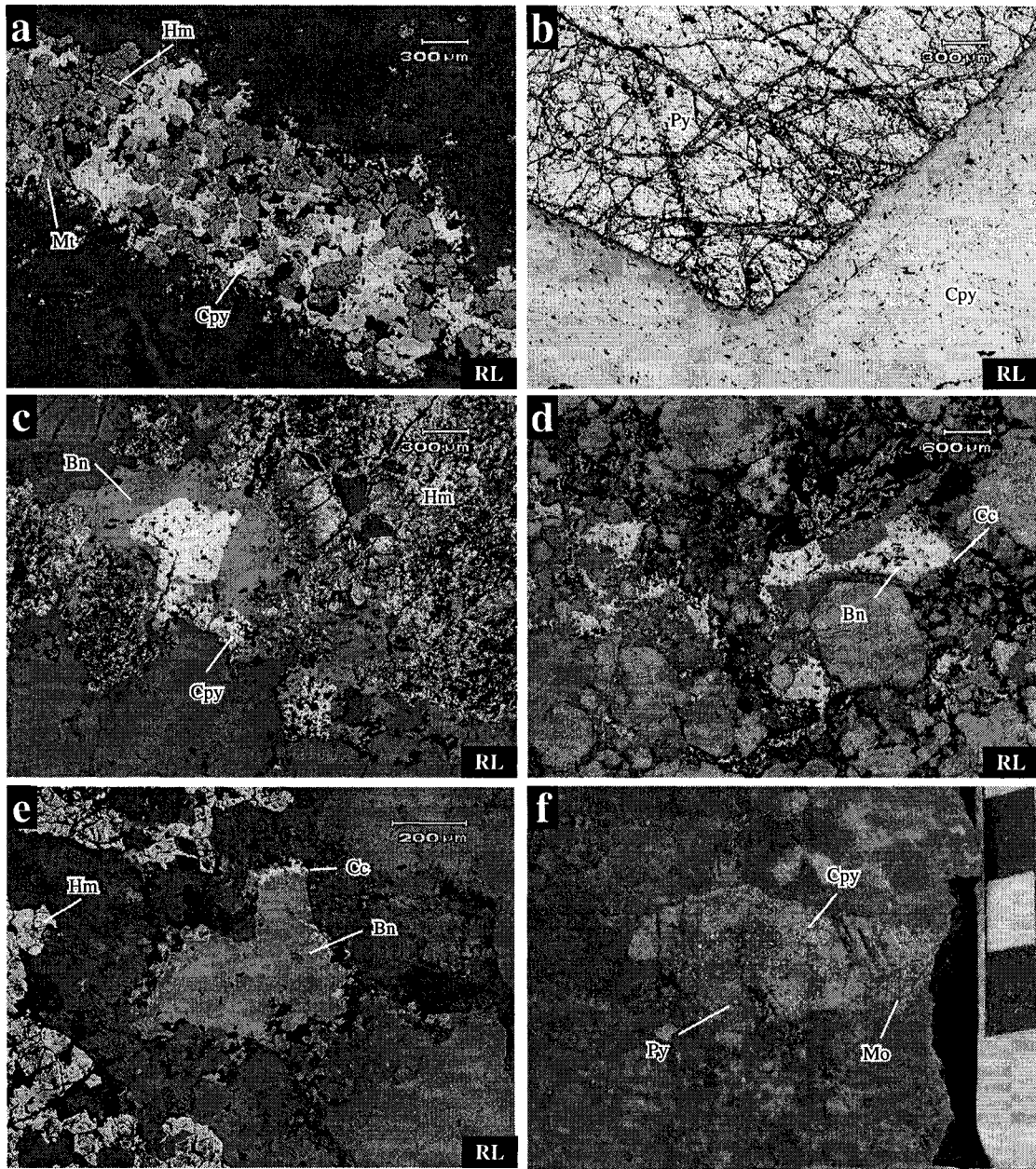


Figure 5.15 - (a) Magnetite, partly altered to hematite, being replaced by chalcopyrite in a vein. Sample 05-JES-086. (b) A large euhedral pyrite grain being replaced along fractures by chalcopyrite. Sample 06CF287-281-8. (c) Chalcopyrite partly replaced by bornite and hematite. Sample 05-JES-155. (d & e) Bornite grains rimmed by chalcocite and possibly covellite. Sample 05-JES-155. (f) Zoned sulphide grain within the intrusive breccia unit from the Paramount zone. At the core is pyrite, followed by chalcopyrite, then partly rimmed by molybdenite. Drillhole 06CF287 at 18.3 m. Abbreviations: Bn = bornite, Cc = chalcocite, Cpy = chalcopyrite, Hm = hematite, Mo = molybdenite, Mt = magnetite, Py = pyrite.

observed to have chalcocite and covellite rims likely indicating later supergene alteration of the copper sulphides (Fig. 5.15d and e). Linder (1975) also observed trace amounts of covellite and tetrahedrite in some polished sections, whereas Fox et al. (1976) reported the local presence of rare pyrrhotite, although tetrahedrite and pyrrhotite were not observed during the current study.

The vast majority of ore minerals within the Schaft Creek deposit are hosted within veins, and only minor amounts occur as disseminations in wall rocks. In instances where mineralization forms disseminations, it typically occurs in association with zones of pervasive potassic alteration, and rarely with pervasive sericite-chlorite alteration. Potassic and sericite-chlorite alteration in general contain the highest grade intersections, and the best grades are where multiple alteration facies overprint each other. Copper mineralization occurs prominently in each of the three deposit zones in both potassic and sericite-chlorite alteration facies, but molybdenite tends to be restricted to zones with prominent potassic alteration. In zones of potassic alteration, copper and molybdenum mineralization are largely coincident, commonly occurring together within single veins (Figs. 4.17b, 5.6a, and 5.8e). A later phase of molybdenite mineralization occurs as fracture-coatings which cross-cut earlier mineralization, as discussed above (Fig. 5.12a).

At the surface and in some weathered fractures recovered from drillcore, malachite and azurite are sometimes observed as weathering products of copper-bearing sulphides. Single grains of cuprite and native copper were also observed on some fractures in drillcore, but these minerals are exceedingly rare and are related to supergene alteration.

The three mineralization zones are broadly similar, but each has characteristic features: most importantly, all three zones contain significant amounts of chalcopyrite. However the Paramount zone is enriched in bornite with respect to the other zones, whereas the West Breccia zone contains more pyrite and less bornite with respect to the other zones. The unique mineralization style of each of the deposit zones is discussed below.

5.2.3.1 - Paramount zone

Mineralization in the Paramount zone occurs in a number of different modes: as disseminations within the granodiorite dykes and intrusive breccias, within hydrothermal quartz-dominated breccias and stockworks, within quartz-dominated veins, and as sulphide-dominated silica-deficient veins. The dominant sulphide minerals in this zone are bornite, chalcopyrite, molybdenite, and rare pyrite. The Cu-bearing sulphides tend to occur widely throughout the zone, whereas distribution of molybdenite is more specific in that it tends to occur preferentially within quartz-dominated veins and stockworks, and rarely as disseminations. In some instances, Cu- and Mo-sulphide disseminations occur as large (up to 3 cm wide) zoned breccia clasts within the intrusive matrix (Fig. 5.15f). The order of mineral zoning in these sulphide grains consists of a pyrite core surrounded by chalcopyrite, and rimmed by molybdenite.

The granodiorite and the corresponding intrusive breccia are both subsequently cross-cut by the mineralized quartz-dominated veins. However, the most common veins in the Paramount zone are barren quartz-dominated veins with wide potassic alteration halos.

5.2.3.2 - Main zone

The Main zone is the largest mineralized zone in the deposit both in size and in terms of total contained metal, and is dominantly hosted by volcanic rocks which are locally intruded by granodiorite dykes. Intrusive breccias are typically not observed in the Main zone. Mineralization primarily occurs within abundant veins and stringers that cross cut each other at varying orientations. Mineralized hydrothermal breccias are observed locally, and these breccias are zoned outwards into the mineralized vein sets. Disseminations are rare, but occur locally in wallrock with pervasive potassic and sericite-chlorite altered wallrock. Mineralization is dominantly associated with potassic and sericite-chlorite alteration; however, chalcopyrite also occurs locally in zones of propylitic alteration. Molybdenite

occurs dominantly in veins within the potassic zone, but also less commonly within veins in the sericite-chlorite zone. Molybdenite is very rarely observed as disseminations, but does occur as late fracture coatings which cross cut all other features. Where narrow potassic halos surround mineralized veins, the ore minerals within these veins may be some combination of any of the three dominant ore minerals.

5.2.3.3 - West Breccia zone

The West Breccia zone is geologically distinct from the Paramount and Main zones, which appear to be similar in terms of alteration and basic mineralization styles. The West Breccia zone is instead dominated by a quartz-carbonate-tourmaline hydrothermal breccia system which propylitically alters the wall rock. Mineralization in this zone is an assemblage of chalcopyrite and pyrite with rare bornite and molybdenite. Ore grades are high in this zone due to a high density of mineralized structures, notably the quartz-carbonate-tourmaline hydrothermal breccia system.

5.2.4 – *Nature of ore distribution*

In order to better understand the controls on ore distribution, a series of plan maps was constructed at 850 m a.s.l. through the deposit. The 850 m a.s.l. elevation was chosen because it offered the greatest number of drillhole pierce points to the plane, in addition to including all three deposit zones. Grade distribution plans for Cu, Mo, Au, and Ag are shown in Figures 5.16 through 5.19.

The four elements are distributed similarly, with each element's high-grade zones largely coinciding with those of the others. There are two notable gaps in the grade zones from all four elements. One low-grade zone lies between the West Breccia and Main zones, and the other between the Main and Paramount zones.

By comparing the ore distribution plans (Figs. 5.16–5.19), the alteration plan (Fig. 5.2), and the geology plan (Fig. 4.2), a number of relationships may be observed. First,

in the Main and Paramount zones, the host rock lithology appears to have little effect on ore grades. The West Breccia zone is the exception to this generalization, a feature which can be attributed to the “Hydrothermal Breccia” rock type being distinguished from the surrounding rocks by the presence of significant hydrothermal quartz and tourmaline with chalcopyrite.

Ore grade distribution appears to be much more closely related to alteration, in particular with potassic and sericite-chlorite alteration facies. This is particularly notable in the Main and Paramount zones, where the highest ore grades in general closely follow potassic and sericite-chlorite alteration facies. In a number of instances the ore grades deviate from what would be expected from the mapped alteration facies, particularly to the south of the Paramount zone and to the north of the Main zone. The reasons for these inconsistencies are unclear, but may be directly related to the structural modification of the deposit.

Finally, the low-grade zone between the Paramount and Main zones should be addressed. This area does not exhibit significant potassic alteration, and thus the abundance of mineralization is low. However, due to different ownership of claim groups in the Paramount and Main zones in the past, the area has not been subjected to the same drilling density of other areas of the deposit, and therefore the nature of alteration and mineralization in the area is less well constrained.

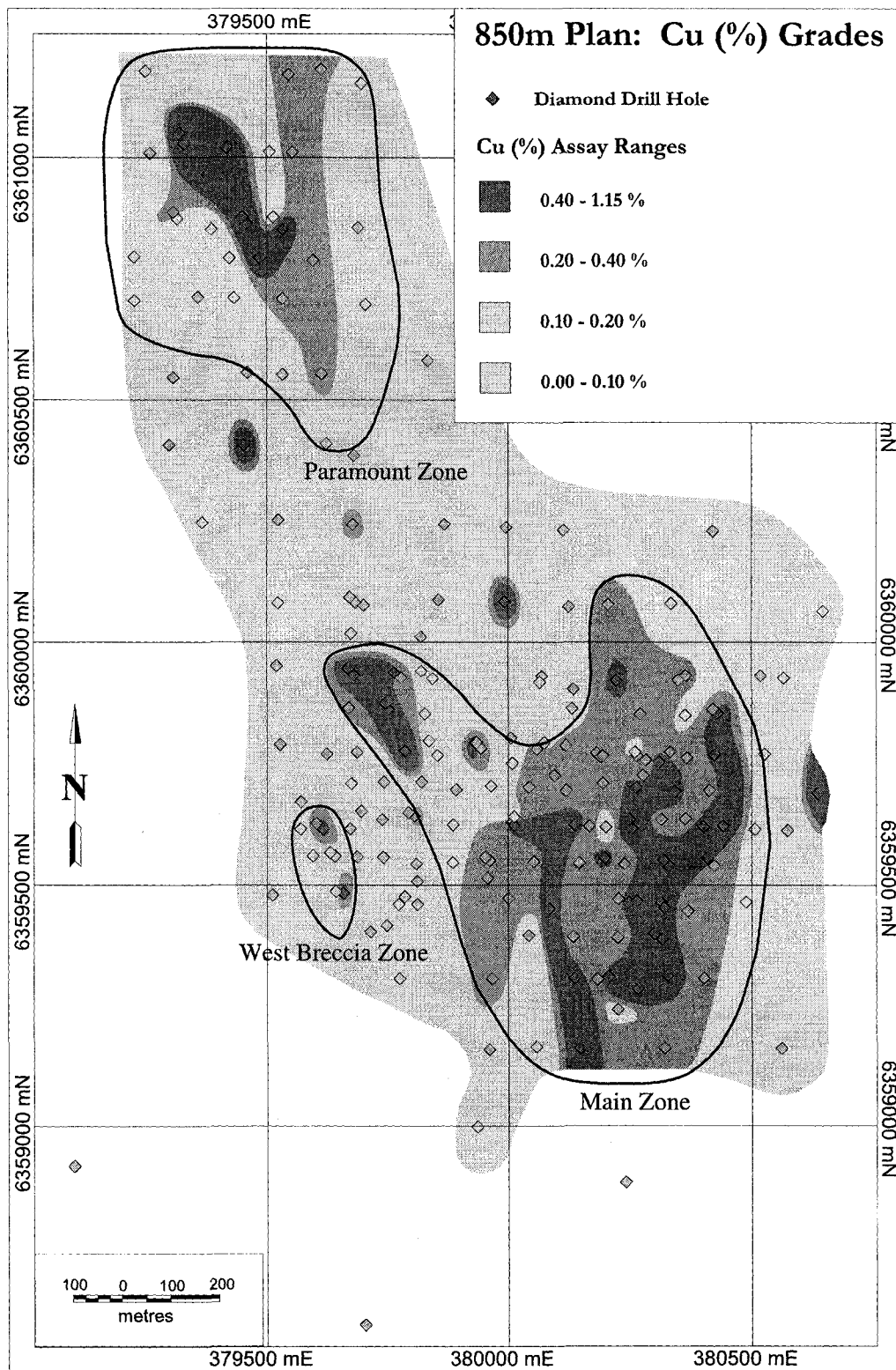


Figure 5.16 - 850 m elevation plan - Copper grades. Drillhole pierce points are calculated from surface elevation, drillhole azimuth, and dip. Grades are from the three metre sample interval that pierces the plane. Coordinates are in UTM Zone 9V (NAD 83 datum).

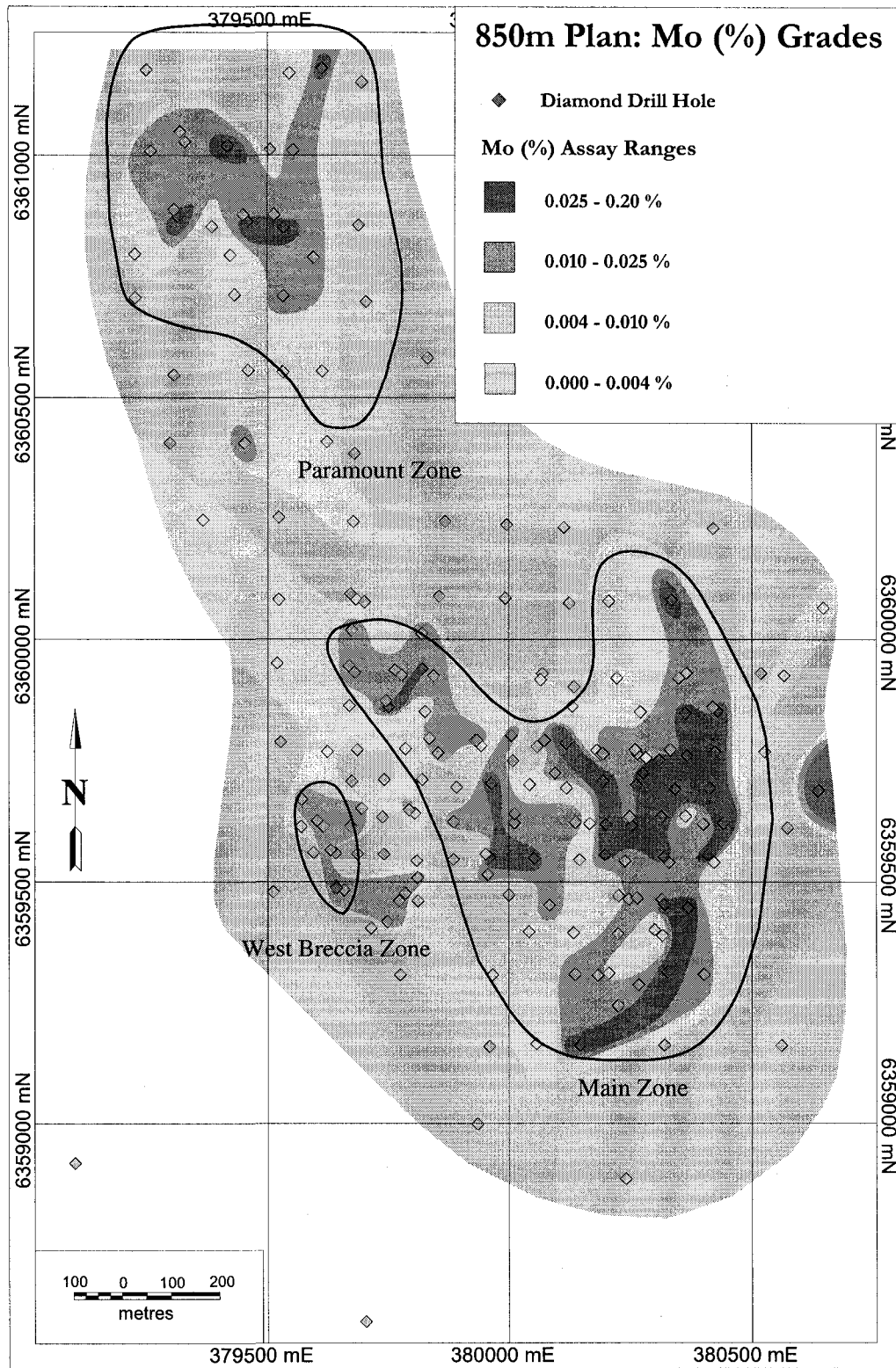


Figure 5.17 - 850 m elevation plan - Molybdenum grades. Drillhole pierce points are calculated from surface elevation, drillhole azimuth, and dip. Grades are from the three metre sample interval that pierces the plane. Coordinates are in UTM Zone 9V (NAD 83 datum).

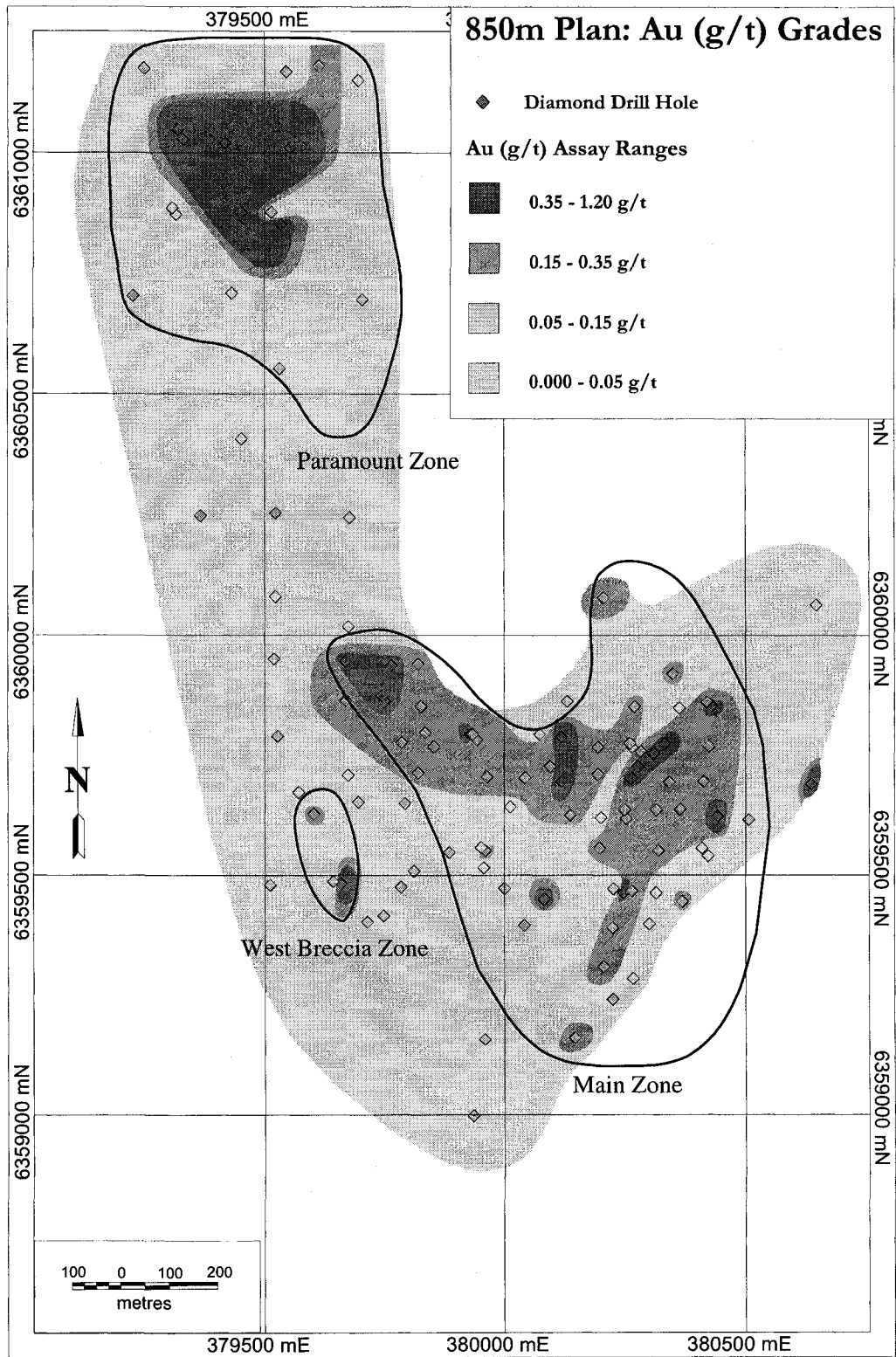


Figure 5.18 - 850 m elevation plan - Gold grades. Drillhole pierce points are calculated from surface elevation, drillhole azimuth, and dip. Grades are from the three metre sample interval that pierces the plane. Coordinates are in UTM Zone 9V (NAD 83 datum).

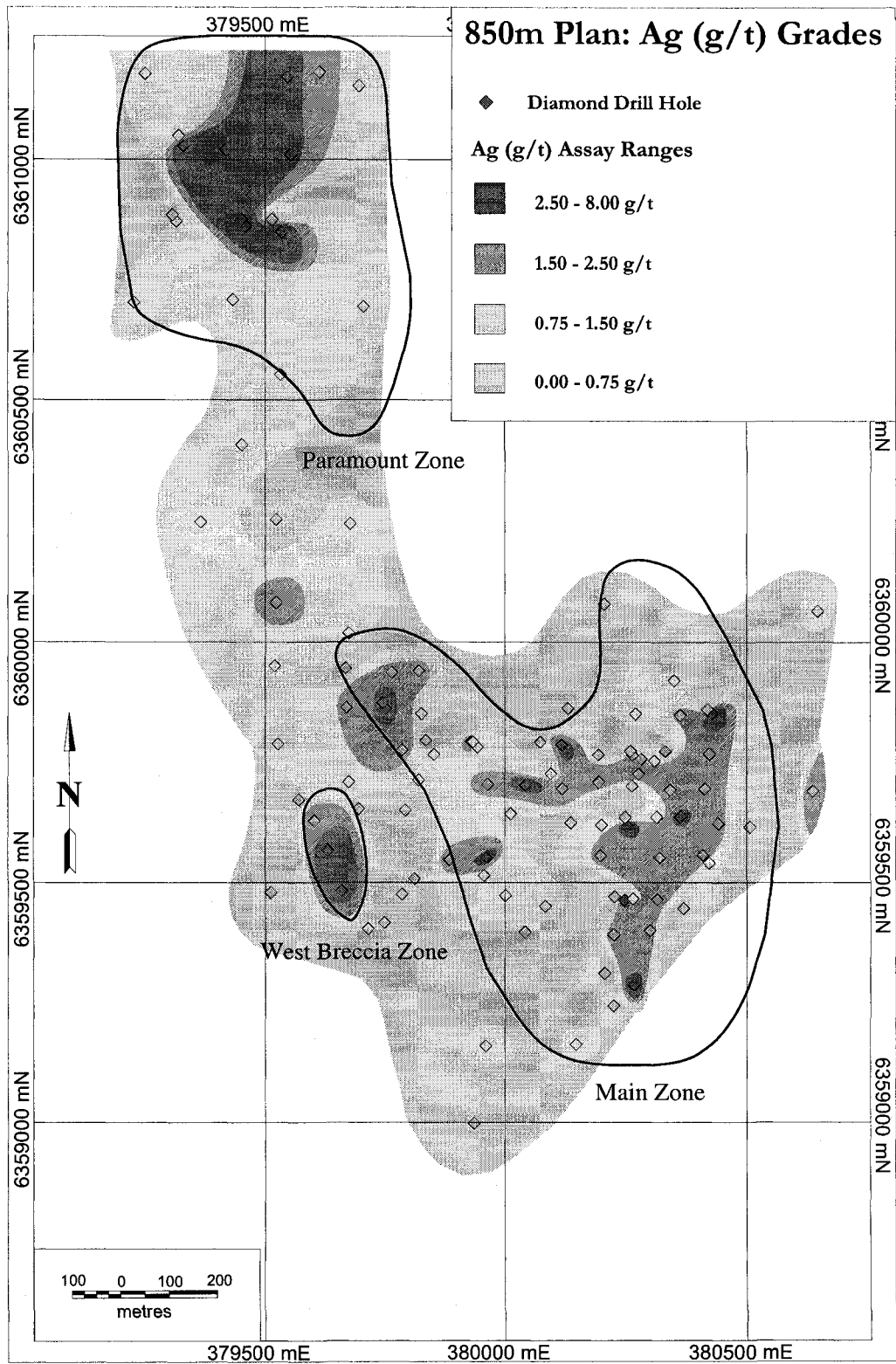


Figure 5.19 - 850 m elevation plan - Silver grades. Drillhole pierce points are calculated from surface elevation, drillhole azimuth, and dip. Grades are from the three metre sample interval that pierces the plane. Coordinates are in UTM Zone 9V (NAD 83 datum).

6 – DISCUSSION

6.1 – Tectonic Setting

The Schaft Creek deposit is hosted by basaltic to andesitic volcanic rocks that exhibit notable Ta-Nb-Ti anomalies which are typical of arc magmas (Brenan et al., 1994; Foley et al., 2000). In these rocks, Mg-rich augite phenocrysts are common, as are phenocrysts of albitized plagioclase. These volcanic rocks were subsequently intruded by evolved, commonly feldspar-phyric, granodioritic rocks that exhibit largely similar, but more evolved, trace element and rare earth element patterns (figures 4.13 and 4.14) that indicate evolution from a common magmatic source.

Although the relatively mafic composition of the associated volcanic rocks suggests an island arc environment, the presence of magmatic zircons with older inherited cores in the granodiorite bodies suggests that they were intruded through older continental crust. These conflicting lines of evidence might be explained in terms of the arc being formed on a back-arc rifted continental fragment, analogous to the modern-day Japanese archipelago. The Schaft Creek deposit is therefore interpreted to have formed during the Late Triassic prior to amalgamation and accretion of this continental fragment to ancestral North America during the Jurassic.

At 222.0 ± 0.8 Ma (best estimate of age of mineralization) the Schaft Creek deposit is notably older than other similar calc-alkaline porphyry Cu deposits in northern Stikinia, which range from ~196 to ~202 Ma (Table 6.1). Alkaline porphyry deposits from the same area (Galore Creek and Red Chris) are roughly 10 m.y. younger than this age, possibly indicating a regional evolution from calc-alkalic to alkalic magmatism with time.

The origin of mineralization at Schaft Creek has been debated in the literature, as have the nature and relationships of the Hickman and Yehiniko batholiths. Brown et al. (1996) and Logan et al. (2000) described the Hickman batholith as a complex multi-zoned intrusive body of largely granodioritic composition which is cross-cut by the younger quartz

monzonitic Yehiniko batholith. The geochemistry of the Hickman batholith, Yehiniko batholith, and the felsic intrusive dykes within the deposit are indistinguishable, however, all exhibiting similar major element chemistry, trace element chemistry, and listric REE patterns. In addition, the geochronological data indicate that the ages of the Yehiniko batholith, Hickman batholith, and mineralized dykes cannot be distinguished outside of error, and were all emplaced sometime in the period 235–220 Ma. Together, these data indicate that the Yehiniko batholith may not be a unique intrusive body, but may instead simply be a separate phase of the Hickman batholith.

Only three intrusive bodies with a similar age to Schaft Creek are known in the region, and together these plutons make up the Stikine Plutonic Suite. This suite includes the Hickman batholith (best estimate age of 222.1 ± 9.6 Ma; this study), the Cake Hill pluton of the Hotailuh batholith (221 ± 3 Ma; Anderson and Bevier, 1992), and the Stikine batholith which is believed to be of roughly the same age (Anderson, 1993). Based largely on field relationships, these three batholiths are thought to be co-magmatic with the Stuhini Group volcanic rocks (Holbek, 1988; Anderson, 1989; Anderson, 1993; Logan and Koyanagi, 1994; Brown et al., 1995; Logan et al., 2000). Woodsworth et al. (1991) observed that the Late Triassic Stikine Suite plutons only occur within the Stikine Arch to the north and west of the Bowser basin, and suggested that a number of other batholiths in the Stikinia terrane may also belong to the Stikine Plutonic suite.

Geochemical and geochronological evidence support the conclusion that the Stikine Suite plutons and the Stuhini Group volcanic rocks are co-magmatic. The Mess Lake facies Stuhini Group volcanic rocks and the felsic intrusive rocks of the Hickman batholith exhibit broadly similar trace element and REE patterns, with the volcanic rocks exhibiting more flat-lying and less fractionated REE patterns than the intrusive rocks. Two separate studies of the Stuhini Group volcanic rocks from two different areas yielded U-Pb zircon ages of 227 ± 1 Ma (Gunning, 1993, in Brown et al., 1995) and $212.8 +4.2/-3.5$ Ma (Logan et al., 2000), the latter date being interpreted to represent an upper bound to the age of the group

(Logan et al., 2000) possibly indicating a protracted period of volcanic activity. Additional U-Pb zircon geochronology on the Mess Lake facies of the Stuhini Group volcanic rocks in the deposit area would help to further constrain the relative timing of the volcanic and intrusive rocks.

6.2 – Nature of the Schaft Creek Porphyry System

The northern Stikinia terrane hosts a number of significant porphyry copper deposits of both calc-alkaline and alkaline affinity. The seven deposits listed in Table 6.1 can also be classified as conforming to one of three porphyry deposit models: the Lowell and Guilbert (1970) felsic calc-alkalic porphyry model, the Hollister (1975) diorite calc-alkalic porphyry model, or the alkalic porphyry model (Lang et al., 1995a; Lang et al. 1995b). The differences in these models derive from the chemistry of the host rocks and the mineralizing intrusive bodies. The Schaft Creek deposit broadly falls into the felsic porphyry category, but has some features in common with dioritic porphyries. The alkalic model pertains only to deposits hosted in alkalic host volcanic rocks, and is therefore not considered further here.

In the Lowell and Guilbert (1970) model, the mineralizing intrusive rocks are typically granodioritic to quartz-monzonitic in composition, and quartz diorite intrusions are also commonly observed nearby. In the Hollister (1975) model, the associated intrusive rocks are potassium feldspar rich and silica deficient syenites to monzonites. Commonly associated with these syenitic to monzonitic intrusives are dioritic intrusive bodies, from which this model derives its name.

One key distinction between the Lowell and Guilbert (1970) and Hollister (1975) models is the lack of quartz-sericite-pyrite phyllic alteration assemblages in the latter. This facies is absent from the diorite model because the intrusive rocks generating the hydrothermal fluids have lower silica and higher iron contents, so alteration assemblages

Table 6.1 - A comparison of northern Cordilleran porphyry deposits to classic porphyry deposit models.

Deposit	Type	Coordinates	Age (Method)	Measured and Indicated resources				Host Rocks	Intrusive Rocks	Alteration
				Size (Mt)	Cu (wt. %)	Mo (wt. %)	Au (g/t)			
Lowell and Guilbert, 1970	Felsic cal-alkaline		-	deposit model	-	-		Granodiorite to quartz-monzonite, quartz diorite	Potassic (orthoclase-biotite or orthoclase-chlorite), phyllic (quartz-sericite-pyrite), argillic, and propylitic.	
Hollister, 1975	Dioritic cal-alkaline		-	deposit model	-	-		Syenite-monzonite, diorite	Potassic (orthoclase-biotite or orthoclase-chlorite), and propylitic.	
Schaff Creek	Calc-alkaline	57°21' N 131°00' W	222.4 ± 2.3 Ma (Re-Os)	718	0.30	0.020	0.22	Late Triassic Stuhini Group.	Potassic, phyllic (chlorite-sericite), propylitic, hematite, carbonate.	
Keness North	Calc-alkaline	57°02' N 126°47' W	~202 Ma (U-Pb)	407	0.22	-	0.41	Late Triassic to Early Jurassic Takla Group Early Jurassic Hazelton Group.	Early potassic alteration (biotite-rich) overprinted by phyllic alteration (quartz-sericite ± pyrite).	
Keness South	Calc-alkaline	57°02' N 126°47' W	~202 Ma (U-Pb)	109.4	0.23	-	0.71	Late Triassic to Upper Jurassic Takla group Early Jurassic Hazelton group.	Early potassic alteration (K-feldspar rich) overprinted by phyllic alteration (quartz-sericite ± pyrite); second potassic alteration event. Supergene zone: 20% of mineralization.	

Table 6.1 cont.

Deposit	Type	Coordinates	Age (Method)	Measured and Indicated resources				Host Rocks	Intrusive Rocks	Alteration
				Size (Mt)	Cu (wt. %)	Mo (wt. %)	Au (g/t)			
Kerr	Calc-alkaline	56°28' N 130°16' W	~197 Ma (U-Pb)	74	0.74	-	0.34	Late Triassic Stuhini Group.	Porphyritic potassic monzonite.	Chlorite-bearing alteration, which is flanked by a phyllic alteration (sericite-quartz ± pyrite).
Sulphurets	Calc-alkaline	56°30' N 130°15' W	~196 Ma (U-Pb)	39.3	0.32	-	1.05	Early Jurassic Hazelton Group.	Feldspar porphyry (Main Copper zone) Raewyn quartz monzonite (Gold zone).	Potassic, phyllic, propylitic, advanced argillic.
Galore Creek	Alkaline	57°08' N 131°27' W	~210 Ma (U-Pb)	748.9	0.52	-	0.30	Late Triassic Stuhini Group.	Galore Creek syenite intrusions.	Ca-K-silicate (garnet), potassic, propylitic. Late sericite-anhydrite-carbonate alteration overprints earlier alteration.
Red Chris	Alkaline	57°42' N 129°47' W	~210 Ma (U-Pb)	446.1	0.36	-	0.29	Late Triassic Stuhini Group.	Early Jurassic monzonite to quartz monzodiorite porphyry.	Potassic, phyllic, argillic, propylitic. Abundant late carbonate alteration.

Table 6.1 cont.

Deposit	Metallic minerals	Veining	Grade Distribution	Structure	References
Lowell and Guilbert, 1970	Copper and molybdenum sulphides.	Quartz-dominated veins hosting sulphides sometimes with minor orthoclase, biotite, or sericite.	Copper mineralization is highest at or near the boundary between phyllic and potassic alteration zones. The propylitic zone is typically barren. Ore typically occurs as disseminations in the potassic zone and in quartz veins in the phyllic zone.	Not part of original model.	Lowell and Guilbert, 1970
Hollister, 1975	Copper sulphides, abundant magnetite	Quartz veins are present, as are veins of chlorite, epidote, and albite. Carbonate veins maybe important in some deposits.	Copper mineralization will occur in the potassic zone as both disseminations and fracture fillings. Mineralization may extend outwards into the propylitic zone. High gold, low molybdenum:chalcopyrite ratios.	Not part of original model.	Hollister, 1975
Schaft Creek	Cpy, Bn, Mo, Py.	Early barren quartz, quartz-dominated veins with bornite and chalcopyrite, carbonate-dominated veins with chalcopyrite and pyrite, late carbonate-dominated veins.	Highest grade zones associated with potassic alteration and hydrothermal stockwork zones. Most mineralization is vein-hosted.	Significant syn- and post-mineralization deformation.	Spilsbury (1995) and this paper
Kemess North	Cpy, Py, weak Bn, Mo; supergene-native Cu, Cct.	Mineralized veins contain quartz, pyrite, and chalcopyrite. Late-stage pyrite stringers are cut by post-mineralization carbonate-rich, anhydrite-rich, and chlorite-rich veins.	Highest grade zone is characterized by secondary biotite.	Post-mineralization faults have modified final distribution of the ore body to present configuration.	1, 2, 3, 4
Kemess South	Pyrite: Veins, fracture coatings, and quartz stringers Chalcopyrite: disseminations and quartz stockwork veins	Similar vein petrography as Kemess North.	Highest grades in zones of intense quartz stockwork and potassic alteration vein halos.	Same as Kemess North.	1, 2, 3, 4

Table 6.1 cont.

Deposit	Metallic minerals	Veining	Grade Distribution	Structure	References
Kerr	Cpy, Bn, Py, tetrahedrite, temantite.	Quartz stockwork mineralization is dominant; py ± qtz, ser, minor cpy; qtz ± py, carb, anh, ser, chl, cpy; anh ± cpy; carb ± minor cpy, bn; qtz + carb, chl, cpy.	Mineralization is related to a north-trending pyritic zone which follows the monzonitic intrusions. Strongly deformed with significant remobilization of mineralization. Highest grades are associated with chlorite-bearing alteration.	Deformation coincides with period of carbonate veining with minor chalcopyrite and bornite which follows main mineralization event. Significant late deformation resulting in remobilization of metallic minerals.	2, 5, 6
Sulphurets	Cpy, gold, Py, Mo, Mt.	Quartz stockwork mineralization, fluorite veins.	Disseminations in potassic alteration, and in argillic alteration as veins and in wall rock.	Syn- and post-mineralization deformation.	2, 5, 7, 8, 9
Galore Creek	Cpy, Bn, Mt, Py, sphalerite.	Magmatic-hydrothermal breccia system.	Highest grades occur in potassically-altered host rocks. Lower grades are associated with sericite-anhydrite-carbonate alteration overprint, indicating possible leaching or remobilization. Mineralization dominantly occurs as disseminations.	Pre-mineralization mylonite zone, mineralized breccia zones are aligned to regional structures. Late faults subtly deformed the system.	1, 2, 7, 10, 11, 16, 17
Red Chris	Cpy, Bn, Fringe zones - Py, Mt.	Quartz stockwork mineralization. Local gypsum veins. Late quartz-carbonate veins carrying trace galena and sphalerite.	Mineralization largely occurs in stockwork veins. A high-grade core contains sheeted quartz-chalcopyrite veins.	Complex faulting within the deposit area which makes correlation between drillholes difficult.	2, 13, 14, 15, 16, 17

Abbreviations: Bn = bornite; Cct = chalcocite; Cpy = chalcopyrite; Mo = molybdenite; Mt = magnetite; Py = pyrite. References: 1 = Mortensen et al. (1995); 2 = McMillan et al. (1995); 3 = Duuring et al. (2006); 4 = Rebagliati et al. (1995); 5 = Seabridge Gold Inc. (2007); 6 = Ditson et al. (1995); 7 = Margolis and Britten (1995); 8 = Fowler and Wells (1995); 9 = Kirkham and Margolis (1995); 10 = Logan and Koyanagi (1994); 11 = Lechner (2006); 12 = Enns et al. (1995); 13 = Newell and Peatfield (1995); 14 = Baker et al. (1995); 15 = Collins et al. (2004); 16 = Lang et al. (1995a); 17 = Lang et al. (1995b).

tend to be less quartz rich with more abundant chlorite in place of sericite. The propylitic alteration facies thus tends to directly abut the potassic alteration zone in the diorite model.

Hollister (1975) observed that mineralization in dioritic porphyries continues beyond the potassic alteration facies and into the surrounding propylitic alteration facies, similar to the mineralization extending into the phyllic alteration zone of Lowell and Guilbert (1970). No differences in alteration style were observed by Hollister (1975) that could be used to predict the presence of mineralization in the propylitic alteration facies. However, a possible method of identifying the mineralized portion of propylitic alteration in dioritic porphyries was identified at Schaft Creek, where it was observed that the potassic alteration facies gave way to a surrounding transitional alteration facies of sericite and chlorite, which was mineralized. This zone in turn gives way to the surrounding poorly mineralized propylitic alteration facies, which is distinguished from the sericite-chlorite facies by the additional presence of epidote.

A number of other differences exist between the two calc-alkalic models. Whereas deposits that conform to the Lowell and Guilbert (1970) model have abundant quartz veins which carry mineralization, deposits of the Hollister (1975) model often display mineralized veins of chlorite, epidote, albite, and carbonate. This is again a direct result of the lower silica contents of the host dioritic intrusive rocks.

Another major difference between the two calc-alkalic deposit models is that deposits of the diorite model typically bear no appreciable molybdenum, whereas this element is common in more felsic deposits. Gold mineralization behaves oppositely, with diorite model deposits being richer in gold compared with more felsic systems.

The Schaft Creek deposit does not fit perfectly into either of the calc-alkalic models. Although the deposit is spatially associated with dioritic intrusive rocks, these are not the mineralizing bodies. Instead, the mineralizing fluids at Schaft Creek are thought to have been derived from a more felsic granodioritic intrusion. However, the style of alteration at

Schaft Creek does largely conform to that proposed by Hollister (1975), with the addition of the sericite-chlorite alteration described above. The nature of veins at Schaft Creek is also consistent with the diorite model because of the importance of carbonate veins in mineralization. The high abundance of molybdenite and relatively low grades of Au in the Schaft Creek deposit are, however, more in agreement with the Lowell and Guilbert (1970) model.

None of the deposits used as examples by Lowell and Guilbert (1970) are hosted by volcanic country rocks that are as mafic as those at Schaft Creek. It is possible that the hybrid nature of the Schaft Creek deposit arises as a result of the combination of the more mafic composition of the dominant country rocks and the fluids being generated by a granodioritic body. The difference in chemistry of the wall-rocks could explain the quartz-poor sericite-chlorite alteration assemblage, whereas the Mo-rich nature of the mineralization could be explained by derivation of the ore fluids from a more felsic granodioritic intrusive system.

The large volume of fluid that would be required to form a major porphyry deposit would require an intrusive body of at least 100 km³ (Cline and Bodnar, 1991; Ulrich et al., 1999; Liu and McPhail, 2005; Richards, 2005). The Hickman batholith to the west of the deposit is greatly in excess of the minimum required size and is the most likely source pluton. Orientation of measured strata (~292°/67°NE) indicates that the Hickman batholith would likely have intruded directly beneath the volcanic rocks that host the deposit. Some authors believe that a satellite pluton to the Hickman batholith may currently directly underlie the deposit, and that the intrusion of this undiscovered pluton may have caused much of the small-scale deformation observed in the deposit (Fox et al., 1976; Ewanchuk et al., 2007). Such a hypothesis would be consistent with the mapping of Logan et al. (2000), who described a roughly north-south-trending dioritic body ~4 km in length and less than 1 km wide occurring 4 km east of the Schaft Creek deposit, on the western slope of the Mess Creek valley. Logan et al. (2000) suggested that this dioritic body might be

a border phase of the larger equigranular Hickman batholith. If this is the case, then it is possible that the Stuhini Group volcanic rocks in the Schaft Creek area are all underlain by intrusive rocks of the Hickman batholith, consistent with identification of this body as the source of mineralizing fluids.

6.3 – Schaft Creek Compared with other Porphyry Systems in Northern British Columbia

Most of the deposits listed in Table 6.1 are found within volcanic rocks of the Stuhini Group. Exceptions are the Kemess and Sulphurets deposits, which are both hosted in younger Early Jurassic Hazelton Group volcanic rocks (Rebagliati et al., 1995; Kirkham and Margolis, 1995). The Kemess deposit is also partly hosted by Late Triassic Takla Group volcanic rocks (Rebagliati et al., 1995), which are believed to be the southerly equivalent to the more northern and western Stuhini Group volcanic rocks (Logan and Koyanagi, 1994).

Whereas most calc-alkaline deposits in northern Stikinia are associated with monzonitic to monzodioritic intrusive rocks (Table 6.1), the Schaft Creek deposit is associated with granodioritic rocks of the Hickman batholith. Schaft Creek is also unique in that it is the only deposit in the area to host significant amounts of molybdenum (Table 6.1). Alteration amongst the various calc-alkaline deposits in northern Stikinia typically conforms to that described by the models of either Lowell and Guilbert (1970) or Hollister (1975). As in the diorite model, alkalic deposits are also missing typical phyllic alteration zones due to the low abundance of silica in these systems (Lang et al., 1995a; Lang et al., 1995b). Therefore, the alteration observed at Galore Creek and Schaft Creek is similar, because neither of these deposits exhibit quartz-sericite-pyrite phyllic alteration (Margolis and Britten, 1995). However, alteration at Galore Creek is unique in this part of the Cordillera because it exhibits a garnet-bearing Ca-K-silicate alteration phase which is similar to that observed in skarn environments (Logan and Koyanagi, 1994; Margolis and

Britten, 1995). This unusual alteration at Galore Creek is subsequently overprinted by late carbonate alteration, a feature shared by the Red Chris and Schaft Creek deposits (Logan and Koyanagi, 1994; Margolis and Britten, 1995; Newell and Peatfield, 1995; Baker et al., 1997).

In general, porphyry copper deposits of the northern Stikinia terrane have their highest ore grades within zones of potassic alteration and quartz stockworks or breccias (Table 6.1). The Kerr deposit is the exception to this rule, with the highest grades occurring in chlorite-bearing alteration facies (Ditson et al., 1995). However, these workers report a high degree of deformation which has resulted in the remobilization of metallic minerals and also possibly the alteration of potassic zone biotite to chlorite (Ditson et al., 1995). The Kerr deposit is also unusual in that it hosts significant amounts of mineralization within carbonate-dominated veins (Ditson et al., 1995), in the same way as at Schaft Creek. This observation is consistent with the Hollister (1975) porphyry model.

All deposits in the area have experienced significant structural modification since original formation, and thus have been subjected to varying degrees of dislocation from the typical concentric zonation of the Lowell and Guilbert (1970) model. The structural modification reported in these deposits likely arises as a result of the multiple collisional events suggested for this area of the northern Cordillera (Logan et al., 2000).

6.4 – Deposit Exploration

This study of the Schaft Creek deposit was limited by a number of factors which must be considered in further exploration work on the property. The primary difficulty in interpretation of the system is lack of exposure within the deposit. This, coupled with the intense structural modification of the system during and after formation, makes it difficult to develop a robust geological model for the deposit. However, a number of observations were made that may help in future exploration on the property, including clarification of the

nature of the Purple Volcanic unit and the distribution of deposit zones.

The origin of the Purple Volcanic unit has been debated in the literature, in part because any contact between the Purple Volcanics and the underlying green volcanic rocks has been largely obscured by overburden. However, a number of workers report observing a several-metre wide fault separating the two colours of volcanic rocks (Linder, 1975; Fox et al., 1976; Seraphim et al., 1976). Linder (1975) argued that the hematized volcanic rocks are late and unconformably overlie the green volcanic rocks. For these reasons, the hematized volcanic rocks have largely been treated as a hard boundary to mineralization, and exploration and drilling in the hematized volcanic rocks thus remains limited.

Some authors, however, have observed weak mineralization locally in the hematized volcanic rocks (Fox et al., 1976; Seraphim et al., 1976). Fox et al. (1976) observed the hematized rocks to grade into the magnetite-rich green volcanic rocks to the north of the deposit, a feature confirmed by this author. In the current drilling program, hematization has also been encountered at depth (drillhole 06CF284 at 216m depth), where it overprints potassic alteration and mineralization (Fig. 5.5c). These observations, coupled with the abundance of hematite-bearing carbonate veins, provide strong evidence that the hematized volcanic rocks are simply a late hydrothermal alteration feature, and are not representative of a late distinct volcanic unit, nor are they related to a late supergene alteration phase. Weak chalcopyrite mineralization was also observed within the hematized volcanic rocks to the north of the deposit area. For these reasons, the hematite-altered volcanic rocks may in fact host mineralization, and should be considered in future exploration of the deposit.

It may be possible to indirectly constrain the relative timing of the hematite veining and alteration event and the major barren carbonate veining observed throughout the area by comparing the relationships of each of these events with the intruding late mafic dykes. In one instance, a fine-grained basaltic dyke was observed to follow an earlier carbonate breccia vein within the Main zone of the deposit (Fig. 4.8f), indicating that at least one period of dyke formation followed at least one period of carbonate vein emplacement. In

the peripheries of the Main zone in surface outcrop, late basaltic dykes are observed to cross-cut the earlier volcanic rocks. However, in a number of instances to the south-east of the deposit, these late mafic dykes exhibit a strong red to purple colouration characteristic of hematization (Fig. 4.8d). This would indicate that it is possible that the carbonate breccia veins were emplaced first, followed by intrusion of the late mafic dykes, and subsequently the hematite \pm carbonate veins and alteration. However, very fine carbonate veins (<1 mm wide) cross-cut the mafic dyke. This may indicate that the carbonate veining period was protracted and occurred over the same time period as mafic dyke emplacement, or that there may have been multiple carbonate veining events.

These late alteration and veining events followed the main mineralization period and the formation of the three deposit zones. The three different zones of the Schaft Creek deposit each have distinct geology, alteration, and mineralization with respect to each other. Although inadequate structural information exists in order to develop a robust model, it is possible to draw a number of conclusions regarding the orientation of the deposit as a result of the unique features of the three deposit zones. The Paramount zone, is dominated by granodioritic intrusive rocks and intrusive breccias, and also has the highest proportion of potassic alteration. The zone is host to a large number of early barren quartz veins which would be the earliest and highest-temperature fluids released from a cooling magma body. In addition, the zone is strongly mineralized, and hosts the highest proportion of bornite relative to chalcopyrite and pyrite. Collectively, these features indicate that in a classical porphyry shell model such as the Lowell and Guilbert (1970) model, the Paramount zone forms one of the lower-most and deepest sections of the porphyry system.

The Main zone contains less granodioritic intrusive material in narrower dykes. Potassic alteration in this zone remains abundant but is less pervasive, occurring instead as variable-width potassic haloes around veins. Sericite-chlorite alteration is also abundant, and the zone exhibits a lower proportion of bornite relative to chalcopyrite. These features suggest that the zone is genetically similar to the Paramount zone, but is further from the

source of the mineralizing fluids.

The West Breccia zone is somewhat unique when compared to the other two zones. This zone exhibits some of the intrusive breccias that are characteristic of the Paramount zone, but exhibits none of the corresponding potassic alteration. The West Breccia zone is instead dominated by low-temperature propylitic alteration and quartz-tourmaline hydrothermal breccias rich in pyrite and chalcopyrite. All of these properties lead to the conclusion that the West Breccia zone is a lower-temperature part of the hydrothermal system. Because the hydrothermal breccia overprints earlier intrusive brecciation, it appears likely that the West Breccia zone is a late rather than a more distal feature of the system. If the zone were more distal, it would likely not be coincident with the intrusive breccia phase. Several authors have suggested that the West Breccia zone is fault-controlled (Linder, 1975; Fox et al., 1976; Spilsbury, 1995), which would be consistent with the roughly linear distribution of the zone.

7 – CONCLUSIONS

The Schaft Creek deposit is a major unexploited porphyry copper deposit in the northern Cordillera of British Columbia. The deposit is hosted by the basaltic to andesitic Mess Lake facies of the Stuhini Group volcanic rocks, which were formed in a continental-arc setting in the Late Triassic. The crystallization of the underlying Hickman/Yehiniko batholith complex resulted in the release of fluids and granodioritic porphyritic dykes into the overlying Stuhini Group volcanic sequence, creating the Schaft Creek porphyry Cu-Mo deposit.

The age of intrusion of the Hickman batholith is approximately constrained by a composite U-Pb zircon date of 222.1 ± 9.6 Ma, which is in broad agreement with a well-constrained age for Schaft Creek mineralization of 222.0 ± 0.8 Ma (Re-Os molybdenite). No evidence was found to indicate that the Yehiniko batholith represents a distinct younger intrusive event, and it is therefore believed that this batholith represents a part of the larger complexly zoned Hickman batholith.

The deposit is not unique in the northern Cordillera, and shares many features with other nearby deposits such as Galore Creek, Red Chris, Kerr, and Kemess. The Schaft Creek porphyry system largely conforms to a traditional porphyry model, but shares aspects of both the Lowell and Guilbert (1970) and Hollister (1975) models because of the effect of the mafic host volcanic rocks on the fluids exsolved from the felsic to intermediate Hickman batholith. The result of this interaction is a typical high-grade potassic alteration zone that abuts a lower-grade sericite-chlorite alteration zone with an outer barren propylitic zone.

Sulphide minerals in the Schaft Creek deposit include bornite, chalcopyrite, pyrite, molybdenite, and trace covellite and chalcocite. Magnetite and hematite are also present, with hematite commonly appearing as a late hydrothermal alteration phase. The deposit can be separated into three distinct, but related, zones. The northernmost of these zones is the Paramount zone, which comprises abundant granodioritic porphyry and intrusive breccias,

and hosts more bornite and less pyrite with respect to the other zones. Mineralization in the Paramount zone occurs within hydrothermal veins and breccias, and as disseminations. The Main zone is the largest of the mineralized zones and occurs south of the Paramount zone. Basaltic to andesitic volcanic rocks are the dominant lithology in the Main zone, and these rocks host chalcopyrite, bornite, and molybdenite in hydrothermal veins and breccias. The West Breccia zone is unique from the other two zones and occurs south of the Paramount zone and west of the Main zone. The West Breccia zone is dominated by a quartz-carbonate-tourmaline hydrothermal breccia system that hosts abundant chalcopyrite and pyrite with rare bornite and molybdenite.

Two phases of mineralization are observed in the deposit. The main phase is observed in all deposit zones, is associated with potassic and sericite-chlorite alteration, and comprises the bulk of mineralization in the deposit. Mineralization consists mainly of bornite, chalcopyrite, pyrite, and molybdenite occurring within quartz- and carbonate-dominated veins and breccias, sulphide-dominated veins and breccias, and tourmaline-bearing veins and breccias. The second phase of mineralization is minor and does not exhibit any appreciable alteration. It consists of veins of molybdenite \pm specularite as well as Cu-Pb-Zn veins which contain variable amounts of chalcopyrite, galena, and sphalerite. The molybdenite \pm specularite veins are observed throughout the deposit, whereas the Cu-Pb-Zn veins are mainly restricted to the West Breccia Zone.

Significant structural modification coincided with and followed deposit formation, making deposit reconstruction at the time of formation difficult. Conclusions that can be drawn without structural reconstruction are that the Paramount zone represents the earliest and deepest zone of the deposit, the Main zone is stratigraphically higher or later than the Paramount zone, and the West Breccia zone represents a fault-bound phase of deposit formation. Further structural analysis may help to reconstruct and resolve the orientation of the deposit.

REFERENCES

- Anderson, R.G., 1989, A stratigraphic, plutonic, and structural framework for the Iskut River map area, northwestern British Columbia: Current Research, Part E, Geological Survey of Canada, Paper 89-1E, p. 145-154.
- Anderson, R.G., 1993, A Mesozoic stratigraphic and plutonic framework for northwestern Stikinia (Iskut River area), northwestern British Columbia, Canada: *in* Dunn, G. and McDougall, K., eds., Mesozoic Paleogeography of the Western United States – II, Pacific Section Society of Economic Paleontologists and Mineralogists, Book 71, p. 477-494.
- Anderson, R.G., and Bevier, M.L., 1992, New Late Triassic and Early Jurassic U-Pb zircon ages from the Hotailuh Batholith, Cry Lake map area, north-central British Columbia: Radiogenic Age and Isotopic Studies: Report 6, Geological Survey of Canada, Paper 92-2, p. 145-152.
- Baker, T., Ash, C.H., and Thompson, J.F.H., 1997, Geological setting and characteristics of the Red Chris porphyry copper-gold deposit, northwestern British Columbia: Exploration Mining Geology, v. 6, p. 297-316.
- Brenan, J.M., Shaw, H.F., Phinney, D.L., and Ryerson, F.J., 1994, Rutile – aqueous fluid partitioning of Nb, Ta, Hf, Zr, U and Th: Implications for high field strength element depletions in island arc basalts: Earth and Planetary Science Letters, v. 128, p. 327-339.
- Brown, D.A., Gunning, M.H., and Greig, C.J., 1996, The Stikine Project: Geology of Western Telegraph Creek Map Area, Northwestern British Columbia (NTS 104G/5, 6, 11W, 12 and 13): British Columbia Ministry of Employment and Investment – Energy and Minerals Division, Bulletin 95, 182 p.
- Cline, J.S., and Bodnar, R.J., 1991, Can Economic Porphyry Copper Mineralization be Generated by a Typical Calc-Alkaline Melt?: Journal of Geophysical Research, v. 96, p. 8113-8126.
- Collins, J., Colquhoun, W., Giroux, G.H., Nilsson, J.W., and Tenney, D., 2004, Technical report on the Red Chris copper-gold project, Liard Mining Division: Red Chris Development Company Ltd. and bcMetals Corporation, December 16, 229 p.
- Deer, W.A., Howie, R.A., and Zussman, J., 1992, An introduction to the rock-forming minerals – second edition: Pearson – Prentice Hall, Toronto, 696 p.
- Ditson, G.M., Wells, R.C., and Bridge, D.J., 1995, Kerr: The geology and evolution of a deformed porphyry copper-gold deposit, northwestern British Columbia: *in* Schroeter, T.G., ed., Porphyry deposits of the northwestern Cordillera, Canadian Institute of Mining, Metallurgy, and Petroleum Special Volume 46, p. 509-523.
- Duuring, P., Rowins, S.M., McKinley, B., and Orr, A.J., 2006, Porphyry cousins? Geological comparison of the Kemess South and Kemess North porphyry Au-Cu (Mo) deposits, Toadogone district, British Columbia: Geological Society of America Abstracts with Programs, v. 38, No. 5, p. 70.
- Enns, S.G., Thompson, J.F.H., Stanley, C.R., and Yarrow, E.W., 1995, The Galore Creek porphyry copper-gold deposits, northwestern British Columbia: *in* Schroeter, T.G., ed., Porphyry deposits of the northwestern Cordillera, Canadian Institute of Mining, Metallurgy, and Petroleum Special Volume 46, p. 630-644.
- Ewanchuk, S., Fischer, P., and Hanych, W., 2007, 2006 Diamond Drill Report, Schaft Creek Property, Northwestern British Columbia: CopperFox Metals Inc. report, p. 60.

- Foley, S.F., Barth, M.G., and Jenner, G.A., 2000, Rutile/melt partition coefficients for trace elements and an assessment of the influence of rutile on the trace element characteristics of subduction zone magmas: *Geochimica et Cosmochimica Acta*, v. 64, p. 933-938.
- Fowler, B.P., and Wells, R.C., 1995, The Sulphurets Gold zone, northwestern British Columbia: *in* Schroeter, T.G., ed., *Porphyry deposits of the northwestern Cordillera*, Canadian Institute of Mining, Metallurgy, and Petroleum Special Volume 46, p. 484-498.
- Fox, P.E., Grove, E.W., Seraphim, R.H., and Sutherland Brown, A., 1976, Schaft Creek: *in* Sutherland Brown, A., ed., *Porphyry Deposits of the Canadian Cordillera*, CIM Special Volume 15, p. 219-226.
- Frey, F.A., Chappell, B.W., and Roy, S.D., 1978, Fractionation of rare-earth elements in the Tuolumne intrusive series, Sierra Nevada batholith, California: *Geology*, v. 6, p. 239-242.
- Gabrielse, H., and Yorath, C.J., 1991, Tectonic Synthesis, Chapter 18: *in* Gabrielse, H., Yorath, C.J., eds., *Geology of the Cordilleran Orogeny in Canada*, Geological Survey of Canada, *Geology of Canada*, No. 4, p. 677-705.
- Hanes, J.A., 1991, K-Ar and $^{40}\text{Ar}/^{39}\text{Ar}$ geochronology: Methods and applications: *in* Heaman, L.M., Ludden, J.N., eds., *Applications of Radiogenic Isotope Systems to Problems in Geology*, Mineralogical Association of Canada Short Course Handbook, v. 19, p. 27-57.
- Hanson, G.N., 1980, Rare earth elements in petrogenetic studies of igneous systems: *Annual Reviews of Earth Planetary Science*, v. 8, p. 371-406.
- Heaman, L.M., Erdmer, P., and Owen, J.V., 2002, U-Pb geochronological constraints on the crustal evolution of the Long Range Inlier, Newfoundland: *Canadian Journal of Earth Sciences*, v. 39, p. 845-865.
- Holbek, P.M., 1988, Geology and mineralization of the Stikine assemblage, Mess Creek area, northwestern British Columbia: Unpublished M.Sc. Thesis, University of British Columbia, 184 p.
- Hollister, V.F., 1975, An appraisal of the nature and source of porphyry copper deposits: *Minerals Science Engineering*, v. 7, p. 225-233.
- Irvin, T.N., and Baragar, W.R.A., 1971, A guide to the chemical classification of the commonplace volcanic rocks: *Canadian Journal of Earth Science*, v. 8, p. 523-548.
- Kirkham, R.V., and Margolis, J., 1995, Overview of the Sulphurets area, northwestern British Columbia: *in* Schroeter, T.G., ed., *Porphyry deposits of the northwestern Cordillera*, Canadian Institute of Mining, Metallurgy, and Petroleum Special Volume 46, p. 473-483.
- Lang, J.R., Stanley, C.R., and Thompson, J.F.H., 1995a, Porphyry copper-gold deposits related to alkalic igneous rocks in the Triassic-Jurassic arc terranes of British Columbia: *in* Pierce, F.W., and Bolm, J.G., eds., *Porphyry copper deposits of the American Cordillera*, Arizona Geological Society Digest 20, p. 219-236.
- Lang, J.R., Stanley, C.R., Thompson, J.F.H., and Dunne, K.P.E., 1995b, Na-K-Ca magmatic hydrothermal alteration in alkalic porphyry Cu-Au deposits, British Columbia: *in* Thompson, J.F.H., ed., *Magma, fluids, and ore deposits*: Mineralogical Association of Canada Short Course, v. 23, p. 339-366.
- Lechner, M.J., 2006, Updated Galore Creek mineral resources, northwestern British Columbia: NovaGold Resources Inc., 403 p.
- Linder, H., 1975, Geology of the Schaft Creek Porphyry Copper-Molybdenum Deposit, Northwestern B.C.:

CIM Bulletin, v. 68, p. 49-63.

Liu, W., and McPhail, D.C., 2005, Thermodynamic properties of copper chloride complexes and copper transport in magmatic-hydrothermal solutions: *Chemical Geology*, v. 221, p. 21-39.

Logan, J.M., Drobe, J.R., and McClelland, W.C., 2000, British Columbia Geological Survey Bulletin 104: Geology of the Forrest Kerr-Mess Creek area, Northwestern British Columbia (NTS 104B/10, 15 & 104G/2 and 7W): British Columbia Ministry of Energy and Mines, Victoria, 164 p.

Logan, J.M., and Koyanagi, V.M., 1994, Geology and mineral deposits of the Galore Creek area (104G/3, 4), Bulletin 92: British Columbia Ministry of Energy, Mines and Petroleum Resources, 102 p.

Lowell, J.D., and Guilbert, J.M., 1970, Lateral and vertical alteration-mineralization zoning in porphyry ore deposits: *Economic Geology*, v. 65, p. 373-408.

Ludwig, K.R., 2003, Isoplot/Ex, A geochronological toolkit for Microsoft Excel, Version 3.00: Berkeley Geochronology Centre Special Publication No. 4, California.

Margolis, J., and Britten, R.M., 1995, Porphyry-style and epithermal copper-molybdenum-gold-silver mineralization in the northern and southeastern Sulphurets district, northwestern British Columbia: *in* Schroeter, T.G., ed., *Porphyry deposits of the northwestern Cordillera*, Canadian Institute of Mining, Metallurgy, and Petroleum Special Volume 46, p. 473-483.

McMillan, W.J., 1992a, Overview of the tectonic evolution and setting of mineral deposits in the Canadian Cordillera: *Ore Deposits, Tectonics and Metallogeny in the Canadian Cordillera*, British Columbia Ministry of Energy, Mines, and Petroleum Resources, Paper 1991:4, p. 5-24.

McMillan, W.J., 1992b, Porphyry deposits in the Canadian Cordillera: *Ore Deposits, Tectonics and Metallogeny in the Canadian Cordillera*, British Columbia Ministry of Energy, Mines, and Petroleum Resources, Paper 1991:4, p. 253-276.

McMillan, W.J., Thompson, J.F.H., Hart, C.J.R., and Johnston, S.T., 1995, Regional geological and tectonic setting of porphyry deposits in British Columbia and Yukon Territory: *in* Schroeter, T.G., ed., *Porphyry Deposits of the Northwestern Cordillera of North America*, CIM Special Volume 46, p. 40-57.

Monger, J.W.H., 1977, Upper Paleozoic rocks of the western Canadian Cordillera and their bearing on Cordilleran evolution: *Canadian Journal of Earth Sciences*, v. 14, p. 1832-1859.

Monger, J.W.H., 1989, Overview of Cordilleran Geology: *in* Ricketts, B., ed., *Western Canada Sedimentary Basin: A Case History*, Canadian Society of Petroleum Geologists, Chapter 2, p. 9-32.

Monger J.W.H., Souther J.G., and Gabrielse, H., 1972, Evolution of the Canadian Cordillera; a plate-tectonic model: *American Journal of Science*, v. 272, p. 577-602.

Monger, J.W.H., Richards, T.A., and Paterson, I.A., 1978, The hinterland belt of the Canadian Cordillera; new data from northern and central British Columbia: *Canadian Journal of Earth Sciences*, v. 15, p. 823-830.

Monger, J.W.H., Price, R.A., and Tempelman-Kluit, D.J., 1982, Tectonic accretion and the origin of the two major metamorphic and plutonic belts in the Canadian Cordillera: *Geology*, v. 10, p. 70-75.

Monger, J., and Price, R., 2002, The Canadian Cordillera; Geology and tectonic evolution: *Canadian Society of Exploration Geophysicists Recorder*, v. 27, February 2002, p. 17-36.

- Mortensen, J.K., Ghosh, D.K., and Ferri, F., 1995, U-Pb geochronology of intrusive rocks associated with copper-gold porphyry deposits in the Canadian Cordillera: *in* Schroeter, T.G., ed., Porphyry deposits of the northwestern Cordillera, Canadian Institute of Mining, Metallurgy, and Petroleum Special Volume 46, p. 142-158.
- Müntener, O., Keelman, P.B., and Grove, T.L., 2001, The role of H₂O during crystallization of primitive arc magmas under uppermost mantle conditions and genesis of igneous pyroxenites: an experimental study: *Contributions to mineralogy and petrology*, v. 141, p. 643-658.
- Newell, J.M., and Peatfield, G.R., 1995, The Red-Chris porphyry copper-gold deposit, northwestern British Columbia: *in* Schroeter, T.G., ed., Porphyry deposits of the northwestern Cordillera, Canadian Institute of Mining, Metallurgy, and Petroleum Special Volume 46, p. 674-688.
- Panteleyev, A., and Dudas B.M., 1972, SNO, BIRD (Liard Copper); NABS (Paramount): *Geology, Exploration and Mining in British Columbia 1972*, British Columbia Department of Mines and Petroleum Resources, p. 527-528.
- Rebagliati, C.M., Bowen, B.K., Copeland, D.J., and Niosi, D.W.A., 1995, Kemess South and Kemess North porphyry gold-copper deposits, northern British Columbia: *in* Schroeter, T.G., ed., Porphyry deposits of the northwestern Cordillera, Canadian Institute of Mining, Metallurgy, and Petroleum Special Volume 46, p. 377-396
- Richards, J.P., 2003, Tectono-Magmatic Precursors for Porphyry Cu-(Mo-Au) Deposit Formation: *Economic Geology*, v. 98, p. 1515-1533.
- Richards, J.P., 2005, Cumulative factors in the generation of giant calc-alkaline porphyry Cu deposits: *in* Porter, P.M., ed., Super porphyry copper and gold deposits: A global perspective, PGC Publishing, Adelaide, South Australia, v. 1, p. 7-25.
- Seabridge Gold Inc., 2007, Kerr-Sulphurets Project, British Columbia: Corporate report, www.seabridgegold.net/PKerrSulSum, accessed 15/09/2007.
- Selby, D., and Creaser, R.A., 2001, Late and Mid-Cretaceous mineralization in the northern Canadian Cordillera: Constraints from Re-Os molybdenite dates: *Economic Geology*, v. 96, p. 1461-1467.
- Seraphim, R.H., Sutherland Brown, A., Grove, E.W., and Linder, H.W., 1976, Geology of the Schaft Creek Porphyry Copper-Molybdenum Deposit, Northwestern B.C. – Discussion and Reply: *CIM Bulletin*, v. 69, p. 96-102.
- Sillitoe, R.H., 1973, The tops and bottoms of porphyry copper deposits: *Economic Geology*, v. 68, p. 799-815.
- Simonetti, A., Heaman, L.M., Chacko, T., and Banerjee, N.R., 2006, In-situ petrographic thin section U-Pb dating of zircon, monazite, and titanite using laser ablation – MC-ICP-MS: *International Journal of Mass Spectrometry*, v. 253, p. 87-97.
- Souther, J.G., 1971, Geology and mineral deposits of the Tulsequah map-area, British Columbia: Geological Survey of Canada, Memoir 362, 84 p.
- Spilsbury, T.W., 1995, The Schaft Creek copper-molybdenum-gold-silver porphyry deposit, northwestern British Columbia: *in* Schroeter, T.G., ed., Porphyry Deposits of the Northwestern Cordillera of North America, CIM Special Volume 46, p. 239-246.

Streckeisen, A.L., 1974, Classification nomenclature of plutonic rocks: *Geologische Rundschau*, v. 63, p. 773-786.

Streckeisen, A.L., 1976, To each plutonic rock its proper name: *Earth Science Reviews*, v. 12, p. 1-33.

Sun, S.-s, and McDonough, W.F., 1989, Chemical and isotopic systematics of oceanic basalts: implications for mantle composition and processes: *in* Saunders, A.D., Norry, M.J., eds., *Magmatism in the Ocean Basins*, Vol. 42, Geological Society of London, Special Publication, p. 313-345.

Ulrich, T., Günter, D., and Heinrich, C.A., 1999, Gold concentrations of magmatic brines and the metal budget of porphyry copper deposits: *Nature*, v. 399, p. 676-679.

Woodsworth, G.J., Anderson, R.G., and Armstrong, R.L., 1991, Plutonic regimes, Chapter 15: *in* Gabrielse, H., and Yorath, C.J., eds., *Geology of the Cordilleran Orogen in Canada*, Geological Survey of Canada, *Geology of Canada*, no. 4, p. 491-531.

SCHAFT CREEK: APPENDICES

	Page
Appendix 1 Geochemical Quality Control: Standards and Duplicates	94
Appendix 1.1 ICP-OES analyses	94
Appendix 1.2 Instrumental neutron activation analyses	96
Appendix 1.3 ICP-MS analyses	97
Appendix 1.4 Total dissolution ICP-OES analyses	101
Appendix 2 Litho geochemistry	102
Appendix 2.1 Major element geochemistry	102
Appendix 2.2 Trace element geochemistry	105
Appendix 3 Mineral Chemistry	110
Appendix 4 Sample descriptions and Locations	122
Appendix 5 Selected petrographic descriptions	140
Appendix 6 2006 mapping outcrop data	155

Appendix I.1 - Inductively Coupled Plasma - Optical Emission Spectroscopy (ICP-OES) geochemical standards and duplicates

Analyte Symbol	SiO ₂	Al ₂ O ₃	Fe ₂ O ₃	MnO	MgO	CaO	Na ₂ O	K ₂ O	TiO ₂	P ₂ O ₅	LOI	Total	Ba	Be	Sr	V	Y	
Unit Symbol	%	%	(T) %	%	%	%	%	%	%	%	%	%	ppm	ppm	ppm	ppm	ppm	
Detection Limit	0.01	0.01	0.01	0.001	0.01	0.01	0.01	0.01	0.001	0.01	0.01	0.01	1	1	2	5	1	
Batch One																		
SY-3 Meas	60.11	11.77	6.25	0.329	2.60	8.27	4.13	4.39	0.147	0.56			447	21	313	51	723	
SY3 Cert	59.62	11.75	6.49	0.320	2.67	8.26	4.12	4.23	0.150	0.54	1.16		450	20	302	50	718	
NIST 694 Meas	11.44	1.93	0.72	0.010	0.37	43.46	0.88	0.57	0.116	30.10			111	4	937	1531	156	
NIST 694 Cert	11.20	1.80	0.79	0.012	0.33	43.60	0.86	0.51	0.110	30.20						1736		
W-2 Meas	52.57	15.46	10.94	0.165	6.36	10.92	2.26	0.64	1.099	0.15	0.60		176	2	196	283	21	
W-2 Cert	52.44	15.35	10.74	0.163	6.37	10.87	2.14	0.63	1.060	0.13			182	1	194	262	24	
DNC-1 Meas	46.54	18.30	9.75	0.148	10.22	11.30	1.92	0.21	0.487	0.08			105	1	140	155	17	
DNC-1 Cert	47.04	18.30	9.93	0.149	10.05	11.27	1.87	0.23	0.480	0.09	0.60		114	1	145	148	18	
BIR-1 Meas	47.81	15.64	11.32	0.171	9.59	13.22	1.83	-0.03	0.977	0.03			9	1	108	338	14	
BIR-1 Cert	47.77	15.35	11.26	0.171	9.68	13.24	1.75	0.03	0.960	0.05			8	1	108	313	16	
GBW 07113 Meas	72.89	13.01	3.16	0.141	0.14	0.59	2.52	5.69	0.284	0.06			495	4	40	6	46	
GBW 07113 Cert	72.78	12.96	3.21	0.140	0.16	0.59	2.57	5.43	0.300	0.05			506	4	43	4	43	
NIST 1633b Meas	48.61	28.27	11.00	0.016	0.79	2.15	0.30	2.37	1.283	0.59			701	13	1029	302	87	
NIST 1633b Cert	49.24	28.43	11.13	0.020	0.80	2.11	0.27	2.26	1.320	0.53			709		1041	296		
NIST 696 Meas	59.68	18.24	4.78	0.219	0.10	1.15	8.79	4.28	0.135	0.18			591	9	706	2	43	
NIST 696 Cert	59.64	18.39	5.22	0.220	0.10	1.09	8.94	4.28	0.135	0.16			560	10	700	9	46	
FK-N Meas	64.35	18.33	0.09	0.003	0.01	0.10	2.45	12.31	0.006	0.02			200	2	38	3	0	
FK-N Cert	65.02	18.61	0.09	0.005	0.01	0.11	2.58	12.81	0.020	0.02			200	1	39	3	0	
05-JES-152 Org	66.88	15.99	3.40	0.038	2.03	1.71	5.82	2.23	0.487	0.17	1.95	100.71	942	2	330	86	12	
05-JES-152 Dup	66.85	16.04	3.43	0.038	2.06	1.74	5.86	2.20	0.496	0.17	1.95	100.84	937	2	328	87	13	

* Meas = measured value; Cert = certified value; Org = original sample; Dup = duplicate sample.

Appendix I.1 cont.

Analyte Symbol	SiO ₂	Al ₂ O ₃	Fe ₂ O ₃	MnO	MgO	CaO	Na ₂ O	K ₂ O	TiO ₂	P ₂ O ₅	LOI	Total	Ba	Be	Sr	V	Y	
Unit Symbol	%	%	(T) %	%	%	%	%	%	%	%	%	%	ppm	ppm	ppm	ppm	ppm	
Detection Limit	0.01	0.01	0.01	0.001	0.01	0.01	0.01	0.01	0.001	0.01	0.01	0.01	1	1	2	5	1	
<i>Batch Two</i>																		
SY-3 Meas	59.51	11.53	6.44	0.327	2.6	8.36	4.05	4.14	0.147	0.58	97.68	443	20	306	53	719		
SY-3 Cert	59.62	11.76	6.49	0.32	2.67	8.25	4.12	4.23	0.15	0.54	97.68	450	20	302	50	718		
NIST 694 Meas	11.52	1.92	0.75	0.011	0.34	43.47	0.88	0.56	0.115	30.13	89.13	115	5	936	1675	148		
NIST 694 Cert	11.2	1.8	0.79	0.012	0.33	43.6	0.86	0.51	0.11	30.2	89.13	115	5	936	1675	148		
W-2a Meas	51.31	15.1	10.5	0.164	6.2	10.67	2.21	0.63	1.066	0.14	97.66	172	1	193	273	20		
W-2a Cert	52.44	15.35	10.74	0.163	6.37	10.87	2.14	0.63	1.06	0.13	97.66	182	1	190	262	24		
DNC-1 Meas	47.35	18.51	9.81	0.147	10.23	11.33	1.93	0.23	0.492	0.07	99.59	107	<1	143	156	17		
DNC-1 Cert	47.04	18.3	9.93	0.149	10.05	11.27	1.87	0.23	0.48	0.09	99.59	114	1	145	148	18		
BIR-1 Meas	48.08	15.65	11.32	0.171	9.76	13.37	1.83	0.04	0.979	0.03	100.7	7	<1	108	342	15		
BIR-1 Cert	47.77	15.35	11.26	0.171	9.68	13.24	1.75	0.03	0.96	0.05	100.7	7	0.6	108	313	16		
GBW 07113 Meas	72.3	12.77	3.16	0.14	0.15	0.6	2.48	5.42	0.285	0.05	98.69	502	4	41	<5	47		
GBW 07113 Cert	72.78	12.96	3.21	0.14	0.16	0.59	2.57	5.43	0.3	0.05	98.69	506	4	43	5	43		
NIST 1633b Meas	49.1	28.33	11.22	0.017	0.78	2.16	0.28	2.35	1.309	0.58	95.68	717	13	1042	309	89		
NIST 1633b Cert	49.24	28.43	11.13	0.02	0.8	2.11	0.27	2.35	1.32	0.53	95.68	709	13	1041	296	89		
NIST 696 Meas	3.8	53.33	8.45	0.004	0.01	0.02	0.02	0.02	2.598	0.05	68.09	15	<1	23	401	13		
NIST 696 Cert	3.79	54.5	8.7	0.004	0.01	0.02	0.02	0.009	2.64	0.05	68.09	15	<1	23	401	13		
FK-N Meas	66.02	18.75	0.1	0.004	<0.01	0.1	2.49	12.86	0.006	0.01	>101.0	212	<1	39	<5	<1		
FK-N Cert	65.02	18.61	0.09	0.005	0.01	0.11	2.58	12.81	0.02	0.02	>101.0	200	1	39	5	0.5		

* Meas = measured value; Cert = certified value; Org = original sample; Dup = duplicate sample.

Appendix 1.2 - Instrumental neutron activation analysis (INAA) geochemical standards and duplicates.

Analyte Symbol	Au	Ag	As	Br	Co	Cr	Hg	Ir	Sb	Sc	Se	W	Zn	Mass
Unit Symbol	ppb	ppm	ppm	ppm	ppm	ppm	ppm	ppb	ppm	ppm	ppm	ppm	ppm	g
Detection Limit	1	5	1	0.5	0.1	0.5	1	1	0.1	0.01	0.5	1	50	
<i>Batch One</i>														
WMG-1 Meas	125		9	1.2	200	775	1.4	51	2.7	27.2	15.5	<1		1.359
WMG-1 Cert	110	3	7		200	770		46	1.8	26	15	1	110	
WMG-1 Meas	121		8	1.9	196	763	1.4	50	2.4	26.7	15.6	<1		1.714
WMG-1 Cert	110	3	7		200	770		46	1.8	26	15	1	110	
<i>Batch two</i>														
WMG-1 Meas	106	<5	7	0.9	202	790	<1	53	2	25.9	13.5	<1	120	1.145
WMG-1 Cert	110	3	7		200	770		46	1.8	26	15	1	110	
WMG-1 Meas	127	<5	7	1.1	202	790	<1	55	2.1	26.2	13.7	<1	140	1.16
WMG-1 Cert	110	3	7		200	770		46	1.8	26	15	1	110	
C-161	53	<5	<1	<0.5	10	8.2	<1	<1	<0.1	11.8	<0.5	<1	<50	1.193
C-161 Split	56	<5	2	<0.5	9.8	8.2	<1	<1	<0.1	11.9	<0.5	<1	<50	1.377

* Meas = measured value; Cert = certified value; Org = original sample; Dup = duplicate sample.

Appendix 1.3 - Inductively Coupled Plasma Mass Spectrometry (ICP-MS) geochemical standards and duplicates.

Analyte Symbol	Bi	Cs	Ga	Ge	Hf	In	Nb	Rb	Sn	Ta	Th	U	Zr	La	Ce	Pr
Unit Symbol	ppm	ppm	ppm	ppm	ppm	ppm	ppm	ppm	ppm	ppm	ppm	ppm	ppm	ppm	ppm	ppm
Detection Limit	0.1	0.1	1	0.5	0.1	0.1	0.2	2	1	0.1	0.05	0.05	1	0.05	0.1	0.02
Batch One																
Blank	<0.1	<0.1	<0.5	<0.1	<0.1	<0.1	<0.2	<1	<1	<0.01	<0.05	<0.01	<1	<0.05	<0.05	<0.01
SY-3 Meas	4.5	2.8	40	4	10.9	<0.2	196	209	5	23.6	922	631	356	1220	2090	222
SY-3 Cert	0.8	2.5	27	1.4	9.7	<0.1	148	206	6.5	30	1003	650	320	1340	2230	223
W-2 Meas	0.2	0.7	19	1.7	2.5	<0.1	7.0	19	2	0.45	2.21	0.54	92	10.8	23.4	2.97
W-2 Cert	0.03	0.99	20	1	2.56	<0.1	7.9	20	<1	0.5	2.2	0.53	94	11.4	24	5.9
DNC-1 Meas	0.5	<0.1	12	0.8	1.0	<0.1	1.4	4	<1	0.07	0.27	0.06	32	3.93	8.69	1.12
DNC-1 Cert	0.02	0.34	15	1.3	1.01	<0.1	3	4.5	<1	0.098	0.2	0.1	41	3.8	10.6	1.3
BIR-1 Meas	<0.1	<0.1	16	1.3	0.6	<0.1	0.5	<1	<1	0.02	0.05	0.02	13	0.77	2.08	0.40
BIR-1 Cert	0.02	0.005	16	1.5	0.6	<0.1	0.6	0.25	0.65	0.04	0.03	0.01	15.5	0.62	1.95	0.38
WMG-1 Meas	3.7	0.4	10	1.8	1.5	<0.1	4.9	3	1	0.29	1.17	0.66	56	7.76	16.2	2.08
WMG-1 Cert	0.48	0.48	10.3	1.7	1.3	<0.1	6	4	2.2	0.5	1.1	0.65	43	8.2	16	
MAG-1 Meas	0.2	8.7	23	1.7	3.6	<0.1	14.8	151	3	1.18	11.6	2.84	123	43.8	89.6	10.27
MAG-1 Cert	0.34	8.6	20.4	1.1	3.7	0.18	12	149	3.6	1.1	11.9	2.7	126	43	88	9.3
GXR-2 Meas	0.2	5.4	44	1.1	6.5	<0.1	10.8	79	1	0.82	8.16	2.83	246	25.1	51.3	5.40
GXR-2 Cert	0.69	5.2	37	1.1	8.3	0.252	11	78	1.7	0.9	8.8	2.9	269	25.6	51.4	
LKSD-3 Meas	<0.5	2.2	15	1.2	4.4	0.1	8.4	74	1	0.66	10.2	4.40	160	48.6	91.0	11.6
LKSD-3 Cert	2.3	2.3	15	1.2	4.8	0.1	8	78	3	0.7	11.4	4.6	178	52	90	
MICA-FE Meas	0.5	178	92	3.1	26.6	0.6	288	2020	70	33.3	163	86.9	829	200	405	51.2
MICA-FE Cert	1.9	180	95	3.2	26	0.6	270	2200	70	35	150	80	800	200	420	49
GXR-1 Meas	1380	2.3	16	3	0.8	0.8	1.3	3	49	0.18	2.7	39.3	28	9.0	16.7	2.13
GXR-1 Cert	1380	3	13.8	3	0.96	0.77	0.8	14	54	0.175	2.44	34.9	38	7.5	17	
STM-1 Meas	2.3	1.5	37	1.9	27.5	<0.1	250	116	6	18.7	29.8	8.8	1200	151	258	25.6
STM-1 Cert	0.13	1.54	36	1.4	28	0.12	268	118	6.8	18.6	31	9.06	1210	150	259	19
05-JES-152 ORG	1.4	1.9	21	1.9	3.0	<0.1	4.3	46	3	0.30	3.53	2.00	113	11.8	24.7	2.97
05-JES-152 REP	1.2	1.7	19	1.8	2.9	<0.1	4.1	43	9	0.31	3.49	1.97	112	11.9	24.7	2.99

* Meas = measured value; Cert = certified value; Org = original sample; Rep = repeated sample (duplicate).

Appendix 1.3 cont.

Analyte Symbol	Nd	Sm	Eu	Gd	Tb	Dy	Ho	Er	Tl	Tm	Yb	Lu
Unit Symbol	ppm	ppm	ppm	ppm	ppm	ppm	ppm	ppm	ppm	ppm	ppm	ppm
Detection Limit	0.05	0.01	0.005	0.02	0.01	0.02	0.01	0.01	0.05	0.005	0.01	0.002
Batch One												
Blank	<0.05	<0.01	<0.005	<0.01	<0.01	<0.01	<0.01	<0.01	<0.05	<0.005	<0.01	<0.002
SY-3 Meas	718	123	18.8	122	22.1	134	27.4	85.5	1.8	13.1	69.4	8.50
SY-3 Cert	670	109	17	105	18	118	29.5	68	1.5	11.6	62	7.9
W-2 Meas	12.6	3.23	1.14	3.71	0.66	3.92	0.75	2.18	<0.05	0.332	2.06	0.311
W-2 Cert	14	3.25	1.1	3.6	0.63	3.8	0.76	2.5	0.2	0.38	2.05	0.33
DNC-1 Meas	5.09	1.50	0.626	2.08	0.44	2.89	0.62	1.93	<0.05	0.325	2.02	0.306
DNC-1 Cert	4.9	1.38	0.59	2	0.41	2.7	0.62	2	<0.05	0.33	2.01	0.32
BIR-1 Meas	2.41	1.15	0.559	1.91	0.41	2.69	0.57	1.73	<0.05	0.281	1.72	0.260
BIR-1 Cert	2.5	1.1	0.54	1.85	0.36	2.5	0.57	1.7	0.01	0.26	1.65	0.26
WMG-1 Meas	9.01	2.28	0.760	2.51	0.43	2.44	0.47	1.38	<0.05	0.207	1.29	0.196
WMG-1 Cert	9	2.3	0.8	2.8	0.4	2.8	0.5	2.83	0.2	0.2	1.3	0.21
MAG-1 Meas	38.0	7.48	1.55	6.47	1.00	5.32	0.96	2.83	0.26	0.419	2.71	0.381
MAG-1 Cert	38	7.5	1.55	5.8	0.96	5.2	1.02	3	0.59	0.43	2.6	0.40
GXR-2 Meas	19.3	3.60	0.785	3.15	0.51	2.84	0.54	1.68	0.86	0.263	1.75	0.267
GXR-2 Cert	19	3.5	0.81	3.3	0.48	3.3	0.54	1.68	1.03	0.3	2.04	0.27
LKSD-3 Meas	43.0	7.90	1.52	6.77	0.93	4.95	0.93	2.86	0.45	0.431	2.74	0.418
LKSD-3 Cert	44	8	1.5	7.7	1	4.9	0.93	2.86	0.45	0.431	2.7	0.4
MICA-FE Meas	183	35.1	0.665	24.2	2.72	10.6	1.37	3.76	16.0	0.552	3.45	0.468
MICA-FE Cert	180	33	0.7	21	2.7	11	1.6	3.8	16	0.48	3.5	0.5
GXR-1 Meas	9.3	3.12	0.71	4.43	0.91	5.25	0.98	2.79	0.3	0.43	2.43	0.327
GXR-1 Cert	18	2.7	0.69	4.2	0.83	4.3	0.98	2.79	0.39	0.43	1.9	0.28
STM-1 Meas	79.4	12.3	3.59	8.7	1.49	8.06	1.44	4.37	0.39	0.655	4.39	0.628
STM-1 Cert	79	12.6	3.6	9.5	1.55	8.1	1.9	4.2	0.26	0.69	4.4	0.6
05-JES-152 ORG	12.0	2.68	0.766	2.33	0.38	2.09	0.41	1.19	0.39	0.185	1.21	0.181
05-JES-152 REP	12.1	2.73	0.738	2.41	0.38	2.12	0.40	1.20	0.35	0.181	1.20	0.184

* Meas = measured value; Cert = certified value.

Appendix 1.3 cont.

Analyte Symbol	Bi	Cs	Ga	Ge	Hf	In	Nb	Rb	Sn	Ta	Th	U	Zr	La	Ce	Pr
Unit Symbol	ppm	ppm	ppm	ppm	ppm	ppm	ppm	ppm	ppm	ppm	ppm	ppm	ppm	ppm	ppm	ppm
Detection Limit	0.1	0.1	1	0.5	0.1	0.1	0.2	2	1	0.1	0.05	0.05	1	0.05	0.1	0.02
<i>Batch two</i>																
Method Blank	<0.1	<0.1	<1	<0.5	<0.1	<0.1	<0.2	<2	<1	<0.1	<0.05	<0.05	<1	<0.05	<0.1	<0.02
SY-3 Meas	0.6	2.7	35	2.8	10.6	<0.1	163	204	5	23.6	907	664	332	1360	2290	223
SY-3 Cert	0.8	3	27	1.4	9.7	<0.1	148	206	7	30	1000	650	320	1340	2230	223
W-2a Meas	<0.1	0.9	18	1.6	2.4	<0.1	6	20	2	0.5	2.01	0.52	85	11.1	23.9	3.03
W-2a Cert	0.03	1	17	1	2.6	<0.1	7.9	21	1	0.5	2.4	0.53	94	10	23	
DNC-1 Meas	<0.1	0.2	14	1.3	1	<0.1	1.2	4	1	<0.1	0.24	0.06	33	3.81	8.4	1.11
DNC-1 Cert	0.02	0.3	15	1.3	1	<0.1	3	5	1	0.1	0.2	0.1	41	3.8	11	1.3
BIR-1 Meas	<0.1	<0.1	16	1.5	0.6	<0.1	0.4	<2	1	<0.1	0.06	<0.05	14	0.74	2.1	0.38
BIR-1 Cert	0.02	0.005	16	1.5	0.6	<0.1	0.6	0.3	0.6	0.04	0.03	0.01	16	0.62	2	0.38
WMG-1 Meas	0.9	0.4	11	1.5	1.5	<0.1	4.4	3	2	0.3	1.11	0.68	53	8.18	16.8	2.15
WMG-1 Cert	<0.1	0.5	10	1.7	1.3	<0.1	6		2	0.5	1.1	0.65	43	8.2	16	
MAG-1 Meas	<0.1	8.6	23	1.7	3.4	<0.1	12.1	149	3	1.2	10.6	2.78	112	42.5	86.7	9.89
MAG-1 Cert	0.3	8.6	20	1.1	3.7	0.2	12	149	4	1.1	11.9	2.7	126	43	88	9.3
GXR-2 Meas	<0.1	5.1	34	1.1	5.9	<0.1	8	77	2	0.8	7.52	2.74	212	25.4	51.1	5.39
GXR-2 Cert	0.7	5.2	37	1.1	8.3	0.3	11	78	2	0.9	8.8	2.9	269	25.6	51.4	
LKSD-3 Meas	<0.1	2.3	16	1.1	4.7	<0.1	7.4	75	2	0.7	9.96	4.53	164	49.2	92.4	11.6
LKSD-3 Cert	0.4	177	96	3.2	4.8	0.6	8	78	3	0.7	11.4	4.6	178	52	90	
MICA-FE Meas	2	180	95	3.2	26.1	0.6	270	2270	71	34.8	150	85.1	823	201	433	50.2
MICA-FE Cert	1380	2.8	14	2.8	0.7	0.8	1.1	3	52	<0.1	2.46	34.5	24	8.28	15.6	2.03
GXR-1 Meas	1380	3	14	1	1	0.8	0.8	10	54	0.2	2.44	34.9	38	7.5	17	

* Meas = measured value; Cert = certified value.

Appendix 1.3 cont.

Analyte Symbol Unit Symbol Detection Limit	Nd ppm	Sm ppm	Eu ppm	Gd ppm	Tb ppm	Dy ppm	Ho ppm	Er ppm	Tl ppm	Tm ppm	Yb ppm	Lu ppm
<i>Batch two</i>												
Method Blank	< 0.05	< 0.01	< 0.005	< 0.02	< 0.01	< 0.02	< 0.01	< 0.01	< 0.05	< 0.005	< 0.01	< 0.002
SY-3 Meas	733	120	18.8	111	22	136	27.5	86.5	1.41	12.6	69.2	8.55
SY-3 Cert	670	109	17	105	18	118	29.5	68	1.5	11.6	62	7.9
W-2a Meas	13.2	3.2	1.19	3.48	0.68	4.07	0.78	2.34	0.11	0.333	2.13	0.314
W-2a Cert	13	3.3	1		0.63	3.6	0.76	2.5	0.2	0.38	2.1	0.33
DNC-1 Meas	4.98	1.4	0.633	1.87	0.43	2.88	0.62	2.02	< 0.05	0.315	2	0.31
DNC-1 Cert	4.9	1.38	0.59	2	0.41	2.7	0.62	2	0.03	0.38	2.01	0.32
BIR-1 Meas	2.48	1.14	0.566	1.7	0.42	2.74	0.57	1.8	< 0.05	0.273	1.7	0.263
BIR-1 Cert	2.5	1.1	0.54	1.85	0.36	2.5	0.57	1.7	0.01	0.26	1.65	0.26
WMG-1 Meas	9.66	2.37	0.8	2.41	0.45	2.62	0.5	1.48	< 0.05	0.213	1.36	0.204
WMG-1 Cert	9	2.3	0.82		0.3	2.8	0.5			0.2	1.3	0.21
MAG-1 Meas	37.8	7.12	1.54	5.77	0.97	5.35	0.96	2.84	0.28	0.404	2.59	0.384
MAG-1 Cert	38	7.5	1.6	5.8	0.96	5.2	1	3	0.59	0.43	2.6	0.4
GXR-2 Meas	19.7	3.54	0.782	2.94	0.52	2.96	0.56	1.77	0.88	0.269	1.76	0.271
GXR-2 Cert	19	3.5	0.81	3.3	0.48	3.3			1	0.3	2.04	0.27
LKSD-3 Meas	43.7	7.69	1.54	6.04	0.96	5.24	0.97	3.06	0.56	0.445	2.88	0.431
LKSD-3 Cert	44	8	1.5		1	4.9					2.7	0.4
MICA-FE Meas	180	33.1	0.639	21.1	2.69	10.8	1.39	3.88	16	0.529	3.49	0.491
MICA-FE Cert	180	33	0.7	21	2.7	11	1.6	3.8	16	0.48	3.5	0.5
GXR-1 Meas	8.9	2.93	0.697	3.96	0.9	5.31	0.99	2.89	0.42	0.421	2.41	0.343
GXR-1 Cert	18	2.7	0.69	4.2	0.83	4.3			0.39	0.43	1.9	0.28

* Meas = measured value; Cert = certified value.

Appendix 1.4 - Total dissolution inductively coupled plasma optical emission spectrometry (ICP-OES) geochemical standards.

Analyte Symbol	Ag	Cd	Cu	Ni	Pb	S	Zn
Unit Symbol	ppm	ppm	ppm	ppm	ppm	%	ppm
Detection Limit	0.5	0.5	1	1	5	0.001	1
<i>Batch One</i>							
AN-G Meas	< 0.3	< 0.3	17	35	3	0.010	15
AN-G Cert		0.08	19	35	2	0.014	20
SDC-1 Meas	< 0.3	< 0.3	29	36	24	0.061	104
SDC-1 Cert	0.041	0.08	30	38	25	0.065	103
DNC-1 Meas	< 0.3	< 0.3	92	246	11	0.055	55
DNC-1 Cert	0.027	0.182	96	247	6.3	0.039	66
SCO-1 Meas	0.5	< 0.3	29	28	31	0.064	99
SCO-1 Cert	0.134	0.14	28.7	27	31	0.063	103
GXR-6 Meas	0.5	< 0.3	65	25	101	0.011	123
GXR-6 Cert	1.3	1	66	27	101	0.016	118
GXR-2 Meas	17.0	4.2	76	20	716	0.019	527
GXR-2 Cert	17	4.1	76	21	690	0.031	530
GXR-1 Meas	32.9	2.5	1104	40	797	0.263	725
GXR-1 Cert	31	3.3	1110	41	730	0.257	760
GXR-4 Meas	3.5	< 0.3	6126	40	54	1.712	73
GXR-4 Cert	4	0.86	6520	42	52	1.770	73
05-1008-2 Org	-0.3	-0.3	3	6.62	9	0.007	45
05-1008-2 Dup	-0.3	-0.3	4	6.96	10	0.005	44
<i>Batch Two</i>							
SDC-1 Meas	< 0.5	< 0.5	40	36	25	0.067	100
SDC-1 Cert	0.04	0.08	30	38	25	0.065	100
DNC-1 Meas	< 0.5	< 0.5	97	250	9	0.064	56
DNC-1 Cert	0.03		96	247	6	0.039	66
SCO-1 Meas	< 0.5	0.6	29	25	32	0.073	91
SCO-1 Cert	0.1	0.1	29	27	31	0.063	100
GXR-6 Meas	< 0.5	< 0.5	70	25	96	0.01	120
GXR-6 Cert	1	1	66	27	100	0.016	118
GXR-2 Meas	17	4.1	87	20	704	0.02	525
GXR-2 Cert	17	4.1	76	21	690	0.031	530
GXR-1 Meas	30.7	3.7	1120	37	740	0.272	685
GXR-1 Cert	31	3.3	1110	41	730	0.257	760
GXR-4 Meas	3.4	< 0.5	6360	39	55	1.9	73
GXR-4 Cert	4	0.9	6520	42	52	1.77	73

* Meas = measured value; Cert = certified value; Org = original sample; Dup = duplicate sample.

Appendix 2.1 - Major element geochemistry for Schaft Creek samples.

Sample	Detection Limit	Analytical Method	05-JES-149	05-JES-187	05-JES-208	05-1008-1	05-1008-2	05-1008-6
Lithology			Granodiorite	Granodiorite	Granodiorite	Granodiorite	Granodiorite	Granodiorite
Drillhole			T-136 @119'	Surface	T-217 @ 122'	Surface	Surface	Surface
Easting			379212	378797	379086	386734	375895	376940
Northing			6360720	6358180	6359951	6359984	6367684	6371904
<i>Weight Percent</i>								
SiO ₂	0.01	FUS-ICP	64.92	66.58	65.98	67.14	66.82	66.21
Al ₂ O ₃	0.01	FUS-ICP	16.19	14.99	15.63	15.71	15.75	15.95
Fe ₂ O ₃ (T)	0.01	FUS-ICP	4.02	2.88	3.01	3.52	2.59	2.72
MnO	0.001	FUS-ICP	0.402	0.042	0.070	0.110	0.139	0.158
MgO	0.01	FUS-ICP	1.73	0.70	1.65	1.45	0.94	1.13
CaO	0.01	FUS-ICP	3.64	3.77	2.88	3.44	2.45	2.85
Na ₂ O	0.01	FUS-ICP	4.60	4.57	5.44	4.45	4.61	5.09
K ₂ O	0.01	FUS-ICP	2.81	2.51	2.01	2.97	2.61	2.61
TiO ₂	0.001	FUS-ICP	0.454	0.403	0.438	0.431	0.298	0.342
P ₂ O ₅	0.01	FUS-ICP	0.17	0.14	0.16	0.15	0.12	0.13
LOI	0.01	FUS-ICP	1.44	3.97	2.86	1.01	2.66	1.84
TOTAL	0.01	FUS-ICP	100.37	100.55	100.12	100.38	99.00	99.03

Appendix 2.1 cont.

Sample	05-JES-013 Feldspar Porphyry H-050 @ 713'	05-JES-152 (1) Feldspar Porphyry T-136 @ 662'	05-JES-152 (2) duplicate	06-JES-011 Gabbro Surface	06CF268 151.90 Diorite - Altered 06CF268 @ 152m	05-JES-151 Basalt T-136 @ 419'	05-JES-210 Basalt T-217 @ 170'	05-JES-097 Andesite - Altered H-073 @ 132'
Drillhole	380140	379212		378985	380452	379212	379086	380235
Easting	6359765	6360720		6358540	6359622	6360720	6359951	6360246
Nothing								
<i>Weight Percent</i>								
SiO ₂	66.80	66.88	66.85	48.86	48.85	46.91	49.12	52.10
Al ₂ O ₃	15.86	15.99	16.04	12.35	17.66	15.59	11.75	15.92
Fe ₂ O ₃ (T)	2.72	3.40	3.43	12.63	10.76	9.54	12.09	9.07
MnO	0.001	0.038	0.038	0.216	0.050	0.371	0.421	0.299
MgO	1.39	2.03	2.06	9.41	3.78	10.15	10.05	6.35
CaO	2.69	1.71	1.74	8.26	3.52	10.40	10.69	5.69
Na ₂ O	5.53	5.82	5.86	3.65	2.90	1.92	2.22	5.71
K ₂ O	1.98	2.23	2.20	0.64	2.72	0.49	1.22	0.21
TiO ₂	0.337	0.487	0.496	0.716	1.448	1.029	0.699	0.788
P ₂ O ₅	0.13	0.17	0.17	0.32	0.38	0.21	0.30	0.23
LOI	3.23	1.95	1.95	2.48	7.11	3.72	1.85	4.46
TOTAL	100.67	100.71	100.84	99.54	99.18	100.33	100.43	100.82

Appendix 2.1 cont.

Sample	05-JES-136	05-JES-144	05-JES-203	05-1006-3	06-JES-069	06-JES-070	06-JES-071	06-JES-061
Lithology	Andesite - Altered	Andesite	Andesite	Andesite	Andesite	Andesite	Andesite	Rhyolite
Drillhole	Surface	Surface	T-128 @ 22'	Surface	Surface	Surface	Surface	Surface
Easting	380604	380449	380399	380618	380111	380052	380687	381871
Northing	6359783	6359951	6360234	6360164	6360384	6360433	6360196	6361936
<i>Weight Percent</i>								
SiO ₂	49.98	51.00	52.73	54.93	52.43	52.81	52.43	74.65
Al ₂ O ₃	17.55	17.40	16.33	15.03	16.48	16.63	14.94	12.68
Fe ₂ O ₃ (T)	9.01	9.16	9.11	8.65	9.67	9.40	9.17	1.81
MnO	0.126	0.290	0.151	0.414	0.167	0.178	0.155	0.045
MgO	5.62	5.25	5.66	4.82	5.37	5.02	5.53	0.43
CaO	4.84	7.48	5.87	4.01	6.36	5.94	5.07	0.53
Na ₂ O	5.31	3.06	3.10	4.20	3.43	4.00	2.96	2.76
K ₂ O	1.07	1.46	1.37	0.63	1.11	1.04	1.42	5.91
TiO ₂	0.974	0.951	0.827	0.749	0.943	0.884	0.853	0.112
P ₂ O ₅	0.30	0.29	0.24	0.22	0.26	0.26	0.25	0.03
LOI	5.52	3.87	5.20	6.77	4.02	3.51	7.10	0.97
TOTAL	100.31	100.21	100.58	100.41	100.20	99.66	99.86	99.92

Appendix 2.2 - Trace element geochemistry for Schaft Creek samples.

Sample	Detection Limit	Analytical Method	05-JES-149	05-JES-187	05-JES-208
Lithology			Granodiorite	Granodiorite	Granodiorite
<i>Parts Per Million</i>					
Au	1	INAA	-1	-1	-1
Ag	0.5	MULT INAA / TD-ICP	-0.3	-0.3	-0.3
As	1	INAA	2	2	2
Ba	1	FUS-ICP	1014	1117	761
Be	1	FUS-ICP	2	2	2
Bi	0.1	FUS-MS	0.5	1.0	1.6
Br	0.5	INAA	0.9	-0.5	0.9
Cd	0.5	TD-ICP	-0.3	-0.3	-0.3
Co	0.1	INAA	8.4	5.7	5.9
Cr	0.5	INAA	13.2	14.2	12.8
Cs	0.1	FUS-MS	1.3	1.2	2.0
Cu	1	TD-ICP	80	33	82
Ga	1	FUS-MS	17	16	17
Ge	0.5	FUS-MS	1.8	1.5	1.4
Hf	0.1	FUS-MS	3.4	3.7	3.2
Hg	1	INAA	-1	-1	-1
In	0.1	FUS-MS	-0.1	-0.1	-0.1
Ir	1	INAA	-1	-1	-1
Nb	0.2	FUS-MS	4.2	4.6	4.6
Ni	1	TD-ICP	8	17	91
Pb	5	TD-ICP	11	8	-3
Rb	2	FUS-MS	53	55	46
S	0.001	TD-ICP	0.034	0.004	-0.001
Sb	0.1	INAA	0.5	0.9	1.6
Sc	0.01	INAA	8.21	6.03	7.32
Se	0.5	INAA	-0.5	-0.5	-0.5
Sn	1	FUS-MS	-1	-1	14
Sr	2	FUS-ICP	602	361	453
Ta	0.1	FUS-MS	0.4	0.5	0.4
Th	0.05	FUS-MS	5.04	6.08	4.95
U	0.05	FUS-MS	2.65	2.67	3.07
V	5	FUS-ICP	83	64	75
W	1	INAA	6	-1	2
Y	1	FUS-ICP	12	10	12
Zn	1	MULT INAA / TD-ICP	32	117	63
Zr	1	FUS-MS	113	130	118
La	0.05	FUS-MS	13.81	9.96	13.57
Ce	0.1	FUS-MS	26.7	18.2	27.6
Pr	0.02	FUS-MS	3.19	2.18	3.20
Nd	0.05	FUS-MS	12.37	8.24	12.16
Sm	0.01	FUS-MS	2.78	1.87	2.65
Eu	0.005	FUS-MS	0.825	0.647	0.781
Gd	0.02	FUS-MS	2.41	1.77	2.24
Tb	0.01	FUS-MS	0.39	0.28	0.37
Dy	0.02	FUS-MS	2.14	1.57	2.17
Ho	0.01	FUS-MS	0.42	0.32	0.41
Er	0.01	FUS-MS	1.22	0.97	1.22
Tl	0.05	FUS-MS	0.31	0.40	0.34
Tm	0.005	FUS-MS	0.196	0.152	0.197
Yb	0.01	FUS-MS	1.33	1.09	1.34
Lu	0.002	FUS-MS	0.204	0.172	0.207
Mass		INAA	1.281	1.280	1.451

Appendix 2.2 cont.

Sample	05-1008-1	05-1008-2	05-1008-6	05-JES-013	05-JES-152 (1)
Lithology	Granodiorite	Granodiorite	Granodiorite	Feldspar Porphyry	Feldspar Porphyry
<i>Parts Per Million</i>					
Au	-1	-1	9	26	-1
Ag	-0.3	-0.3	-0.3	-0.3	0.3
As	3	2	3	1	3
Ba	1212	1022	1124	1339	942
Be	2	2	2	2	2
Bi	1.2	0.9	0.9	3.7	1.4
Br	0.9	-0.5	1.0	-0.5	0.8
Cd	-0.3	-0.3	-0.3	-0.3	-0.3
Co	7.1	5.5	5.6	4.3	7.9
Cr	19.0	16.1	19.2	12.8	26.2
Cs	1.3	0.5	0.6	2.9	1.9
Cu	3	4	3	434	58
Ga	18	16	17	17	21
Ge	2.2	1.4	1.4	1.7	1.9
Hf	3.5	2.6	2.9	2.8	3.0
Hg	-1	-1	1	-1	-1
In	-0.1	-0.1	-0.1	-0.1	-0.1
Ir	-1	-1	-1	-1	-1
Nb	4.7	2.6	3.5	3.0	4.3
Ni	7	7	7	7	12
Pb	9	10	13	5	-3
Rb	71	50	48	36	46
S	0.007	0.005	-0.001	0.040	0.009
Sb	0.4	0.5	0.5	1.3	1.5
Sc	7.37	5.02	5.19	4.45	8.64
Se	-0.5	-0.5	-0.5	-0.5	-0.5
Sn	4	2	-1	3	3
Sr	572	510	796	509	330
Ta	0.5	0.2	1.8	0.3	0.3
Th	5.53	3.37	3.37	2.91	3.53
U	2.22	1.26	1.29	1.45	2.00
V	72	45	50	52	86
W	-1	-1	-1	3	2
Y	12	6	10	7	12
Zn	45	44	47	23	34
Zr	124	94	105	98	113
La	15.00	9.65	11.62	9.40	11.85
Ce	28.6	17.7	23.7	19.1	24.7
Pr	3.44	2.04	2.97	2.38	2.97
Nd	13.06	7.45	11.17	9.36	12.01
Sm	2.69	1.62	2.32	2.04	2.68
Eu	0.783	0.529	0.656	0.619	0.766
Gd	2.37	1.37	1.95	1.75	2.33
Tb	0.38	0.21	0.30	0.26	0.38
Dy	2.01	1.10	1.56	1.37	2.09
Ho	0.39	0.22	0.30	0.27	0.41
Er	1.17	0.66	0.90	0.78	1.19
Tl	0.47	0.39	0.36	0.29	0.39
Tm	0.183	0.103	0.139	0.122	0.185
Yb	1.25	0.70	0.95	0.82	1.21
Lu	0.192	0.115	0.147	0.128	0.181
Mass	1.405	1.247	1.334	1.326	1.205

Appendix 2.2 cont.

Sample	05-JES-152 (2)	06-JES-011	06CF268 151.90	05-JES-151	05-JES-210
Lithology	duplicate	Gabbro	Diorite - Altered	Basalt	Basalt
<i>Parts Per Million</i>					
Au		< 1	267	9	-1
Ag	-0.3	< 0.5	1.4	0.4	-0.3
As		9	2	8	7
Ba	937	271	121	239	366
Be	2	1	1	2	2
Bi	1.2	0.3	1.1	0.3	0.7
Br		< 0.5	< 0.5	-0.5	1.0
Cd	-0.3	< 0.5	< 0.5	-0.3	-0.3
Co		44.5	20.8	47.5	46.4
Cr		347.0	6.7	374.3	409.0
Cs	1.7	0.4	8.4	0.4	0.8
Cu	13	242	> 10000	57	8
Ga	19	15	19	14	13
Ge	1.8	1.8	1.5	2.1	2.7
Hf	2.9	1.3	2.0	2.2	1.2
Hg		< 1	< 1	-1	-1
In	-0.1	< 0.1	0.2	-0.1	-0.1
Ir		< 1	< 1	-1	-1
Nb	4.1	2.1	4.0	4.7	1.5
Ni	6	83	7	164	26
Pb	9	< 5	12	4	3
Rb	43	15	102	8	30
S	0.010	0.005	1.430	0.084	0.006
Sb		4.4	2.5	1.0	1.1
Sc		33.30	25.30	33.11	40.04
Se		< 0.5	< 0.5	-0.5	-0.5
Sn	9	< 1	2	-1	2
Sr	328	382	198	364	397
Ta	0.3	0.2	0.3	0.3	0.1
Th	3.49	0.87	1.55	1.29	0.97
U	1.97	0.82	1.32	0.41	0.67
V	87	295	305	227	294
W		3	24	-1	-1
Y	13	13	15	20	13
Zn	36	78	48	70	90
Zr	112	40	74	84	37
La	11.94	7.06	11.30	14.38	5.70
Ce	24.7	15.2	25.4	32.5	12.6
Pr	2.99	2.06	3.35	4.54	1.84
Nd	12.14	9.76	15.20	18.58	8.40
Sm	2.73	2.65	3.56	4.14	2.44
Eu	0.738	0.975	1.320	1.328	0.819
Gd	2.41	2.61	3.07	4.27	2.71
Tb	0.38	0.45	0.54	0.67	0.45
Dy	2.12	2.81	3.30	3.79	2.50
Ho	0.40	0.56	0.65	0.75	0.47
Er	1.20	1.63	1.89	2.16	1.35
Tl	0.35	0.08	0.37	0.09	0.21
Tm	0.181	0.240	0.273	0.323	0.199
Yb	1.20	1.50	1.70	2.07	1.27
Lu	0.184	0.223	0.261	0.307	0.185
Mass		1.451	1.328	1.474	1.426

Appendix 2.2 cont.

Sample Lithology	05-JES-097 Andesite - Altered	05-JES-136 Andesite - Altered	05-JES-144 Andesite	05-JES-203 Andesite	05-1006-3 Andesite	06-JES-069 Andesite
<i>Parts Per Million</i>						
Au	-1	-1	4	-1	-1	< 1
Ag	-0.3	0.3	0.5	-0.3	-0.3	< 0.5
As	9	3	5	4	12	10
Ba	129	717	842	682	205	570
Be	2	2	2	2	2	1
Bi	3.1	0.6	0.6	0.6	0.8	1.3
Br	-0.5	-0.5	-0.5	-0.5	-0.5	< 0.5
Cd	-0.3	-0.3	-0.3	-0.3	-0.3	< 0.5
Co	26.0	27.8	30.1	26.2	26.4	26.6
Cr	92.2	45.0	57.4	61.6	81.3	44.3
Cs	0.2	0.3	0.4	0.9	1.1	1.0
Cu	15	51	49	205	11	12
Ga	16	17	16	17	14	18
Ge	2.1	2.2	2.0	1.5	1.7	1.8
Hf	1.6	2.7	2.6	1.7	1.7	1.7
Hg	-1	-1	-1	-1	-1	< 1
In	-0.1	-0.1	-0.1	-0.1	-0.1	< 0.1
Ir	-1	-1	-1	-1	-1	< 1
Nb	1.7	5.6	5.4	1.9	1.6	2.3
Ni	31	40	37	16	8	14
Pb	-3	-3	6	9	8	10
Rb	3	18	27	20	11	22
S	0.010	0.019	0.004	0.012	0.004	0.031
Sb	4.3	1.2	4.8	2.0	1.7	5.9
Sc	28.41	23.13	25.89	31.54	29.30	29.50
Se	-0.5	-0.5	-0.5	-0.5	-0.5	< 0.5
Sn	-1	-1	1	2	2	< 1
Sr	452	613	546	362	293	427
Ta	0.1	0.4	0.3	0.1	0.1	0.1
Th	1.17	2.27	2.17	1.19	1.26	0.95
U	0.56	0.87	0.80	0.65	0.67	0.54
V	251	237	231	261	297	286
W	-1	-1	-1	-1	-1	2
Y	17	21	20	19	18	19
Zn	95	79	74	48	46	83
Zr	50	105	101	53	52	53
La	6.70	16.11	15.42	6.80	6.62	8.13
Ce	14.6	33.6	31.4	15.3	14.1	18.1
Pr	2.04	4.28	4.08	2.06	2.02	2.44
Nd	9.33	17.61	16.45	9.26	9.22	11.20
Sm	2.65	4.15	3.83	2.52	2.60	3.01
Eu	0.889	1.285	1.233	0.883	0.853	1.170
Gd	3.04	4.21	3.94	2.99	2.96	3.05
Tb	0.53	0.70	0.65	0.54	0.53	0.59
Dy	3.17	3.76	3.54	3.32	3.18	3.75
Ho	0.62	0.75	0.70	0.67	0.63	0.75
Er	1.85	2.22	2.08	2.05	1.91	2.21
Tl	-0.05	0.23	0.37	0.23	0.10	0.21
Tm	0.284	0.335	0.336	0.306	0.294	0.344
Yb	1.88	2.21	2.17	2.00	1.91	2.25
Lu	0.284	0.337	0.313	0.303	0.289	0.316
Mass	1.234	1.225	1.144	1.526	1.320	1.507

Appendix 2.2 cont.

Sample	06-JES-070	06-JES-071	06-JES-061
Lithology	Andesite	Andesite	Rhyolite
<i>Parts Per Million</i>			
Au	12	< 1	< 1
Ag	< 0.5	< 0.5	< 0.5
As	9	62	1
Ba	549	269	943
Be	1	< 1	3
Bi	0.2	0.2	0.7
Br	1.0	< 0.5	0.8
Cd	< 0.5	0.5	< 0.5
Co	26.5	28.0	2.6
Cr	36.2	55.5	12.0
Cs	0.9	1.7	0.5
Cu	30	29	12
Ga	18	16	15
Ge	1.7	1.3	1.3
Hf	1.8	1.6	4.3
Hg	< 1	< 1	< 1
In	< 0.1	< 0.1	< 0.1
Ir	< 1	< 1	< 1
Nb	2.2	2.0	15.1
Ni	12	15	3
Pb	14	6	20
Rb	21	35	137
S	0.006	0.003	< 0.001
Sb	3.6	2.8	0.4
Sc	28.00	27.70	3.15
Se	< 0.5	< 0.5	< 0.5
Sn	< 1	< 1	4
Sr	509	226	156
Ta	0.1	0.1	1.7
Th	1.04	0.78	10.30
U	0.70	0.38	5.24
V	267	120	9
W	< 1	< 1	2
Y	20	16	32
Zn	116	104	41
Zr	56	49	127
La	8.53	5.95	34.10
Ce	19.3	14.2	65.7
Pr	2.57	1.83	7.09
Nd	11.90	8.73	24.20
Sm	3.12	2.40	4.91
Eu	1.110	0.892	0.245
Gd	3.14	2.57	4.09
Tb	0.57	0.49	0.86
Dy	3.73	3.17	5.59
Ho	0.77	0.65	1.17
Er	2.23	1.94	3.75
Tl	0.15	0.19	0.79
Tm	0.331	0.290	0.627
Yb	2.16	1.84	4.17
Lu	0.326	0.297	0.659
Mass	1.237	1.423	1.34

Appendix 3 - Pyroxene and plagioclase mineral chemistry.

Sample	05-JES-210A1	05-JES-210A2	05-JES-210A3	05-JES-210B4	05-JES-210B5	05-JES-210C7	05-JES-210C8	05-JES-210C9
Mineral	Diopside	Diopside	Diopside	Augite	Augite	Augite	Augite	Augite
Lithology	Andesite	Andesite	Andesite	Andesite	Andesite	Andesite	Andesite	Andesite
<i>Weight percent</i>								
SiO ₂	53.10	53.31	53.14	51.31	51.14	50.27	50.29	50.26
TiO ₂	0.21	0.16	0.23	0.49	0.47	0.55	0.54	0.58
Al ₂ O ₃	1.73	1.40	1.66	3.48	3.49	4.05	4.16	4.00
FeO	4.85	4.32	4.58	8.34	7.99	8.02	8.16	8.40
MnO	0.12	0.12	0.12	0.27	0.18	0.18	0.16	0.23
MgO	16.74	16.99	17.02	14.98	15.26	14.64	14.74	14.44
CaO	22.72	22.68	22.94	20.94	21.26	21.53	21.32	21.33
Na ₂ O	0.21	0.20	0.23	0.40	0.42	0.40	0.36	0.39
Total	99.67	99.19	99.92	100.21	100.22	99.63	99.73	99.63
<i>Atomic Proportions</i>								
Si	1.95	1.96	1.95	1.90	1.89	1.88	1.88	1.88
Ti	0.01	0.00	0.01	0.01	0.01	0.02	0.02	0.02
Al	0.07	0.06	0.07	0.15	0.15	0.18	0.18	0.18
Al ^{iv}	0.05	0.04	0.05	0.10	0.11	0.12	0.12	0.12
Al ^{vi}	0.03	0.02	0.02	0.05	0.05	0.06	0.06	0.06
Cr	0.00	0.00	0.00	0.00	0.00	0.00	0.00	0.00
Total Fe	0.15	0.13	0.14	0.26	0.25	0.25	0.25	0.26
Mn	0.00	0.00	0.00	0.01	0.01	0.01	0.01	0.01
Mg	0.92	0.93	0.93	0.83	0.84	0.81	0.82	0.80
Ca	0.89	0.90	0.90	0.83	0.84	0.86	0.85	0.85
Na	0.01	0.01	0.02	0.03	0.03	0.03	0.03	0.03
Total cations	4	4	4	4	4	4	4	4
Oxygens	6	6	6	6	6	6	6	6

Appendix 3 cont.

Sample Mineral Lithology	05-JES-210C10 Augite Andesite	05-JES-210D11 Augite Andesite	05-JES-210D12 Augite Andesite	05-JES-210D13 Augite Andesite	05-JES-210D14 Augite Andesite	05-JES-210D15 Augite Andesite	05-JES-210D16 Augite Andesite	05-JES-210D17 Diopside Andesite
<i>Weight Percent</i>								
SiO ₂	51.19	51.39	51.35	52.85	50.71	51.27	51.24	51.65
TiO ₂	0.44	0.55	0.60	0.31	0.48	0.47	0.40	0.32
Al ₂ O ₃	3.33	4.43	4.90	3.38	3.44	3.34	3.05	3.01
FeO	8.05	11.51	11.56	10.42	8.05	7.83	6.96	6.59
MnO	0.20	0.34	0.35	0.34	0.22	0.19	0.18	0.13
MgO	15.20	16.29	16.15	17.00	15.12	15.33	15.57	15.71
CaO	21.22	12.14	12.10	12.44	21.13	21.23	21.85	22.40
Na ₂ O	0.40	0.56	0.65	0.48	0.36	0.38	0.34	0.28
Total	100.03	97.20	97.65	97.22	99.51	100.04	99.58	100.07
<i>Atomic Proportions</i>								
Si	1.90	1.94	1.93	1.98	1.89	1.90	1.90	1.91
Ti	0.01	0.02	0.02	0.01	0.01	0.01	0.01	0.01
Al	0.15	0.20	0.22	0.15	0.15	0.15	0.13	0.13
Al ^{IV}	0.10	0.06	0.07	0.02	0.11	0.10	0.10	0.09
Al ^{VI}	0.05	0.13	0.14	0.13	0.05	0.05	0.04	0.04
Cr	0.00	0.00	0.00	0.00	0.00	0.00	0.00	0.00
Total Fe	0.25	0.36	0.36	0.33	0.25	0.24	0.22	0.20
Mn	0.01	0.01	0.01	0.01	0.01	0.01	0.01	0.00
Mg	0.84	0.92	0.90	0.95	0.84	0.85	0.86	0.87
Ca	0.84	0.49	0.49	0.50	0.85	0.84	0.87	0.89
Na	0.03	0.04	0.05	0.04	0.03	0.03	0.02	0.02
Total cations	4	4	4	4	4	4	4	4
Oxygens	6	6	6	6	6	6	6	6

Appendix 3 cont.

Sample	05-JES-210D18	05-JES-210D19	05-JES-210E20	05-JES-210E21	05-JES-210E22	05-JES-210F23	05-JES-210F24	05-JES-210F25
Mineral	Augite	Diopside	Diopside	Diopside	Diopside	Augite	Augite	Augite
Lithology	Andesite	Andesite	Andesite	Andesite	Andesite	Andesite	Andesite	Andesite
<i>Weight percent</i>								
SiO ₂	51.36	51.13	53.41	52.47	53.30	50.36	50.39	51.56
TiO ₂	0.33	0.40	0.14	0.24	0.17	0.55	0.59	0.44
Al ₂ O ₃	3.33	3.45	1.57	2.23	1.67	4.18	4.01	2.96
FeO	6.95	7.10	4.19	5.08	4.68	8.34	8.62	7.92
MnO	0.17	0.18	0.11	0.10	0.11	0.18	0.23	0.23
MgO	15.65	15.34	17.12	16.48	17.01	14.87	14.64	15.62
CaO	21.98	22.02	22.87	22.84	22.81	21.40	21.00	20.84
Na ₂ O	0.30	0.32	0.21	0.22	0.23	0.39	0.44	0.37
Total	100.07	99.95	99.61	99.66	99.98	100.26	99.91	99.93
<i>Atomic Proportions</i>								
Si	1.90	1.90	1.96	1.93	1.95	1.87	1.88	1.91
Ti	0.01	0.01	0.00	0.01	0.00	0.02	0.02	0.01
Al	0.15	0.15	0.07	0.10	0.07	0.18	0.18	0.13
Al ^{iv}	0.10	0.10	0.04	0.07	0.05	0.13	0.12	0.09
Al ^{vi}	0.04	0.05	0.03	0.03	0.02	0.05	0.06	0.04
Cr	0.00	0.00	0.00	0.00	0.00	0.00	0.00	0.00
Total Fe	0.21	0.22	0.13	0.16	0.14	0.26	0.27	0.25
Mn	0.01	0.01	0.00	0.00	0.00	0.01	0.01	0.01
Mg	0.86	0.85	0.94	0.91	0.93	0.82	0.81	0.86
Ca	0.87	0.87	0.90	0.90	0.90	0.85	0.84	0.83
Na	0.02	0.02	0.02	0.02	0.02	0.03	0.03	0.03
Total cations	4	4	4	4	4	4	4	4
Oxygens	6	6	6	6	6	6	6	6

Appendix 3 cont.

Sample	05-JES-210G26	05-JES-210G27	05-JES-210G28	05-JES-094A29	05-JES-094A30	05-JES-094A31	05-JES-094B32	05-JES-094B33
Mineral	Augite	Augite	Augite	Augite	Augite	Augite	Augite	Augite
Lithology	Andesite	Andesite	Andesite	Andesite	Andesite	Andesite	Andesite	Andesite
<i>Weight percent</i>								
SiO ₂	49.61	51.11	51.40	51.49	51.70	50.21	52.88	49.82
TiO ₂	0.57	0.43	0.37	0.45	0.40	0.64	0.29	0.73
Al ₂ O ₃	4.18	3.32	3.22	2.75	2.92	4.60	2.30	4.54
FeO	8.52	7.87	7.85	9.76	9.29	7.92	6.69	8.17
MnO	0.19	0.21	0.22	0.33	0.31	0.21	0.17	0.17
MgO	14.73	15.37	15.44	14.35	14.96	14.89	16.68	14.88
CaO	21.22	20.96	21.61	20.15	20.16	21.44	20.73	21.21
Na ₂ O	0.41	0.36	0.35	0.45	0.38	0.28	0.30	0.30
Total	99.44	99.64	100.46	99.72	100.09	100.18	100.04	99.81
<i>Atomic Proportions</i>								
Si	1.86	1.90	1.90	1.93	1.92	1.86	1.94	1.86
Ti	0.02	0.01	0.01	0.01	0.01	0.02	0.01	0.02
Al	0.19	0.15	0.14	0.12	0.13	0.20	0.10	0.20
Al ^{IV}	0.14	0.10	0.10	0.07	0.08	0.14	0.06	0.14
Al ^{VI}	0.05	0.05	0.04	0.05	0.05	0.06	0.04	0.06
Cr	0.00	0.00	0.00	0.00	0.00	0.00	0.00	0.00
Total Fe	0.27	0.24	0.24	0.31	0.29	0.25	0.21	0.25
Mn	0.01	0.01	0.01	0.01	0.01	0.01	0.01	0.01
Mg	0.82	0.85	0.85	0.80	0.83	0.82	0.91	0.83
Ca	0.85	0.84	0.86	0.81	0.80	0.85	0.82	0.85
Na	0.03	0.03	0.03	0.03	0.03	0.02	0.02	0.02
Total cations	4	4	4	4	4	4	4	4
Oxygens	6	6	6	6	6	6	6	6

Appendix 3 cont.

Sample Mineral Lithology	05-JES-094B34	05-JES-097A35	05-JES-097A36	05-JES-097A37	05-JES-097B38	05-JES-097B39	05-JES-097B40	05-JES-097C41
	Augite	Augite	Augite	Augite	Augite	Augite	Augite	Augite
	Andesite	Andesite	Andesite	Andesite	Andesite	Andesite	Andesite	Andesite
<i>Weight Percent</i>								
SiO ₂	52.72	49.57	50.94	48.13	54.12	54.07	51.51	51.59
TiO ₂	0.30	1.04	0.71	0.56	0.35	0.37	0.39	0.55
Al ₂ O ₃	2.14	6.99	5.53	8.78	2.61	3.02	4.88	4.94
FeO	7.12	8.36	8.96	9.46	6.61	7.70	8.84	7.72
MnO	0.17	0.47	0.55	0.47	0.46	0.64	0.51	0.35
MgO	17.37	17.60	17.50	16.55	20.11	19.44	18.03	18.43
CaO	19.33	11.77	11.76	11.54	12.16	11.93	11.98	12.17
Na ₂ O	0.20	1.17	0.95	1.49	0.56	0.56	0.99	0.86
Total	99.34	96.97	96.89	96.97	96.97	97.73	97.12	96.62
<i>Atomic Proportions</i>								
Si	1.95	1.85	1.91	1.81	1.99	1.99	1.92	1.92
Ti	0.01	0.03	0.02	0.02	0.01	0.01	0.01	0.02
Al	0.09	0.31	0.24	0.39	0.11	0.13	0.21	0.22
Al ^{iv}	0.05	0.15	0.09	0.19	0.01	0.01	0.08	0.08
Al ^{vi}	0.04	0.16	0.15	0.20	0.11	0.12	0.14	0.14
Cr	0.00	0.00	0.00	0.00	0.00	0.00	0.00	0.00
Total Fe	0.22	0.26	0.28	0.30	0.20	0.24	0.28	0.24
Mn	0.01	0.01	0.02	0.02	0.01	0.02	0.02	0.01
Mg	0.96	0.98	0.98	0.93	1.10	1.06	1.00	1.02
Ca	0.76	0.47	0.47	0.47	0.48	0.47	0.48	0.49
Na	0.01	0.09	0.07	0.11	0.04	0.04	0.07	0.06
Total cations	4	4	4	4	4	4	4	4
Oxygens	6	6	6	6	6	6	6	6

Appendix 3 cont.

Sample	05-JES-097C42	05-JES-097C43	05-JES-097D44	05-JES-097D45	05-JES-097D46	05-JES-097E47	05-JES-097E48	05-JES-097F50
Mineral	Augite	Augite	Augite	Augite	Augite	Augite	Augite	Augite
Lithology	Andesite	Andesite	Andesite	Andesite	Andesite	Andesite	Andesite	Andesite
<i>Weight percent</i>								
SiO ₂	53.58	52.58	51.57	50.25	50.99	52.53	49.76	52.77
TiO ₂	0.18	0.49	0.60	1.01	0.64	0.50	0.92	0.46
Al ₂ O ₃	3.72	4.13	5.25	6.66	4.99	3.99	7.44	4.34
FeO	7.45	8.18	8.57	8.49	9.24	8.78	7.93	8.47
MnO	0.43	0.58	0.45	0.36	0.60	0.55	0.43	0.52
MgO	18.92	18.47	17.92	17.55	17.66	18.17	17.76	18.09
CaO	12.28	11.99	12.13	12.04	11.76	11.90	11.73	11.79
Na ₂ O	0.58	0.73	0.91	1.12	1.00	0.65	1.29	0.67
Total	97.14	97.15	97.40	97.49	96.89	97.07	97.28	97.11
<i>Atomic Proportions</i>								
Si	1.98	1.95	1.92	1.87	1.91	1.96	1.85	1.96
Ti	0.00	0.01	0.02	0.03	0.02	0.01	0.03	0.01
Al	0.16	0.18	0.23	0.29	0.22	0.17	0.33	0.19
Al ^{iv}	0.02	0.05	0.08	0.13	0.09	0.04	0.15	0.04
Al ^{vi}	0.14	0.13	0.15	0.16	0.13	0.13	0.18	0.15
Cr	0.00	0.00	0.00	0.00	0.00	0.00	0.00	0.00
Total Fe	0.23	0.25	0.27	0.26	0.29	0.27	0.25	0.26
Mn	0.01	0.02	0.01	0.01	0.02	0.02	0.01	0.02
Mg	1.04	1.02	0.99	0.97	0.99	1.01	0.98	1.00
Ca	0.49	0.48	0.48	0.48	0.47	0.47	0.47	0.47
Na	0.04	0.05	0.07	0.08	0.07	0.05	0.09	0.05
Total cations	4	4	4	4	4	4	4	4
Oxygens	6	6	6	6	6	6	6	6

Appendix 3 cont.

Sample	05-JES-097F51	05-JES-097F52	05-JES-097G53	05-JES-097G54	05-JES-097G55	05-JES-144A56	05-JES-144A57	05-JES-144A58
Mineral	Augite	Augite	Augite	Augite	Augite	Augite	Augite	Augite
Lithology	Andesite	Andesite	Andesite	Andesite	Andesite	Andesite	Andesite	Andesite
<i>Weight percent</i>								
SiO ₂	52.45	50.57	50.91	51.27	53.17	51.76	50.59	51.46
TiO ₂	0.40	0.87	0.67	0.75	0.35	0.66	0.82	0.67
Al ₂ O ₃	4.30	6.39	6.21	5.38	3.39	2.61	3.96	2.66
FeO	7.21	7.97	8.53	7.69	8.56	9.49	8.92	10.32
MnO	0.49	0.46	0.48	0.42	0.63	0.32	0.24	0.31
MgO	19.09	18.29	17.83	18.52	18.80	15.34	15.01	15.12
CaO	11.96	11.72	11.46	11.85	11.93	19.56	20.45	19.26
Na ₂ O	0.76	1.12	1.14	0.91	0.60	0.34	0.33	0.37
Total	96.65	97.40	97.23	96.79	97.42	100.07	100.32	100.16
<i>Atomic Proportions</i>								
Si	1.95	1.88	1.89	1.91	1.97	1.92	1.88	1.92
Ti	0.01	0.02	0.02	0.02	0.01	0.02	0.02	0.02
Al	0.19	0.28	0.27	0.24	0.15	0.11	0.17	0.12
Al ^{IV}	0.05	0.12	0.11	0.09	0.03	0.08	0.12	0.08
Al ^{VI}	0.14	0.16	0.17	0.15	0.12	0.04	0.05	0.03
Cr	0.00	0.00	0.00	0.00	0.00	0.00	0.00	0.00
Total Fe	0.22	0.25	0.27	0.24	0.27	0.29	0.28	0.32
Mn	0.02	0.01	0.02	0.01	0.02	0.01	0.01	0.01
Mg	1.06	1.01	0.99	1.03	1.04	0.85	0.83	0.84
Ca	0.48	0.47	0.46	0.47	0.47	0.78	0.81	0.77
Na	0.05	0.08	0.08	0.07	0.04	0.02	0.02	0.03
Total cations	4	4	4	4	4	4	4	4
Oxygens	6	6	6	6	6	6	6	6

Appendix 3 cont.

Sample	05-JES-144B59	05-JES-144B60	05-JES-144B61	05-JES-144C62	05-JES-144C63	05-JES-144C64	05-JES-144D65	05-JES-144D66
Mineral	Augite	Augite	Augite	Augite	Augite	Augite	Augite	Augite
Lithology	Andesite	Andesite	Andesite	Andesite	Andesite	Andesite	Andesite	Andesite
Weight percent								
SiO ₂	51.58	51.64	51.64	51.37	50.55	50.33	50.60	50.49
TiO ₂	0.50	0.47	0.67	0.64	0.69	0.68	0.74	0.72
Al ₂ O ₃	3.13	2.91	2.91	3.32	4.28	3.85	3.74	4.09
FeO	8.00	8.09	7.90	7.67	7.86	8.42	8.46	8.36
MnO	0.21	0.19	0.21	0.19	0.18	0.21	0.18	0.23
MgO	16.06	16.07	15.63	15.62	15.26	15.16	15.17	15.15
CaO	19.98	20.06	20.39	20.71	20.42	20.66	20.58	20.43
Na ₂ O	0.38	0.36	0.34	0.33	0.35	0.35	0.36	0.38
Total	99.84	99.79	99.69	99.86	99.58	99.66	99.84	99.85
<i>Atomic Proportions</i>								
Si	1.91	1.91	1.92	1.90	1.88	1.88	1.88	1.88
Ti	0.01	0.01	0.02	0.02	0.02	0.02	0.02	0.02
Al	0.14	0.13	0.13	0.15	0.19	0.17	0.16	0.18
Al ^{iv}	0.09	0.09	0.08	0.10	0.12	0.12	0.12	0.12
Al ^{vi}	0.05	0.04	0.04	0.05	0.07	0.05	0.05	0.06
Cr	0.00	0.00	0.00	0.00	0.00	0.00	0.00	0.00
Total Fe	0.25	0.25	0.25	0.24	0.24	0.26	0.26	0.26
Mn	0.01	0.01	0.01	0.01	0.01	0.01	0.01	0.01
Mg	0.89	0.89	0.86	0.86	0.85	0.84	0.84	0.84
Ca	0.79	0.80	0.81	0.82	0.81	0.83	0.82	0.81
Na	0.03	0.03	0.02	0.02	0.03	0.03	0.03	0.03
Total cations	4	4	4	4	4	4	4	4
Oxygens	6	6	6	6	6	6	6	6

Appendix 3 cont.

Sample	05-JES-144D67	05-JES-144D68	05-JES-144D69	05-JES-144D70	05-JES-144D71	05-JES-144D72	05-JES-144E73	05-JES-144E74
Mineral	Augite	Augite	Augite	Augite	Augite	Augite	Augite	Augite
Lithology	Andesite	Andesite	Andesite	Andesite	Andesite	Andesite	Andesite	Andesite
<i>Weight percent</i>								
SiO ₂	50.82	51.66	50.74	50.98	50.47	51.91	52.28	52.34
TiO ₂	0.62	0.49	0.60	0.71	0.78	0.54	0.36	0.28
Al ₂ O ₃	4.32	3.45	4.21	3.39	4.10	2.43	2.25	2.25
FeO	6.84	7.00	7.05	9.72	9.41	9.17	8.23	8.20
MnO	0.17	0.18	0.17	0.24	0.22	0.29	0.24	0.22
MgO	15.49	16.23	15.71	15.20	14.97	15.83	15.68	15.52
CaO	21.13	20.89	20.87	19.32	19.34	19.38	20.82	20.84
Na ₂ O	0.32	0.29	0.34	0.43	0.37	0.35	0.36	0.36
Total	99.70	100.18	99.69	99.99	99.67	99.88	100.22	100.00
<i>Atomic Proportions</i>								
Si	1.88	1.90	1.88	1.90	1.88	1.93	1.93	1.94
Ti	0.02	0.01	0.02	0.02	0.02	0.02	0.01	0.01
Al	0.19	0.15	0.18	0.15	0.18	0.11	0.10	0.10
Al ^{iv}	0.12	0.10	0.12	0.10	0.12	0.07	0.07	0.06
Al ⁱⁱⁱ	0.07	0.05	0.06	0.05	0.06	0.03	0.03	0.04
Cr	0.00	0.00	0.00	0.00	0.00	0.00	0.00	0.00
Total Fe	0.21	0.22	0.22	0.30	0.29	0.28	0.25	0.25
Mn	0.01	0.01	0.01	0.01	0.01	0.01	0.01	0.01
Mg	0.85	0.89	0.87	0.84	0.83	0.88	0.86	0.86
Ca	0.84	0.82	0.83	0.77	0.77	0.77	0.83	0.83
Na	0.02	0.02	0.02	0.03	0.03	0.03	0.03	0.03
Total cations	4	4	4	4	4	4	4	4
Oxygens	6	6	6	6	6	6	6	6

Appendix 3 cont.

Sample Mineral Lithology	05-JES-144E75 Augite Andesite	05-JES-144F76 Augite Andesite	05-JES-144F77 Augite Andesite	05-JES-144F78 Augite Andesite	05-JES-136A2 Albite Andesite	05-JES-136A3 Albite Andesite	05-JES-136B4 Albite Andesite	05-JES-136B5 Albite Andesite	05-JES-136B6 Albite Andesite
<i>Weight percent</i>									
SiO ₂	51.25	50.82	51.43	52.22	67.29	66.67	66.62	67.13	67.05
TiO ₂	0.52	0.61	0.48	0.27					
Al ₂ O ₃	3.18	4.43	3.39	2.51	20.29	20.64	20.31	20.31	20.60
FeO	8.31	7.00	7.17	8.74	0.02	0.04	0.03	0.07	0.03
MnO	0.22	0.19	0.25	0.31	0.01	0.00	0.00	0.00	0.00
MgO	15.31	15.54	16.08	15.70	0.00	0.01	0.01	0.03	0.03
CaO	20.56	20.63	20.55	20.28	0.62	0.89	0.90	0.59	0.90
Na ₂ O	0.38	0.34	0.32	0.32	11.31	11.09	11.18	11.44	11.03
Total	99.72	99.54	99.66	100.34	99.53	99.34	99.05	99.57	99.64
<i>Atomic Proportions</i>									
Si	1.91	1.88	1.90	1.93	2.96	2.94	2.94	2.95	2.94
Ti	0.01	0.02	0.01	0.01	0.00	0.00	0.00	0.00	0.00
Al	0.14	0.19	0.15	0.11	1.05	1.07	1.06	1.05	1.07
Al ^{iv}	0.09	0.12	0.10	0.07	0.04	0.06	0.06	0.05	0.06
Al ^{vi}	0.05	0.08	0.05	0.04	1.01	1.01	1.00	1.00	1.01
Cr	0.00	0.00	0.00	0.00	0.00	0.00	0.00	0.00	0.00
Total Fe	0.26	0.22	0.22	0.27	0.00	0.00	0.00	0.00	0.00
Mn	0.01	0.01	0.01	0.01	0.00	0.00	0.00	0.00	0.00
Mg	0.85	0.86	0.89	0.87	0.00	0.00	0.00	0.00	0.00
Ca	0.82	0.82	0.82	0.80	0.03	0.04	0.04	0.03	0.04
Na	0.03	0.02	0.02	0.02	0.96	0.95	0.96	0.98	0.94
Total cations	4	4	4	4	5.00	5.00	5.00	5.00	5.00
Oxygens	6	6	6	6	8	8	8	8	8

Appendix 3 cont.

Sample	05-JES-136C7	05-JES-136C8	05-JES-136C9	05-JES-136D10	05-JES-136D11	05-JES-136D12	05-JES-136E13	05-JES-136E14	05-JES-136E15
Mineral	Albite	Albite	Albite	Albite	Albite	Albite	Albite	Albite	Albite
Lithology	Andesite	Andesite	Andesite	Andesite	Andesite	Andesite	Andesite	Andesite	Andesite
Weight percent									
SiO ₂	66.87	66.35	66.07	66.36	66.28	66.25	66.65	67.00	66.97
TiO ₂									
Al ₂ O ₃	20.40	20.87	20.96	20.75	20.26	20.96	20.67	20.58	20.52
FeO	0.03	0.01	0.06	0.06	0.01	0.00	0.03	0.01	0.04
MnO	0.01	0.00	0.03	0.00	0.00	0.00	0.01	0.00	0.00
MgO	0.01	0.02	0.02	0.04	0.01	0.02	0.01	0.02	0.01
CaO	0.86	1.20	1.43	1.25	0.79	1.09	0.98	0.87	0.76
Na ₂ O	11.12	11.02	10.64	11.05	7.64	10.91	11.30	11.38	11.28
Total	99.31	99.45	99.21	99.49	94.99	99.24	99.66	99.87	99.58
<i>Atomic Proportions</i>									
Si	2.95	2.92	2.92	2.92	3.00	2.92	2.93	2.94	2.94
Ti	0.00	0.00	0.00	0.00	0.00	0.00	0.00	0.00	0.00
Al	1.06	1.08	1.09	1.08	1.08	1.09	1.07	1.06	1.06
Al ^{IV}	0.05	0.08	0.08	0.08	0.00	0.08	0.07	0.06	0.06
Al ^{VI}	1.01	1.01	1.01	1.00	1.08	1.01	1.00	1.00	1.01
Cr	0.00	0.00	0.00	0.00	0.00	0.00	0.00	0.00	0.00
Total Fe	0.00	0.00	0.00	0.00	0.00	0.00	0.00	0.00	0.00
Mn	0.00	0.00	0.00	0.00	0.00	0.00	0.00	0.00	0.00
Mg	0.00	0.00	0.00	0.00	0.00	0.00	0.00	0.00	0.00
Ca	0.04	0.06	0.07	0.06	0.04	0.05	0.05	0.04	0.04
Na	0.95	0.94	0.91	0.94	0.67	0.93	0.96	0.97	0.96
Total cations	5.00	5.00	5.00	5.00	5.00	5.00	5.00	5.00	5.00
Oxygens	8	8	8	8	8	6	6	6	6

Appendix 3 cont.

Sample Mineral Lithology	05-JES-136F16 Albite Andesite	05-JES-136F17 Albite Andesite	05-JES-136F18 Albite Andesite	05-JES-136G19 Albite Andesite	05-JES-136G20 Albite Andesite	05-JES-136G21 Albite Andesite
<i>Weight percent</i>						
SiO ₂	67.09	65.85	66.44	66.86	65.24	65.25
TiO ₂						
Al ₂ O ₃	20.40	20.61	20.50	20.42	21.37	20.65
FeO	0.02	0.06	0.05	0.01	0.01	0.08
MnO	0.00	0.01	0.00	0.00	0.02	0.00
MgO	0.01	0.01	0.00	0.01	0.02	0.03
CaO	0.61	1.06	0.78	0.71	1.89	0.72
Na ₂ O	11.34	11.15	11.34	11.33	10.58	7.06
Total	99.47	98.74	99.10	99.34	99.15	93.79
<i>Atomic Proportions</i>						
Si	2.95	2.92	2.94	2.95	2.89	2.99
Ti	0.00	0.00	0.00	0.00	0.00	0.00
Al	1.06	1.08	1.07	1.06	1.12	1.11
Al ^{iv}	0.05	0.08	0.06	0.05	0.11	0.01
Al ^{vi}	1.01	1.00	1.00	1.01	1.01	1.10
Cr	0.00	0.00	0.00	0.00	0.00	0.00
Total Fe	0.00	0.00	0.00	0.00	0.00	0.00
Mn	0.00	0.00	0.00	0.00	0.00	0.00
Mg	0.00	0.00	0.00	0.00	0.00	0.00
Ca	0.03	0.05	0.04	0.03	0.09	0.04
Na	0.97	0.96	0.97	0.97	0.91	0.63
Total cations	5.00	5.00	5.00	5.00	5.00	5.00
Oxygens	6	6	6	6	6	6

Appendix 4 - Schaft Creek sample descriptions and locations.

Sample ID	Drillhole/ Station	Depth (m)	Easting	Northing	Location	Field Description
05-JES-001	T-107	42.4	379943	6359173		Green volcanic with lithic fragments and euhedral to subhedral phenocrysts. Veins of Qtz-carbonate, one type of which bears chalcocopyrite and bornite. Pyrite is fg and disseminated.
05-JES-002	T-107	44.2	379943	6359173		Altered green volcanic to sericitic. Intense veining and mineralization.
05-JES-003	T-107	46.6	379943	6359173		Intensely altered volcanics. Pink in colour with intense veining.
05-JES-004	T-107	51.5	379943	6359173		Sample of "sheeted" vein in volcanics for thin-section only.
05-JES-005	T-107	136.4	379943	6359173		Highly mineralized vein containing abundant chalcocopyrite and bornite with possible pyrite in a green volcanic porphyry with 5-10% dark-green phenocrysts.
05-JES-006	T-107	142.7	379943	6359173		K-spar altered wall rock (after porphyritic green volcanics) with very intense quartz veining containing extensive chalcocopyrite and bornite mineralization.
05-JES-007	T-107	164.7	379943	6359173		Strongly potassically altered porphyritic volcanic. Veins of quartz are present which host chalc and born, but vast majority appears to be disseminated, comprising 5-10% of the rock by volume.
05-JES-008	T-107	178.7	379943	6359173		Highly potassically altered green volcanics brecciated by quartz-carbonate vein. Fluid movement was forcable, as wall rock clasts within vein are sharp and angular - contact is also sharp. Some fragments (clasts) bear quartz veins within, showing the episodes may be unrelated. Appearance of veins is different too - earlier vein mainly Qtz, while new vein strongly carbonitic. No mineralization seems to be associated with this event.
05-JES-009	H-050	49.7	380141	6359765		Grey-green fine-grained intermediate volcanics with plagioclase and pyroxene/hornblende. Minor quartz-carbonate veining. Disseminated pyrite. Moderate to strong chlorite/epidote alteration.
05-JES-010	H-050	160.1	380141	6359765		Grey-green volcanics with vein of chalcocopyrite 0.5cm wide cutting across core. Disseminated pyrite within the wallrock accounts for 5-8% of the rock by volume.
05-JES-011	H-050	195.1	380141	6359765		Quartz fragments within green fine grained groundmass likely of chlorite. Chalcocopyrite and pyrite are observed to occur both as fragments and within the groundmass. Possible shear zone - a fabric exists within the rocks.
05-JES-012	H-050	199.4	380141	6359765		Quartz Diorite to Tonalite dyke, fine- to medium-grained. Mafic minerals account for ~5-10%; hornblende or pyroxene. Sulphides are disseminated - mainly pyrite, but trace chalcocopyrite is also present. Potassic mineralizing dyke cuts across. Contact with volcanics is very sharp.
05-JES-013	H-050	217.4	380141	6359765		Quartz-feldspar porphyry dyke (quartz-monzonitic in composition) with 60-70% phenocrysts of quartz and feldspar with occasional mafics in a very fine grained matrix/groundmass. May be potassically altered. Intersected by very few quartz or carbonate veins - only few that do cut are very narrow (hairline). Disseminated chalcocopyrite and pyrite.
05-JES-014	H-091	95.1	379623	6359575		Tourmaline Breccia
05-JES-015	H-091	103.0	379623	6359575		Tourmaline Breccia
05-JES-016	H-091	104.3	379623	6359575		Tourmaline Breccia
05-JES-017	H-091	107.0	379623	6359575		Tourmaline Breccia - Quartz-Carbonate-Tourmaline vein
05-JES-018	H-091	111.3	379623	6359575		Tourmaline Breccia with quartz vein and associated sulphides
05-JES-019	H-091	124.7	379623	6359575		Tourmaline Breccia

Appendix 4 cont.

Sample ID	Drillhole/ Station	Depth (m)	Location		Field Description
			Eastings	Northing	
05-JES-020	H-091	124.7	379623	6359575	Tourmaline Breccia showing multiple events
05-JES-021	H-091	123.2	379623	6359575	Tourmaline Breccia with cross-cutting chlorite veins
05-JES-022	H-091	128.7	379623	6359575	Tourmaline Breccia with epidote and chalcopyrite
05-JES-023	H-091	135.1	379623	6359575	Tourmaline Breccia
05-JES-024	H-091	134.1	379623	6359575	Tourmaline Breccia
05-JES-025	H-091	139.6	379623	6359575	Tourmaline Breccia - very nice with potassically altered quartz monzonite clasts
05-JES-026	H-091	142.7	379623	6359575	Tourmaline Breccia - very highly mineralized
05-JES-027	H-091	144.8	379623	6359575	Tourmaline Breccia showing concentration of sulphides within the matrix
05-JES-028	H-091	160.4	379623	6359575	Tourmaline Breccia with veins of vuggy quartz-carb vein (vein composition uncertain)
05-JES-029	H-091	159.5	379623	6359575	Tourmaline Breccia
05-JES-030	H-091	157.3	379623	6359575	Tourmaline Breccia - Clast not as fractured - lower alteration and mineralization
05-JES-031	H-091	163.1	379623	6359575	Tourmaline Breccia
05-JES-032	H-091	164.6	379623	6359575	Tourmaline Breccia
05-JES-033	H-091	179.6	379623	6359575	Tourmaline Breccia
05-JES-034	H-091	186.0	379623	6359575	Tourmaline Breccia with chalcopyrite vein cross-cutting
05-JES-035	H-091	187.5	379623	6359575	Tourmaline Breccia with multiple cross-cutting veins
05-JES-036	H-091	197.9	379623	6359575	Tourmaline Breccia with possible phyllic overprint after potassic alteration
05-JES-037	H-091	201.2	379623	6359575	Wide quartz vein
05-JES-038	H-091	202.7	379623	6359575	Cross-cutting and offset quartz veins
05-JES-039	H-091	212.2	379623	6359575	Tourmaline Breccia with vuggy quartz-carbonate veins filling matrix space
05-JES-040	H-091	213.4	379623	6359575	Tourmaline Breccia with vuggy quartz-carbonate veins filling matrix space
05-JES-041	H-091	214.9	379623	6359575	Tourmaline Breccia - well defined with sharp, angular clasts
05-JES-042	H-091	226.2	379623	6359575	Tourmaline Breccia with clast showing fracture-controlled hematite
05-JES-043	H-091	225.6	379623	6359575	Tourmaline Breccia - Quartz vein within clast cut by brecciation
05-JES-044	H-091	260.1	379623	6359575	Tourmaline Breccia - Quartz Monzonite with bornite and chalcopyrite
05-JES-045	H-093	59.1	379976	6360099	Multiple generation quartz-carbonate veins in green volcanics
05-JES-046	H-093	197.9	379976	6360099	Nice wide quartz vein in green volcanics
05-JES-047	H-093	199.4	379976	6360099	Nicely sheeted quartz veins
05-JES-048	H-093	255.2	379976	6360099	Possible volcanic breccia
05-JES-049	H-093	256.7	379976	6360099	Strong alteration overprinting feldspar porphyry. Epidote is present, overprinting potassic alteration. Chalcopyrite and bornite present (trace).
05-JES-050	T-132	123.5	379537	6361025	Possibly late mafic dyke
05-JES-051	T-132	260.1	379537	6361025	Felsic intrusive breccia with chalcopyrite
05-JES-052	T-132	257.6	379537	6361025	Bornite and chalcopyrite in possibly sericitized porphyritic volcanics
05-JES-053	T-132	268.0	379537	6361025	Intense bornite and chalcopyrite within quartz-carbonate vein within potassically-altered igneous breccia
05-JES-054	T-132	275.3	379537	6361025	Possible secondary biotite in porphyritic tonalite or quartz monzonite (PPFQ)

Appendix 4 cont.

Sample ID	Drillhole/ Station	Depth (m)	Location		Field Description
			Easting	Northing	
05-JES-055	T-132	298.8	379537	6361025	Hydrothermal breccia - intense quartz veining with moderate chalcocopyrite
05-JES-056	T-132	314.3	379537	6361025	Variably altered quartz-feldspar porphyry with intense bornite and chalcocopyrite
05-JES-057	T-132	319.5	379537	6361025	Intrusive breccia with bornite
05-JES-058	T-132	320.7	379537	6361025	Intrusive breccia with bornite and chalcocopyrite
05-JES-059	T-132	400.0	379537	6361025	Intrusive breccia with intense chalcocopyrite and bornite
05-JES-060	T-132	407.0	379537	6361025	Altered but 'barren' quartz monzonite to quartz diorite
05-JES-061	T-132	407.0	379537	6361025	Intrusive breccia with clast containing quartz veins which are cross cut by the brecciation
05-JES-062	T-132	410.1	379537	6361025	Intrusive breccia with trace chalcocopyrite. Potassically altered with propylitic overprint.
05-JES-063	T-132	410.7	379537	6361025	Intrusive breccia with trace chalcocopyrite and bornite. Representative textural sample.
05-JES-064	T-132	411.0	379537	6361025	Intrusive breccia with disseminated chalcocopyrite, bornite, and magnetite, and molybdenite. Porphyry is brecciating body.
05-JES-065	T-132	421.3	379537	6361025	Heterolithic intrusive breccia with chlorite/epidote veining. Good representative sample.
05-JES-066	T-132	423.2	379537	6361025	Intrusive breccia with intense chlorite/epidote veining and significant hematite.
05-JES-067	T-132	445.7	379537	6361025	Intrusive breccia with x-cutting quartz vein in turn being cut by carbonate vein containing some Fe-rich carbonate such as ankerite.
05-JES-068	T-132	481.4	379537	6361025	Intrusive breccia (feldspar porphyry clasts) with quartz vein hosting impressive bornite mineralization without associated chalcocopyrite.
05-JES-069	T-132	484.5	379537	6361025	Intrusive breccia shear zone hosting very impressive molybdenite mineralization within.
05-JES-070	H-084	27.4	380406	6359555	Diorite potassically altered then overprinted by phyllic - secondary biotite is replaced by chlorite, k-spar is sericitized. Disseminated chalcocopyrite, plus vein-hosted x-cutting quartz vein. Total 2-3% chalcocopyrite.
05-JES-071	H-084	28.0	380406	6359555	As 05-JES-070, but with a magnetite vein. Potassic alteration overprinted by phyllic.
05-JES-072	H-084	32.3	380406	6359555	Already stained, shows intense potassic alteration of diorite. Potassic alteration overprinted by phyllic.
05-JES-073	H-084	71.6	380406	6359555	Very nice sample. Diorite with disseminated pyrite and chalcocopyrite plus x-cutting vein of chalcocopyrite. Local hematite. Sulphides ~6-10%. Potassic alteration overprinted by phyllic.
05-JES-074	H-084	72.6	380406	6359555	Diorite with quartz veins cross cutting, hosting chlorite and magnetite. Potassic alteration overprinted by phyllic.
05-JES-075	H-084	75.3	380406	6359555	Diorite with disseminated pyrite. Chalcocopyrite is restricted to quartz vein with magnetite. Potassic alteration overprinted by phyllic.
05-JES-076	H-084	86.3	380406	6359555	Diorite with x-cutting quartz vein hosting chalcocopyrite. Some chalcocopyrite is disseminated. Potassic alteration overprinted by phyllic.
05-JES-077	H-084	90.2	380406	6359555	Diorite - intensely potassically altered with light phyllic alteration overprint. Extensive quartz veining (almost brecciating), hosting chalcocopyrite and molybdenite.
05-JES-078	H-084	91.2	380406	6359555	Diorite (coarser grained), potassically altered with large quartz vein hosting significant molybdenite and chalcocopyrite (and bornite) - also possible covellite (CuS).

Appendix 4 cont.

Sample ID	Drillhole/ Station	Depth (m)	Location		Field Description
			Easting	Northing	
05-JES-079	H-084	98.2	380406	6359555	Much more fine-grained - quartz vein cuts hosting molybdenite and chalcopyrite.
05-JES-080	H-084	108.2	380406	6359555	Volcanic breccia to fragmental. Intense chloritic alteration (propylitic) with disseminated pyrite (~2%) and trace chalcopyrite. Local quartz filling.
05-JES-081	H-084	260.1	380406	6359555	Very intense phyllic alteration possibly overprinting potassic. Cream coloured with no discernable textures - protolith possibly volcanic. Barren.
05-JES-082	H-084	257.6	380406	6359555	As 05-JES-081, but with some disseminated pyrite and barren hairline quartz veinlets.
05-JES-083	H-084	276.8	380406	6359555	Very nice sample. Beautifully aligned plagioclase phenocrysts with intense chalcopyrite and bornite vein hosted in two generations. Quartz vein x-cuts, which is then cut again by bornite vein. Disseminated chalcopyrite is also present. Plagioclase porphyry. Hematite is found in veins with chalcopyrite.
05-JES-084	H-084	277.1	380406	6359555	Diorite. Potassically altered with phyllic overprint. Disseminated pyrite and chalcopyrite (~5%). Chalcopyrite veins and quartz vein with chalcopyrite and molybdenite.
05-JES-085	H-084	281.4	380406	6359555	As 05-JES-084.
05-JES-086	H-084	298.2	380406	6359555	Fine-grained diorite with quartz+chalcopyrite+magnetite veins.
05-JES-087	H-084	304.9	380406	6359555	Volcanic breccia with phyllic alteration after potassic with disseminated pyrite and vein-hosted chalcopyrite. Local quartz fracture filling. Some possible tourmaline.
05-JES-088	H-084	308.2	380406	6359555	Feldspar porphyry (plagioclase phenocrysts). Propylitically altered with quartz vein hosting chalcopyrite and moly with 1cm wide potassic rim. A Chalcopyrite vein cross-cuts. Epidote is present.
05-JES-089	T-109	213.4	379795	6359475	Andesite with variable but very intense chloritization (propylitic alteration). May be brecciating. Cross-cut by quartz veins. No sulphides.
05-JES-090	H-060	363.4	380121	6359638	Fragmented andesite (or Volcanic Breccia) with variably altered clasts. Strongly chloritized (propylitic alteration). Possibly related to some hydrothermal brecciation event - tourmaline matrix with sharp clasts of angular andesite.
05-JES-091	H-045	364.3	380524	6359468	Quartz monzonite (possibly porphyritic) with cross-cutting quartz veins contributing potassic alteration to wall rock, the depth of penetration is directly proportional to the size of the vein. No sulphides. Interesting texturally.
05-JES-092	T-147	22.9	380109	6360089	Andesitic volcanic breccia with variably altered heterolithic clasts, some large up to 5cm. Local intense chloritic/epidote alteration. This interval logged by teck as "P.V.L.P.". No purple colouration was observed.
05-JES-093	T-147	24.4	380109	6360089	Intensely altered clast from unit described in 05-JES-092. Complete epidote replacement.
05-JES-094	T-147	59.5	380109	6360089	Andesite porphyry. Well formed euhedral plagioclase with anhedral pyroxene phenocrysts. Epidote (propylitic) alteration with hematite. Hematite is often directly associated with chlorite.
05-JES-095	T-147	81.1	380109	6360089	Heterolithic volcanic breccia/fragmental volcanic. Groundmass/matrix is andesitic, and is intensely epidotized (propylitic alteration). Clast boundaries are sharp, while clasts are variable: some are intensely hematized (andesite with intense purple/red appearance), while others are more mafic (possibly clasts of PPAU).

Appendix 4 cont.

Sample ID	Drillhole/ Station	Depth (m)	Location		Field Description
			Easting	Northing	
05-JES-096	H-073	8.5	380235	6360246	mg. Diorite. Potassically altered with later light chloritic alteration of secondary biotite. Plagioclase grains are euhedral and cumulate. Some trace pyrite, apparently associated with chlorite. Veins of chlorite and quartz cross-cut.
05-JES-097	H-073	40.2	380235	6360246	fg Andesite, grey to black in appearance. Possibly phyllic partially overprinted by propylitic. Vfg sericitic alteration with locally concentrated intense chlorite. Fine quartz veins cut, offsetting chlorite vein.
05-JES-098	H-073	55.5	380235	6360246	Andesite - possibly volcanic breccia or fragmental volcanic. "clasts" or "splotches" of very highly chloritized andesite, or could almost be described as chloritic "nodules". Disseminated pyrite seems to be spatially associated with chlorite. Dark selvages appear around chloritic nodules. Clasts of granodiorite are adjacent, pointing towards heterolithic breccia origin. Pyrite ~5%, often euhedral showing good typical cubic habit.
05-JES-099	H-073	118.3	380235	6360246	Granodiorite (possibly a dyke). Potassically altered with propylitic overprint. Disseminated pyrite account for ~2% of the rock by volume. Hairline quartz veins, locally hosting trace chalcopyrite. Chlorite vein cuts.
05-JES-100	H-073	129.3	380235	6360246	Intensely sheared and/or brecciated volcanics. Brown in colour. Intense quartz-carbonated veining with local tourmaline. Likely a hydrothermal breccia. Local molybdenite paint on fracture surfaces.
05-JES-101	H-073	188.1	380235	6360246	Pyroxene-Plagioclase Andesite Porphyry. Euhedral phenocrysts. Green/brown colouration. Sericite and chlorite alteration - multiple phases? Quartz tourmaline veins cut and host chalcopyrite. Quartz vein cross-cuts these veins.
05-JES-102	H-073	219.5	380235	6360246	Intensely altered - protolith is indistinguishable, likely Andesite. Purple colouration preserved in centres of "clasts", possibly relic potassic alteration (or hematization?). Brownish/tan colour and clay and/or sericitic minerals point to possible argillic alteration.
05-JES-103	H-073	222.3	380235	6360246	Intensely altered. Possibly fragmental volcanic or hydrothermal breccia. Relic texture consistent with tourmaline matrix and highly potassically altered (purple-reddist) clasts. Multiple veining events. Similar in texture to 05-JES-102, but alteration is less intense. Possibly some chlorite alteration, but sericitic and/or clay alteration is dominant.
05-JES-104	H-073	232.9	380235	6360246	Green andesitic volcanics. Local vein-related potassic alteration overprinted by chloritization. Multiple generations of quartz veins, at least two pulses. Later one is possibly associated with spectacular pyrite mineralization - well formed euhedral, cubic pyrite approaching 4mm diametre. Locally some chalcopyrite is associated, but limited. Pyrite accounts for ~10% of the rock by volume. Earlier generations of veining, at least one of which contains tourmaline - which may rather be purple "dusty" hematite - red streak. Very nice sample.
05-JES-105	H-073	304.9	380235	6360246	Zone of sheeted quartz veins cutting andesite. Andesite is highly altered, brown/tan colour, possibly potassic alteration overprinted by silic or phyllic (argillic?). Good intact veins, possibly for fluid inclusion work. Sample taken ~5' from 8" wide quartz vein containing chlorite and possible ankerite. Local molybdenite paint on fractured surfaces.

Appendix 4 cont.

Sample ID	Drillhole/ Station	Depth (m)	Location		Field Description
			Easting	Northing	
05-JES-106	H-064	13.7	380243	6359176	"Augite Porphyry Unit - PPAU". 2mm euhedral plagioclase phenocrysts in a dark fine-grained groundmass, with smaller "blady plagioclase phenocrysts. Some (~10%) of phenocrysts may be k-spar. Possible quartz phenocrysts. Unit is cross-cut by quartz veins.
05-JES-107	H-064	14.9	380243	6359176	Coarser-grained "PPAU", as a medium- to fine-grained gabbro or gabbronorite. Chloritic alteration of pyroxenes is moderate to low. Hematite/quartz dyke cuts, local chalcocopyrite veins are present.
05-JES-108	H-064	23.8	380243	6359176	"PPAU" - porphyritic gabbronorite. Plag and pyroxene with chlorite alteration of pyroxenes. Sample taken is very typical and representative of the unit. Fine fracture-filling quartz veins are present, along with narrow (~0.5mm) chalcocopyrite veins.
05-JES-109	H-064	52.7	380243	6359176	ANPF unit is not observably porphyritic, but of not is again the vein-hosted nature of the chalcocopyrite mineralization.
05-JES-110	H-064	76.2	380243	6359176	Fine-grained "PPAU" - porphyritic gabbronorite. Near contact with andesite, so smaller grain size can be attributed to chill margin, possibly indicating intrusive nature of the unit. Intense chalcocopyrite and magnetite mineralization along veins. These veins are surrounded by chloritic wall-rock alteration, the depth of penetration being proportional to vein size.
05-JES-111	H-064	77.7	380243	6359176	Beautiful porphyritic mafic volcanic (gabbronorite) with large euhedral pyroxene grains up to 1cm in diameter. Disseminated and vein-hosted pyrite account for ~5% by volume. Local chalcocopyrite occurring along fine veins ~0.5mm wide. Groundmass is fine grained. Chloritic alteration is moderate and pervasive. Very much modally gabbroic to noritic.
05-JES-112	H-064	80.8	380243	6359176	Melanogabbronorite (PPAU). Local disseminated magnetite. Coarse- to medium-grained cumulate pyroxenes. Chlorite alteration, particularly of "interstitial" material (possibly groundmass of porphyry). No disseminated sulphides were observed. Chalcocopyrite is restricted to narrow veins with pyrite.
05-JES-113	H-064	85.7	380243	6359176	More porphyritic gabbronorite with well-formed euhedral phenocrysts of pyroxene up to 4mm in diameter. Locally intense chalcocopyrite and pyrite veining. Cross-cut by later quartz veins with tourmaline. Chlorite alteration, particularly of groundmass. Observations by other geos: Possibly a diorite - hornblende rather than pyroxene. Possibly amphibole pseudomorphs after augite.
05-JES-114	H-064	104.3	380243	6359176	Gabbronorite porphyry with fewer, larger phenocrysts up to 1.2cm diameter. Shows offsetting of quartz veins providing evidence for at least two phases of quartz veining. Local hematite staining. Local tourmaline veining.
05-JES-115	H-064	106.7	380243	6359176	Porphyritic gabbronorite with substantial tourmaline-quartz veins. **Throughout hole, all mineralization is vein-hosted, and predominantly chalc-only. Locally some moly is present, and bornite is rare.

Appendix 4 cont.

Sample ID	Drillhole/ Station	Depth (m)	Easting	Location Northing	Field Description
05-JES-116	H-064	189.0	380243	6359176	Porphyritic quartz monzodiorite to tonalite. No mafic minerals were observed. Possibly replaced by chalcopyrite and bornite, which appear to be disseminated and fine grained, account for ~5% of the rock. Possibly ankerite alteration - vfg. Brownish reddish tan coloured alteration, semi-fracture controlled. If volcanic, would be rhyolitic. Possibly a QZMZ that has been intensely sericitized - this would explain the lack of primary textures and the "washed-out" appearance. Fresh nicely formed plagioclase phenocrysts. Carbonate alteration present/likely. Sulphides are likely controlled by microveinlets.
05-JES-117	H-064	214.3	380243	6359176	Volcanic sediment - possibly greywacke. Fine grained, well sorted, with graded bedding oblique to core axis. Lithic fragments present, but predominantly fine subrounded grains of plag, k-spar, and possibly pyroxene. Groundmass is green in colour. Weak to moderate chloritic alteration. No sulphides.
05-JES-118	H-064	251.5	380243	6359176	Volcanic sedimentary conglomerate. Large lithic clasts up to 5cm of andesite with smaller heterolithic fragments. Groundmass is fine-grained, mostly lithic clasts with very intense chloritic alteration.
05-JES-119	H-064	255.2	380243	6359176	Volcanic sedimentary conglomerate. Heterolithic lithic clasts ranging in size from 3cm to 0.2mm and possibly smaller. Groundmass and clasts are both intensely altered to likely chlorite, but alteration of the groundmass is more intense. Locally some possible argillic/clay alteration interpreted from brown/greyish colour along hairline fractures. Locally trace vein-hosted chalcopyrite.
05-JES-120	H-064	276.2	380243	6359176	Purple-coloured volcanic sediments. Fine-grained (sandstone-sized). Contact is subvertical to core axis. Fine veins of possible tourmaline cross-cut, locally hosting trace chalcopyrite.
05-JES-121	H-064	276.8	380243	6359176	Orange coloured volcanics. Contact with purple volcanics is sharp (and included in sample). Lithic fragments are present. Cut by two vein generations, one quartz with probably magnetite selvages, the other more chloritic. Colour possibly imparted by an argillic alteration.
05-JES-122	H-064	297.6	380243	6359176	Fine-grained igneous felsic rock. Alignment of shards/phenocrysts - veins are also aligned. Microveining is intense - shatter the rock, mm spacing veins. Sericitic alteration. Sheared/hydrothermally veined very strongly. Potassic alteration overprinted by phyllic or possibly argillic alteration. Reddish/pink colour overprinted by brown/grey colouration. Very fine grained sericite or possibly clay minerals. Some trace disseminated pyrite present. Numerous veins cut, but are all strongly deformed by shearing. Large quartz vein hosts ~10-20% pyrite and chalcopyrite, with pyrite being dominant -4:1.
05-JES-123	H-053	50.0	379749	6360092	Semi-massive pyrite mineralization. Pyrite hosted by quartz veins which cut brownish-coloured andesitic volcanics. Pyrite content is roughly 50% with no chalcopyrite, bornite, or molybdenite. Interval directly follows shear zone (or fracture zone - core is fine pebbles). Later fine (~0.5mm) quartz-carbonate veins cut. This is consistently observed throughout the deposit as minor fracture-controlled quartz-carbonate veins represent the last event in the system. This sample could possibly be assayed for Au content (05-JES-123A)

Appendix 4 cont.

Sample ID	Drillhole/ Station	Depth (m)	Easting	Location Northing	Field Description
05-JES-124	H-053	56.1	379749	6360092	Intensely altered undifferentiated andesite, or possibly porphyritic quartz-feldspar (quartz-monzonitic) dyke, as it is near/at the lithologic boundary. Rock altered to light brownish/tan/grey and appears to possibly have been carbonically altered? (Argillic?) as interpreted from the reddish tan colour and carbonate mineralization. Pyrite is vein hosted along fine fractures and accounts for 1% by volume of the rock.
05-JES-125	H-053	60.4	379749	6360092	Granodiorite? Plag and K-spar are roughly equal (if K-spar is primary) with quartz and some replaced biotite. Possibly potassic alteration. Definite sericitic alteration. Pyrite occurs along veins and apparently disseminated, usually associated with relic biotite. Quartz-pyrite vein also bears notable concentration of a black non-opaque mineral along the vein boundaries. Pyrite is ~2%.
05-JES-126	H-053	71.6	379749	6360092	Quartz Monzonite, potassically altered. Disseminated pyrite (~1%). Vein hosted pyrite created alteration halo which is dark-grey to brown and ~1.2cm wide around pyrite vein. Black non-opaque mineral vein cross-cuts all.
05-JES-127	H-053	199.7	379749	6360092	Potassically altered andesite - fine-grained, pink colouration. Fragmented, brecciated by tourmaline. Clasts are sharp and angular, with no wall-rock alteration. Matrix is locally pyritized ~10%.
05-JES-128	H-053	143.6	379749	6360092	Potassically altered porphyritic andesite to a heterolithic fluid breccia with a greyish carbonitic matrix/groundmass. Clasts are variably potassically altered with sharp boundaries, and are subangular. Local massive pyrite overprint, but occurs preferentially in the matrix. Black mineral in matrix may be an opaque - to be determined in thin-section.
05-JES-129	H-053	145.7	379749	6360092	Porphyritic andesite with fine disseminated pyrite (~1%). Black, possibly carbonate veins are intense, and locally brecciate - spatially associated with spectacular pyrite.
05-JES-130	H-053	216.5	379749	6360092	Tourmaline breccia. All clasts are green andesite. Trace pyrite - some disseminated, most hosted in quartz. Tourmaline matrix is locally quartz-rich. Trace chalcopyrite occurs in tourmaline. Fragments are sharp and angular.
05-JES-131	H-053	218.0	379749	6360092	Potassically altered porphyritic andesite to quartz-feldspar porphyry - overprinted by light chloritic alteration. Strongly brecciated by tourmaline (fluid) matrix. Clast size ranges from 10cm to <1mm, and are sharp and angular to subangular.
05-JES-132	H-053	221.0	379749	6360092	Tourmaline breccia. Sample clearly shows restriction of sulphides (chalcopyrite and pyrite) to the matrix. Breccia is heterolithic, and clasts are potassically altered. Sulphides account for roughly 2% of the rock, or 20% of the matrix. Visible sharp fluid alteration boundary.
05-JES-133	H-053	267.1	379749	6360092	Andesite - dark grey, moderately sericitized. Cross-cut by pyrite/quartz vein, subparallel to core axis. Magnetite is closely associated, and contained within the vein. End of the sample interval is intensely altered by a greenish-tanish-yellow fibrous mineral.
05-JES-134	H-053	268.9	379749	6360092	Heterolithic tourmaline BX with potassically altered clasts. Pyrite mineralization is spectacular, but restricted to matrix along with lesser chalcopyrite. ~40% of matrix, or 5-10% of the rock by volume.

Appendix 4 cont.

Sample ID	Drillhole/ Station	Depth (m)	Location		Field Description
			Easting	Northing	
05-JES-135	H-053	297.6	379749	6360092	Heterolithic tourmaline breccia with massive pyrite mineralization within the matrix. ~80% of the matrix is pyrite, or roughly 20% of the rock by volume. Sample 05-JES-135A was taken for assay for gold. Clasts of feldspar porphyry.
05-JES-136	N/A	Surface	380604	6359783	Plagioclase-Augite porphyritic volcanics. Very little veining, massive. Outcrop is 3m x 2m.
05-JES-137	N/A	Surface	380591	6360015	Fine-grained andesite with chloritic alteration. Outcrop is poorly exposed and rubbly in appearance. No structures were clearly visible.
05-JES-138	N/A	Surface	380817	6360168	5m outcrop on side of road cut. Fine-grained andesite with sericitic and chloritic alteration. Fracture plain is oriented at 008/52.
05-JES-139	N/A	Surface	380817	6360168	Same location, opposite end of outcrop. Porphyritic andesite. Subhedral plagioclase phenocrysts, sericitically altered. Chloritic alteration of groundmass.
05-JES-140	N/A	Surface	380575	6360148	Locally strongly sheared, highly weathered andesitic volcanics. Strike and dip of plain of preferential failure (possible bedding?) is oriented 256/50.
05-JES-141	N/A	Surface	380544	6360146	Purple volcanics, massive and unaltered.
05-JES-142	N/A	Surface	380460	6360128	Andesitic conglomerate, strongly weathered, weakly veined
05-JES-143	N/A	Surface	380437	6360144	Massive plagioclase porphyritic andesite. Weakly weathered, unaltered, with weak fracturing. Contact with Andesite conglomerate unit is at 245/55.
05-JES-144	N/A	Surface	380449	6359951	Massive plagioclase-pyroxene porphyritic andesite. Low weathering, fracture and vein-free. 4m downhill a zone of intense alteration and mineralization - gossanous, chalcopyrite, rusty staining. Immediately followed by ANPF again, though more sheared and altered.
05-JES-145	N/A	Surface	380449	6359951	Sample number not used
05-JES-146	T-136	29.9	379212	6360720	Granodiorite, medium-grained. Mineralized. Sulphides occur both as disseminations and in veins, however those appearing disseminated may be hosted in very fine grains. Vuggy quartz vein cuts, host light (trace) pyrite and chalcopyrite mineralization. Total sulphides for the sample is trace. Locally brecciated by quartz. Zones of variably intense chlorite replacement, apparently overprinting potassic alteration.
05-JES-147	T-136	30.8	379212	6360720	Granodiorite, potassically altered. Trace sulphides (as disseminations). Trace pyrite is associated with carb-quartz veins which cut. Potassic alteration is overprinted by vein-controlled chloritic alteration.
05-JES-148	T-136	32.6	379212	6360720	Potassically altered granodiorite with possible bornite mineralization as disseminations. Associated with a fine-grained black metallic mineral which is also disseminated.
05-JES-149	T-136	36.3	379212	6360720	Very weakly potassically altered granodiorite, likely from the Hickman pluton (from spatial association). No visible sulphides, nice petrographic sample. Medium- to coarse-grained.
05-JES-150	T-136	46.6	379212	6360720	Logged as D/BS. HOWEVER: Contact with the granodiorite unit is like a mafic/intermediate dyke, but moving away from the contact, unit is strongly porphyritic with subhedral plagioclase grains (medium-grained phenocrysts). The groundmass is fine-grained and appears to possibly be plagioclase and pyroxene. The whole unit is very intensely altered to chlorite and epidote. Some <1mm quartz veins cross cut, but occur only two times over four feet.

Appendix 4 cont.

Sample ID	Drillhole/ Station	Depth (m)	Location		Field Description
			Easting	Northing	
05-JES-151	T-136	127.7	379212	6360720	Fine-grained gabbro to gabbronorite. Euhedral lath-shaped plagioclase. Dark-coloured (green to black). Disseminated pyrite is associated with epidote and chlorite. The unit described as BRIV in the drill log is invalid. The interval is composed of a number of small late dykes cutting through porphyritic volcanics, fine-grained gabbros, and granodiorite. There are no brecciation textures. These units are variably altered by epidote, chlorite, and disseminated pyrite. Locally becoming very intense.
05-JES-152	T-136	201.8	379212	6360720	Quartz-feldspar porphyry (medium-grained). Relatively unaltered, good representative sample. Some disseminated pyrite occurs. Chloritic and possible sericitic alteration are light. Phenocrysts account for approximately 70% of the rock.
05-JES-153	T-150	26.2	379769	6359789	Quartz-feldspar porphyry, potassically altered to moderate pink. Carbonate (Fe-rich - Ankerite?) veins cross cut. Disseminated trace molybdenite and chalcopyrite.
05-JES-154	T-150	41.5	379769	6359789	Intense vein-hosted molybdenic mineralization. Significant quartz veining is almost stockwork-type. Quartz cuts highly and intensely potassically altered quartz-feldspar porphyry. Molybdenum accounts for rough 2% of the rock by volume, but all is restricted to veins and fractures. Quartz veining is locally associated with Fe-rich carbonates (ankerite). Texture is though a quartz-rich hydrothermal breccia. Host rock is feldspar porphyry, but is now 80% quartz-carbonate veins of multiple generations. Some molybdenite is disseminated within quartz vein.
05-JES-155	T-150	45.7	379769	6359789	Highly altered andesite with intense chloritic alteration. Intense quartz veining, could possibly be described as hydrothermally brecciating, as in a stockwork. Hosted within quartz is significant bornite and chalcopyrite, accounting for ~25% of the veins, and 5% of the rock. Black mineral occurring in quartz vein is hematite (red streak). Mostly epidote alteration.
05-JES-156	T-150	56.1	379769	6359789	Coarse-grained disseminated chalcopyrite in highly altered andesite. Andesite is potassically altered with an intense sericitic overprint. Ore minerals are of unusually large size for this deposit.
05-JES-157	T-150	71.6	379769	6359789	Tectonic breccia, not mylonitic. Clasts of variably altered andesite are intensely fractured and rounded. Evidence of movement is observed in groundmass surrounding clasts. Groundmass is purply-reddish brown with patches of white (colour possibly from hematite?). A clear fabric exists, and is cross-cut by later quartz-carbonate veins.
05-JES-158	T-150	85.7	379769	6359789	Protolith is unrecognizable, likely andesite (observed to be fine-grained, but this may be a function of intense alteration by vfg minerals), and potassically altered. Intensely altered to locally brecciated by (light hydrothermal fracturing) by epidote/chlorite alteration. This alteration is most intense in the groundmass and as veins.
05-JES-159	T-150	90.5	379769	6359789	Intensely altered - some sort of breccia, but so intensely chloritized/epidotized that the protolith is not recognizable. Appears to be sheared or possibly faulted.
05-JES-160	T-150	90.9	379769	6359789	Cuts lithology of 05-JES-159. "Tectonic" breccia. Narrow zone ~8cm, cuts subvertical to core axis. Matrix and fragments and texture is similar to 05-JES-157.
05-JES-161	H-098	39.0	379926	6359796	Fine-grained gabbro, equigranular, no visible sulphides. Chloritically and sericitically altered.

Appendix 4 cont.

Sample ID	Drillhole/ Station	Depth (m)	Location		Field Description
			Easting	Northing	
05-JES-162	H-098	41.8	379926	6359796	Fine-grained porphyritic gabbro to diorite. Augite phenocrysts are ~0.5mm. Groundmass is moderately to strongly chloritically altered.
05-JES-163	H-098	117.1	379926	6359796	Fine-grained quartz monzonite (possibly a dyke intruding ANXX which makes up the majority of the hole). Phyllic alteration (light grey colour). Disseminated pyrite and chalcocopyrite accounting for ~2%.
05-JES-164	H-098	159.8	379926	6359796	Porphyritic to quartz monzonitic. Veins are well preserved for possible fluid inclusion work. Quartz-carbonate with local chlorite. Phyllic (sericitic) alteration. No sulphides.
05-JES-165	H-098	204.6	379926	6359796	Quartz veins cutting andesite. Veins host coarse-grained molybdenite. Possibly for geochron and fluid inclusion work.
05-JES-166	H-098	255.8	379926	6359796	Highly altered feldspar porphyry. Hydrothermally brecciated, potassically altered with an intense chlorite and sericite overprint. Very intense moly fracturing and vein-filling (~5% of the rock by volume).
05-JES-167	H-098	257.9	379926	6359796	Hydrothermally brecciated andesite with a chlorite and sericite overprint on potassic. A quartz vein hosts molybdenite. Disseminated (matrix-hosted?) chalcocopyrite and pyrite. Total sulphides ~5% (1% moly, 3% chalcocopyrite, 1% pyrite).
05-JES-168	H-098	268.0	379926	6359796	Fine-grained gabbro. No visible sulphides. Possibly serpentinized - fractures are filled by a glassy black mineral. Chloritically altered.
05-JES-169	H-098	272.0	379926	6359796	Highly altered andesite. Highly sericitically altered (with associated chlorite). Strongly deformed with light shearing. Fabric is present, indicating a possible tectonic brecciation.
05-JES-170	H-098	272.9	379926	6359796	Hydrothermal breccia with a fabric - possibly tectonic in origin. Highly altered by sericite and chlorite. Quartz and black non-metallic mineral matrix to the breccia.
05-JES-171	H-098	300.0	379926	6359796	Fine-grained gabbro. Mostly unmineralized. Light chlorite and possible serpentine alteration. No sulphides. Homogeneous.
05-JES-172	H-039	35.1	379817	6359321	"ANCG" - volcanic breccia or fragmental volcanic (not conglomeritic). Sericitic and chloritic alteration. Veins of chalcocopyrite cut subvertical to the core axis, and contain quartz and possible carbonates. No disseminated sulphides are present, but total pyrite accounts for ~2% by volume. Typical of unit (hosting of sulphides only within veins).
05-JES-173	H-039	140.2	379817	6359321	Highly potassically altered plagioclase-quartz-porphyrific andesite. Locally disseminated fine-grained molybdenite (trace). Cut by quartz veins hosting molybdenite and local chalcocopyrite (trace), which is then cut by later Fe-rich carbonate which locally brecciates the rock.
05-JES-174	H-039	142.4	379817	6359321	Highly potassically altered plagioclase-porphyrific andesite. Highly fractured and cut by quartz vein hosting trace molybdenite.
05-JES-175	H-039	143.9	379817	6359321	Quartz stockwork or hydrothermal breccia hosting notable pyrite (~1%) with trace chalcocopyrite. Carbonate veins are also present, but do not cross-cut.

Appendix 4 cont.

Sample ID	Drillhole/ Station	Depth (m)	Location		Field Description
			Easting	Northing	
05-JES-176	H-039	146.6	379817	6359321	Interval runs from 474' to 484'. Very intensely mineralized - most well-mineralized interval observed to date. Chalcopyrite - 10%; Pyrite - 10%; Molybdenite - 5%; with possible (probable?) pentlandite. The Matrix is a fine-grained brownish/reddish mineral which occurs along with quartz.
05-JES-177	H-039	158.2	379817	6359321	Host unit for mineralization. Hydrothermally brecciated heterolithic material overprinted by very fine veins of Fe-rich carbonate (ankerite). Some clasts of andesite and quartz, with an average size of ~1cm.
05-JES-178	H-039	189.0	379817	6359321	Tourmaline hydrothermal breccia. Later altered by carbonate veining. A possible fabric exists. Logged as a "FAULT", could possibly offset mineralized and unmineralized zones? While the fault seems to be an ore 'boundary', it has not affected alteration. Very intense potassic alteration within PPFQ exist downhole.
05-JES-179	H-039	310.1	379817	6359321	Pyroxene-phenocrystic mafic to intermediate volcanic. Highly chloritized, pyroxene phenocrysts have well-developed chlorite rims. Cut by carbonate+quartz+tourmaline vein(s).
05-JES-180	N/A	Surface	379574	6359684	Supergene alteration of variably altered andesite. Likely a conglomerate/volcanic breccia with clasts showing intense potassic alteration. Significant chalcopyrite (~5%) with trace malachite.
05-JES-181	H-066	129.3	380083	6359486	Feldspar porphyry with large black 'spots' - possibly hornblende pseudomorphs. Numerous hydrous phases - chlorite with bornite and hematite. Black zones are not veins, but possibly rather "channelways"? Feldspars have been saussuritized (sericitic alteration), and rock is generally very soft. Fine brownish colour was imparted by ankerite.
05-JES-182	H-066	175.9	380083	6359486	Porphyritic andesite. Highly altered by sericitic, chlorite, and likely epidote. Possibly light late carbonitic alteration. Quartz veins cut (<0.5cm), carrying varying amounts of chalcopyrite, magnetite, and hematite. In places veins are only metallic with no quartz.
05-JES-183	H-066	225.3	380083	6359486	Very nice sample representative of unit. Relic porphyry texture, now highly altered - first to chlorite and sericite, then strongly overprinted by epidote. Fine chalcopyrite veins cut (~2mm) along with quartz-chalcopyrite-magnetite/hematite veins which have resulted in potassic alteration of the wall rock to a depth proportional to vein width.
05-JES-184	H-066	350.0	380083	6359486	Unit was logged as mylonite, an interpretation which is false. Some textural evidence for displacement and/or possible movement does exist, but the fabric is by no means "mylonitic". The rock is more like a possible tectonic breccia with heterolithic clasts. The most pervasive clast lithology is highly potassically altered-quartz-feldspar porphyry. The "groundmass" may in fact be the same material, simply overprinted by intense chloritic alteration, which was then destroyed by very intense epidote alteration. The epidote exhibits a well-defined texture within the rock, and there is some possible evidence for clast rotation. Prior to tectonic alteration, this unit could have acted as a hydrothermal pathway. The rest of the interval is not mylonitic at all, and only locally shows any evidence of shearing or fabric. The unit should have rather been logged as a highly altered quartz-feldspar porphyry to porphyritic andesite.

Appendix 4 cont.

Sample ID	Drillhole/ Station	Depth (m)	Location		Field Description
			Easting	Northing	
05-JES-185	N/A	Surface	378797	6358180	Medium-grained potassically altered (with possible later sericitic alteration overprinting) rock with ~10% quartz and more plagioclase than k-spar - Granodiorite? Light brown/tan in appearance. Quartz is more visible on weathered surface.
05-JES-186	N/A	Surface	378797	6358180	4m upstream of 05-JES-185. Mostly unaltered. Medium- to Coarse-grained quartz, k-spar, biotite and plagioclase. Appearance is of a typical Granite. Possible trace disseminated sulphides.
05-JES-187	N/A	Surface	378797	6358180	15m upstream of 05-JES-186. Same lithology, unaltered. For geochemical analysis.
05-JES-188	H-104	42.7	379816	6360596	Felsic cumulate (granodiorite?). Highly potassically altered, disseminated pyrite (<1%). Likely later Fe-rich carbonate alteration. Sample is representative of interval. (comparable to 05-JES-186)
05-JES-189	H-104	55.5	379816	6360596	Felsic cumulate (granodiorite?) with weak potassic alteration and disseminated pyrite (<1%). Secondary biotite replacing earlier biotite? Possible geochron sample. Epidote is associated with biotite as replacement.
05-JES-190	H-104	204.3	379816	6360596	Porphyritic andesite with pyroxene and plagioclase phenocrysts. Very-fine-grained pyrite is disseminated evenly throughout and accounts for roughly 5% by volume. Locally epidote "nodules" occur. Rock is fairly soft, and lightly tinted green from black, so chloritic alteration is likely. The degree of alteration is variable along the unit, and varies directly with epidote. Appearance of the dry surface is comparable to D/BS unit. Locally fine (<1mm) fracture-filling veins.
05-JES-191	H-104	235.1	379816	6360596	Highly altered andesite, grey in colour with strong evidence for sericitic (phyllitic?) alteration. Vein of quartz and black hard mineral bearing intense chalcopyrite, pyrite, and possible pyrrhotite with trace molybdenite. Nice well-mineralized sample. The same ore minerals are "vein disseminated" throughout the rock as fine veins of only sulphides. Later quartz veins cut the mineralization.
05-JES-192	H-104	238.4	379816	6360596	Logged as QZMZ, and is near contact with above volcanics. Rock is strongly porphyritic, and not cumulate. Very felsic, with little primary biotite which where present has been replaced by sericite or chlorite. Disseminated chalcopyrite occurs throughout, but is very fine-grained and accounts for <1% by volume. Beautiful porphyritic texture with lath-shaped plagioclase phenocrysts. Possible secondary biotite. Colouration is grey to white.
05-JES-193	H-104	251.2	379816	6360596	Medium-grained felsic intrusive with plagioclase +/- k-spar with biotite. Relic biotite has been replaced by chlorite. Quartz and plagioclase have been strongly replaced by sericite. Disseminated sulphides account for roughly 5% of the rock: 4% pyrite, 1% chalcopyrite. Grey to greenish tint.
05-JES-194	H-104	305.8	379816	6360596	Green volcanics (andesite) - fine grained. Sericitically altered. Pyrite +/- chalcopyrite veins cut subvertical to the core axis and alter the wallrock to a light tan colour. Sulphides (pyrite) also occur as disseminations. In total sulphides account for ~10% of the interval.
05-JES-195	N/A	Surface	380537	6360166	Purple volcanics. Contact must be ~5m south. Vuggy with local chlorite and epidote. Outcrop is 4m x 3m. Elevation: 4210'
05-JES-196	N/A	Surface	380589	6360550	Purple volcanics. Relatively homogeneous. Carbonate + Quartz veining. Variable zones of green, which have possibly escaped oxidation of magnetite to hematite. Elevation: 4513'

Appendix 4 cont.

Sample ID	Drillhole/ Station	Depth (m)	Location		Field Description
			Easting	Northing	
05-JES-197	N/A	Surface	380656	6360680	Purple volcanic breccia? Heterolithic clasts, which may be zones of more or less intense alteration. Chlorite and epidote alteration is extensive and locally intense. Elevation: 4654'
05-JES-198	N/A	Surface	380632	6361054	Fine- to Medium-grained andesite. Outcrop is 5m x 8m with extensive downslope rubble. Sample collected for geochemistry. Light chloritic alteration is observed. Elevation: 5050'
05-JES-199	N/A	Surface	380593	6361389	Fine-grained green andesite, with plagioclase phenocrysts (subhedral). Local fine (<1mm) quartz veins. Chloritically altered. Elevation: 5530'
05-JES-200	N/A	Surface	380511	6361580	Subcrop (frost-heaved). Mineralized volcanics. Lots of sulphur burns. Pyrite present (trace) and is restricted to fractures. Chert present. Elevation 5626'
05-JES-201	N/A	Surface	380611	6362587	Porphyritic green volcanics in large outcrop surrounded by rubble at highest point of traverse. Elevation 6430'
05-JES-202	T-128	7.5	380400	6360234	Purple volcanics. Cut by calcite veins 0.5-2mm diameter. Local epidote alteration ("nodules"). Locally reddish colouration of surface.
05-JES-203	T-128	8.5	380400	6360234	Purple volcanics. Local epidote, particularly as veins fracturing and locally brecciating volcanics.
05-JES-204	T-128	13.4	380400	6360234	Purple volcanics. Strong reddish overprint. Possible quartz phenocrysts. Extensive calcite/quartz veining. Some disseminated silver-coloured sulphides - possible arseno pyrite. Form of sulphide is roughly cubic, but appears to be made up of smaller grains.
05-JES-205	T-128	15.2	380400	6360234	Contact between purple and green volcanics, if in fact separate lithologies. No notable fault or discontinuity was observed between the colour changes. Nice calcite vein for possible fluid inclusion work (~2mm width). Rock is porphyritic with pyroxene? phenocrysts replaced by chlorite. Rock very strongly chloritically altered (could be chloritically altered purple volcanics, or as-yet-unoxidized 'green' volcanics. Numerous fine calcite/quartz veins (<1mm). Further downhole (@-69') are disseminated trace sulphides, likely chatcopyrite.
05-JES-206	T-128	33.8	380400	6360234	Crystal Lapilli tuff. Phenocrysts of both pyroxene and plagioclase. Heterolithic clasts. Chloritic alteration. Locally intense hematization. Cut by quartz-carbonate veins. Fragments (clasts) are lapilli-sized. Some are mafic. At 135', return into 'purple' volcanic unit. "Interfingering" of purple and green volcanics could point to a number of possible origins: 1) Green volcanics are fresh, while purple volcanics were exposed at surface and oxidized, and were then buried by another layer of fresh volcanics, the top layer of which was again oxidized, producing alternating green-purple layers of variable thickness. 2) The purple volcanics are an alteration phase of the green volcanics caused by a change of oxidation state which was controlled by some fluid or other means. 3) The purple volcanics are a separate distinct unit which has been deformed along with the green volcanics (there is insubstantial evidence for this)

Appendix 4 cont.

Sample ID	Drillhole/ Station	Depth (m)	Location		Field Description
			Easting	Northing	
05-JES-207	T-217	23.2	379086	6359950	Medium- to Coarse-grained intrusive. Quartz, K-spar, and plagioclase with hornblende and biotite. Extensive K-spar clearly differentiates this lithology from the "GRDR" unit observed elsewhere (and likely associated with the Hickman Batholith). Composition is Quartz Monzonitic to Granitic. Very nice primary cumulate texture. Mostly unaltered, with some sericitic alteration. Over interval, some degree of light quartz-carbonate veining. Carbonate veining appears to become more pervasive and less Iron-rich upon movement to the periphery of the currently defined system - could possibly be used to define zonation and extent of mineralization.
05-JES-208	T-217	37.2	379086	6359950	Similar to 05-JES-207, fairly vein free, and sample specifically for geochemistry.
05-JES-209	T-217	40.9	379086	6359950	Medium- to Coarse-grained intrusive. Primarily plagioclase with ~20% quartz and associated biotite. Compositionally plots within the Granodiorite field as defined by the IUGS. Possible sericitic alteration. Chalcocopyrite occurs in veins accounting for ~2% of the rock with possible trace bornite associated.
05-JES-210	T-218	51.8	379087	6358932	Logged as "PPAU". Unit is a porphyritic mafic volcanic with pyroxene phenocrysts. Epidote/chlorite alteration is light, with possible sericitic. Light quartz-chlorite veining, with veins typically <0.2mm. Sample for geochemistry.
05-JES-211	T-219	34.1	379686	6358598	Logged as "PPAU". This is incorrect, rather the unit is intermingled fine-grained mafic material (possibly D/BS?) with porphyritic clast material hosting magnetite within the matrix. Bladed plagioclase crystals and unusual euhedral 5-sided prismatic crystals replaced by granular green mineral, likely epidote.
05-JES-212	T-219	55.2	379686	6358598	Agite porphyry unit. Lightly altered by epidote/chlorite and carbonate. Three generations/pulses of veining are present. 1) Straight crossing (perpendicular) carbonate veins (~1mm across), which are possibly associated with 2) Fracture-filling veins <1mm. 3) Later calcite vein cutting and offsetting earlier veining (~1mm, not straight). Possibly use for fluid inclusion.
05-JES-213	T-219	60.4	379686	6358598	Strongly porphyritic (plagioclase) andesite. Chloritically altered. Multiple veining events/pulses. Some disseminated grey anhedral metallic mineral which is non-magnetic. Carbonate veins represent at least two pulses, one of which is bearing hematite. One of the hematite veins cuts the vein of a black non-metallic, non-magnetic mineral (possibly tourmaline?).
05-JES-214	T-219	68.9	379686	6358598	Shear Zone. Shears were later infilled by carbonate veining. Extensive magnetite, often oxidized to hematite locally giving a purply appearance. Protolith is indiscernable. Groundmass is chloritically(+/- epidote) altered, while clasts are preferentially hematized. A moderate fabric exists. The shear extends from 218-231'.
05-JES-215	T-204	29.9	379299	6360889	Quartz-feldspar porphyry, hydrothermally brecciated by quartz. Bornite and chalcocopyrite are restricted to the brecciating quartz, accounting for ~60% of the vein material, or ~5% of the rock. Bornite dominates chalcocopyrite ~2:1 by volume.
05-JES-216	05CF234	48.1	379669	6359503	Late Pb-Zn-quartz vein hosting significant sphalerite and galena. Vein walls are diffuse.
05-JES-217	05CF234	53.0	379669	6359503	Quartz tourmaline hydrothermal breccia as 05-JES-216.

Appendix 4 cont.

Sample ID	Drillhole/ Station	Depth (m)	Location		Field Description
			Easting	Northing	
05-JES-218	05CF234	60.9	379669	6359503	Zone of intense chalcopyrite mineralization (up to 20% locally), but overall ~ 8% cpy. Quartz-tourmaline hydrothermal breccia.
05-JES-219	05CF234	67.4	379669	6359503	Highly potassically altered porphyritic wall rock overprinted by sericite, quartz, and chlorite. Cross-cut by quartz-tourmaline veining. Chalcopyrite is restricted almost exclusively to the hydrothermal veins.
05-JES-220	05CF234	84.7	379669	6359503	Quartz-tourmaline hydrothermal breccia. Epidote alteration is moderate. Disseminated chalcopyrite appears in the breccia matrix.
05-JES-221	05CF234	105.5	379669	6359503	Quartz-tourmaline hydrothermal breccia. Intense alteration of the wall-rock obscuring lithology.
05-JES-222	05CF234	110.6	379669	6359503	Quartz-tourmaline hydrothermal breccia. Moderate to strong epidote alteration, low abundance of cpy (<1%), trace gypsum as late fracture-fill.
05-JES-223	05CF234	121.6	379669	6359503	Felsic intrusive breccia. Matrix is felsic, fine-grained, and roughly equigranular with either clasts, or zones, of variable alteration of locally intense epidote alteration.
05-JES-224	05CF234	123.4	379669	6359503	Felsic intrusive breccia.
05-JES-225	05CF234	124.9	379669	6359503	Felsic intrusive breccia.
05-JES-226	05CF234	128.0	379669	6359503	Large andesitic clast within felsic intrusive breccia. Chalcopyrite occurs along fine epidote veins and in fractures. Epidote alteration is intense.
05-JES-227	05CF234	131.4	379669	6359503	Quartz-tourmaline hydrothermal breccia in andesite. Abundant chalcopyrite, molybdenite, and pyrite are present in the sample.
05-JES-229	05CF234	151.8	379669	6359503	Quartz-tourmaline hydrothermal breccia.
05-JES-230	05CF234	161.5	379669	6359503	Pyroxene-phyric andesite with quartz-tourmaline veins. Propylitic alteration overprinting potassic. Local epidote.
05-JES-231	05CF234	25.8	379669	6359503	Quartz-tourmaline hydrothermal breccia. 70% rock clasts to 30% hydrothermal material. Rock clasts are andesitic and subangular to angular.
06-JES-003	Stn 3	Surface	380257	6359669	Lapilli to breccia tuffaceous andesite, cross-cut by hematite vein. Sericite + chlorite alteration.
06-JES-004	Stn 5	Surface	380402	6359554	Andesite with chalcopyrite + bornite. Phyllic alteration.
06-JES-005	Stn 8	Surface	380388	6359935	Intensely potassically altered aphanitic andesite.
06-JES-006	Stn 9	Surface	380262	635995	Porphyritic basaltic andesite.
06-JES-007	Stn 13	Surface	379147	6359419	Medium-grained quartz-feldspar porphyry.
06-JES-008	Stn 13	Surface	379147	6359419	Lapilli tuff facies andesite.
06-JES-009	Stn 17	Surface	379161	6359581	Augite-phyric andesite with vein-hosted chalcopyrite (~1%), pyrite (~3%), and malachite (~1%).
06-JES-010	Stn 23	Surface	379420	6358927	Late mafic dyke.
06-JES-011	Stn 26	Surface	378985	6358540	Gabbro with coarse-grained phenocrysts.
06-JES-012	Stn 26	Surface	378985	6358540	Gabbro with coarse-grained phenocrysts.
06-JES-013	Stn 29	Surface	380434	6359789	Aphanitic andesite. Potassic alteration overprinted by phyllic.
06-JES-014	Stn 29	Surface	380434	6359789	Quartz-feldspar porphyry. Potassic alteration overprinted by phyllic.
06-JES-015	Stn 30	Surface	380384	6360049	Quartz-feldspar porphyry. Potassic alteration overprinted by phyllic.
06-JES-016	Stn 31	Surface	380376	6360083	Late mafic dyke with calcite-filled vesicles.

Appendix 4 cont.

Sample ID	Drillhole/ Station	Depth (m)	Location		Field Description
			Easting	Northing	
06-JES-017	Stn 38	Surface	380470	6359708	Aphyric andesite.
06-JES-018	Stn 44	Surface	380617	6360094	Plagioclase-phyric basaltic andesite. Phyllic alteration. Abundant pyrite.
06-JES-019	Stn 45	Surface	379226	6359950	Quartz-feldspar porphyry, medium grained and largely equigranular. Potassic alteration.
06-JES-020	Stn 47	Surface	379245	6359950	Quartz-feldspar porphyry. Potassic alteration.
06-JES-021	Stn 50	Surface	382911	6361590	Diorite; intense propylitic alteration obscures original texture.
06-JES-022	Stn 51	Surface	382981	6361570	Diorite, propylitic alteration.
06-JES-023	Stn 52	Surface	383048	6361604	Andesite, intense propylitic alteration.
06-JES-024	Stn 53	Surface	382939	6361534	Diorite, propylitic alteration.
06-JES-025	Stn 54	Surface	382637	6361458	Diorite, propylitic alteration.
06-JES-026	Stn 55	Surface	380111	6360384	Andesitic lapilli tuf to lapilli breccia. Propylitic alteration.
06-JES-027	Stn 58	Surface	380052	6360433	"Purple volcanics" hematite alteration overprinting propylitic.
06-JES-028	Stn 60	Surface	379626	6361304	Intrusive breccia. Potassic and phyllic alteration. Highly mineralized with chalcocopyrite.
06-JES-029	Stn 29	Surface	380434	6359789	Aphanitic andesite.
06-JES-030	Stn 61	Surface	379606	6361362	Intrusive breccia in plagioclase-phyric andesite.
06-JES-031	Stn 64	Surface	379546	6361479	Aphanitic andesite, propylitic alteration.
06-JES-032	Stn 64	Surface	379546	6361479	Quartz-feldspar porphyry. Phyllic alteration overprinting potassic.
06-JES-033	Stn 65	Surface	379486	6361549	Aphanitic andesite. Hematite alteration. Weak mineralization.
06-JES-034	Stn 70	Surface	380619	6358904	Purple to green volcanics. Weakly magnetic. Propylitic alteration.
06-JES-035	Stn 71	Surface	380640	6358762	Augite-phyric andesite.
06-JES-036	Stn 71	Surface	380640	6358762	Augite-phyric andesite with hematite alteration.
06-JES-037	Stn 71	Surface	380640	6358762	Crystal lapilli tuff.
06-JES-038	Stn 73	Surface	380747	6358723	Hematized late mafic dyke.
06-JES-039	Stn 75	Surface	380840	6358888	Augite-phyric andesite, propylitically altered.
06-JES-040	Stn 81	Surface	379564	6359674	Hydrothermal breccia with intense mineralization. Hydrothermal matrix is dominantly sulphide-only. Clast protolith is obscured by intense phyllic alteration and silicification.
06-JES-041	Stn 82	Surface	379545	6359918	Quartz feldspar porphyry. Potassic alteration overprinted by phyllic alteration.
06-JES-042	Stn 82	Surface	379545	6359918	Intrusive breccia float.
06-JES-043	Stn 88	Surface	380487	6360085	Plagioclase phyric andesite, phyllic alteration.
06-JES-044	Stn 88	Surface	380487	6360085	Augite-plagioclase-phyric andesite. Potassic alteration overprinted by phyllic alteration.
06-JES-045	Stn 88	Surface	380487	6360085	Quartz-feldspar porphyry. Potassic alteration overprinted by phyllic.
06-JES-046	Stn 95	Surface	380741	6360251	Plagioclase-phyric andesite. Propylitic alteration overprinted by hematite.
06-JES-047	Stn 105	Surface	379706	6357404	Medium-grained felsic intrusive. Potassic alteration overprinted by phyllic alteration.
06-JES-048	Stn 107	Surface	379740	6357397	Dacite to rhyolite. Chlorite alteration.
06-JES-049	Stn 116	Surface	380484	6363281	Dacite to rhyolite, possibly silicically altered.
06-JES-050	Stn 118	Surface	380675	6363209	Diorite.
06-JES-051	Stn 119	Surface	380671	6363202	Layered magnetite-rich rock.

Appendix 4 cont.

Sample ID	Drillhole/ Station	Depth (m)	Location		Field Description
			Easting	Northing	
06-JES-052	Stn 120	Surface	380641	6363037	Quartz-feldspar porphyry.
06-JES-053	Stn 123	Surface	380632	6362873	Dacite to rhyolite. Chlorite alteration.
06-JES-054	Stn 126	Surface	380587	6362717	Dacite to rhyolite. Propylitic alteration.
06-JES-055	Stn 129	Surface	380590	6362511	Fine-grained granodiorite.
06-JES-056	Stn 136	Surface	380449	6361735	Gossanous aphanitic andesite.
06-JES-058	Stn 137	Surface	379906	6359857	Highly altered andesite. Potassic alteration overprinted by propylitic.
06-JES-059	Stn 157	Surface	382085	6362242	Quartz feldspar porphyry. Potassic alteration.
06-JES-060	Stn 158	Surface	382052	6362168	Augite-phyrlic andesite, weak propylitic alteration.
06-JES-061	Stn 161	Surface	381871	6361936	Dacite, phyllically altered.
06-JES-062	Stn 161	Surface	381871	6361936	Equigranular gabbro.
06-JES-063	Stn 163	Surface	381698	6361712	Plagioclase-rich bedded tuff.
06-JES-064	Stn 165	Surface	381563	6361452	Breccia zone within outcrop with heterolithic clasts and hematization.
06-JES-066	06CF258	147.0	380194	6359467	Sampled to examine possible tetrahedrite.
06-JES-067	06CF257	246.0	380250	6359635	Sampled to identify possible sphalerite.
06-JES-068	Stn 10	Surface	380300	6360159	Aphyritic basaltic andesite.
06-JES-069	Stn 55	Surface	380111	6360384	Andesitic lapilli tuff to lapilli breccia.
06-JES-070	Stn 58	Surface	380052	6360433	Hematized aphanitic andesite.
06-JES-071	Stn 93	Surface	380687	6360196	Hematized aphanitic basaltic andesite. Propylitic alteration.

Appendix 5 - Selected petrographic descriptions for Schaft Creek samples.

Sample: 05-1006-2

Lithology: Phyllically altered feldspar porphyry

Primary Minerals/Textures:

Little of the primary textures are preserved due to the pervasive alteration.

-60% phenocrysts

-40% plagioclase

-15% k-feldspar

-5% quartz

-50% groundmass?

-textures are obscured and destroyed by alteration, percentages are highly speculative

Alteration Minerals:

Intense pervasive phyllic alteration

-abundant and intense sericitic alteration

-abundant quartz alteration

-weak chlorite alteration, typically of the groundmass

-carbonate alteration overprint is late and is strong

Vein Minerals/Textures:

~1mm wide quartz veins are barren and are fine-grained. The veins tend to be straight and parallel-walled, sometimes with carbonate walls which are narrow (~100-200microns). These veins are sometimes offset by later carbonate-only veins which are also barren. The carbonate veins tend to be narrower than the quartz veins (<0.5mm) and are irregular in shape. The late carbonate veins are associated with the strong late carbonate veining.

Opaque/Sulphide Minerals:

<1% Cpy as disseminations, typically associated with sericite or secondary chlorite. Rarely associated with either vein type. Trace magnetite as disseminations.

Sample: 05-1006-3

Lithology: Hematized plagioclase-phyric andesite (phyllically altered?)

Primary Minerals:

Phenocrysts: (25%)

-Plagioclase (85%)

-coarse grained and medium grained (bimodal)

-coarse grained are anhedral to subhedral

-medium grained are euhedral

-altered weakly to sericite and/or carbonate

-Pyroxene (15%)

-coarse grained

-complete pseudomorphed by carbonate and lesser chlorite

Groundmass: (75%)

-Plagioclase

-euhedral lath-shaped grains

-seem to form flow patterns and alignment around larger phenocrysts

Alteration Minerals:

Very strong dominant carbonate alteration (possibly clay alteration...). Extensive hydrothermal quartz, either brecciating or filling existing fractures in the rock. Carbonate may be replacing pyrophyllite (clay).

Opaque/Sulphide Minerals:

Hematite and Magnetite, occurrence is mutually exclusive – magnetite rich zones do not bear hematite and vice-versa

Sample: 05-1008-1

Lithology: Granodiorite - Hickman

Primary Minerals:

Quartz: Dominant (40%)

-medium to coarse grained, typically subhedral

-weakly replaced by sericite

Plagioclase: Abundant (40%)

-some show very nicely developed zoning

-medium to coarse grained, typically euhedral

-moderately replaced by sericite – locally becoming intense

K-Feldspar: Rare (5%)

-common simple twins

-medium grained (occasionally fine grained), typically euhedral to subhedral

-moderately replaced by sericite

Amphibole/Hornblende: Common (10%)

-subhedral, medium to fine grained (medium dominant)

-strongly pleochroic – yellow to dark green

-weakly replaced by chlorite – locally intense

Biotite: Rare (5%)

Appendix 5 cont.

-usually distinct discrete medium grained crystals, typically subhedral

Alteration Minerals:

A narrow (~1mm) calcite-quartz vein cuts through and imparts a narrow (~5mm) halo of intense sericitic alteration upon the surrounding plagioclase and K-feldspar, and complete chlorite replacement of the amphibole/hornblende resulting in pseudomorphs. The calcite portion of the vein is fairly coarse-grained and terminates rather suddenly, giving way to dominant very fine grained quartz. The alteration assemblage surrounding the vein does not change with this change in vein mineral dominance. Fairly extensive secondary or re-crystallized quartz (fine grained and subhedral).

Opaque/Sulphide Minerals:

Magnetite, ilmenite, and hematite, not necessarily intergrown. All however are usually associated spatially with the occurrence of amphibole. Rare, fine grained (not medium grained), and appear to be disseminated.

Sample: 05-1008-2

Lithology: Granodiorite - Yehiniko

Primary Minerals:

Plagioclase: Dominant (50%)

- euhedral and medium grained. Nice lath-shaped grains.
- pervasively altered to sericite – locally pseudomorphed

Quartz: Abundant (35%)

- anhedral and medium to coarse grained
- locally secondary quartz which is fine grained

K-Feldspar: Common to rare (10%)

- often shows simple twins
- euhedral and medium grained. Typically lath-shaped

Amphibole: Rare (5%)

- subhedral to anhedral, typically fine to medium grained
- weakly altered to chlorite (locally intense)

Alteration Minerals:

Locally some carbonate alteration which appears to be loosely forming a vein.

Opaque/Sulphide Minerals:

Ilmenite, hematite, and magnetite. Minerals occur as disseminations and typically independently, but sometimes in clusters. Commonly spatially associated with amphibole. Ilmenite is dominant, followed by hematite. Hematite is often an alteration phase replacing magnetite.

Notes:

Plagioclase and K-feldspar occur together and are euhedral. Quartz is interstitial and crystallized later, along with amphibole.

Sample: 05-1008-4

Lithology: Granodiorite - Yehiniko

Primary Minerals:

Plagioclase: Dominant (45%)

- typically euhedral and medium grained
- well-developed oscillatory zoning is very common
- typically moderately altered to sericite (usually a core-dominant feature, or along certain zones or twins)

Quartz: Abundant (40%)

- typically anhedral and medium to coarse grains
- occurs as intergrowths between dominant euhedral plagioclase grains

K-Feldspar: Rare (5%)

- typically subhedral to euhedral and medium grained
- common simple twins

-moderately sericitically altered

Amphibole: Rare (5%)

- typically anhedral to subhedral
- weakly altered to chlorite

Biotite: Rare (5%)

- medium grained and subhedral
- commonly altered moderately to chlorite

Titanite: trace

- typically euhedral, medium grained, exhibits characteristic diamond shape

Cassiterite: trace

- very fine prismatic grains (euhedral), occurring mainly within chlorite
- may be secondary

Alteration Minerals:

Secondary potassium feldspar is observed overgrowing rims of plagioclase grains.

Opaque/Sulphide Minerals:

Magnetite/ilmenite/hematite assemblage, typically fine grained

Appendix 5 cont.

Sample: 05-1008-6

Lithology: Granodioritic – Yehiniko

Primary Minerals:

Quartz: Dominant (45%)

- forms pegmatitic-sized oikocrysts which enclose all other minerals
- also occurs as medium to coarse grained anhedral grains

Plagioclase: Abundant (40%)

- typically euhedral to subhedral and fine to medium grained (medium dominant)
- strongly sericitized

K-Feldspar: Common (5%)

- typically euhedral to subhedral and fine to medium grained
- strongly sericitized

Amphibole/Hornblende: Common (10%)

- anhedral to subhedral and typically fine grained (some medium)
- rare simple twinning
- moderate to weak replacement by chlorite

Chlorite: Rare

- some may be primary, but likely mostly secondary – difficult to determine if pseudomorphs
- some discrete grains are fine to medium grained and subhedral

Biotite: Rare

- subhedral and fine to medium grained
- weakly to moderately replaced by chlorite

Zircon: Trace

- medium grained
- euhedral to subhedral
- occurs in association with titanite

Titanite: Trace

- medium grained for titanite
- euhedral – exhibits characteristic diamond shape
- occurs in association with zircon

Alteration Minerals:

Potassic feldspar alteration of rims of plagioclase grains.

Opaque/Sulphide Minerals:

-typical association of magnetite/ilmenite/hematite, although grain size is commonly medium grained

Notes:

Poikilitic texture of very coarse-grained quartz oikocryst enclosing chadacrysts of plagioclase, K-feldspar, amphibole etc. in the abundances described above.

Sample: 05-JES-004

Lithology: Phyllically altered feldspar porphyry

Primary Minerals/Textures:

Phenocrysts: 70%

- Plagioclase: 40%
- K-spar: 30%
- both subhedral, strongly altered

Groundmass: 30%

Alteration Minerals:

Strong phyllic alteration is pervasive with strong sericite and weak quartz. Later carbonate alteration overprints.

Vein Minerals/Textures:

~2cm wide quartz-carbonate vein which has quartz and carbonate forming at the same time. Possibly a number of different fluid flow events re-using, but this is unclear. Vein walls are sharp, with finer-grained quartz along the vein margins, and coarser grained quartz and carbonate towards the centre.

Opaque/Sulphide Minerals:

The main vein hosts chalcopyrite and bornite mineralization as distinct small grains throughout, and distinct molybdenite locally. Mineralization also continues into the wallrock, where it occurs as very fine-grained disseminations. In the wallrock, the sulphides occur at roughly equal abundance as within the vein. The wallrock also hosts magnetite+hematite disseminations throughout. A later hairline vein cross-cuts and is intensely mineralized with chalcopyrite and bornite coexisting.

Sample: 05-JES-006

Lithology: Potassically altered plagioclase-phyric andesite, or potassically altered feldspar porphyry

Primary Minerals/Textures:

Mostly destroyed by alteration

- Phenocrysts ~60%
- plagioclase ~30%
- k-spar ~30% (may be through replacement)
- groundmass ~50% completely replaced

Appendix 5 cont.

Alteration Minerals:

Very strong potassic alteration with a very strong late carbonate overprint

- potassic rims of feldspars are common
- groundmass some combination of secondary k-spar and quartz
- late carbonate is fine grained and pervasive

Vein Minerals/Textures:

Quartz veins are earlier, parallel-walled and ~0.5mm wide. Re-used by very narrow (<100um) carbonate veins. Additional carbonate veins are randomly oriented and irregular with varying widths of less than 0.2mm.

Opaque/Sulphide Minerals:

~1% chalcopyrite in carbonate veins and as disseminations, anhedral, fine to medium grained.
Trace bornite, typically occurring with chalcopyrite.

Sample: 05-JES-007

Lithology: Potassically altered plagioclase-phyric andesite

Primary Minerals/Textures:

Most of the primary textures have been obliterated by alteration.

Phenocrysts: ~60%?
-dominantly plagioclase

Groundmass: ~40%

Alteration Minerals:

Potassic alteration is intense, replacing groundmass and phenocrysts. Biotite is not observed. Late carbonate alteration overprints.

Vein Minerals/Textures:

~1 cm quartz vein with carbonate walls. Irregular narrow (<0.2mm) carbonate veins occur at random orientations. Both vein types are barren.

Opaque/Sulphide Minerals:

Common fine-grained disseminated chalcopyrite with trace bornite (total sulphides <1%), and some trace oxides with hematite partly replacing magnetite.

Sample: 05-JES-013

Lithology: Porphyritic granodiorite

Primary Minerals:

Phenocrysts: (50%)
-Plagioclase: Dominant (80%)
-medium to coarse grained and euhedral
-zoning common
-strongly altered
-Quartz: Common (10%)
-medium to coarse grained and subhedral – tend to appear “rounded”
-K-feldspar: Rare to trace
-fine to medium grained and subhedral
-strongly altered
-Amphibole/Hornblende (10%)
-complete pseudomorphed by chlorite (and possibly sericite)

Groundmass: (50%)

-Quartz (90%)
-typically very fine grained and subhedral to anhedral

Alteration Minerals:

Numerous late cross-cutting calcite veins. Narrow – typically <2mm. Dominant alteration appears to be associated with these veins. Unclear if major alteration mineral is sericite, pyrophyllite, or carbonate, or some combination thereof.

Opaque/Sulphide Minerals:

Magnetite and ilmenite with trace hematite. Magnetite and ilmenite are intergrown, and typically occur as aggregates of individual grains or as disseminations (fine grained). Trace pyrite.

Notes:

Texture is classic porphyritic texture with mostly euhedral phenocrysts and a quartz-only groundmass.

Unit appears to be more granodioritic than quartz monzonitic, implying a genetic relationship with the Hickman batholith

Sample: 05-JES-041

Lithology: Tourmaline-quartz hydrothermal breccia

Primary Minerals/Textures:

Some form of plagioclase- (and possibly pyroxene)-phyric andesitic volcanic rock. Original textures have been destroyed. Clasts within the tourmaline stockwork appear to be heterolithic, although this may be an artefact of variable degrees of alteration.

Alteration Minerals:

All clast lithologies have been intensely silicified to the point of obliterating any original textures. Some rare phenocrysts of plagioclase have been preserved. Silicification is frequently accompanied by chloritization of the mafic minerals, although chlorite is largely absent from the stockwork save as vug in-filling often along with quartz. Locally carbonate and/or calcite is intense. Sericite

Appendix 5 cont.

is common as a replacement mineral of plagioclase, and occurs together with the assemblage quartz-sericite-chlorite with later calcite/carbonate

Vein Minerals/Textures:

Veins are dominated by tourmaline which is acicular and medium grained at vein margins and at centers (vugs), particularly at stockwork intersections. Quartz is also present, but within the vein/stockwork itself, is fairly minor in comparison to tourmaline. Carbonate is also present and is locally abundant.

Opaque/Sulphide Minerals:

Hematite is dominant and occurs mainly within the hydrothermal stockwork. Trace chalcopyrite is also found in the stockwork.

Sample: 05-JES-058

Lithology: Intrusive breccia

Primary Minerals/Textures:

Intrusive phase (matrix)

- plagioclase phenocrysts
 - medium grained, euhedral lath-shaped
 - variably altered by sericite (weak to moderate)
- groundmass
 - some plagioclase, but dominantly quartz (which may likely be secondary), carbonate is also present and abundant

Andesite tuff (clast)

- plagioclase phenocrysts
 - fine grained, subhedral
 - variably altered by sericite (weak to moderate)
- groundmass similar to intrusive phase, but with more intense sericitic alteration

Alteration Minerals:

Chlorite is notably absent from the intrusive phase. Quartz is dominant, followed by sericite and then carbonate

Vein Minerals/Textures:

None

Opaque/Sulphide Minerals:

Extensive bornite mineralization, with some (trace) chalcopyrite. Bornite is not controlled by veins but instead appears to occur as interstitial intergrowths between plagioclase phenocrysts. Seems to possibly be dominantly occurring at the margin between the igneous intrusive breccia matrix and the andesitic clast. There may be some evidence that the bornite is occurring in "dry" veins.

Sample: 05-JES-073

Lithology: Potassically-altered leucogabbro to diorite

Primary Minerals/Textures:

Medium to coarse-grained intrusive

- plagioclase (60%)
 - typically euhedral forming nice lath-shaped grains which are intergrown
 - shows a later k-feldspar overgrowth texture, where the cumulate euhedral plagioclase underwent rim growth of later k-feldspar
- pyroxene (30%)
 - only pseudomorphs of nearly-euhedral pyroxene remain
 - near-complete replacement by chlorite and biotite (near vein), or by intense calcite/carbonate alteration
- biotite (10%)
 - likely secondary after pyroxene

Alteration Minerals:

Intense chlorite and biotite alteration of pyroxene with weak sericitic alteration of plagioclase throughout the slide, however, a later carbonate vein cuts and within a fairly wide halo (~1-2cm) has altered the mafic minerals completely to carbonate. Plagioclase also exhibits significant k-feldspar overgrowths.

Vein Minerals/Textures:

Two veins: Earlier – chalcopyrite, Later – carbonate/calcite

Chalcopyrite vein appears to be directly associated with the occurrence of shreddy secondary biotite, indicating the vein has a "potassic" alteration nature. The later calcite/carbonate vein locally overprints.

Opaque/Sulphide Minerals:

Abundant chalcopyrite related to secondary biotite. Occurs both within a major (~2mm wide) "dry" vein, and as fine to medium-grained disseminations throughout.

Sample: 05-JES-078

Lithology: Sericitically altered potassically altered leucogabbro to diorite

Primary Minerals/Textures:

A medium grained largely equigranular intrusive composed primarily of plagioclase (~70%) and pyroxene (~30%). Plagioclase has undergone k-feldspar and subsequent sericitic alteration with some (weak) carbonate alteration. Pyroxenes have undergone complete replacement by hydrothermal biotite and subsequent moderate replacement by chlorite.

Alteration Minerals:

Typical "potassic" alteration of a mafic host rock – dominant assemblage is secondary k-feldspar with abundant secondary "shreddy"

Appendix 5 cont.

biotite. It appears a later alteration converted some secondary biotite to chlorite and some of the potassically-altered plagioclase weakly to sericite. Some carbonate alteration is also observed.

Vein Minerals/Textures:

Major vein (~2cm width) is dominantly quartz with associated carbonate. This vein and associated veins of similar quartz-carbonate composition host the major proportion of ore minerals in the sample. The vein margins exhibit a microcrystalline mosaic quartz texture which grades into comb quartz and eventually coarse-grained vein centre. The major vein does not appear to have been reused.

Opaque/Sulphide Minerals:

Abundant chalcopyrite with common bornite intergrowths and discrete grains. Molybdenite is also common and occurs both as discrete aggregates or intergrown with chalcopyrite (and sometimes bornite). Pyrite is trace. Ore minerals are more abundant within the dominant quartz-carbonate veins, but also occur as disseminations within the highly altered wall rock. Later carbonate-only veins also carry chalcopyrite, but in lesser amounts and also are not observed to host either bornite or molybdenite.

Sample: 05-JES-091

Lithology: Phyllically altered potassically altered plagioclase-quartz porphyritic andesite to dacite

Primary Minerals/Textures:

Slide appears to be divided into two different rock types, one which is phenocrysts-rich, and which is phenocrysts-poor. Both are highly altered to sericite, almost obscuring original textures.

The former bears significant medium to coarse grained euhedral plagioclase which are strongly altered (early K-feldspar – weak, later sericite+chlorite – strong) with common euhedral to subhedral coarse-grained quartz phenocrysts which are unaltered. Mafic phenocrysts are common to trace, and medium to fine grained, and are commonly replaced by biotite which has subsequently been replaced by clays (possibly after chlorite?)

The later is similarly altered, however it bears significantly fewer phenocrysts. However, the rare phenocrysts that occur in the later unit are subhedral to anhedral medium grained plagioclase and subhedral to euhedral coarse-grained quartz. The groundmass is fine-grained quartz and rare plagioclase with abundant chlorite which likely is replacing earlier mafic minerals. This portion appears to have locally undergone more pervasive carbonate alteration.

Alteration Minerals:

It appears an earlier phase of potassic alteration (observed in poorly-developed hydrothermal K-feldspar rims around plagioclase) has been strongly overprinted by pervasive phyllic alteration with an assemblage of sericite and chlorite. Groundmass appears to have been altered to quartz. Clay is also abundant in the groundmass, and in particular rimming quartz phenocrysts.

Vein Minerals/Textures:

A number of minor (<1mm) carbonate±chlorite veins cross cut the section.

Opaque/Sulphide Minerals:

Intergrown magnetite-ilmenite is common, locally occurring as coarse grains.

Sample: 05-JES-094

Lithology: Andesite to basaltic andesitic lapilli breccia lithic tuff

Collection Purpose:

Primary Minerals/Textures:

Clast:

Phenocrysts: (40%)

-Plagioclase

-exhibits a trachytic texture of rough alignment

-medium grained and typically euhedral showing good lath texture

-moderately altered to sericite

-Pyroxene

-typically medium grained and subhedral

-variably altered to amphibole (some intense, others intact)

Groundmass: (60%)

-plagioclase (Strongly altered to sericite)

-chlorite and amphibole after mafic minerals/glass

-appears to exhibit some sort of flow banding/layering in narrow (~5mm) bands, the contacts of which undulate subtly

Lapilli Breccia Tuff:

-lithic-clast dominated by clasts of various lithologies and of varying size and abundance

-unclear if anhedral crystals are fragments or comagmatic

-crystal fragments are dominated by plagioclase (~70%) and pyroxene (20%) with trace amphibole (10%). Pyroxene has largely been pseudomorphed by amphibole.

Alteration Minerals:

Clast:

-sericitization of the matrix is very strong, and is moderate in the plagioclase phenocrysts

-uralitic amphibole alteration of pyroxenes is strong to weak, amphibole is common in the groundmass

-chlorite alteration of the groundmass is intense, locally becoming medium grained

Matrix:

-similar alteration to clast

-a number of calcite/carbonate veins cut the matrix portion, but do not penetrate the larger clast. Vein diameter is ~1mm

Vein Minerals/Textures:

No significant veins observed

Appendix 5 cont.

Opaque/Sulphide Minerals:

Dominantly hematite, but some relict magnetite remains at the centre of large hematite veins – indicates hematite is a replacement feature.

Notes:

Volumetrically dominant portion of the slide represents a “clast” of material incorporated into the later volcanic breccia. Note the breccia is volcanic, not intrusive, in nature. The “matrix” portion is lithic clast dominated and hosts clasts of numerous lithologies of varying size and abundance.

Sample: 05-JES-095

Lithology: Basaltic andesitic heterolithic lapilli tuff breccia

Primary Minerals/Textures:

-Heterolithic breccia

-clasts are dominantly plagioclase-phyric andesite to basaltic andesite showing nice euhedral lath-shaped plagioclase grains of medium size. Other clast types are minor.

-matrix is comprised of an anhedral to subhedral plagioclase with amphibole (possibly pseudomorphing pyroxene), and common chlorite replacing the finer-grained matrix and mafic minerals.

Alteration Minerals:

-sericite alteration of plagioclase is ubiquitous and moderate to intense

-chlorite alteration of mafic minerals is abundant and moderate to intense. Frequently observed to be directly associated with (and possibly replacing) uraltic amphibole after pyroxene

Vein Minerals/Textures:

A number of minor (<1mm) calcite/carbonate veins cross-cut, but appear to be late and do not correspond to any significant alteration haloes

Opaque/Sulphide Minerals:

Hematite is dominant, trace magnetite

Notes:

Nearly texturally identical to 05-JES-094. This sample is more centered upon the matrix portion than any major clasts.

Sample: 05-JES-097

Lithology: Hematized andesite to basaltic andesite lapilli tuff

Primary Minerals:

Phenocrysts: (~5%)

-pyroxene

-euhedral to subhedral, as well as occurring as aggregates

-typically medium to fine grained

-moderately replaced by chlorite

Groundmass: (~95%)

-plagioclase: dominant

-characteristic lath-shaped grains

-alteration to groundmass is weak

-possibly glass or mafic minerals: abundant

-moderately altered to chlorite

Alteration Minerals:

-at least two generations of veins cross-cut the slide

-the earlier vein is made up almost exclusively of calcite

-later vein is carbonate-quartz

-alteration through slide is carbonate + chlorite

Opaque/Sulphide Minerals:

Magnetite dominated (poss. ilmenite and/or hematite), but very fine grained, and disseminated

Sample: 05-JES-098

Lithology: Propylitically altered andesitic to dacitic volcanic breccia

Primary Minerals/Textures:

Fine-grained volcanic breccia. Clasts are completely replaced by epidote. Evidence for clast origin of epidote “nodules”, which shows a “trail” of epidote-rich clast material being lost from the larger clast. Groundmass was once porphyritic with medium to fine grained subhedral feldspars and medium to fine grained pyroxenes or amphiboles. These minerals have been pervasively replaced by sericite+chlorite and chlorite±epidote respectively. Quartz is also present in the groundmass, and may be secondary or primary – the distinction is not possible. Epidote-rich clasts also bear common quartz.

Alteration Minerals:

Typical “propylitic” alteration assemblage, with the clasts exhibiting nearly complete epidote replacement of all minerals. The matrix is dominated by chlorite+sericite+epidote. Also the presence of abundant pyrite indicates a propylitic alteration facies. It is possible that the high abundance of sericite and the pervasiveness of alteration indicates an earlier phyllic phase existed which has since been overprinted. Trace clay is present and spread throughout.

Vein Minerals/Textures:

No significant veins observed. Trace carbonate veins cross cut but are typically <<1mm

Opaque/Sulphide Minerals:

Appendix 5 cont.

Abundant euhedral to subhedral medium to coarse grained pyrite with trace anhedral fine-grained chalcopyrite. Large euhedral pyrite and the chalcopyrite are restricted to the breccia matrix. Epidote-rich clasts only host fine-grained subhedral to anhedral pyrite grains. Magnetite is largely absent.

Sample: 05-JES-104

Lithology: Plagioclase-phyric andesite

Primary Minerals/Textures:

Phenocryst: (30%)

-Plagioclase

-euhedral to subhedral, and medium to coarse grained

-moderately replaced by sericite

Groundmass (70%)

-very fine grained, and possibly once glassy, now completely replaced by quartz and sericite and lesser carbonate (replacing sericite?)

Alteration Minerals:

Dominant assemblage is sericite, quartz, and carbonate

Vein Minerals/Textures:

Carbonate ± Quartz vein: hosts pyrite+chalcopyrite, tends to be coarse-grained

Later finer-grained quartz vein is barren and cross-cuts, along the same orientation as the Carbonate-dominated vein, actually re-using the vein.

Opaque/Sulphide Minerals:

Pyrite: abundant euhedral to subhedral and coarse-grained

Chalcopyrite: Rare, anhedral locally distributed, and restricted to the vein

Sample: 05-JES-111

Lithology: Basaltic andesitic crystal to lapilli tuff

Primary Minerals:

Crystal tuff:

Phenocrysts: (15%)

-Pyroxene phenocrysts completely pseudomorphed by fine-grained amphibole which has formed fibrous infillings which go extinct at the same time

-pyroxenes were coarse grained and euhedral to subhedral

Groundmass: (85%)

-Plagioclase (50%)

-typically euhedral lath-shaped grains (fine grained)

-weakly sericitically altered

-Amphibole (50%)

-possibly secondary after pyroxene or glass

-typically fine-grained and subhedral

Lapilli tuff:

-contains a number of different lithologic fragments, most of which are of very similar lithology to the crystal tuff with subtle variations. Phenocrystic phases are the same, as is amphibole alteration. The groundmass in this portion is more highly altered by uraltic amphibole.

Alteration Minerals:

Amphibole is dominant with some weak sericitic alteration

Opaque/Sulphide Minerals:

Pyrite is dominant, and is typically medium grained and anhedral. Chalcopyrite is common and is fine to medium grained and anhedral.

Notes:

Sample actually spans two different volcanic layers (one is a crystal tuffs, while the other is a lapilli tuff). Two phases appear to be petrographically similar, only one has a finer-grained matrix.

Sample: 05-JES-116

Lithology: Porphyritic dacitic volcanic. (or plagioclase-phyric tonalite?)

Primary Minerals/Textures:

Phenocrysts: (40%)

Plagioclase (100%)

-euhedral, coarse to medium grained

-weakly altered to sericite, with later moderate alteration to carbonate

Groundmass: (60%)

Dominated by quartz and possibly feldspars. Mafic minerals in the groundmass (or glass) have been replaced by late carbonate alteration, with weak earlier sericitic alteration throughout.

Alteration Minerals:

Weak sericitic alteration is early with later moderate carbonate alteration. Primary textures are nicely preserved.

Vein Minerals/Textures:

Carbonate veins typically <1mm width cross-cut

Appendix 5 cont.

Opaque/Sulphide Minerals:

Abundant disseminated fine-grained anhedral chalcopyrite with trace anhedral pyrite. Chalcopyrite locally appears to be hosted in dry to nearly-dry veins which contain carbonate and/or quartz. Trace magnetite.

Sample: 05-JES-120

Lithology: Basaltic andesite plagioclase crystal tuff

Primary Minerals/Textures:

Only preserved primary textures are plagioclase phenocrysts (~25%) which are typically subhedral and medium to fine grained.

Alteration Minerals:

Calcite+quartz alteration is so intense so as to nearly obscure all earlier textures save plagioclase phenocrysts.

Vein Minerals/Textures:

Main vein phase is chlorite dominated with lesser calcite/carbonate (possibly ankerite) and associated quartz, which is typically restricted to vein margins. Vein width varies from ~1mm to 5mm. A later phase of calcite-only veins cross-cuts and these veins are typically ≤ 1 mm width. It is with these later calcite-only veins that chalcopyrite is hosted.

Opaque/Sulphide Minerals:

Magnetite is common as fine-grained disseminations, sometimes with ilmenite intergrowths and rarely with hematite rims. Chalcopyrite is common and typically occurs within or closely spatially associated with later carbonate/calcite veins which cross-cut. Lesser chalcopyrite is hosted by the major chlorite-calcite vein, where it is again associated with the carbonate phase. No pyrite was observed

Sample: 05-JES-123

Lithology: Quartz-carbonate-tourmaline-hosted semi-massive pyrite mineralization with rare sphalerite and trace chalcopyrite

Primary Minerals/Textures:

N/A – vein only

Alteration Minerals:

N/A – vein only

Vein Minerals/Textures:

Assemblage of quartz+tourmaline+carbonate. Tourmaline and pyrite are locally intimately intergrown. Later minor calcite/dolomite veins cross-cut and are not mineralized.

Opaque/Sulphide Minerals:

Semi-massive pyrite mineralization with trace chalcopyrite as disseminations within pyrite grains. Also rare sphalerite with well-developed chalcopyrite disease. Sphalerite typically occurs interstitially to larger pyrite grains. Pyrite may be replacing chalcopyrite (and sphalerite).

Sample: 05-JES-136

Lithology: Pyroxene-phyric basaltic andesite

Primary Minerals:

Phenocrysts: (~20%)

-Plagioclase: dominant (~80%)

-euhedral to subhedral, typically coarse to medium grained

-not observed to be zoned

-moderately altered by carbonates (possibly after sericite?)

-Pyroxene: common (~20%)

-euhedral to subhedral, typically medium grained

-completely pseudomorphed by calcite, serpentine, and chlorite

-calcite replacement in places is so intense to form complete grains (coarse) which have adopted the relict pyroxene euhedra

Groundmass: (~80%)

-Plagioclase: Dominant

-nice lath-shaped plagioclase groundmass

-moderately to weakly replaced by carbonates

-mafic minerals: Abundant

-completely replaced by an assemblage of carbonate and chlorite

Alteration Minerals:

Calcite: Abundant, intense, commonly completely pseudomorphing pyroxene along with chlorite and sometimes epidote. Also throughout the matrix where it is abundant (may be another carbonate – too fine-grained to differentiate)

Chlorite: Abundant, intense – locally occurs as veins. Occurs throughout the groundmass.

Epidote: Rare, but typically euhedral and fine grained

Opaque/Sulphide Minerals:

Magnetite/ilmenite abundant in the groundmass as fine disseminations

Notes:

Well-developed porphyritic texture with large (coarse to medium grained) phenocrysts of plagioclase and pyroxene and a fine-grained matrix of lath-shaped nearly euhedral plagioclase. Matrix is however also dominated by chlorite and calcite which likely have replaced the mafic minerals which would have been present.

Appendix 5 cont.

Sample: 05-JES-144

Lithology: Pyroxene- plagioclase-phyric basaltic andesite

Primary Minerals:

Phenocrysts: (~15%)

- Pyroxene: dominant (75%)
 - euhedral to subhedral and medium grained
 - occurs as single grains (commonly twinned) or occasionally as aggregates
 - only weakly altered – grains are largely pristine
- Feldspars: abundant (15%)
 - likely plagioclase
 - almost completely pseudomorphed
 - replaced by calcite/carbonate, and possibly sericite
 - grains were originally subhedral, with rare euhedra

Groundmass: (~75%)

- Plagioclase: dominant
 - euhedral plagioclase laths only weakly altered to calcite
- Mafic components: abundant
 - completely replaced by an assemblage of chlorite and carbonate

Alteration Minerals:

- Carbonate/calcite replacing plagioclase phenocrysts and mafic groundmass.
 - locally find medium-grained calcite grains
- chlorite replacing mafic groundmass and locally replacing mafic phenocrysts

Opaque/Sulphide Minerals:

Magnetite/ilmenite dominant, pyrite is trace. Abundant and widespread as fine grained disseminations.

Sample: 05-JES-149

Lithology: Granodiorite

Primary Minerals and Alteration:

Plagioclase: dominant (50%)

- typically euhedral, nice lath-shaped medium to coarse grains
- some observed to be zoned
- strongly altered to sericite

Quartz: abundant (30%)

- typically anhedral, occurring interstitially between dominant plagioclase, medium to coarse grained
- often show undulose extinction
- weakly altered to sericite

K-Feldspar: common to rare (5-10%)

- typically euhedral to subhedral, exhibit good simple twinning
- moderately to strongly altered to sericite

Hornblende: common (10%)

- typically anhedral and fine to medium grained
- exhibit strong pleochroism from yellow to pistachio green
- moderately altered to biotite
 - biotite strongly pleochroic from deep brown to clear
- moderately altered to chlorite

Opaque/Sulphide Minerals:

Magnetite, ilmenite, and hematite are common and are usually intergrown. Hematite may be an alteration phase of both magnetite and ilmenite. Grains are typically fine grained and anhedral.

Sample: 05-JES-151

Lithology: Gabbro

Primary Minerals:

Coarse-grained (phenocrystic) phase: Completely pseudomorphed by an alteration assemblage of chlorite and/or pyrophyllite and/or carbonate

Medium-grained phase:

- Plagioclase (70%)
 - typically euhedral and lath-shaped
 - weakly altered
- Clinopyroxene (30%)
 - typically subhedral to anhedral
 - almost unaltered

Alteration Minerals:

Assemblage of chlorite, pyrophyllite (clay), and carbonate/calcite. Appears carbonate/calcite is most recent and overprints others. Chlorite appears to be earliest.

Opaque/Sulphide Minerals:

None

Appendix 5 cont.

Sample: 05-JES-152

Lithology: Porphyritic granodiorite

Primary Minerals:

Phenocrysts: (50%)

- Plagioclase: dominant (70%)
 - euhedral, typically medium grained
 - weakly altered
- Quartz: common (20%)
 - subhedral, typically coarse grained, tends to appear "rounded"
- K-feldspar: rare (5%)
 - euhedral, typically medium grained
 - weakly altered
- Amphibole/hornblende pseudomorphs (5%)
 - replaced by chlorite
- biotite and/or chlorite
 - chlorite may be secondary, but relationship remains unclear
- fine to medium grained and subhedral

Groundmass: (50%)

- Quartz (~100%)
 - fine grained to very fine grained

Alteration Minerals:

Calcite occurs as veins, and dominant alteration may be carbonitic, or sericitic

Opaque/Sulphide Minerals:

Pyrite: rare

- disseminated and very fine grained

Magnetite/ilmenite/hematite: rare

- fine grained and intergrown
- no direct spatial association with pyrite

Notes:

Texturally very similar to 05-JES-013

Sample: 05-JES-153

Lithology: Carbonitically altered phylically altered potassically altered plagioclase porphyritic andesite

Primary Minerals/Textures:

Phenocrysts: (60%)

- Plagioclase: 80%
 - typically euhedral lath-shaped and medium grained
 - early alteration of K-feldspar (rim alteration) with later intense sericite (core alteration), and later local carbonate alteration
- Mafic minerals (amphibole or pyroxene or primary biotite) (~10%)
 - subhedral and fine to medium grained
 - replaced by secondary biotite and subsequently an assemblage of chlorite and sericite (becoming coarse-grained to muscovite) with later clay alteration along fractures
- K-feldspar: 5%
 - typically euhedral and medium grained
 - alteration comparable to plagioclase
- Quartz: 5%
 - typically medium grained and subhedral
 - unaltered

Alteration Minerals:

Hydrothermal K-feldspar alteration and overgrowth of feldspars+groundmass along with biotite alteration of fine grained mafic phenocrysts. A secondary alteration event involved an assemblage of sericite+chlorite. A later alteration phase included an overprint of local carbonate/calcite, followed by (or syngenetic with) local clay alteration.

Vein Minerals/Textures:

Main veins are calcite/carbonate veins with rare quartz. Typically wide (~1cm to ~1mm) and hosting significant chalcopyrite.

Opaque/Sulphide Minerals:

Fine-grained anhedral disseminated chalcopyrite is abundant. Chalcopyrite is also often hosted within, or at the margins of calcite/carbonate veins. Pyrite is absent. Trace molybdenite is present as disseminations. Bornite is rare and typically anhedral fine grains which may be intergrown with chalcopyrite. Trace sphalerite is also present and is typically associated with the chalcopyrite/bornite assemblage.

Sample: 05-JES-155

Lithology: Hydrothermal quartz-carbonate brecciated plagioclase-porphyritic andesite

Primary Minerals/Textures:

Plagioclase-porphyritic andesite

Appendix 5 cont.

- plagioclase is euhedral to subhedral and typically medium grained
- undergone intense k-feldspar alteration destroying any groundmass textures, and subsequent sericitic alteration of the feldspars and chlorite alteration of the mafic minerals. Clay alteration was later and dominantly effected the mafic minerals

Alteration Minerals:

- intense K-feldspar alteration followed by sericitic and chloritic (phyllitic) alteration and later minor clay alteration.

Vein Minerals/Textures:

Dominantly coarse-grained quartz which becomes finer-grained around clasts. Carbonate is also abundant, and some carbonate seems to occur as cross-cutting veins. The later veins of carbonate seem to be scavenging hematite and depositing bornite. Carbonate minerals in the main quartz-dominated vein appear to be interstitial to quartz, indicating that the carbonate was carried in by a later event. Locally K-feldspar and plagioclase are present within the vein material, and have been preferentially altered by carbonate.

Opaque/Sulphide Minerals:

Abundant coarse-grained magnetite/ilmenite intergrown, with magnetite preferentially replaced by hematite. Hematite is volumetrically dominant. Chalcopyrite, bornite, and covellite are also frequently intergrown, in addition to occurring as discrete or intergrown grains. Covellite is most commonly a replacement or rim replacement of bornite. No pyrite is present. Bornite & covellite are often associated spatially with carbonate, the occurrence of some of which appears to be later than the quartz-dominated mineralizing event. Carbonate fluids may be locally remobilizing metals and re-depositing them.

Sample: 05-JES-172

Lithology: Propylitically altered intrusive breccia

Primary Minerals/Textures:

Fine-grained intrusive matrix:

- plagioclase-dominated, forming euhedral laths (altered to sericite and quartz)
- groundmass is either quartz-dominated, or has been intensely silicified. Chlorite is also abundant, and later calcite/carbonate is present.

Crystal tuff clast:

- contains large plagioclase grains (coarse grained to pegmatitic), which have been truncated by the intrusive brecciation event.
- groundmass is fine to very fine grained and is comprised of plagioclase which has been moderately altered to sericite, along with chlorite and carbonate/calcite which appear to have replaced the mafic constituents of the matrix. Groundmass contains significant magnetite+ilmenite+hematite.

Epidote-rich clast:

- parent lithology is completely unrecognizable, but the clast must have been dominated by hornblende or pyroxene in order to be altered to such a high degree by epidote. Epidote is the dominant mineral, but quartz is also significant, and calcite/carbonate is later.

Alteration Minerals:

Intrusive matrix:

- Sericite and quartz with chlorite and later calcite

Crystal tuff clast:

- Sericite and chlorite, with later calcite

Epidote-rich clast:

- Epidote and lesser quartz with later calcite

Vein Minerals/Textures:

Quartz-chlorite-carbonate veins (<1mm to ~3mm) cross-cut all lithologies and have transported significant chalcopyrite. The occurrence of chlorite and calcite/carbonate in the vein appears to be mutually exclusive. Later minor calcite/carbonate-only veins which are typically <1mm wide cross-cut and are not barren, but contain significantly less chalcopyrite than the earlier quartz-rich veins.

Opaque/Sulphide Minerals:

Dominantly ilmenite with magnetite (intergrown), with later replacement by hematite. Chalcopyrite is significant and occurs in spatial association with the quartz-chlorite-carbonate veins.

Sample: 05-JES-187

Lithology: Potassically altered granodiorite

Primary Minerals and Alteration:

Plagioclase: dominant (60%)

- medium grained (rarely coarse), typically subhedral
- strongly replaced by sericite
- rim replacement/overgrowth by secondary k-feldspar

Quartz: abundant (15%)

- medium to coarse grained, typically anhedral
- weakly to moderately replaced by sericite

Amphibole/hornblende: common (15%)

- fine to coarse grained, typically subhedral
- weakly replaced by biotite
- weakly replaced by chlorite

K-Feldspar: common to rare (5-10%)

Appendix 5 cont.

- medium (rarely coarse) grained, typically euhedral to subhedral
 - strongly replaced by sericite
- Biotite: rare (<5%)
- medium grained, subhedral

Opaque/Sulphide Minerals:

Magnetite and ilmenite intergrown, partly replaced by hematite. Typically occur as anhedral fine grains. Rare to trace.

Sample: 05-JES-202

Lithology: Hematized pyroxene-phyric basaltic andesite

Primary Minerals:

Phenocrysts: (15%)

Pyroxene and/or plagioclase

-coarse to medium grained

-completely pseudomorphed by an assemblage of chlorite and carbonate

Groundmass: (75%)

-Plagioclase

-euhedral, lath-shaped, and typically fine grained (coarse for a matrix)

-Chlorite and carbonate – likely replacing mafic minerals in the groundmass

Alteration Minerals:

Very intense carbonate/chlorite alteration, with a number of generations of cross-cutting carbonate veins

Opaque/Sulphide Minerals:

Almost completely hematite, but some magnetite remains

Sample: 05-JES-204

Lithology: Hematized propylitically altered plagioclase-pyroxene phyric andesite to basaltic andesite

Primary Minerals/Textures:

Phenocrysts: (20%)

-Plagioclase (80%)

-typically medium to fine grained euhedral lath-shaped grains

-variably altered to chlorite+sericite and later carbonate

-K-feldspar (5%)

-typically medium to fine grained euhedral grains

-similar alteration to plagioclase

-mafics (15%)

-pseudomorphs appear to reflect more pyroxene habit, however grains were subhedral to anhedral

-completely replaced by carbonate, possibly after chlorite

Groundmass: (80%)

-plagioclase

-euhedral lath-shaped grains, fine to very fine grained, moderately altered to sericite

-rest of matrix is presently composed of chlorite and hematite (hematite after magnetite), likely both after mafic minerals and/or glass

Alteration Minerals:

Propylitic first alteration phase consisting of moderate to intense chloritization and sericitization with significant magnetite. This was followed by oxidation of the magnetite to hematite, and another phase of intense carbonate alteration and veining. The timing of the oxidation and carbonate alteration is unclear, as no cross-cutting relationships could be observed. Locally quartz is present as an alteration phase which seems to be associated with the carbonate event.

Vein Minerals/Textures:

The only veins are calcite/carbonate veins of ~1-2mm width (down to hairline), which carried in the significant late-stage carbonate alteration

Opaque/Sulphide Minerals:

Abundant hematite which occurs as large opaque grains, and as very fine translucent bright red grains throughout the groundmass.

Sample: 05-JES-208

Lithology: Potassically altered granite

Primary Minerals:

K-Feldspar: dominant (50%)

-mainly subhedral, mainly medium grained. Also some anhedral and some coarser-grained, but these are more rare

-simple twins are common

-potassic alteration around rim

Quartz: abundant (30%)

-typically medium to coarse grained and anhedral

-weak sericite alteration

-undulose extinction common, also often show consertal texture (intergrown boundaries)

Amphibole/hornblende: common (10%)

-fine to medium grained (medium dominant) and subhedral

Appendix 5 cont.

-completely replaced – only pseudomorphs remain
-replaced by intense chlorite and strong muscovite
Plagioclase: rare (10%)
-strong sericite alteration

Biotite: trace

Alteration Minerals:

Some very thin (<1mm) carbonate veins, sericitic alteration is moderate, potassic alteration is moderate.

Opaque/Sulphide Minerals:

Intergrown fine-grained magnetite-ilmenite are rare, with trace hematite replacing rims. Opaque minerals commonly occur in close spatial association with hornblende.

Sample: 05-JES-210

Lithology: Gabbro

Primary Minerals:

Clinopyroxene: (45%)

-euhedral to subhedral, medium to coarse grained
-moderately altered to amphibole (locally strong), particularly rim replacement

Plagioclase: (50%)

-euhedral to subhedral, typically nice lath-shaped grains
-strongly to moderately replaced by sericite (possibly later clay?)

Orthopyroxene: (5%)

-euhedral to subhedral, medium to coarse grained
-moderately altered to amphibole, particularly rim replacement

Alteration Minerals:

Amphibole:

-uralitic (hydrothermal in origin)
-some may be secondary magmatic due to inequilibrium of pyroxene
-abundant replacing pyroxenes, also occurs in veins and together as coarse to medium grained aggregates

Sericite and/or clay:

-fine grained replacement of plagioclase

Quartz locally forms minor veins

Opaque/Sulphide Minerals:

Magnetite, medium grained, disseminated

Sample: 05-JES-211

Lithology: Augite-plagioclase-phyric basaltic andesite

Primary Minerals:

Phenocrysts: (40%)

-Clinopyroxene (50%)

-typically coarse grained and subhedral (rarely euhedral)
-variably altered by an assemblage of uralitic amphibole and chlorite, with chlorite typically altering fractures and mineral cores, while amphibole tends to be more restricted to the rim (possibly indicating amphibole alteration is later)

-Plagioclase (50%)

-typically subhedral (almost appear "rounded")
-weakly to moderately altered to sericite, which may be overprinted by later carbonitic and/or clay alteration

Groundmass: (60%)

-nice euhedral lath-shaped plagioclase grains along with intense chloritic alteration, disseminated opaque minerals (magnetite) are common and fine-grained

Alteration Minerals:

Chlorite is dominant and replaces both clinopyroxene phenocrysts and mafic minerals/glass in the groundmass. Sericite is also abundant, dominantly replacing plagioclase phenocrysts and locally becoming fairly coarse grained (for an alteration mineral). Carbonate/calcite alteration is later and minor, typically occurring as narrow cross-cutting veins.

Opaque/Sulphide Minerals:

Magnetite is common and typically has ilmenite intergrowths. Typically fine to medium grained and subhedral to anhedral.

Pyrite is trace, typically fine to very fine grained and anhedral.

Notes:

Clinopyroxene phenocrysts appear to be the earliest phase of mineral precipitation, followed by plagioclase phenocrysts and finally the groundmass.

Sample: 05-JES-212

Lithology: Intensely altered rock

Primary Minerals/Textures:

Primary mineral textures have been completely destroyed by very intense pervasive carbonate alteration. It is apparent that some coarse-grained phenocrysts existed as primary minerals.

Appendix 5 cont.

Alteration Minerals:

Intense carbonate flooding throughout the slide, with less chlorite alteration which is being overprinted. Carbonate alteration seems to be coeval with lesser quartz alteration.

Vein Minerals/Textures:

At least four pulses of carbonitic fluid passed through the rock, based on cross cutting relationships of the veins. Vein 1 is ~1mm wide and exhibits perpendicular-wall crystal growth with parallel growth in the vein centre, this vein is cut by Vein 2 which is narrower but of similar composition to the parallel-growth vein centre of vein 1. Vein 3 cuts and terminates vein 2 and is much wider (~5mm) and much coarser-grained and does not exhibit the characteristic twinning lamellae of the earlier more calcite-dolomite-like veins. Vein 3 is in turn cross cut by vein 4 which is again similar to the earlier two vein types.

Opaque/Sulphide Minerals:

The veins are completely barren. However fine-grained disseminated sphalerite aggregates are present throughout the sample in addition to magnetite/hematite which is fine grained and disseminated.

Sample: 05-JES-216

Lithology: Tourmaline-quartz hydrothermal breccia

Primary Minerals/Textures:

N/A

Alteration Minerals:

N/A

Vein Minerals/Textures: (65%)

An assemblage of dominant tourmaline and lesser quartz. The tourmaline is very low-Fe due to its near colourlessness but strong pleochroism from clear to deep tan. In addition the tourmaline only exhibits first-order greys and whites.

A later phase of sericitic alteration of the vein material is moderately replacing tourmaline.

Still later carbonate veins cross-cut the mineralization and other vein material. Locally coarse to medium grained carbonate minerals are present in the primary vein. It is unclear if these grains are coeval with the earlier vein or developed during carbonate vein cross-cutting.

Opaque/Sulphide Minerals: (35%)

Sphalerite: 50%

Galena: 25%

Chalcopyrite: 20%

-Sphalerite and galena occur together and form very large anhedral grains (sphalerite tending to be more euhedral)

-Chalcopyrite mineralization was later, and is observed to be replacing/overprinting galena and the sphalerite has developed strong chalcocopyrite disease

Pyrite: 5%

Sample: 05-JES-227

Lithology: Hydrothermal stockwork

Primary Minerals/Textures:

N/A

Alteration Minerals:

N/A

Vein Minerals/Textures:

Primary vein: The main vein portion is divided into two halves

-fine grained quartz-rich portion

-there is some evidence that the silicification is post-ore deposition, as the sulphides in this portion appear to be dissolved and are perforated by quartz, whereas in the tourmaline portion they are more massive

-Microcrystalline tourmaline portion

-both sides host carbonate and fluorite, but these are overprinting

-trace fine-grained epidote is present in both portions, but is dominant in the tourmaline portion

Secondary veins:

-cross-cut earlier more massive vein

-calcite/carbonate + chlorite, ranging in width from <1mm to ~2mm (the larger of which was re-used)

-where the vein is chlorite rich abundant chalcocopyrite ± pyrite is present

-resulted in alteration of primary vein minerals observed as carbonate alteration throughout the sample

Tertiary vein:

-later event, but resulted in abundant fluorite within the wallrock

-composed almost entirely of fluorite, although there is some evidence that the vein is being reused after carbonate

-resulted in fluorite alteration of surrounding wall rock

Opaque/Sulphide Minerals:

Rare acicular rutile grains occur within carbonate-dominated portions of the slide

Abundant chalcocopyrite (~30%) with rare pyrite and trace sphalerite

Appendix 6 - 2006 Schaft Creek outcrop mapping data.

Station	NAD83		Size	Lithology	Description	Modal Mineralogy	Samples
	Easting	Northing					
1	380316	6359648	~5m	PPFQ - GRDR	Page lost in river		06-JES-001, 06-JES-002
2	380294	6359660	3 x 12m	ANDS to ANTF	Magnetite-bearing aphyric andesite to basaltic andesite to andesitic lapilli tuff to breccia		none
3	380257	6359669	2 x 1m	ANTF	Lapilli to breccia tuffaceous andesite.		06-JES-003: sample of 1cm-wide hematite vein in ANDS
4	380252	6359659	20 x 8m	ANDS	Aphanitic andesite		none
5	380402	6359554	4 x 25m	ANPF	Andesite to pyroxene-phyric andesite		06-JES-004: Andesite with cpy+bn, variably altered (ANXX)
6	380413	6359694	3 x 25m	ANPF	Plagioclase-porphyrific to aphyric basaltic andesite. Plagioclase phenocrysts are subrounded and mg-cg.		none
7	380420	6359741		ANPF	Weakly porphyritic andesite		None
8	380388	6359935		ANDS	Intensely altered ANDS or potassically altered PPFQ - distinction is difficult due to intensity of alteration		06-JES-005: representative
9	380262	635995	10 x 2.5m	ANPF	Porphyritic basaltic andesite		06-JES-006: representative

Appendix 6 cont.

Station	NAD83		Size	Lithology	Description	Modal Mineralogy	Samples
	Easting	Northing					
10	380300	6360159	3 x 3m	ANDS	Aphyric basaltic andesite		06-JES-068: geochem
11	379130	6359300		ANPF	Porphyritic andesite (~10% plag, 5% px phenos)		
12	379107	6359330		ANPF	Pillowed flows of porphyritic andesite		
13	379147	6359419	20 x 20 x 4m	ANPF	Lapilli tuff facies andesitic volcanic		06-JES-008
14	379141	6359440		PPFQ	Medium-grained quartz-feldspar porphyry		06-JES-007
15	379132	6359461	1.5 x 15m	ANDS with PPFQ	As at station 13		
16	379116	6359442	100 x 50m	ANPF with PPFQ	ANPF: Augite-phyric pillowed andesite		
17	379161	6359581	10 x 10m	ANPF, ANLT, and PPFQ	Both porphyritic pillow facies and lapilli tuff facies		06-JES-009: Collected from W end of trench and is ANPF with vein-hosted cpy (~1%), py (~3%), and mal (~1%).
18	379180	6359638	4 x 30m	ANPF	Augite-phyric andesite		
19	379148	6359657	4 x 4m	PPFQ	Quartz-feldspar porphyry		

Appendix 6 cont.

Station	NAD83		Size	Lithology	Description	Modal Mineralogy	Samples
	Easting	Northing					
20	379159	6359646	10 x 6m	PPFQ and ANPF	Plagioclase-phyric andesite and quartz-feldspar porphyry		
21	379497	6359272		ANPF	Augite-phyric andesite		
22	379451	6358991	3 x 3m	ANPF	Augite-phyric andesite		
23	379420	6358927	20 x 10m	ANPF and D/BS	Plagioclase-Augite-phyric andesite and late mafic dyke	Phenocrysts: plag (~10%), augite (~5%)	06-JES-010: representative of D/BS
24	379454	6358451	20 x 15m	ANPF	Plagioclase-Augite-phyric andesite	Phenocrysts: plag (~10%), augite (~10%)	
25	379052	6358436	8 x 10m	ANDS	Aphanitic andesite		
26	378985	6358540	6 x 30m	PPAU	Gabbro with coarse-grained augite phenocrysts		06-JES-011; 06-JES-012
27	378987	6358569	4 x 10m	PPAU	Gabbro with coarse-grained augite phenocrysts		
28	378976	6358597	10 x 10m	PPAU	Gabbro with coarse-grained augite phenocrysts		
29	380434	6359789		ANDS and PPFQ	Aphanitic andesite and Quartz-feldspar porphyry		06-JES-013: rep of PPFQ 06-JES-014: rep of ANDS 06-JES-029: ANDS geochem

Appendix 6 cont.

Station	NAD83		Size	Lithology	Description	Modal Mineralogy	Samples
	Easting	Northing					
30	380384	6360049	4 x 2m	PPFQ	Quartz-feldspar porphyry		06-JES-015: representative
31	380376	6360083	4 x 5m	D/BS	Late mafic dyke		06-JES-016: vesiculation and representative
32	380417	6359997	50 x 3m	PPFQ and D/BS	Quartz-feldspar porphyry and locally vesiculated late mafic dyke		
33	380434	6359986	15 x 15m	ANDS and ANPF	Aphanitic andesite (strongly altered), and plagioclase-augite-phyric andesite	ANPF: plag (20%), cpx (10%)	
34	380467	6359940	5 x 2m	ANPF	Plagioclase-phyric andesite	plag (35%), fg	
35	380502	6359917	10 x 8m	ANPF	Plagioclase-phyric andesite	plag (40%), mg	
36	380604	6359782	2 x 3m	ANPF	Augite-phyric andesite	plag (10%), mg	Last year: 05-JES-136
37	380487	6359667	15 x 1m	ANPF	Plagioclase-phyric andesite	plag (10%), fg	

Appendix 6 cont.

Station	NAD83		Size	Lithology	Description	Modal Mineralogy	Samples
	Easting	Northing					
38	380470	6359708	3 x 1m	ANDS	Aphyric andesite		06-JES-017
39	380530	6359161	15 x 4m	ANLT to ANLB	Andesitic lapilli tuff to andesitic lapilli tuff breccia. Andesite fragments are subrounded "pebbles" and are very poorly sorted	Clast size ranges from <1cm to >15cm	
40	380584	6359438	3 x 3m	ANPF	Plagioclase-phyric andesite	Plag (20%), eg, subhedral, largely replaced by epidote	
41	380560	6359456	8 x 2m	ANPF	Plagioclase-phyric andesite	Plag (20%), eg, subhedral, largely replaced by epidote	
42	380544	6359535	3 x 4m	ANPF	Plagioclase-phyric andesite	Plag (15%), mg, subhedral	
43	380579	6360014		ANDS	Aphanitic andesite		Sampled last year: 05-JES-137
44	380617	6360094	8 x 10m	ANPF	Plagioclase-phyric basaltic andesite	Plag (10%), mg, subrounded	06-JES-018: shows representative andesite texture and alteration with elevated py
45	379226	6359950	2 x 1m	PPFQ	Quartz-feldspar porphyry, but mg and largely equigranular, similar in appearance to GRDR		06-JES-019: for thin section
46	379251	6359938	6 x 3m	PPFQ	Quartz-feldspar porphyry, but mg and largely equigranular, similar in appearance to GRDR		
47	379245	6359950		PPFQ and D/BS	Quartz-feldspar porphyry and fg. Late mafic dyke (gabbroic to dioritic in composition)		06-JES-020: for thin section
48	379244	6359882	4 x 2m	ANLT	Andesitic lapilli tuff		

Appendix 6 cont.

Station	NAD83		Size	Lithology	Description	Modal Mineralogy	Samples
	Easting	Northing					
49	378787	6358173	continuous	GRDR	Hickman granodiorite		Sampled last year with a number of samples
50	382911	6361590	3 x 1m	DIOR	Possibly diorite		06-JES-021: representative
51	382981	6361570	4 x 1m	DIOR	Diorite		06-JES-022: representative
52	383048	6361604	5 x 2m	ANDS	Green volcanic		06-JES-023: representative
53	382939	6361534	4 x 1m	DIOR	Diorite		06-JES-024: representative
54	382637	6361458	5 x 3m	DIOR	Diorite		06-JES-025: representative
55	380111	6360384	20 x 4m	ANLT to ANLB	Andesite lapilli tuff to lapilli breccia	Clast size range: <1cm - 5cm, with some much larger (>15cm) Clasts are all the same lithology: Aphanitic andesite	06-JES-026: representative 06-JES-069: Geochem
56	380076	6360420	8 x 3m	ANLT to ANLB	Andesite lapilli tuff to lapilli breccia	Clast size range: <1cm - 5cm, with some much larger (>15cm) Clasts are all the same lithology: Aphanitic andesite	none
57	380059	6360427	Discontinuous	ANLT to ANLB	Andesite lapilli tuff to lapilli breccia	Heterolithic clasts of 1-20 cm. Matrix is fg tuff. Clasts are various varieties of andesite	none
58	380052	6360433	Discontinuous	PVOL	Purple volcanics	Same lithology and clast variety as 057, but groundmass has distinct purple colouration	06-JES-027: representative 06-JES-070: Geochem
59	380036	6360461	8 x 2m	D/BS	Late mafic dyke	Medium-grained diorite to gabbro	none

Appendix 6 cont.

Station	NAD83		Size	Lithology	Description	Modal Mineralogy	Samples
	Easting	Northing					
60	379626	6361304	8 x 2m	INBX D/BS	Intrusive breccia Late mafic dyke	mg PPFQ intrusive matrix, fg dominantly andesitic clasts	06-JES-028 - large sample with beautiful cpy stringers; 06-JES- 029; both representative.
61	379606	6361362	40 x 3m	INBX ANPF	Intrusive breccia Plagioclase-phyric andesite	ANPF: mg-cg plagioclase, subhedral to anhedral, ~35-40%	06-JES-030
62	379578	6361421	8 x 2m	INBX	Intrusive breccia		none
63	379556	6361459	3 x 2m	INBX	Intrusive breccia		none
64	379546	6361479	10 x 3m	ANDS PPFQ D/BS	Aphanitic andesite Quartz-feldspar porphyry Late mafic dyke	Aphanitic andesite bears ~2% of plagioclase phenocrysts, which are anhedral and have been replaced by chlorite	06-JES-031: ANDS sample 06-JES-032: PPFQ sample
65	379486	6361549	10 x 3m	PPFQ PVOL	PPFQ intruding purple volcanics		06-JES-033: PVOL (mineralized)
66	379472	6361590	15 x 4 x 4m	PVOL	Aphanitic purple volcanics		
67	380497	6359103	8 x 4m	ANDS	Aphanitic andesite		
68	380575	6359024	4 x 2m	ANDS	Aphanitic andesite		
69	380597	6359052	10 x 20 x 10	ANDS	Aphanitic andesite		
70	380619	6358904	10 x 10m	PVOL to ANDS	Purple to green volcanic		06-JES-034: representative, for thin section

Appendix 6 cont.

Station	NAD83		Size	Lithology	Description	Modal Mineralogy	Samples
	Eastings	Northing					
71	380640	6358762	60 x 30 x 30m	ANPF, PVPF, and CLTF	Augite-phyric andesite Porphyritic purple volcanics Crystal lapilli tuff	Augite phenos: cg. subhedral to euhedral, ~30%	ANPF: 06-JES-035 PVPF: 06-JES-036 CLTF: 06-JES-037
72	380704	6358716	10 x 4m	PVOL to ANDS	Purple to green volcanic		
73	380747	6358723	60 x 60 x 40m	PVPF, PMDK	Augite-phyric purple volcanic, fine-grained purple mafic dyke		06-JES-038: Purple dyke
74	380805	6358814	10 x 10m	PVPF	Augite-phyric purple volcanic	40% augite, subhedral, mg	
75	380840	6358888	100 x 100m	ANDS, PVOL, PMDK, ANPF	Aphanitic andesite Aphanitic purple volcanics Fine-grained purple mafic dyke Augite-phyric andesite	Augite phyric andesite: phenos are euhedral and up to 2cm long	06-JES-039: augite-phyric andesite
76	380998	6358840	50 x 20 x 10m	ANPF, PVPF	Augite-phyric andesite Augite-phyric purple volcanics		
77	381039	6358765	10 x 10m	PVOL, PMDK	Purple volcanics Purple mafic dyke		
78	380961	6359024	50 x 20 x 20m	ANDS	Aphanitic andesite		
79	380939	6359081	50 x 20 x 20m	PVOL	Purple volcanic, locally showing a lapilli or breccia texture		
80	380934	6359138	30 x 30 x 30m	PVOL, ANDS	Aphanitic purple and green volcanics		

Appendix 6 cont.

Station	NAD83		Size	Lithology	Description	Modal Mineralogy	Samples
	Easting	Northing					
81	379564	6359674	4 x 1m	WBX	Hydrothermal breccia to stockwork	Aphanitic andesitic clasts	06-JES-040
82	379545	6359918	20 x 10m	PPFQ	Quartz feldspar porphyry		06-JES-041: representative 06-JES-042: of breccia float nearby
83	380214	6359575	10 x 3m	ANPF	Plagioclase-phyric andesite	Plag phenos: ~30%, subhd, mg	
84	380195	6359583	5 x 2m	ANPF	Plagioclase-phyric andesite	Plag phenos: ~30%, subhd, mg	
85	380202	6359613	3 x 3m	ANPF	Plagioclase-Augite-phyric andesite	Plag phenos: ~30%, subhd, mg; Augite phenos: ~15%, subhd, mg	
86	380532	6360046	3 x 2m	ANDS	Aphanitic andesite		
87	380494	6360082	8 x 2m	ANPF	Augite-phyric andesite	Augite phenos: ~25%, mg, subhedral	
88	380487	6360085	4 x 3m	ANPFa, ANPF, PPFQ	Plagioclase-phyric andesite Altered augite-plagioclase-phyric andesite Quartz-feldspar porphyry	ANPF: Plag phenos: ~25%, subhd, mg ANPFa: Plag+Aug: ~20%, mg, subhd	06-JES-045: ANPF 06-JES-043: ANPFa 06-JES-044: PPFQ
89	380493	6360096	10 x 2m	ANPFa	Plagioclase-phyric andesite		
90	380521	6360132	5 x 5m	PVLT	Hematized basaltic andesitic lapilli tuff		
91	380575	6360150	10 x 10m	PVLT	Hematized basaltic andesitic lapilli tuff		
92	380604	6360160	30 x 5m	PVOL	Hematized aphanitic basaltic andesite		
93	380687	6360196	large	PVOL	Hematized aphanitic basaltic andesite		
94	380718	6360194	Large ridge	PVOL	Hematized aphanitic basaltic andesite		06-JES-071: Geochem

Appendix 6 cont.

Station	NAD83		Size	Lithology	Description	Modal Mineralogy	Samples
	Easting	Northing					
95	380741	6360251		PVLT to PVOL ANPD	Hematized basaltic andesitic lapilli tuff to aphanitic basaltic andesite Plagioclase-phyric andesite dykes	ANPF: Plag: mg, subhedral to anhedral ~30%.	06-JES-046: ANPF
96	380551	6360284	Beginning of large o/c ridge	PVOL	Hematized aphanitic basaltic andesite		
97	380498	6360374		PVLT	Hematized basaltic andesitic heterolithic lapilli tuff		
98	380596	6360529	30 x 10m	PVOL	Hematized aphanitic basaltic andesite		
99	380676	6360642		PVCT ANPD	Hematized basaltic andesitic lapilli tuff Plagioclase-phyric andesitic dyke	PVCT: Plag ~50%, fg, euhedral ANPD: Plag ~15%, mg, subhedral	
100	380703	6360669	8 x 4m	ANDS	Aphanitic andesite		
101	380698	6360747	10 x 10m	ANPF	Plagioclase-phyric andesite	Plag: ~25%, mg, subhedral	
102	380678	6360818	10 x 10m	ANPF	Plagioclase-phyric andesite	Plag: ~15%, mg, subhedral	
103	380464	6361068	30 x 20m	ANPF	Plagioclase-phyric andesite	Plag: ~20%, mg, subhedral	
104	380532	6361120	10 x 10m	ANPF	Plagioclase-phyric andesite	Plag: ~20%, mg, subhedral	
105	379706	6357404		GRDR	Medium-grained intrusive		06-JES-047
106	379740	6357397	10 x 2m	PVOL	Hematized aphanitic basaltic andesite		
107	379740	6357397		ANDS PVOL	Aphanitic andesite Hematized aphanitic basaltic andesite		06-JES-048
108	380161	6357634	4 x 3m	ANDS	Aphanitic andesite		
109	380180	6357611	4 x 4m	ANDS	Aphanitic andesite		
110	380213	6357674	6 x 3m	ANDS	Aphanitic andesite		
111	380228	6357693	large	ANDS	Aphanitic andesite		
112	380286	6357843	200 x 100m	ANDS	Aphanitic andesite		

Appendix 6 cont.

Station	NAD83		Size	Lithology	Description	Modal Mineralogy	Samples
	Easting	Northing					
113	380039	6363302	large	ANPF QFP	Plagioclase-phyric andesite Quartz-Feldspar porphyry dyke	Plag: ~5%, subhd, fg QFP: quartz eyes - distinct from PPFQ. Mg with abundant subhd plagioclase phenos	06-JES-048
114	380102	6363251	large	No Code	Dacitic to rhyolitic volcanic	aphanitic	
115	380464	6363302	large	ANPF	Augite-phyric andesite	Augite ~10%, cg, subhedral	
116	380484	6363281	large	ANDS	Aphanitic		06-JES-049
117	380631	6363235	large	ANPF	Augite-phyric andesite	Augite ~5%, mg, anhedral	06-JES-050
118	380675	6363209	large	DIOR	Diorite	Fine-grained	06-JES-051
119	380671	6363202	large		Weird-textured magnetite-rich rock		
120	380641	6363037	large	QFP	Quartz-feldspar porphyry	With nice quartz-eyes and feldspar	05-JES-052
121	380625	6362999	large	QFP No Code	Quartz-feldspar porphyry Dacitic to Rhyolitic volcanic		
122	380641	6362967	large	ANPF	Augite-phyric basaltic andesite	Augite: ~5-10%, mg, subhedral	06-JES-053
123	380632	6362873	large	No Code	Dacitic to rhyolitic volcanic		
124	380628	6362743	large	No Code	Augite-plagioclase-phyric dacite	Plag: ~5-10%, fg, subhedral Augite: ~5%, mg, subhedral	
125	380587	6362717	large	ANPF + ANDS	Augite-phyric andesite to aphanitic andesite		
126	-116	196	large	ANPF No Code	ANPF and Augite-phyric dacite to rhyolite	Augite: ~10%, cg, euhedral	06-JES-054
127	380613	6362588	large	ANPF	Plagioclase-phyric andesite	plag: ~10%, fg, subhedral	Last year: 05-JES-201
128	380590	6362511	large	No Code	Plagioclase-phyric basalt	Plag: ~5%, fg, euhedral	
129			large	ANPF No Code No Code	Plagioclase-phyric andesite Layered unit (Stn 123) Fine-grained granodiorite	Fine-grained diorite bears trace euhedral magnetite	06-JES-055 - collected from granodioritic unit
130	380628	6362288	large	ANPF	Augite-phyric andesite		

Appendix 6 cont.

Station	NAD83		Size	Lithology	Description	Modal Mineralogy	Samples
	Easting	Northing					
131	380632	6362148	large	ANPF	Augite-plagioclase-phyric andesite	Augite: ~5%, mg, euhedral Plag: ~5%, fg, subhedral	
132	380684	6362053	large	ANPF	Augite-plagioclase-phyric andesite	Augite: ~5%, mg, euhedral Plag: ~5%, fg, subhedral	
133	380701	6361842	large	ANPF	Plagioclase-phyric andesite	Augite: ~5%, mg, euhedral Plag: ~5%, fg, subhedral	
134	380638	6361715	large	ANPF	Gossan		
135	380571	6361708	large	ANPF	Augite-phyric andesite	Augite: ~10%, mg, subhedral	06-JES-056
136	380449	6361735	large	ANDS	Aphanitic andesite, Gossanous		
137	379906	6359857	8 x 2m	ANDS	Very highly altered andesite		06-JES-058
138	379920	6359815	20 x 2m	ANDS ANPF	ANDS as at Stn 137 ANPF: Augite-plagioclase-phyric andesite	ANPF: Augite: ~10%, cg, subhedral; Plagioclase: ~3%, mg, subhedral	
139	380240	6360230	5 x 5m	PVLP	Hematized andesite lapilli to breccia	Heterolithic clasts or variably altered porphyritic volcanics	
140	380236	6360226	5 x 3m	D/BS	Late mafic dyke, plagioclase-augite-phyric - Dioritic to Gabbroic in composition	Plag: ~30%, mg, sbhd to euhd Aug: ~20%, mg, sbhd	
141	380229	6360231	5 x 3m	PPFQ D/BS	Feldspar porphyry (equigranular) Late mafic dyke	PPFQ: Monzonite to monzodiorite	
142	380219	6360248	8m	N: D/BS S: PPFQ	Late mafic dyke Feldspar porphyry (equigranular)	PPFQ: Monzonite to monzodiorite	

Appendix 6 cont.

Station	NAD83		Size	Lithology	Description	Modal Mineralogy	Samples
	Easting	Northing					
143	380209	6360247	8m	PPFQ	Feldspar porphyry (equigranular) Late mafic dyke	PPFQ: Monzonite to monzodiorite	
144	380210	6360267	10 x 10m	ANPF PPFQ D/BS	Late mafic dyke intruding Feldspar porphyry intruding plagioclase-augite-phyric andesite.	D/BS as at station 140. PPFQ: Monzonite to monzodiorite ANPF: Plag ~15%, mg, sbhd Aug ~10%, mg, sbhd	
145	380197	6360270	9 x 3m	PPFQ	Feldspar porphyry	PPFQ: Monzonite to monzodiorite	
146	380199	6360282	5 x 5m	PPFQ D/BS	Feldspar porphyry Late mafic dyke	PPFQ: Monzonite to monzodiorite	
147	380179	6360301	5 x 8m	PPFQ D/BS	Feldspar porphyry Late mafic dyke	PPFQ: Monzonite to monzodiorite	
148	380176	6360266	15 x 2m	D/BS	Late mafic dyke	D/BS as at station 140.	
149	380133	6360291	20 x 6m	ANAP	Plagioclase-augite-phyric andesite	Plag: ~10%, mg, sbhd to euhd Aug: ~10%, fg, sbhd	
150	380111	6360304	50 x 4m	ANLP to ANBX ANAP	Andesite lapilli to breccia Plagioclase-augite-phyric andesite	ANLP to ANBX: Aphanitic matrix bearing heterolithic clasts of various andesite lithologies. ANAP: Plag ~40%, mg, sbhd Aug 20%, mg, sbhd	
151	380123	6360336	Same as above	ANAP to ANDS	Fine-grained massive ANDS with rare phenocrysts	Plag and Aug: ~0.5mm	
PF06	380105	6360281	10 x 4m	ANLP to ANBX	Andesite lapilli to breccia	Matrix: fg volcanic Clasts: <1 - 10cm size, heterolithic andesitic volcanic	

Appendix 6 cont.

Station	NAD83		Size	Lithology	Description	Modal Mineralogy	Samples
	Easting	Northing					
PF07	380102	6360259	50 x 8m	PVOL	Hematized aphanitic andesite	Non-porphyritic Non-fragmental	
152	380102	6360246	50 x 8m	PVOL	Hematized aphanitic andesite	Locally euhedral feldspar needles.	
PF08	380102	6360189	6 x 4m	PVCT	Hematized augite crystal tuff	Augite crystals, euhd, fg, exhibiting rough alignment	
153	380212	6360077	30 x 30m	ANDS	Aphanitic andesite		
154			10 x 4m	ANDS	Aphanitic andesite		
PF09	380234	6360054	12 x 6m	ANDS	Aphanitic andesite		
155	380292	6359930	10 x 10m	ANPF D/BS	Plagioclase-phyric andesite Late mafic dyke	ANPF: Plag ~25%, fg, sbhd Aug ~5%, fg, sbhd	
PF10	380287	6359964	10 x 10m	ANPF	Plagioclase-phyric andesite		
PF11	380345	6359885	5 x 5m	ANDS	Aphanitic andesite, but highly altered		
156/PF20	382308	6362579	15 x 30m	DIOR	Fine-grained equigranular diorite	5-10% mafic minerals, which have been replaced by chlorite, and are interstitial to plagioclase	
157/PF21	382085	6362242	35 x 10m	ANAU ANPF PPFQ?	Augite-phyric andesite Plagioclase-phyric andesite Monzonite to Monzodiorite	ANAU: Aug ~25%, mg, euhd ANPF: Plag ~25%, fg, euhd PPFQ: Equigran, no mafics	06-JES-059: PPFQ
158	382052	6362168	5 x 5m	ANPF ANAU	Plagioclase-phyric andesite Augite-phyric andesite	ANPF: Plag ~20%, fg, sbhd ANAU: Aug ~15%, cg, euhd	06-JES-060: ANAU
PF22	382083	6362151	2 x 2m	ANPF	Plagioclase-phyric andesite	Plag 30-40%, mg, euhd	
159	381975	6362052	5 x 5m	ANPF PPFQ	Plagioclase-phyric andesite Feldspar porphyry	ANPF: Plag ~20%, fg, sbhd PPFQ: Monzonite to monzodiorite	
PF23	381964	6362020	8 x 2m	ANDS	Aphanitic andesite		
160	381880	6361946	3 x 1m	ANDS	Aphanitic andesite		

Appendix 6 cont.

Station	NAD83		Size	Lithology	Description	Modal Mineralogy	Samples
	Eastings	Northing					
161	381871	6361936	5 x 3m	Dacite Gabbro	Very felsic feldspar-phyric volcanic Equigranular gabbro	Dacite: Feldspar phenos: pink, subhd, mg, ~20%, Qtz eyes, anhhd, mg, 5%	06-JES-061: Dacite 06-JES-062: Gabbro
162			3 x 3m	PVPPF	Hematized plagioclase-phyric andesite	Plag ~15%, mg-fg, sbhd	06-JES-063
163	381698	6361712	10 x 5m	ANTF	Plagioclase-rich bedded air-fall tuff		
PF24	381632	6361584	100 x 30m	ANDS	Aphanitic andesite		
164			100 x 30m	ANTF	Bedded andesite tuff	Beds ~0.3cm thick	
PF25	381616	6361555	100 x 30m	ANTF	Bedded andesite tuff	Beds ~0.3cm thick	
WS01	381627	6361555	100 x 30m	D/BS Gabbro Mylonite ANTF	Late mafic dyke Equigranular gabbro Mylonitic shear zone/fault bx Bedded andesite tuff		
PF26	381571	6361461	20 x 7m	ANPF	Plagioclase-phyric andesite	Plag 20-30%, mg, subhd	06-JES-064 - breccia zone within o/c with heterolithic clasts and purple colouration
165	381563	6361452	3 x 3m	DIOR	Augite-phyric diorite	Phenos: Aug mg, sbhd Matrix: plagioclase with vfg mafics	
PF27	381449	6361235	2 x 1m	DIOR	Diorite porphyry	Close packing augite phenocrysts ~70%	
166	381328	6361011	3 x 2m	ANAP	Plagioclase-augite-phyric andesite	Plag ~25%, fg, sbhd Aug ~15%, mg, sbhd	
PF28	381319	6361005	2 x 2m	ANAP to ANLP	Plagioclase-augite-phyric andesitic lapilli tuff	Plag ~20%, fg, sbhd Aug ~5%, mg, sbhd Rare heterolithic clasts	
PF29	381280	6360952	3 x 2m	ANAP to ANLP	Plagioclase-augite-phyric andesitic lapilli tuff	Plag ~40%, fg, sbhd Aug ~5%, mg, sbhd Minor heterolithic clasts	
167	381170	6360780	3 x 2m	ANAP	Plagioclase-augite-phyric andesite	Plag ~25%, fg, sbhd Aug ~15%, mg, sbhd	

Appendix 6 cont.

Station	NAD83		Size	Lithology	Description	Modal Mineralogy	Samples
	Easting	Northing					
PF30	381104	6360643	3 x 3m	ANAP to ANLP	Plagioclase-augite-phyric andesitic lapilli tuff	Plag ~40%, fg, sbhd Aug ~5%, mg, sbhd Minor heterolithic clasts	
168	381079	6360596	3 x 2m	ANDS	Hematized aphanitic andesite		
PF31	381087	6360584	8m	ANBX	Andesitic breccia		
169	381043	6360559	5 x 2m	ANDS	Aphanitic andesite	Heterolithic volcanic breccia with clasts of <1cm to ~20cm.	
170	380841	6360252	3 x 2m	ANDS	Aphanitic andesite	Aug phenos ~2%, mg, sbhd to euhd	

Note: For appendix 6, the following abbreviations are used.

Field lithologic codes: ANAP, augite- and plagioclase-phyric andesite; ANAU, augite-phyric andesite; ANBX, andesite breccia; ANDS, aphanitic andesite; ANLT, andesite lapilli tuff; ANPF, plagioclase-phyric andesite; ANTF, andesite tuff; CLTF, crystal lapilli tuff; D/BS, late mafic dyke; DIOR, diorite; GRDR, granodiorite; INBX, intrusive breccia; PMDK, hematized mafic dyke; PPAU, gabbro; PPFQ, quartz-feldspar porphyry; PVCT, hematized crystal tuff; PVLT, hematized lapilli tuff; PVOL, hematized aphanitic andesite; PVPF, hematized plagioclase-phyric andesite; QFP, quartz feldspar porphyry with quartz eyes; WBX, hydrothermal breccia with tourmaline and quartz.

Alteration codes: W, weak; M, moderate; I, intense; Pot, potassic; Phyl, phylitic; Prop, propylitic.

Mineral Abbreviations: Aug, augite; Bn, bornite; Bt, biotite; Carb, carbonate; Chl, chlorite; Cpx, clinopyroxene; Cpy, chalcopyrite; Epi, epidote; Hm, hematite; K-spar, potassium feldspar; Mal, malachite; Mo and Moly, molybdenite; Mt, magnetite; Plag, plagioclase; Py, pyrite; Qtz, quartz; Ser, sericite.

Mineral occurrence: V, vein; D, dissemination; T, trace; P, pervasive.

Grain size: Vfg, very fine grained; Fg, fine-grained; Mg, medium-grained; Cg, coarse-grained.

Other abbreviations: Anhhd, anhedral; Subhd, subhedral; Euhd, euhedral; Equgran, equigranular; Phenos, phenocrysts.

Appendix 6 cont.

Station	Alteration (Intensity)									
	Assemblage	K-feld	Bt	Chl	Ser	Epidote	Carb	Silica	Mal	
1		I								W-M
2		I (local)		M	W				W	
3				M	M				M	
4				W	W					
5		I (local)		W-M	W-M		W (local) (late)			
6				W	W				t - surface	
7				W	W					
8		I			M-I					
9					W	W (local)				

Appendix 6 cont.

Station	Alteration (Intensity)									
	Assemblage	K-feld	Bt	Chl	Ser	Epidote	Carb	Silica	Mal	
10					W	W (local)	W (local) (late)			
11				M	M		W (local) (late)			
12				M	M		W (local) (late)			
13				M	M					
14			I As at station 13							
15		PPFQ: M	PPFQ: W	ANPF: M		ANPF: M				
16		PPFQ: W		AN: M-I		AN: M-I				
17				M	M	W				W
18				I	M					M-I
19		M								

Appendix 6 cont.

Station	Assemblage	K-feld	Bt	Alteration (Intensity)				Silica	Carb	Mal
				Chl	Ser	Epidote				
20	PPFQ: Potassic; ANPF: Phyllic	PPFQ: W		ANPF: M	ANPF: W					
21	Phyllic overprinting potassic	W - early		M - late	M - late					
22	Propylitic			M						
23	ANPF: Propylitic			ANPF: M D/BS: W	ANPF: W	ANPF: M (local)				
24	Propylitic			M		Locally I				
25	Propylitic			M		Locally I				
26	Phyllic			W	W					
27	Phyllic			W	W					
28	Phyllic			W	W					
29	PPFQ: Potassic overprinted by chloritic ANDS: Potassic overprinted by phyllic	I, early		M - late	M - late					

Appendix 6 cont.

Station	Assemblage	K-feld	Bt	Alteration (Intensity)				Silica	Carb	Mal
				Chl	Ser	Epidote	Chl			
30	Potassic overprinted by phyllic	I, early		I - late	I - late					
31	Very weak chloritic			W						
32	PPFQ: Potassic D/BS: Light Chloritic	PPFQ: M		D/BS: W					Abundant	
33	ANDS: Propylitic ANPF: Propylitic			M	M	M (locally I)			none	
34	Phyllic			M	W				local	
35	Phyllic			M	W					
36	Chloritic			M						
37	Propylitic (no epidote)			I						

Appendix 6 cont.

Station	Assemblage	K-feld	Bt	Alteration (Intensity)				Silica	Mal
				Chl	Ser	Epidote	Carb		
38	Chloritic	M (locally)		M					
39	Propylitic			M-I		M, I (locally)			
40	Propylitic			I		I			
41	Propylitic			M		I			
42	Propylitic			M		I			
43	Phyllic			M		W		Local	
44	Phyllic			M		M			
45	Potassic (maybe light phyllic overprint)	I	M			M			
46	Potassic (maybe light phyllic overprint)	I	M			M			
47	PPFQ: potassic (maybe light phyllic overprint) D/BS: chloritic	PPFQ: I	PPFQ: M	D/BS: W		PPFQ: M			
48	Chloritic and carbonate							I	

Appendix 6 cont.

Station	Assemblage	K-feld	Bt	Alteration (Intensity)					Mal
				Chl	Ser	Epidote	Carb	Silica	
49	Potassic and carbonate	M			M			M	
50	Propylitic			I		I			
51	Propylitic			I		M (local)			
52	Propylitic			I		M (local)			
53	Propylitic			I		I		I	
54	Propylitic			W	W	M (local)			
55	Propylitic			M		I (local)			
56	Propylitic			M		I (local)			
57	Phyllic			M	M	I (clasts)			
58	Oxidation - hematite								
59	Chloritic			M					

Appendix 6 cont.

Station	Assemblage	K-feld	Bt	Alteration (Intensity)	Epitote	Carb	Silica	Mal
				Chl	Ser			
60	Matrix: Potassic to Phyllic Clasts: Variable D/BS: Chloritic	Mtx: M		Clst: M D/BS: M	Mtx: M	Clst: M	Clst: M	Common
61	Matrix: Potassic to Phyllic Clasts: Variable ANPF: phyllic	Mtx: M		Clst: M ANPF: W	Mtx: M ANPF: W	Clst: M	Clst: M	Common
62	Matrix: Potassic to Phyllic Clasts: Variable	Mtx: M		Clst: M	Mtx: M	Clst: M	Clst: M	Common
63	Matrix: Potassic to Phyllic Clasts: Variable	Mtx: M		Clst: M	Mtx: M	Clst: M	Clst: M	Common
64	ANDS: Propylitic PPFQ: Phyllic over Potassic D/BS: Chloritic	PPFQ: I (early)		ANDS: M PPFQ: W D/BS: M	ANDS: W PPFQ: M	ANDS: M		Common
65	PPFQ: Phyllic over potassic PVOL: oxidation	PPFQ: I (early)		PPFQ: W	PPFQ: W			Common
66	PVOL: oxidation							rare
67	Propylitic			I-M				I (local)
68	Propylitic			I-M				I-M
69	Propylitic			I-M				I-M
70	Propylitic			M				

Appendix 6 cont.

Station	Assemblage	Alteration (Intensity)							
		K-feld	Bt	Chl	Ser	Epidote	Carb	Silica	Mal
71	ANPF: Sericitic (phyllitic?) PVPF: Propylitic CLTF: Propylitic			ANPF: W PVPF: I CLTF: I	ANPF: M	PVPF: I CLTF: I			ANPF: Common
72	Propylitic			I-M		I-M			
73	Propylitic			I-M		I-M			
74	Propylitic			I		I			
75	ANDS: Propylitic PVOL: Propylitic + hematite PMDK: Hematite ANPF: Chloritic			ANDS: M PVOL: I ANPF: M		ANDS: W PVOL: I			
76	ANPF: Propylitic PVPF: Propylitic			ANPF: M PVPF: I		ANPF: W PVPF: I			
77	PVOL: Propylitic PMDK: Hematite			PVOL: I		PVOL: I			
78	Propylitic			I		I (local)			
79	Propylitic			I		I			
80	Propylitic			I		I			

Appendix 6 cont.

Station	Assemblage	K-feld	Bt	Alteration (Intensity)					Silica	Carb	Mal
				Chl	Ser	Epidote	Carb	Silica			
81	Clas: silicification + chlorite			M				M		Abundant	
82	Potassic overprinted by phyllic	M-W	M		M					Abundant	
83	Phyllic alteration			M	M					Abundant	
84	Phyllic alteration			M	M					Abundant	
85	Phyllic alteration			M-I	M					Abundant	
86	Sericite + silica				M					trace	
87	Propylitic (over phyllic?)			M	I						
88	ANPF: Chloritic ANPFa: Potassic overprinted by Phyllic PPFQ: Potassic overprinted by Phyllic	ANPFa: W PPFQ: M		ANPF: M ANPFa: M PPFQ: M	ANPFa: M PPFQ: M					Abundant	
89	Phyllic			M	I					Abundant	
90	Hematized propylitic			M			M				
91	Hematized propylitic			M							
92	Hematized propylitic			I				I (local)			
93	Hematized propylitic			I				I (local)			
94	Hematized propylitic			I			M				

Appendix 6 cont.

Station	Assemblage	K-feld	Bt	Alteration (Intensity)					Silica	Mal
				Chl	Ser	Epidote	Carb			
95	Hematized propylitic Propylitic			I		I				
96	Hematized propylitic			I		M				
97	Hematized propylitic			I		M				
98	Hematized propylitic			I		M	M (local)			
99	PVCT: Hematized propylitic ANPD: Chloritic			PVCT: M ANPD: M		PVCT: M				
100	Propylitic			M		W				
101	Chloritic			M						
102	Phyllic?			M	M					
103	Propylitic			I		M (local)				
104	Propylitic			M		W (local)				
105	Potassic overprinted by phyllic			M	M				Weak	
106	Hematized propylitic			M	M					
107	Propylitic Hematized propylitic			ANDS: M-I PVOL: M		PVOL: M				
108	Propylitic			I						
109	Propylitic			I						
110	Propylitic			I						
111	Propylitic			I						
112	Propylitic			M						

Appendix 6 cont.

Station	Assemblage	Alteration (Intensity)									
		K-feld	Bt	Chl	Ser	Epidote	Carb	Silica	Mal		
113	ANPF: Chlorite QFP: Potassic overprinted by Carbonate	QFP: M		ANPF: M			QFP: I				
114	Chlorite with carbonate			M			M				
115	Chlorite			M							
116	Cherty possibly over chloritic			W					M-I		
117	Chlorite + chert			M					M		
118	Very weakly altered										
119											
120	Carbonate								I		
121	Sericite + chlorite			M		M			I		
122	Chloritic			M							
123	Chloritic with chert?			M						I?	
124	Chloritic			M							
125	Propylitic			M				I - local			
126	Propylitic			M		M					
127	Chloritic			M							
128	Chloritic			M							
129											
130	Chloritic			M							

Appendix 6 cont.

Station	Assemblage	K-feld	Bt	Alteration (Intensity)					Silica	Carb	Mal
				Chl	Ser	Epidote	Carb	Mal			
131	Chloritic			M							
132	Chloritic			M							
133	Phyllic?			M	M				W		
134											
135	Chloritic			M							
136	Chloritic			M				I- local			
137	Potassic + chlorite	M-local		M-pervasive	W					Common	
138	ANDS: Potassic + chlorite ANPF: chloritic	ANDS: M-local		ANDS: M-perv ANPF: M	ANDS: W ANPF: W						
139	Hematite + Propylitic?			W	W	W-M					
140	Chlorite + sericite, very light			VW	VW						
141	PPFQ: Potassic D/BS: chloritic	PPFQ: W-M		D/BS: W	PPFQ: W						
142	PPFQ: Potassic D/BS: chloritic	PPFQ: W-M		D/BS: W	PPFQ: W						

Appendix 6 cont.

Station	Assemblage	K-feld	Bt	Alteration (Intensity)				Carb	Silica	Mal
				Chl	Ser	Epidote				
143	Potassic	W-M		W	W					
144	PPFQ: Potassic + epidote ANPF: Phyllic, propylitic D/BS: Chloritic	PPFQ: W		ANPF: M D/BS: W	PPFQ: W ANPF: M	ANPF: M PPFQ: M				
145				not recorded						
146	PPFQ: weak potassic with phyllic overprint D/BS: chloritic	PPFQ: W		PPFQ: W D/BS: W	PPFQ: M					
147	PPFQ: weak potassic with phyllic overprint D/BS: chloritic	PPFQ: W		PPFQ: W D/BS: W	PPFQ: M					
148	Chloritic			W	W					
149	Phyllic to propylitic with hematite			W-M	W-M	W				
150	Alteration same for both lithologies. Phyllic to Propylitic with weak hematite			M	W	W -local				
151	Phyllic to propylitic with hematite and epidote nodules			M	W	M-local				
PF06				not recorded						

Appendix 6 cont.

Station	Assemblage	K-feld	Bt	Alteration (Intensity)					Silica	Mal
				Chl	Ser	Epidote	Carb			
PF07	Hematite, others not recorded					M-local				
152	Pervasive hematite; local epidote					I-local				
PF08	Hematite						W-ankerite		W	
153	Phyllic?			W-M	M				W	
154	Phyllic			W-M	W-M			W-local		
PF09	Potassic	M-I			W-M			M		
155	Propylitic			W-M	W-M	W				
PF10					not recorded					
PF11	Potassic	M-I							W	
156/PF20	Phyllic?			M	W					
157/PF21	ANAU & ANPF: Phyllic PPFQ: Potassic	PPFQ: M		AN: W-M	AN: W PPFQ: W-M			ANAU: M		
158	Both same - weak chloritic			W	W					
PF22				not recorded						
159				not recorded						
PF23				not recorded						
160	Phyllic?			W	W					

Appendix 6 cont.

Station	Assemblage	K-feld	Bt	Alteration (Intensity)					
				Chl	Ser	Epidote	Carb	Silica	Mal
161	Dacite: phyllic			Dacite: W-M	Dacite: W-M				
162				W-M	W				
163				W	W				
PF24				not recorded					
164				not recorded					
PF25				not recorded					
WS01				not recorded					
PF26				not recorded					
165				W	W	W-local			
PF27				not recorded					
166				W	W				
PF28				M	W				
PF29				M	W	M-local			
167				W	W				

Appendix 6 cont.

Station	Assemblage	K-feld	Bt	Alteration (Intensity)			Epidote	Carb	Silica	Mal
				Chl	Ser	W				
PF30				M	W	W	M-local			
168				W-M	W	W	W-M (local)			
PF31				W-M	W	W	W-M (local)			
169				W-M			I-pervasive			
170				W-M						

Appendix 6 cont.

Station	Type	Timing	Thick	Veins Halo	Abundance	Shape	Minerals	Mineralization (% Abundance/type)							
								Bn	Cpy	Mo	Pv	Hm	Mt		
1								1/V	1/V						
2									2/D						
3	Dry	Syn- mineralization	~1cm				Hm		t/D				t/D	5/V	
4	Qtz-carb		<1cm				Barren								local/V
5	Qtz+carb	Syn- mineralization	~1cm	Potassic, narrow			Cpy (at centre)	1-2/D, V	5/D, V		1/V				
6	Qtz+carb						Barren		t/D						
7															
8	Carb	Late	<2cm	none			barren		2.5/D				2.5/D		
9															<1/D

Appendix 6 cont.

Station	Type	Timing	Thick	Veins Halo	Abundance	Shape	Minerals	Mineralization (% Abundance/type)							
								Bn	Cpy	Mo	Py	Hm	Mt		
10	Carb	Late	<1cm	none			barren						<1/D		
11	Carb	Late, non-parallel walls	<1cm	none			barren								Lots
12	Carb	Late	<1cm	none			barren								Lots
13	Qtz-Carb	Syn-alteration	~1cm										5/D		
14															
15	Qtz-Carb	Syn-alteration	~1cm	none			barren						5-10/D locally		
16													5/D locally		
17															
18	Qtz-Carb	syn-alteration	<1cm	none			barren						1/D, V locally		
19													3/D, V locally		

Appendix 6 cont.

Station	Type	Timing	Thick	Veins Halo	Abundance	Shape	Minerals	Bn	Cpy	Mo	Py	Hm	Mt
20													
21	Qtz-Carb	Syn-alteration	<1cm	none	Common	Irregular	barren			5/D - very locally			
22											none		
23	Qtz-Carb	Syn-alteration (associated with epidote)	<2cm	Epidote (locally)	Common	Parallel	barren				none		
24											~1/D, vfg		
25	Qtz-carb	syn-alteration	<2cm	Epidote (locally)	Common	Parallel	barren				~5/D, local		
26	Qtz-carb	Syn-alteration?	<1cm	none	rare	Parallel	barren		5/D		2/D		
27	Qtz-carb	Syn-alteration?	<1cm	none	rare	Parallel	barren		5/D		2/D		
28	Qtz-carb	Syn-alteration?	<1cm	none	rare	Parallel	barren		5/D		2/D		
29	Qtz-carb	Syn-mineralization	~2cm	potassic	Common	Parallel	Cpy		PPFQ: 2/D ANDS: 2/D		PPFQ: trace ANDS: 1/D		

Appendix 6 cont.

Station	Type	Timing	Thick	Veins		Abundance	Shape	Minerals	Mineralization (% Abundance/type)							
				Halo	None				Bn	Cpy	Mo	Pv	Hm	Mt		
30									5/D			1/D				
31				None								none				
32	Carb (PPFQ only)	Syn-mineralization	<2cm	not observed	Common	Parallel	Cpy+Py		PPFQ: 5/D, V			PPFQ: 1/D, V D/BS: 3/D, local				
33	Carb	Syn-mineralization	<5cm	not observed	Common	Parallel	Py		ANDS (west): 5/D			ANDS (west): 1/D ANDS (high min): 20/D				
34									2/D, local			2/D				
35	Sulphide (cpy+py)	mineralization	<1cm	none	Common	Parallel	Cpy+Py		2/D							
36				none observed								none				
37				none observed								2-4/D				

Appendix 6 cont.

Station	Type	Timing	Thick	Veins Halo	Abundance	Shape	Minerals	Mineralization (% Abundance/type)						
								Bn	Cpy	Mo	Py	Hm	Mt	
38	Qtz+carb (bt rims)	Syn-mineralization	~3cm	Potassic-chlorite >5cm	Common	Parallel	Cpy+Py		5/D, V			2/D, V		
39	Qtz-carb	Syn-alteration	~1cm	not observed	Common	Parallel	Barren					1/D		
40				not observed								1/D		
41				not observed								1/D		
42				not observed								2/D		Abundant, rare distinct grains
43	Qtz-carb	Syn-mineralization	<1cm	not observed	Abundant	Parallel	Cpy+Py		3/D, V			2/D, V		
44	Carb-Qtz	Syn-alteration	<1cm	not observed	Common	Parallel	Py					1-2/D, V; 8 locally		
45				not observed					2/D			5/D		
46				not observed					2/D			5/D		
47				not observed				PPFQ: 2/D				PPFQ: 5/D D/BS: 1/D		
48	Qtz-carb	syn-alteration	<1cm	not observed	Abundant	Parallel	Barren					1/D		

Appendix 6 cont.

Station	Type	Timing	Thick	Veins Halo	Abundance	Shape	Minerals	Mineralization (% Abundance/type)							
								Bn	Cpy	Mo	Pv	Hm	Mt		
49															
50															
51	Carb	late	<1cm	not observed	Common	Squigly	Barren				t/D				
52	Qtz-carb	syn-alteration	1cm	not observed	Abundant	parallel	Barren				2/D				
53															
54											1/D				
55															
56														none observed	
57														none observed	
58														none observed	
59														none observed	

Appendix 6 cont.

Station	Type	Timing	Thick	Veins Halo	Abundance	Shape	Minerals	Mineralization (% Abundance/type)						
								Bn	Cpy	Mfo	Pv	Hm	Mt	
60	Qtz-Carb Chlorite	Post-brecciation; syn- mineralization	<1cm to 2cm	Pot None	Abundant	Random Parallel	Cpy Barren	5/D, V						
61	PPFQ; Qtz- Carb Chlorite	Post-brecciation; syn- mineralization	<1cm to 2cm	Pot None	Abundant	Random Parallel	Cpy Barren	5/D, V						
62	Qtz-Carb Chlorite	Post-brecciation; syn- mineralization	<1cm to 2cm	Pot None	Common	Random Parallel	Cpy Barren	t/D, V						
63	Qtz-Carb Chlorite	Post-brecciation; syn- mineralization	<1cm to 2cm	Pot None	Common	Random Parallel	Cpy Barren	t/D, V						
64	Qtz-carb	Syn- mineralization	<1cm	not observed	Abundant	Parallel to random	Cpy	3/D, V						
65	Qtz-carb	Syn- mineralization	~2mm to ~1cm	not observed	Abundant	Parallel to random	Barren	2/D						
66	Qtz-carb	Post-alteration	<0.5mm	not observed	Abundant	Parallel to random	Barren	1/V						
67												none observed		
68												none observed		
69												none observed		
70	Calcite	Syn-alteration	<1cm	not observed	Abundant	Parallel	Barren						Abundant	Common

Appendix 6 cont.

Station	Type	Timing	Thick	Veins Halo	Abundance	Shape	Minerals	Mineralization (% Abundance/type)					
								Bn	Cpy	Mo	Pv	Hm	Mt
71	Carb +/- Qtz	Syn-alteration	~2cm	not observed	Abundant	Parallel	Barren					Abundant	Common
72												Abundant	
73	Carb	Syn-alteration	<6cm	not observed	Abundant	Parallel	Barren			t/D		Abundant	
74	Carb+Qtz	Syn-alteration	<1cm	Epidote (~2cm)	Abundant	Parallel	Barren					Abundant	
75	Carb-Qtz	Syn-alteration	<1cm	not observed	Abundant	Parallel	Barren						
76	Carb+Ep Vuggy Qtz	Syn-alteration Syn alteration	<1cm <5cm	Epidote Not observed	Abundant Common	Parallel	Barren			PVPF: t/D		Abundant	
77												Abundant	
78	Qtz	Syn-alteration	<10cm	Sulphur- stained	Abundant	Parallel	Barren					Abundant	
79													
80													PVOL: Abundant

Appendix 6 cont.

Station	Type	Timing	Thick	Veins Halo	Abundance	Shape	Minerals	Mineralization (% Abundance/type)						
								En	Cpy	Mo	Py	Hm	Mt	
81	Sulphide	Mineralization	n/a	Silicious	Pervasive	Stockwork	Cpy, Bn	2-3/V,S	8/V,S					
82									5/D	5/D				
83	qtz-carb	Syn-alteration	<1.5cm	not observed	Common	Parallel	not observed		2/D	2/D				
84	qtz-carb	Syn-alteration	<1.5cm	not observed	Common	Parallel	not observed	1/D,V	2/D,V	1/D,V				
85	qtz-carb	Syn-alteration	<1.5cm	not observed	Common	Parallel	not observed		2/D	2/D				
86									t/D	5-10/D				
87										4/D				
88														
89									2/D	1/D			Abundant	
90													Abundant	
91	Carbonate	unclear	<1cm	not observed	Common	Parallel	Barren							
92													P	
93	Carbonate	syn-alteration	<2cm	not observed	Abundant	Parallel	Barren						P	
94	Carbonate	syn-alteration	<1cm	not observed	Abundant	Parallel	Barren						Abundant	

Appendix 6 cont.

Station	Type	Timing	Thick	Veins Halo	Abundance	Shape	Minerals	En	Cpy	Mo	Py	Hm	Mt
113													
114											1/D		
115	Carbonate	Syn-alteration	<1cm	not observed	Common	Parallel	Barren				5/D		
116													
117													
118													
119													
120											t/D		
121													
122													
123													
124													
125											1-2/D		
126													
127													Abundant
128													
129													Trace
130													

Appendix 6 cont.

Station	Type	Timing	Thick	Veins Halo	Abundance	Shape	Minerals	Bn	Cpy	Mo	Py	Hm	Mt
131	Carbonate	Syn-alteration	<1cm	Not observed	Abundant	Parallel	Barren						
132	Carbonate	Syn-alteration	<1cm	Not observed	Abundant	Parallel	Barren						
133													
134	Carbonate	Syn-mineralization	<1cm	Not observed	Abundant	Parallel	Py				5/D, V		
135													
136											5/D		Veins
137	Quartz	Syn-mineralization	<1cm	Potassic, <2cm	Abundant	Parallel	Bn, Cpy	t/V, D	t/V, D				
138	ANDS: Quartz				ANDS: as above								ANDS: as above ANPF: Barren
139													M
140													
141													
142													

Appendix 6 cont.

Station	Type	Timing	Thick	Veins Halo	Abundance	Shape	Minerals	Mineralization (% Abundance/type)							
								Bn	Cpy	Mo	Py	Hm	Mt		
143															
144	Carbonate in ANPF	Unclear	<0.5cm	Not observed	Common	Parallel	Barren							ANPF: w	
145															
146															
147															
148															
149														W	
150														W	
151														W	
PF06															Not noted

Appendix 6 cont.

Station	Type	Timing	Thick	Veins Halo	Abundance	Shape	Minerals	Bn	Cpy	Mo	Py	Hm	Mt
PF07	Carbonate+epidote	unclear	0.5 -1.0 cm	not observed	Common	Parallel	Barren					W	
152													Abundant
PF08									t				
153	Qtz-carb	Syn-mineralization	<0.5cm	not observed	Common	Parallel	Bn, Cpy	0.5/V,D	t/V,D			possibly very weak	
154	Qtz-carb	Syn-mineralization	<1cm	not observed	Common	Parallel	Cpy		0.5/V,D			W-local, patchy	
PF09	Quartz	Syn-alteration	<2cm	Potassic	Abundant	Parallel	Cpy, Bn	t/V,D	t/V,D				
155													
PF10												W	
PF11	Carbonate (ankerite)				Abundant								
156/PF20													
157/PF21	Qtz (only observed in PPFQ)	Syn-alteration	<0.5cm	Potassic	Common	Parallel	t Cpy		t/V				ANAU: none ANPF: Abundant
158													
PF22													
159													
PF23													
160													Abundant

Appendix 6 cont.

Station	Type	Timing	Thick	Veins Halo	Abundance	Shape	Minerals	Bn	Cpy	Mo	Py	Hm	Mt
161											Gabbro: t/D		
162											t/D	M-S	
163													
PF24													
164													
PF25													
WS01											Gabbro: t/D		
PF26													
165	Qtz-carb	Syn-alteration	<0.5cm	not observed	Common	Parallel	Barren					W - local	
PF27												W - local	
166												W	
PF28												W	
PF29												M	
167												W	

Appendix 6 cont.

Station	Type	Timing	Thick	Veins Halo	Abundance	Shape	Minerals	Bn	Cpy	Mo	Py	Hm	Mt
PF30												M	
168												W	
PF31	Carbonate	Syn-alteration	<1cm	not observed	Common	Parallel	Barren						
169													
170	Chlorite	unclear	<0.5cm	Not observed	Common	Locally brecciating, parallel	Barren					W	

Appendix 6 cont.

Station	Structure Unit	Orientation	Notes
1	Cpy+Bn bearing Qtz-carb vein		Unmineralized, no visible sulphides. Trace malachite is found on fracture surfaces. Towards northern end, fragmental nature of unit becomes apparent. The northern end also hosts Cpy mineralization, and dominantly chlorite alteration with minor sericite. Later carbonate alteration is locally intense, but is not ubiquitous. Some minor veins are dry but bear chalcopyrite and have ~2cm wide potassic halos. Also present is a lense-shaped Qtz vein of ~6cm width with no associated halos.
2			More strongly sericitically altered than at Stn. 2, but with similar chlorite alteration. Fairly strong malachite alteration, but few sulphides observed likely due to high degree of weathering. 1cm-wide hematite vein is also present, and was sampled.
3			Likely a flow, rather than air-fall facies. This would explain the weaker alteration, as well as the absence of fragments.
4			Locally intense chalcopyrite. Alteration is subtle, but pervasive sericite+chlorite. Locally intense potassic alteration, but no corresponding Qtz+carb veins were observed. Chalcopyrite and bornite occur as disseminations or as dry veins. Also Qtz-carb veins, a number of which host Cpy in high abundances at the centre of the vein, and moly at the edges. Orientation recorded. These veins exhibit a narrow (<2cm) potassic alteration halo. Later cross-cutting carbonate alteration is present. Locally trace malachite after Cu-sulphides.
5	Qtz+carb+cpy vein with Cpy at centre and moly at edges. Other less significant veins are adjacent and roughly parallel.	358/87E	Plagioclase porphyritic basaltic andesite. Plagioclase phenocrysts are subhedral but mg-cg (dominantly mg). Porphyritic texture is very strongly locally concentrated - adjacent rocks are aphyric. Alteration is weak sericite + chlorite. Trace disseminated Cpy, with later malachite. Quartz veins cross-cut but do not bear mineralization.
6	Bedding plane (or shear)	003/31 E	Same as station 6. Andesite is weakly porphyritic and weakly altered. There exists evidence for flow textures in the form of undulating patterns in the rock which appear more subtle than a contact.
7			5% sulphides ~50/50 Cpy+Py as disseminations. Alteration assemblage is k-spar + sericite. Late carbonate veins (<2cm width) cross cut and are abundant. Alteration seems to extend vertically up the hill, which can be seen in the discolouration of talus up-slope.
8			More mafic and dark coloured than previous stations. Volcanics have a distinct darker colour and a notable absence of the pervasive green colouration observed elsewhere. Not likely purple volcanics. Aphyric to weakly porphyritic. Alteration is dominantly sericite with local epidote.
9			

Appendix 6 cont.

Station	Structure Unit	Orientation	Notes
10			Same as station 9.
11			Green fg. volcanics, weakly porphyritic. Highly magnetic, but with no visible magnetite. No sulphides were observed.
12	Pillow flow direction	182 or 2	Lithology same as station 11. Pillowed flows. Flow direction 182 or 002. Could not determine keel or vesiculation to determine upwardness.
13	Contact between ANDS and PPFQ	038	Contact between ANDS and PPFQ strikes at 038, but the dip could not be determined. Some cross-cutting epidote veins are late and have no halos. These veins have non-parallel walls and appear "squiggly". The veins cut both lithologies. Often contains clasts of andesite near the contact.
14	30cm PPFQ dyke	004	Contact relationship between PPFQ and ANDS is more clear, in a 30 cm dyke which has a minor 5cm splay coming off at 30NW. Alteration and mineralization is identical to station 13
15	50cm PPFQ dyke Tip of propagating PPFQ dyke	015 240/80W	Dyke contact is sharp with only subtle <2cm chill margins. Contact is also angular. Barren qtz+carb veins run roughly parallel to the dyke. Back in pillow facies, weakly porphyritic with fg-mg augite phenocrysts. PPFQ is variably potassically altered. ANPF is only propylitically altered with local gossanous zones bearing ~ 5-10% Py.
16	PPFQ dyke	~000	Outcrop bears two trenches, which are roughly parallel and ~30m apart. Trenches aimed to expose areas of gossan which are pyrite. We are in the propylitic zone with abundant locally intense epidote +/- chlorite alteration. PPFQ seems to average a northerly strike. Dyke size ranges from 1m to <5cm. Both porphyritic pillow facies and lapilli tuff facies are observed, the latter of which is more abundant at the northern end.
17			Across length of outcrop move from propylitic alteration to weak phyllic alteration at the western end.
18			No visible sulphides. Qtz-carb veins are abundant
19			Potassically altered, approaching equigranular GRDR. No sulphides were observed.

Appendix 6 cont.

Station	Structure Unit	Orientation	Notes
20			Both PPFQ and ANPF units were present, but contact relationship was unclear.
21	Molybdenite "plane" Barren Qtz-carb vein	002/18E 350/55E	Augite-phyiric andesite with cpx ~ 40%. Sericite + chlorite alteration overprinting weak potassic alteration. Some pillow structures are likely, but are subtle. Some molybdenite occurs without other sulphides in a plane (not a smear), and grains are distinct - not a paint. Irregular Qtz-carb veins are common. Due to erosional favourability of cpx over plag, the weathered surface has a 'pockmarked' appearance where the cpx has weathered away.
22			Augit phenocrysts ~5%. Chlorite alteration is dominant. No sulphides were observed.
23	Cross-cutting mafic dyke 2nd mafic dyke Qtz-carb veins Epidote-hosting QC veins	070/68SE 078/64SE 292/71N 343/73E	Diabase is 15cm wide and is unaltered to weakly chloritically altered with no sulphides. Dyke cross-cuts Qtz-carbonate veins and terminates them. 4 dykes in total cross-cut, all roughly parallel. Thickness increases to the south: 15, 25, 60, >40cm.
24			
25	Qtz-carb veins at two orientations. Not quite at conjugate angles of 60. Epidote vein (strike only)	290/70 345/68 280	Pyrite is typically spatially associated with small (mg) epidote concentrations.
26			Mineralization seems to be concentrated locally, however, there does not appear to be any direct relationship with veining. Quartz-carbonate veins are less abundant to rare.
27			Mineralization seems to be concentrated locally, however, there does not appear to be any direct relationship with veining. Quartz-carbonate veins are less abundant to rare.
28			Mineralization seems to be concentrated locally, however, there does not appear to be any direct relationship with veining. Quartz-carbonate veins are less abundant to rare.
29	Cpy-bearing Qtz-carb vein	177/74W	PPFQ may be a zone of intense potassic alteration of the andesite unit.

Appendix 6 cont.

Station	Structure Unit	Orientation	Notes
30			PPFQ, fairly equigranular, highly altered. Weak potassic overprinted by intense sericite+chlorite. Good mineralization. In contact with late mafic dyke on the north side - described in station 31
31			Would appear as a late mafic dyke, were it not for the local presence of vesicles infilled by calcite. The rest appears to be very weakly altered by chlorite and otherwise very competent and not cut by any veins. No sulphides were observed.
32	Carbonate-sulphide veins Mafic dyke contact	164/76W 115/82W	PPFQ unit is similar to station 29, and is very well mineralized with disseminated and vein-hosted cpy and py. The most intense mineralization is found immediately adjacent carbonate veins which are almost completely weathered away. Malachite and sulphur staining are abundant. The mafic dyke is vuggy and locally bears sulphides, however it is otherwise fairly unaltered. Evidence supporting the dyke hypothesis: No chill margins on PPFQ dyke, but do exist in mafic dyke. Mineral grains from PPFQ are terminated by the D/BS. A fair amount of sulphur staining exists in the mafic dyke, but usually in close proximity to the contact. This could be a result of sulphur saturation through wall-rock assimilation.
33	Carb+Py vein Epidote-halo carb+qtz vein Barren carbonate vein	008/80E 082/82S 340/08E	Westernmost o/c is aphanitic andesite which is highly mineralized with ~5% cpy and 1% py, with malachite and sulphur burns and chlorite alteration. A zone of intense mineralization which is dominantly py (~20%) which has 'rotted' the outcrop. This mineralization is hosted in fg andesite of ser+chl alteration with a supergene leech overprint, juxtaposed against nearly unaltered rock. The region above the mineralized zone is strongly altered. Throughout the outcrop, there is an absence of malachite staining, likely indicating the absence of Cu-bearing sulphides. The strongly altered zone is aphanitic, or has had the original textures obscured by intense alteration. Alteration is an assemblage of chl+ser which appears to have been overprinted by silica. However this is uncertain because the rock is highly friable. Py has been carried in by carbonate veins which have subsequently eroded, producing a rubbly appearance of the mineralized zone. Away from the py-rich zone, within ANPF, there are local zones of intense epidote veining and alteration forming "nodules".
34			Sulphides have been strongly altered to sulphur staining and malachite.
35	Dry sulphide vein	012/85E	
36			Possibly part of D/BS. Amygdulites of calcite are present.
37			Outcrop discontinuous over 15m length

Appendix 6 cont.

Station	Structure Unit	Orientation	Notes
38			Aphyric andesite is chloritically altered and cross-cut by qtz-carb veins which carried in opy+py mineralization and which also created potassic+chlorite rims (chlorite is possibly after biotite)
39	Barren qtz-carb vein	290/81	
40			
41			Identical to station 40, but the epidote alteration is weaker
42			Pyrite is fg, euhedral, and is commonly spatially associated with epidote. The outcrop is strongly magnetic and bears some rare euhedral fg magnetite grains
43			Local malachite and sulphur burns
44	Carb-qtz vein Mineralizing veins (parallel) Fault (photos) Mineralized vein (w/ py)	255/61E 236/42E 308/86E 247/55E	Sulphur burns are abundant, imparted by the occurrence of pyrite along dry fractures <<1cm
45			
46			Lithology, alteration, mineralization, same as station 45
47	Fault contact	285/64S	Fault contact of PPFQ and D/BS. Reason for coarseness of grains in PPFQ is a result of size of dyke (>20m). Fault is ~8cm wide, is not annealed, and is filled with gouge. Other evidence for fault: no smaller interfingering dykes. No clasts in either unit. D/BS unit is very competent. Contact also has epidote and sulphur burns adjacent.
48	Dominant vein direction	182/78	

Appendix 6 cont.

Station	Structure Unit	Orientation	Notes
49	Mafic dyke	087/vert	
50			Possibly diorite. Protolith is intensely propylitically altered so as to obscure the original texture. Epidote and chlorite are both abundant. The diorite is medium-grained and bears no sulphides
51			Medium-grained diorite. Strongly chloritically altered with local epidote. Trace vfg pyrite is present. Late carbonate veins cross-cut.
52			Green volcanic. Heavily qtz+carb veining. Intense chloritic alteration. 1-2% Py.
53			Protolith intensely altered by epidote with carbonate and more widespread chlorite.
54			Diorite, locally epidote altered. Fine to medium grained with weak chlorite+sericite alteration. Local pyrite mineralization is generally <1%.
55	Small fault Large fault with pinnate jointing	256/66 275/70	Fragmental volcanic unit. Cross-cut by faults, with a dextral shear sense, which can be interpreted from the pinnate jointing. Smaller fault has a chloritic alteration halo.
56			Identical lithology to station 55
57			Clasts are of variable composition. Some clasts are vfg pinkish volcanics, and some are epidote "nodules".
58			
59	Contact:	~070/90	Contact could not be identified, but northern portion of o/c is as 058. So dyke width is >4m. Contact structure is very approximate.

Appendix 6 cont.

Station	Structure Unit	Orientation	Notes
60	Contact with D/BS	254/81	Intrusive breccia unit. Matrix has been re-used by hydrothermal fluids (Qtz+Carb and Chlorite veins). Mineralization is locally very good with cpy stringers of ~0.5cm width or less. Cpy also occurs as disseminations resulting in common malachite staining. Total Cpy locally can attain 10%. Alteration is possibly phyllic, but andesite clasts are variably altered. Some PPFQ appears to be potassically altered. D/BS is present at the north end of the o/c and is markedly more competent than the adjacent unit. Contact is irregular and seems to follow jointing in INBX unit.
61			Plagioclase-phyrlic andesite is surprisingly competent and difficult to break.
62			Similar to Strn 060, but with less mineralization, and less hydrothermal material
63			Similar to Strn 060 and 062
64	Contact between PPFQ and D/BS	298/72	
65			Purple volcanics are aphanitic. Some of the larger veins cross-cutting are vuggy. Colouration of the purple volcanics is variable from purple to red. Purple volcanics and quartz-feldspar-porphyry units are both mineralized with 1-2% cpy.
66			Cpy + mal do occur locally, but are restricted to veins
67			
68			
69			
70			Purple volcanics to green volcanics. Weakly magnetic, but also locally oxidized to hematite. Cross-cut by calcite veins.

Appendix 6 cont.

Station	Structure Unit	Orientation	Notes
71	Shear plane/Fault (1m width) Qtz-carb vein	332/61 130/88	Two, possibly three lithologies present in a single o/c, yet contact and paragenetic relationships could not be determined, although it appears veins run through all three lithologies. A section of the o/c is covered in a white substance, which may be derived from the dissolution of carbonate veins. Evidence for this comes from the preservation of one of the major veins cross-cutting, which are ~15-20cm wide, and are later cut by Qtz-carb veins of <1cm thickness
72			Similar lithology to stn 70
73	Fault Purple dyke Vuggy carb vein (~6cm wide)	072/46 126/79 133/81	Fault shows well-developed slickenlines. The major carbonate vein is vuggy. The mafic dyke has sharp margins, and the orientations of these margins seem to roughly follow jointing. Some of the surrounding porphyritic volcanic as been included in the margin of the dyke.
74	Qtz-Carb veins	002/75	
75	Purple dyke Thick Qtz-carb dyke Qtz-carb vein	~N-S 095/83 078/54	O/C begins as ANDS, then moving east intersects the purple volcanics. There appears to be a transitional zone between purple and green volcanics which involves variable purple colouration as zones or nodules before taking full purple colouration. Could this represent a change in oxidizing states in the same lithology? Is the purple volcanic necessarily always purple? A later purple dyke cross cuts at 380998E 6358683N. Further, the o/c passes into augite-phyric andesite. The major Quartz-carbonate vein which cross-cuts is ~12cm thick and brecciates the host rock. The halo around this vein is intensely sulphur-burned.
76	Contact	~305	Epidote-carb vein cuts both lithologies and the contact, indicating that this phase of fluid exsolution post-dated formation of either unit.
77	Contact	~120	PVOL locally brecciated. Orientation of mafic dyke is interpreted; dyke is roughly 3m wide.
78	Fault/Shear Brecciating vuggy Qtz vein	130/85 313/88	
79			Separated by slight valley - may indicate fault contact of two lithologies?
80			

Appendix 6 cont.

Station	Structure Unit	Orientation	Notes
81			Hydrothermal breccia to stockwork with intense mineralization. Hydrothermal material is dominantly sulphide-only. Malachite staining is abundant, along with sulphur burns which appear on fracture surfaces.
82			Piece of float ~4m away has a breccia texture similar to that observed in the paramount zone with heterolithic clasts and a PPFQ matrix.
83	Qz-carb vein	070/50	
84			Mineralization occurs as disseminations, or as dry veins. Dry veins most commonly contain Cpy with Mo. Mo also occurs on fracture planes.
85			
86			Highly altered and gossanous.
87			
88			ANPF likely a "raft" of material carried upwards or downwards in a fault which separates the ANPFa and the PPFQ. This fault is observed directly above in station 89
89	Fault	195/81	Large fault cross-cuts. Malachite and sulphur staining are most prevalent immediately adjacent the fault. Sulphides are present as very fine disseminations.
90	Bedding (right way up)	330/52	Fragmental unit overlying flow top or fall top of similar lithology
91	Bedding	280/45	Lapilli are 1cm or less. Sulphur staining is abundant, but no discernable sulphides were observed.
92			Moving north, abundance of plagioclase phenocrysts increases up to ~15%
93	Veins at two orientation	240/81 116/82	
94			Becomes plagioclase-phyrlic to the north. (~15%, mg, subhed)

Appendix 6 cont.

Station	Structure Unit	Orientation	Notes
95	Dyke contacts	330/78 172/70 121/85 165/83 263/66	Dykes exhibit chilled margins. Average dyke width is ~3m.
96			
97			
98	Brecciating carb viens	272/60 298/54	
99			
100			
101			
102			
103			
104			
105			
106			
107	Contact Contact Shear	075/71 050/70 344/32	Pyrite is largely euhedral and fine-grained.
108			
109			
110	Local zones of gossan	210	Similar to str 110, with local zones of gossan
111			
112			North end has PVOL in contact with ANDS, also PVL

Appendix 6 cont.

Station	Structure Unit	Orientation	Notes
113	QFP dyke	NNW	
114			
115			
116	Gossan	NNW	Zone of gossan to south end of o/c trends roughly NNW and is 2m wide, but is open to the east. Trends the same direction as the QFP unit observed further north.
117			
118			
119			
120			
121	Contact (fault/shear?)	~100	
122			Contact lies north
123			Shows bedding of interlayered coarser grained and finer grained aphanitic beds of roughly equal thickness.
124			
125			
126	Contact ~ 20N		
127			
128			Matrix is very mafic and very fine grained
129			
130			

Appendix 6 cont.

Station	Structure Unit	Orientation	Notes
131	Carb veins	~N	
132	Carb veins	~N	
133			
134			
135			
136			Locally cherty gossanous o/c
137			Very highly altered andeste. No phenocrysts were observed. Vein-centered potassic alteration halos are common and <2cm wide. Such halos are centered around mineralizing quartz veins with trace associated chlorite. Bornite and chalcopyrite are trace, and typically occur at the centres of the quartz veins, often adjacent to chlorite. Pervasive chlorite alteration throughout which predates mineralization and potassic alteration.
138			Northern portion is similar to Stn 137, with lesser potassic alteration and no bornite. Trace cpy occurs as stringers and in veinlets. Faulted against fairly unaltered andesite.
139			
140			Becomes plagioclase-phyric to the north. (~15%, mg, subhed)
141	Preferred shear orientation Contact (highly variable orientation)	041/64 097/72	D/BS in contact with PPFQ. PPFQ is very strongly fault fractured. Contact with D/BS is sharp and irregular, and near contact D/BS is locally vuggy, as observed elsewhere. PPFQ is more equigranular than typically observed, and does not bear significant quartz.
142	Contact: (rough)	350/50	D/BS in contact with PPFQ. PPFQ is light pink, massive, with closely spaced 1mm euhedral feldspars. Little matrix. D/BS is locally vuggy and has no phenocrysts near the contact. The weathered surface has a purple appearance, but this is believed to be due to weathering. Fine-grained euhedral plagioclase laths and subhedral augite phenocrysts are of roughly equal abundance, but are only ~10% together. (PF01)

Appendix 6 cont.

Station	Structure Unit	Orientation	Notes
143			Feldspar porphyry has good weathered surface. Pink, massive, no quartz. 0.5 to 1.0 mm pink feldspar, closely packed, subhedral. (PF02)
144	ANPF/PPFQ contact: Carb veins:	220/52 029/56	Three lithologies in contact. Contact between D/BS and PPFQ is irregular and sharp. D/BS has negative weathering relief relative to PPFQ.
145			
146	Contact	059/49	"Multi-branching, bifurcating, PPFQ dyke" - Walter Hanyeh.
147	Contact	300/65 334/80 120/90	Contacts exhibit chill margins in D/BS.
148			Very competent.
149			North part competent, South part more strongly fractured.
150			ANAP possibly a syngenetic subvolcanic feeder to the volcanic pile.
151			
PF06			Volcanoclastic, massive, competent.

Appendix 6 cont.

Station	Structure Unit	Orientation	Notes
PF07			
152			
PF08	Crystal fabric	318/90?	
153			
154	Qtz-carb veins (mineralized)	178/80	
PF09	Qtz-carb veins	354/80	
155	Late mafic dyke (rough orientation)	070/subvert	
PF10			
PF11			
156/PF20			
157/PF21	Contact	205/38	PPFQ?: Very felsic, very fine-grained but equigranular intrusive underlying andesitic volcanics. Very few mafic minerals and no quartz. Feldspar only and cross-cut by potassically-altering quartz veins which bear trace chalcopyrite. Likely a finer-grained version of the PPFQ equigranular phase observed on the western side of Mount LaCasse on the July 29th traverse. The intrusive cuts through and under the mountain.
158			
PF22			
159	Contact (very rough)	WNW-ESE	
PF23			
160			

Appendix 6 cont.

Station	Structure Unit	Orientation	Notes
161	Contact	005/65	
162			
163	Bedding	271/78	Some mafics are present in the tuff and have been altered strongly to chlorite.
PF24			
164	Bedding	298/64 280/70	Bedding orientation changes by ~20 deg over short distances.
PF25	Bedding	280/70	
WS01	Bedding Mafic dyke contact	280/70 298/vert	Fine-grained mafic dyke (~20-30cm) in contact with a gabbro which bears trace disseminated pyrite. A zone of mylonite ~20-30cm wide lies beside the D/BS contact. Subparallel to the contact is a fault breccia. 2m north of the contact the ANTF unit occurs with mm to 1/2 cm size bedding and some feldspar phenocrysts which may indicate a crystal component or a crystal tuff nature. Some bedding is observed to be hematized. Appearance is similar to that of a siltstone.
PF26			
165			
PF27			
166			
PF28	Phenocryst foliation	260	
PF29			
167			

Appendix 6 cont.

Station	Structure Unit	Orientation	Notes
PF30			
168			
PF31	Carbonate veins	256/39	
169			
170	Chlorite veins	264/45	